FACULTEIT WETENSCHAPPEN

POLY(2-ALKYL-2-OXAZOLINE)S AND POLY(ETHYLENE IMINE)

HOW ONE THING LED TO THE OTHER

Maarten A. Mees

Promotor: Prof.Dr. Richard Hoogenboom
Presented to the Faculty of Sciences, Ghent University, in partial fulfilment of the requirements for the degree of Doctor in Science: Chemistry
2017

UNIVERSITEIT GENT

HEMISTRY UPRAMOLECULAR

POLY(2-ALKYL-2-OXAZOLINE)S AND POLY(ETHYLENE IMINE)
HOW ONE THING LED TO THE OTHER

Members of the examination committee in alphabetical order:
Prof.Dr.Ir. Bruno De Geest (Ghent University; BE)
Prof.Dr Peter Dubruel (Ghent University, BE)
Em.Prof.Dr Eric Goethals (Ghent University, BE)
Prof.Dr. Steve Howdle (University of Nottingham, UK)
Prof.Dr. Annemieke Madder (Ghent University, BE, Chair)
Prof.Dr. José Martins (Ghent University, BE)
Prof.Dr. Stanislav Rangelov (Bulgarian Academia of Sciences, BG)
Prof.Dr. Ulrich S. Schubert (University of Jena, D)

List of abbreviations

ADME	Absorption, Distribution, Metabolism and Excretion
BSA	Bovine serum albumin
b-PEI	Branched Poly(ethylene imine)
BIS	*N,N*-Methylenebisacrylamide
ConA	Concanavalin A
COSY	Correlation spectroscopy
CROP	Cationic ring opening polymerisation
Đ	Dispersity
DCC	*N,N'*-dicyclohexylcarbodiimide
DLS	Dynamic light scattering
DMA	Dimethylaceetamide
DMTMM	4-(4,6-Dimethoxy-1,3,5-triazin-2-yl)-4-methylmorpholinium chloride
DNA	Deoxyribonucleic acid
DOSY	Diffusion-ordered NMR spectroscopy
DP	Degree of polymerisation
EDC	1-ethyl-3-(3-dimethylaminopropyl)carbodiimide
EPO	Erythropoietin
HFIP	Hexafluoro-2-isopropanol
HIV	Human Immunodeficiency Virus
HMBC	Heteronuclear multiple bond correlation
HPMA	N-(2-hydroxypropyl-methacrylamide)
HSQC	Heteronuclear single quantum coherence spectroscopy
LCST	Lower critical solution temperature

L-PEI	Linear poly(ethylene imine)
MALDI-TOF	Matrix assisted laser desorption/ionisation –time of flight
NHS	N-hydroxysuccinimide
NMR	Nuclear magnetic resonance
PAOx	Poly(2-alkyl-2-oxazoline)s
PCL	Polycaprolactone
PEG	Poly(ethylene glycol)
PEtOx	Poly(2-ethyl-2-oxazoline)
PEtOx-PEI	Poly(2-ethyl-oxazoline)-co-poly(ethylene imine)
PDMS	Polydimethylsiloxane
PHPA	Poly(hydroxypropyl acrylate)
PMestOx	Poly(2-methyoxycarbonylethyl-2-oxazoline)
PMMA	Poly(methyl methacrylate)
PNIPAM	Poly(*N*-isopropylacrylamide)
PnPrOx	Poly(2-n-propyl-2-oxazoline)
PPG	Poly(propylene) glycol
PPrOx-PEI	Poly(2-n-propyl-2-oxazoline)-co-poly(ethylene imine)
PPhOx	Poly(2-phenyl-2-oxaoline)
R_H	Hydrodynamic diameter
RID	Refractiv index detector
RGD	Arginylglycylaspartic acid
RNA	Ribonucleic acid
SEC	Size exclusion chromatography
T_{CP}	Cloud point temperature
THPA	N(2-tetrahydropyranyl)aziridine
TNF	Tumor Necrosis Factor

Chapter 1 :
A message in a bottle

CHAPTER 1

1.1 Layman's description

The general purpose of this PhD research was to develop polymers for use in a biomedical context. A difficult question that was raised during this PhD work, not by famous professors or fellow scientists but by the man in the street was, "*So you are putting plastic into a human being?* " In order to answer this question we can compare the human body with the earth globe. Some people are standing on a shore, let us say the Belgian coast and they want to correspond with somebody standing on the coastline of Dover. They throw a bottle, containing a message in the sea, hoping that the person in Dover will receive this. A few things can be done to increase the chance of reaching the person in Dover. You could just increase the number of bottles, increasing the chance that one of these bottles will reach the other coast. This is barely efficient and one depends on a lot of uncontrollable factors that influence the final destination of your bottle, it might as well end up in the Netherlands or France. In addition the sea can be really harsh and your bottle may break due to the current or it can be eaten by a large fish. This could be counteracted by making a stronger bottle that can endure the sea. However, this is still not an efficient way to deliver your message as you rely on the current of the sea that determines the destination of the message. So we propose the following: wouldn't it be possible to make a vessel which is not visible, such as a submarine, which protects the bottle from the dangers of the sea and can be directed to the correct coordinates. Instead of throwing a hundred bottles in the sea, in the hope that one of them will ever reach the coast, you can make a "stealth" vessel with GPS enhanced delivery and protect the message from the sea.

Even though such a sea-submarine would be feasible, as a molecular analogue for drug delivery, this is of course pure fantasy. Nonetheless, encapsulation of an active compound in a biocompatible polymer can protect it from the immune system and enhance its bioavailability. As such, the polymer will protect the message (bioactive compound) from the harsh conditions in the body such as the immune system, renal clearance or the blood current. Molecular recognition could aid to deliver the message/drug to a specific target, which will help in reducing the side effects. However, the pharmaceutical community still mostly focusses on the development of low molecular weight drug molecules rather than macromolecules. It is not easy to introduce macromolecules in this conservative field and a more objective and open view is needed to advance innovations in drug formulation and delivery.

In this thesis, we focused on one specific submarine/type of polymer, namely the biocompatible pseudo-peptides called poly(2-alkyl-2-oxazoline)s (PAOx). The PAOx are also known as the precursors for linear poly(ethylene imine) (L-PEI), a key reference in non-viral vectors for gene delivery. Therefore, in this PhD work, both the development of PAOx and L-PEI for biomedical applications will be examined. First, there will be a thorough examination of the partial hydrolysis of PAOx to understand the copolymer distribution along the chain, which is important to understand the properties and further modification of the resulting

PAOx-PEI copolymers. Subsequently, instead of hydrolysing the usual suspects poly(2-ethyl-2-oxazoline) (PEtOx) and poly(2-methyl-2-oxazoline) (PMeOx), the hydrolysis of poly(2-n-propyl-2-oxazoline)s (PPrOx) will be examined resulting in more hydrophobic cationic copolymers that will be explored for gene delivery. In the final part, the further modification of PEI and PEtOx-PEI polymers will be developed for the preparation of PAOx copolymers with side chain functional groups. A first class was developed by using PEI and PEtOx-PEI for the synthesis of fluorescent copolymers by reaction with super critical CO_2. The second class was obtained by coupling methyl ester containing side-chains onto the copolymers of PEtOx-PEI and their subsequent modification by direct amidation. Finally the reductive amination modification of PEtOx-PEI with carbohydrates yielding sweet polymers was investigated.

1.2 Polymers in a biomedical context

Imagine yourself in a world without polymers? There would be no plastic bottles, no car interior, no electricity housing, etc. Polymers are everywhere around us in the world as it is today in both positive and negative aspects. In less obvious fields, such as medicine polymers are omnipresent in different morphologies, topologies and sizes. However these polymers need to fulfill certain properties to make them applicable in biological context. These strict requirements for polymer properties can be defined in a biological manner or from a chemical point of view.

First of all the polymer needs to be biocompatible. Biocompatibility is defined as the acceptance or rejection of artificial materials by the surrounding tissues or the appropriate immune response. Therefore, so-called stealth behaviour is important as this means that the active compound is not recognized by the immune system. In order to achieve this stealth behaviour, the nonspecific protein adsorption (fouling) has to be minimized. This non-fouling behavior influences the lack of response of the immune system and surrounding tissue. The interaction with the immune system is influenced by the chemical composition or the surface of this polymer material. This controls not only the toxicity, but also the positive effects of the materials.[1] Different interactions at the interface can influence the biocompatibility: 1) chemical structure (branched or linear) and functional groups 2) types and quantity of charges 3) molar mass of the polymer, 4) structural flexibility of the polymer 5) hydrophobicity/hydrophility.[1] Depending on the application these properties can be altered. For biomedical applications the polymers should meet the following chemistry related requirements:

- Minimisation of the heterogeneity of the polymer. A single molecule such as a drug only contains one mass and one specie.[2] On the other hand, polymers have a (broad) statistical mass and size distribution which can have important implications. The different masses (and sizes) may induce important complications, e.g. for renal clearance. The size distribution complicates everything from a pharmaceutical point of view and for regulatory affairs. Therefore, polymers for use in biomedicine should be as defined as possible, in other words, they should have a narrow size distribution.
- Ideal control over the synthetic route makes it possible to tune the physicochemical properties to introduce multiple chemical functionalities.
- The up scaling should be possible and reproducible, including a thorough purification.
- Appropriate formulation, long term stability.
- Characterization of the absorption, distribution, metabolism and excretion (ADME) of the polymer therapeutic.

- It needs to be known what the interaction of the polymer interface is with the biological parts, tissue or fluids, thus mapping the different immunological reactions.

In the early days, the biomedical polymers were used as plasma expanders, wound dressing and antiseptics. In a field dominated by PEG the first polymer-drug-conjugate entering phase I and II of clinical trials was *N*-(2-hydroxypropyl-methacrylamide)-doxorubicin (HPMA-DOX).[3] The biocompatible polymers can have a degradable or non-degradable behaviour. Examples of degradable polymers are poly(glycolic acid) (PGA), polypeptides,[4] dextran, hyaluronic acid, hydroxyethyl starch (HES) and polylactide[3] (FDA approved). Non degradable polymers include PEG, HMPBA, poly(vinyl pyrrolidone) (PVP),[5] and poly(ethylene imine) (PEI).

Polymers used in a biomedical context can be divided in 3 different classes depending on size; a macroscopic class, a microscopic class and a nano class. The macroscopic class contains implantable medical devices, artificial organs, prostheses, dentistry, bone repair or hydrogels. The polymer is either the object itself or the coating.[6] The second class is the micro class[6] consisting of micro particles, and micro needles.[6] In the nano class, drug delivery plays an important role. Polymers in the nano class can have different functions depending on the form of the polymer, the interaction with an active compound and its composition. The polymer drugs are used because small molecules tend to diffuse in the body and hence only a small amount arrives at the desired tissues. The drugs often have low water solubility and are prone to degradation therefore the polymer is used to increase the drug concentration and shell life by solubilisation of drugs into polymer nanoparticles that may protect the drug. Depending on the form of the polymer therapeutic different classes are defined. (Figure 1-1):

- Polymeric drug /sequestrant
- Polymer-protein/peptide conjugates
- Polyplex
- Polymer-drug conjugate
- Block copolymer micelles.

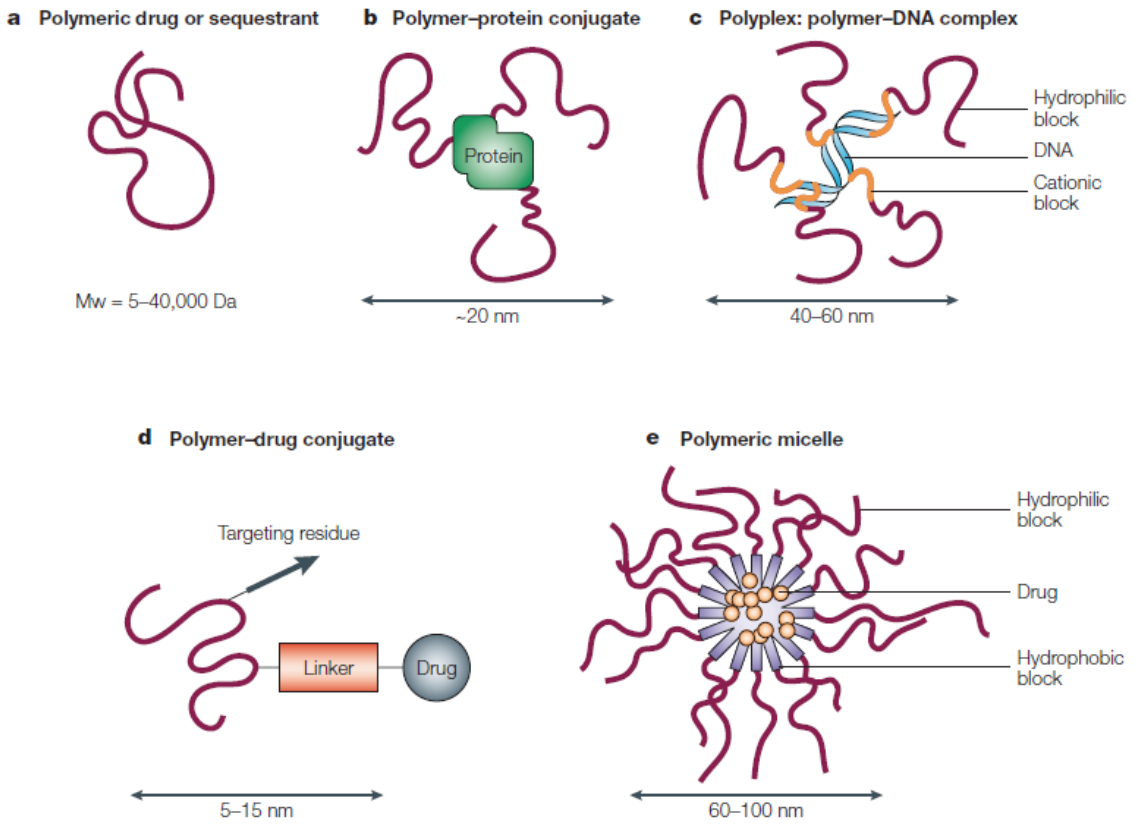

Figure 1-1 Different types of polymer therapeutics [2] With five possible types for the nano class: polymeric drug or sequestrans, polymer-protein conjugate, polyplex, polymer drug conjugate, polymeric micelle.

As seen in Figure 1-1 5 different classes of polymers are shown. The first class are the polymeric drug/sequestrant , such as Renagel. Renagel is a poly(allylamine)s cross linked with epichlorhydrin and is used to bind phosphates.[3] The second class is the polymer-protein conjugate, the polymer dissolves or protect the peptide from the biological environment.[2] The third class is the class of polyplexes, here the polymer interacts with the genetic material often via a cationic charge.[2,7] In the fourth class the polymer is linked with a drug *via a* linker and optional there is a targeting residue linked on the polymer.[6,3] In the last class the drug is often water insoluble and a hydrophobic core is needed to solubilize the drug, the hydrophilic corona makes it possible to have a water soluble vehicle.

Polymer drug conjugates generally consist of three parts, the polymer, a linker and drug/bioactive molecule(Figure 1-1).[2] The polymers can prevent premature degradation and enhance uptake of the drug, while maintaining drug concentration in the therapeutic window, thereby reducing side effects. For its application in polymer therapeutics, the polymer has to be bio-inert, protein resistant and non-fouling.[8]. The most popular polymers that are currently being developed up to clinical trials are PEG and HPMA. A

large drawback of these polymers is the non-degradability and the potential accumulation in different tissue.[3] This can increase the local concentration in certain tissues above the toxicity level. This will activate the immune system and anti-polymer antibodies will be generated. These drawbacks, especially for PEG will be discussed in section 1.4. The focus of polymer therapeutics lays often in cancer research, frequently conjugated drugs are paclitaxel,[9] doxorubicin and camptothecin(quinolone alkaloid found in *Campotheca acuminate,* aka "the happy tree").[10] The different types of polymers for polymer-therapeutics are still rather limited. Table 1 summarizes the polymers which have been used in clinical trials.

Table 1 Examples of polymer therapeutics in clinical trials and current status[3]

Class	Example	Composition	Disease	status
Polymeric drugs	Copaxone[11]	Glu, Ala, Tyr, lysine copolymer(glatiramer)	Multiple sclerosis	Market
	Vivagel	Lysine based dendrimer	HIV/Sex Health	Market
	Synvisc-One	Hyaluronic acid	Osteoarthritis	Market
Polymeric sequestrants	Renagel/Welchol[12]	Cross linked poly(allyl amine)	Lowering phosphate levels in kidney diseases	Market
Polymer-protein conjugates[13]	Zinostatin Stimaler	Polystyrene-comaleic acid	Cancer	market
PEGylated proteins	Cimzia[14]	PEGylated anti TNF fab	Arthritis/chronical diseases	Market
	Mircrera	PEGylated EPO	Kidney diseases	Market
Polymer-drug conjugate	Opaxio	Poly-glutamic acid-paclitaxel	Cancer	Phase III
	Prolindac[15]	HPMA-copolymer-DACH platina	Ovarian Cancer	Phase II
	XMT-1001[16]	Polyacetal-camptoherin derivate	Cancer	Phase II

The biomedical world is continuously evolving and many diseases are better understood and new targets are found. More and more bioactive molecules are used as medicine to interact with newly found molecular targets. Therefore, new delivery systems are needed as molecules like nucleic acids and peptides have to be protected due to their fragility in the hostile biological environment. Polymer-drug conjugates need to be inactive and stable during circulation while releasing the active agent in the target tissue, reducing side effects and avoiding an immune response. The control over the chemistry (hydrophilic/hydrophobic), presence of hydrogen bond donating and accepting groups and

stereochemistry controls are all important factors that influence the biological properties. The field of polymer therapeutics is rapidly expanding, and therefore new polymers are needed to further explore this field. New cures for diseases give new opportunities and new research questions. Therefore there is an urge to create new types of polymers and to develop new systems that are better than the older systems. The choice of poly(2-alkyl-2-oxazoline) will be discussed and explained.

1.3 Poly(2-alkyl-2-oxazoline)s

The field of polymer therapeutics can benefit from the research in poly(2-alkyl-2-oxazoline)s (PAOx) as certain PAOx have been shown to be biocompatible. The large potential chemical versatility makes this class of polymers a real competitor in the field. In each step of the synthesis different functionalities can be introduced.

PAOx are polymers based on the heterocyclic 2-oxazoline monomer. Different methods can be used for the synthesis of 2-oxazolines, (Figure 1-2).[17] Starting from nitriles, carboxylic acids or aldehydes, a large chemical diversity (toolbox) can be obtained due to the broad range of monomers with different 2-substituents that end up as the corresponding PAOx side chains. Together with this diversity a broad range of physical and chemical behaviour can be introduced ranging from very hydrophilic (poly(-2-methyl-2-oxazoline)) to hydrophobic polymers (poly(2-butyl-2-oxazoline). The monomers can be polymerised via the cationic ring opening polymerisation (CROP), Figure 1-2. This means that the monomers cannot have nucleophilic groups as these will interfere with the CROP, which can be overcome with protecting groups. In Figure 1-2 the CROP of 2-oxazolines is depicted. It is a typical chain growth polymerisation, which can be divided in three parts: initiation, propagation and termination. It is a living polymerisation under the ideal conditions, with no termination nor transfer reactions. Since nucleophiles can terminate the polymerisation or induce transfer reactions, extensive measures have to be taken before the polymerisation to ensure the purity of the monomer, solvent and initiator.

The polymerisation (Figure 1-2) is initiated by a nucleophilic attack of the 2-oxazoline monomer onto the electrophilic initiator. In the subsequent propagation step, the newly formed oxazolinium species reacts with the ring of the 2-oxazoline.[17] The polymerisation can be terminated by the addition of a nucleophile. In every step of the polymerisation, functionalities can be introduced. This by using a functional initiator, functional monomers with a functional R side groups or a functional terminating agent. As such the polymers can be tailored to the envisioned application.

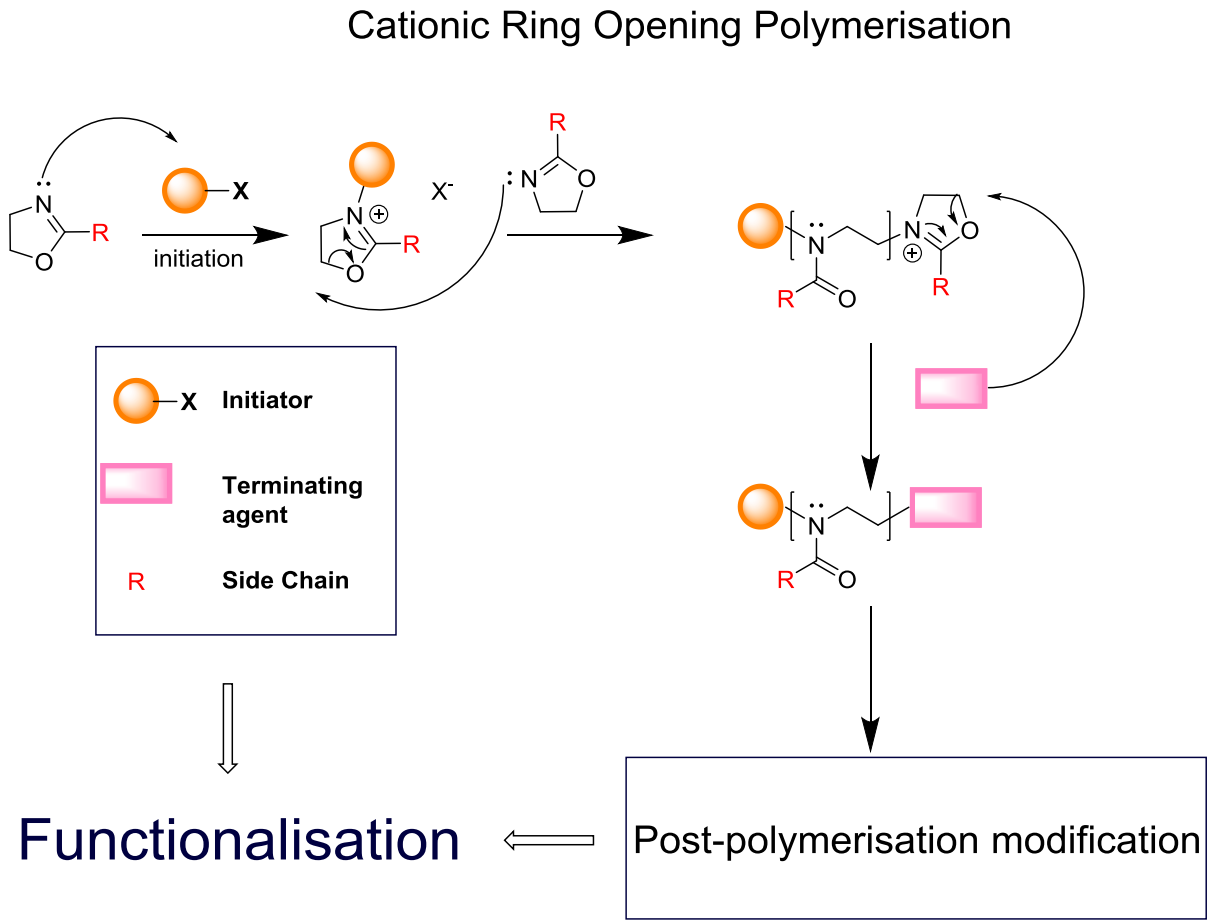

Figure 1-2 Schematic representation of the cationic ring opening polymerisation of 2-oxazolines. The polymer is initiated by the nucleophilic attack of the oxazoline on the initiator. The activated species is subsequently attacked by the oxazoline. Termination is done via a nucleophilic group.

The solution behaviour of PAOx can also be controlled by variation of the 2-substituent of the monomer. Therefore polymers with a different side chain and accompanied different solubility behaviour can be made. Ranking the polymers from water soluble to water insoluble leads to the following order poly(2-methyl-2-oxazoline) (PMeOx) > poly(2-ethyl-2-oxazoline) (PEtOx) (≈ PEG) > poly(2-iso-propyl-2-oxazoline) (PiPrOx) > poly(2-cyclopropyl-2-oxazoline) (PcPrOx) > poly(2-n-propyl-2-oxazoline) (PnPrOx) > poly(2-butyl-2-oxazoline) (PBuOx) with PMeOx being fully water-soluble and PBuOx being fully water insoluble. This control can be used for the synthesis of amphiphilic block copolymers by combining the hydrophilic polymers (PMeOx or PEtOx) with one of the hydrophobic monomers. Such block copolymers can self-assemble into micelles, which can be used for drug loading and delivery.[18] This application will be further discussed in section 5 of this chapter. In some cases, polymers with so called lower critical solution temperature (LCST) behavior are obtained meaning that the polymers are soluble in water below

the cloud point temperature (Tcp). Heating the polymer solution above the T_{CP} leads to phase separation and makes the polymer solution to turn opaque. This interesting property will be discussed in chapter 3. The LCST behaviour can be used for the preparation of responsive surfaces by coating the surface with poly(2-isopropyl-2-oxazoline). The resulting substrate has a different protein and cell adsorption depending on the temperature, whereby the reversible adsorption is much lower below the Tcp induced by the higher hydrophilicity.[19]

1.4 Poly(2-alkyl-2-oxazoline)s vs Poly(ethylene glycol)

PEG polymers are without doubt the gold standard in polymer therapeutics, PEG has a large commercial availability and is the best known polymer in the medical field due to its excellent biocompatible behavior. As discussed before it is important to search for alternatives because PEG has some major drawbacks. Despite that, several PEG based therapeutics have gained FDA approval and are used in the clinic. Therefore both the pro and contras of PEG will be discussed here and the polymer is compared to PAOx as potential alternative.

Polymer drug conjugates, such as PEG,[20] can reduce protein adsorption and aggregation, increase circulation and bioavailability. Most of the drugs are hydrophobic and attachment of a water soluble polymer increases drug circulation and may enhances uptake by the addition of targeting motifs. However, we have to consider that every week papers are published using polymer therapeutics and thereby suggesting a potential cure for the disease. Even though these studies look very promising, only a small part makes it into clinical trials, because *in vitro* or even *in vivo* data from mouse models do not guarantee any success in clinical trials on humans.[21]

PEG is in this context still the most used polymer for developing polymer drug conjugates as it reduces the non-specific adsorption of proteins, including plasma protein adsorption, which is reduced up to 70%. It is, however, not only the reduction of protein adsorption that plays a role in the stealth effect, it is the specific adsorption of certain proteins to the PEG layer that has been suggested to be crucial.[22] When PEG-coated particles were exposed to macrophages without prior protein treatment, the macrophages eliminated the particles, indicating that they could detect the polymer layer. This means that the adsorption of specific types of protein is crucial for the stealth behavior. In fact the clusterin, part of the family of the apolipoproteins, was identified to be crucial. When clusterin adsorption onto PEG was ensured, no uptake in macrophages was observed.[22] This absorption of plasma proteins helps the PEG to avoid recognition by the immune system making the polymer behave as a stealth vessel.

However, several drawbacks to PEG appeared such as the non-degradability and the increased immunogenicity upon repeated treatment.[5] Especially at higher dose treatments, the lack of degradability causes the accumulation of PEG in the body *via* vacuolization, i.e., the formation of vacuoles. Toxicity problems could potentially occur when the concentration of polymer becomes higher than the toxicity threshold of the systems. The immune response is also a concern, as anti-PEG antibodies have been found in multiple cases for PEG causing problems in chronic diseases.[23,24] The anti-PEG antibody is induced by the huge amount of products in pharma and consumer products containing PEG. The antibodies induce inflammation and a faster clearance of these polymer therapeutics making them less effective. There is also a concern for oxidative degradation of PEG *in vivo*. The reason why PEG is still the gold standard lays with the commercial availability in large quantities, in a large range of molar mass and good quality. This is an important asset as a lot of labs do not have the in-house expertise to make the polymers with the required properties. As medicine is quite conservative in changing protocols and they tend to stick to the already approved polymer materials such as PEG, new technologies find it difficult to reach the market.

PAOx receives significant interest as a competitor for PEG because it has similar biomedical properties in combination with some advantages. The pros and cons of PEG and PAOx are listed in Table 1-2. The polymerisation of PEG is often difficult as ethylene oxide is explosive and hazardous. The formed polymers are only stable at low temperatures (-20°C), which is a liability for the shelf life. The limited chemical versatility of PEG provokes low drug loading and difficult active targeting as PEG can only be modified via the end groups. Next to this limited chemical versatility, the above discussed vacuolization and anti-PEG antibodies are in disfavor. To further elaborate on the stealth effect, the protein corona was examined for both PEG and PAOx. They both showed low nonspecific cellular uptake by macrophages, reducing immunologic responses.[25] PEtOx showed less protein adsorption than PEG in fetal calf serum. Remarkably two independent papers report corresponding adsorbed protein patterns with small differences revealing that the formation of the protein corona by specific adsorption of plasma proteins is influenced by the structure of the polymer.[22] Rather than no protein adsorption, the selective adsorption of proteins appears to be important for the stealth behavior. Furthermore, a minor uptake of PEG into macrophages was shown while PEtOx was not taken up in a comparative study.[25]

Table 1-2 PEG vs PAOx

PEG	PAOx
Difficult polymerisation, explosive gaseous monomer	Non explosive, no straightforward purification
Oxidation forms peroxides	No oxidation
Stable at low temperature (-20°C)	Stable in water and at ambient temperature
Diol content	No diol
Highly viscous	Low viscosity
Low drug loading	High drug loading
Difficult for active targeting	Active targeting easy accessible (chemical versatility)
Vacuolization	Cleared from the body
Anti-PEG antibodies	Not enough biological assay and no FDA

The PAOx polymers also show some disadvantages such as difficult monomer synthesis and purification. For the polymerisation a nucleophile free environment is required, nucleophiles can induce termination of the polymerisation which is also true for PEG. However, besides these disadvantages the PAOx polymer appears to be superior, especially with regard to the large chemical versatility, (Figure 1-2). This helps to tailor the desired polymer for a certain application. As not only the bioactive molecule can be coupled but also targeting ligands onto the polymer chain. This helps to tailor the perfect polymer for every specific application. However the main limitation of PAOx is the absence of FDA approved therapeutics posing an important risk as it is uncertain how they will behave in humans.

1.5 Biomedical application of Poly(2-alkyl-2-oxazoline)s

Since the inception of the PAOx-field numerous biomedical applications have been developed and published. The focus of the PAOx field is mainly on polymer therapeutics, namely polymeric micelles, and polymer protein/drug conjugates.

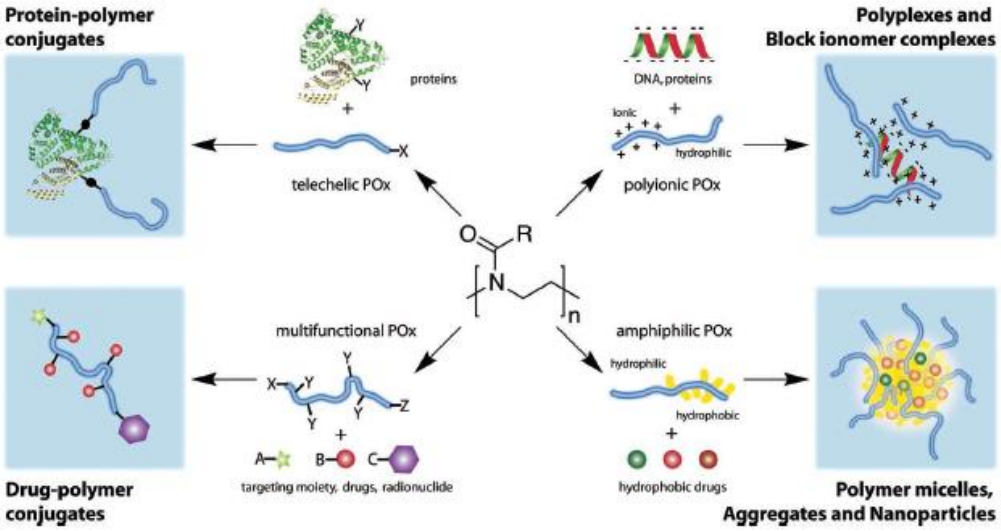

Figure 1-3 Overview of the use of PAOx polymers for polymer therapeutics.[26]

PAOx are gaining interest as biomedical polymers and are often referred to as pseudo-peptides because they are structural isomers of peptides. Similar to other biomedical polymers, a classification of PAOx-based polymer therapeutics can be made in: polymer-drug conjugates, polymeric-drugs, polymer micelles, polymer aggregates, polymer nanoparticles and polyplexes(Figure 1-2).[27] The latter will be discussed in section 7, that focuses on gene therapy and PEI. In the case of a polymer drug conjugate the water solubility is critical, therefore, PMeOx and PEtOx are valuable candidates, although the latter has a Tcp around 65°C, which, is not relevant in a biomedical context. Next to the solubility, the biocompatibility plays a crucial role, which has been tested for PMeOx and PEtOx in different cell lines such as MCF7, HEP G2, CATH cells.[28] The polymers exhibited no toxic effects. *In vivo* data showed excellent behavior for PMeOx as it increased blood circulation times of drugs and is nontoxic against THP-1 cells (acute monocytes leukaemia).[29] The excellent biocompatibility is caused by suppression of protein adsorption although as previously mentioned, specific plasma proteins adsorption may also play a role. This was shown by coating of different surfaces with PMeOx, acting as an anti-fouling coating.[8] Similar, no

hemolytic effect was found for pure PEtOx. PEtOx copolymers with a zwitterionic side chain showed no adverse reaction with human blood, regarding platelet activation or immune system while excellent coagulation behaviour was observed.[30] By using thiolated silica nanoparticles grafted with PMeOx, PEtOx or PPrOx it was shown that PMeOx coated particles had higher mucus penetration. The diffusion speed was correlated with the hydrophilicity, with higher hydrophilicity showing faster diffusion.[31] Similar conclusions were reported for PEtOx and PiPrOx coated poly(organosiloxane) nanoparticles with a rhodamine B core.[25,19] The PEtOx grafted particles showed similar biocompatibility as PEG as discussed in the PAOx vs PEG section. The antibody recognition and cell uptake properties where examined to scan for potential cytotoxicity of PMeOx. The procedure included an alkyne modified tobacco mosaic virus which was coupled to azide containing polymers. An equal immunological response was observed as for PMeOx and the PEGylated virus.[32] Also PMeOx and PEtOx containing lipophiles were made by the coupling of distearoyl phosphatidyl ethanolamine to increase blood halftime and to lower liver uptake in mice. This test showed that the PEtOx performs worse than PMeOx in the context of blood clearance and a minor uptake in liver and spleen was observed. This difference was ascribed to the small change in hydrophilicity.[33]

Not only the PAOx homopolymers showed excellent biocompatibility, various PAOx (tri)block copolymers also showed excellent biocompatible behavior.[28,34] PEtOx-b-PPhOx block copolymers were self-assembled into nanoparticles and examined in a neurotoxicity assay revealing no neurotoxicity. Eventhough there was no apoptosis or necrotic effects, some of the polymers showed activation of the complement system at higher concentration levels.[35]

The excellent biocompatibility of PAOx makes it possible to find a broad range of biomedical applications. In the following, selected biomedical applications of PAOx will be discussed with a distinction on the size of the polymer structure, ranging from the macroscopic level via the microscopic level to the nanoscopic level. At the macroscopic level different topics are discussed, such as thermoresponsive surfaces, bandages, antifouling surfaces and hydrogels.

Different types of anti-fouling surfaces have been developed with different PAOx. The control of surface properties is important as this controls the interface between the material and the blood. It is however a subtle balance, the surface should not be prone to bacterial adsorption as this induces infections and corresponding repelling effects. On the other hand the material needs to be compatible with the tissue, if this is not the case it could induce immunological reactions of the guest organism. As an example polymer brushes on amino-functionalized silicon substrates with different PAOx were discovered to control cell and protein adsorption. Surfaces containing PEtOx or PMeOx showed low cell adsorption.[36] In similar research, copolymers of PiPrOx and PEtOx and PNonOx (poly(2-nonyl-2-oxazoline) were used to make temperature changing surfaces with switchable cell adsorption.[37] Similar anti-fouling containing surfaces were designed based on zwitterionic PAOx to replace heparin. Heparin is an often used anti thrombosis

agent. The coating on implantable devices can prevent thrombosis and opsonisation of proteins which can induce rejection. The zwitterionic PAOx are made starting from PEtOx-PButenOx (poly(2-butenyl-2-oxazoline). The amine is introduced on the double bond using a thiol-ene reaction with cysteine and subsequently a sulfobetaine or a carboxybetaine is prepared. These surfaces showed promising results in the field of anti thrombogenics.[30] Pure PEtOx was spincoated on gold slides and silicon reducing protein adsorption.[38] Poly(l-lysine)-PMeOx were compared with PLL-PEG on a Nb_2O_5 surface yielding non-fouling surfaces. The PMeOx copolymer was reported to be more stable than PEG in physiological and oxidative environment.[39,40] To act as an anti-bacterial agent amines are coupled to the initiator and/or terminator site of PAOx. This helps to disrupt the bacterial cell wall.[41] Different PAOx were developed as anti-micro bacterial materials by the introduction of cationic charges.[41,42] Antibacterial biofilms were developed by making triblock PMeOx-b-Polydimethylsiloxane-b-PMeOx with amine end groups.[43]

The company GATT® showed that PAOx is ready to enter the commercial field of haemostatic agents. The product contains a coating with an electrophilic activated PAOx with excellent biodegradability, strong adhesiveness and haemostatic properties.[44] This agent makes use of a methyl ester containing polymers which will be discussed in chapter 5. The procedure developed in this work was used to couple an ethylene diamine on the polymer.[45]

The last examples for the macroscopic application of biomedical polymers are hydrogels, which are 3D water swollen structures. As PAOx is biocompatible and ideal for cell culture, different types of hydrogels can be synthesized for this purpose. Further applications of hydrogels are found in the area of drug delivery. Two different methods are used for hydrogel synthesis whereby in the first method the cross linked network is formed during the CROP and in the second method a post-polymerisation coupling method is used. The first method is based on the presence of a bifunctional monomer inducing network formation in situ during polymerisation. The network is formed however a solvent exchange needs to be done as no water can be present during the CROP. This means that an extra step is needed as the solvents need to be switched. The second method uses the functional groups on the polymer and cross-linkers to form the hydrogels during a post-polymerisation coupling reaction.[46,47] Such PAOx hydrogels have been used as a scaffold for all kinds of cell growth. PEtOx-PUndecylOx has a undecenyl side chain with a terminal double bond which is cross-linked via a dithiol linker. These hydrogels were used for fibroblast growth and to enhance cell recognition a RGD peptide was added.[48,49] Degradable hydrogels were synthesized by using copolymers with a degradable middle block, namely PEtOx-b-Poly(D,L-lactide)-b-PEtOx. These gels were used to grow skin fibroblast.[50] A triblock polymer, PEtOx-P(ε-caprolactone)-PEtOx, with a thermoresponsive behavior was used to embed the antibody bevacizumab (Avastin). This product prevents neovascularization in certain diseases, such as diabetes.[51] Co-networks were formed with PEtOx and poly(2-hydroxyethyl methacrylate (PHEMA) and poly(hydroxypropyl acrylate) (PHPA) to

release ibuprofen in a controlled way.[52] PEtOx and acrylic acid induced a pH sensitive hydrogel by using γ-gamma irradiation with ibuprofen as model drug.[53]

Hydrogels could not only be used for cell growth but also filter DNA out of solution. During the polymerisation of PEtOx-BocOx was introduced along the chain. This BocOx monomer contains a BOC (tert-butyl oxycarbonyl groep) protected amine in the side chain. After deprotection of the amine a part of the amines are used in crosslinking with chloro-epoxides. The primary amines and the formed secondary amines were demonstrated to interact and bind with DNA.[54]

If we take a step closer to the bottom towards the use of PAOx for microscopic polymer therapeutics, there are only very few examples. Nonetheless microbeads of biodegradable PMeOx were used to grow stem cells. A telechelic PMeOx was formed by using methacrylic end groups. The degradable linker contained a disulfide bridge that is cleaved under reductive conditions and the formation of the microbeads was performed in micro fluidic channels.[55]

We all know that there is plenty of room at the bottom, to cite Richard Feynman. Therefore, and because it is closest to the molecular world of chemists, the nanoscopic polymer therapeutics area has been the broadest research field for PAOx. It is however remarkable that most research groups often use the same model anticancer drugs, such as doxorubicin and paclitaxel. An overview is provided of the reported PAOx drug conjugates (Table 1-3) as well as PAOx micelles that are used for drug encapsulation in the hydrophobic core (Table 1-4)

The most advanced results have been reported by the company Serina therapeutics that is developing a PAOx-drug conjugate to treat Parkinsons' disease, which is currently being evaluated in phase I clinical trials. Serina uses the abbreviation POZ instead of PAOx, which is only a difference in nomenclature. In addition, a manifold of products are in the pipeline of this company: the treatment of epilepsy with PAOx-cannabidiol (SER-228) and treating nausea and vomiting induced by chemotherapy by POZ-tetrahydrocannabinol (SER-232). SER-214 is the first PAOx conjugate in clinical trials and is based on click chemistry to couple the rotigotine to the side chains of PEtOx (DP200) via cleavable ester linkage. The coupling is performed via an alkyne-functionalized 2-oxazoline monomer which was copolymerised with water soluble PAOx polymers.[56]

Table 1-3 PAOx-drug conjugates

PAOx	Linker	Kind	Drug
PBuOx-b-PEtOx; PBuOx-b-PMeOx and homo PMeOx	Amidation reaction end group; NHS Amidation	enzyme	Horse radish peroxidase[57]
PMeOx	Azyde-alkyne cycloaddition (click)	viral	Model virus[32]
PMeOx/PEtOx	Amine termination	Amino-Peptide	HCPC[58]
PMeOx/PEtOx/poly(2-(4-pent-4-ynyl)-2-oxazoline)	Cycloaddition(click)	Protein cage	Icosahedral Virus like particles (180 QB copies) [59]
PMeOx-b-PDMS-b-PMeOx	streptavidin	Macrophage (target) A1	Biotinylated ligands[60]
PMeOx-co-P4-(2-aminophenyl)-2-oxazoline)-BSA	DMTMM (amine+COOH)	Matrix	Antigen coupling[61]
PMeOx-b-PDMS-b-PMeOx(poly G)	Biotin functionalisation	Pravastin	Cholesterol inhibitor[62]
PMeOx/PEtOx	NHS		Insulin and enzyme[63]
PEtOx	Hydrazone linker	Drug	Doxorubicin (micelle formation)[64]

Table 1-4 PAOx-micelles for drug delivery

PAOx	Kind	Drug
PBuOx/PMeOx and PBuOx/PEtOx	enzyme	Horse radish [65]peroxidase
	enzyme	Superoxide [65]dismutase
PMeOx-b-X-b-PMeOx (x=PNonOx,PtBuOx,PBuOx,PiPropenOx,PPhenOx,PHepOx)l	Drug	Paclitaxel[66–70],Docetaxel[67,69]Ampoterin B(antifungal),Cyclosporine A(immune suprenant), etoposide(cancer)[68],17-AAG[27,69], etopside[69],bortezomib[69,70]
Folic acid-PEtOx-b-poly(ε-caprolactone)	Near infrared dye	Indocanine/folic acid(target)[71]
PiPropOx/PEtOx	Organo siloxane NP	Rhodamine[19,25]
Star shape PPCL-b-OEGMA(oligo-2-ethyloxazoline)methacrylate	Drug	Doxorubicine[72]
Poly(l-lactide)-b-PEtOx-b-poly(l-lactide)	Drug	Doxorubicine[73]
PLLA-PEtOx	drug	Doxorubicine[74]
PEtOx-b-PCL	drug	Plaxitaxel[75]
PMeOx-g-PCL	drug	Different types of drug[76]
PMeOx-b-PDMS-b-PMeOx(poly G)	Pravastin	Cholesterol inhibitor[62]
PEtOx-Poly(2-decenyl-2-oxazoline)-fluorescein	model	Fluorescein [77]

1.6 The hydrolysis of Poly(2-alkyl-2-oxazoline)s

Before the excellent qualities of PAOx in biomedical applications were discovered, the polymer was mainly known as the precursor of linear poly(ethylene imine) (L-PEI) (IUPAC name: poly(imino ethylene)),previously only branched PEI (b-PEI) could be obtained by the ring opening of aziridines. The acidic and basic hydrolysis of the PAOx polymers made it possible to obtain L-PEI for the first time. Via this method it became also possible to synthesise copolymers containing both PEI and the original PAOx.

Four different research groups reported the synthesis of PAOx via CROP in 1966.[78–81] The publication of *Kagiya et al* showed that after hydrolysis of the PMeOx, linear PEI (L-PEI) could be obtained by releasing the side chain, herewith forming acetic acid. In a next step the PEI was acetylated with acetic anhydride showing that a post-polymerisation modification of L-PEI is feasible, in this case yielding the original PAOx.[78] *Tomalia et al* reported that during the acidic hydrolysis of PMeOx in sulfuric acid an acetic acid smell was observed; however no full hydrolysis was obtained. In this paper also the alkaline hydrolysis was reported with corresponding acetic acid smell.[80]

Long before the hydrolysis of PAOx into L-PEI, b-PEI was synthesised via the cationic ring opening polymerisation of aziridines (Scheme 1-1).[82] Therefore in nomenclature PEI is referred to either b-PEI making an explicit distinction between both polymers. The b-PEI was first synthesized in 1938 by I.G. Farbenindustry.[83] The b-PEI contains primary, secondary and tertiary amino groups with a 1:2:1 ratio [84] while the L-PEI only contains secondary amines. The b-PEI is water soluble and is 20% protonated at physiologic pH, depending on the polymer concentration.

The ring opening of aziridines yields the b-PEI (Scheme 1-1). The ring opening is initiated by the attack of the aziridine ring onto a Lewis acid. The resulting aziridinium ion is attacked by nucleophiles obtaining the ring opened aziridinium and a new aziridinium ion at the terminus of the chain. The chain is elongated by addition of a new monomer, whereby the formed secondary amine can also further react to a tertiary amine to induce a branching point. A nucleophilic attack terminates the polymerisation, which can occur with nucleophilic impurities or upon deliberate addition of a terminating nucleophile.

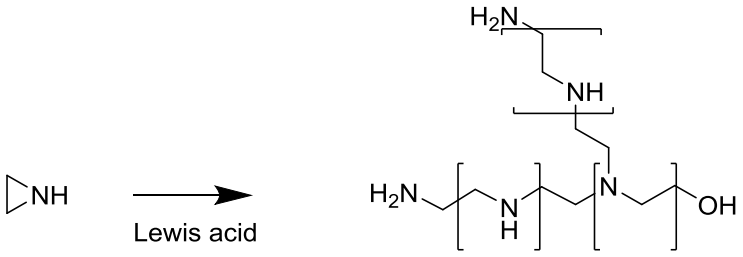

Scheme 1-1 Schematic representation of the ring opening polymerisation of aziridine resulting in b-PEI

The cationic ring-opening polymerisation of substituted aziridines is another option to obtain linear PEI (Scheme 1-2).[83] The aziridines are substituted with different bulky groups lowering the reactivity for the branching points, which promotes the formation of a linear polymer even though 100% linearity is not always reached. Aziridines substituted with different functionalities, such as alkyl, benzyl, sulfonyl, and perfluoro acyl groups have been polymerised. In a final step, some of these linear polyaziridines could be deprotected via cleavage of the side chain yielding linear PEI.[85–87] The branching could also be minimised by using *N*-(2-tetrahydropyranyl)aziridine (THPA), this group could be cleaved under mild conditions to obtain L-PEI as was shown by Goethals et al.[88]

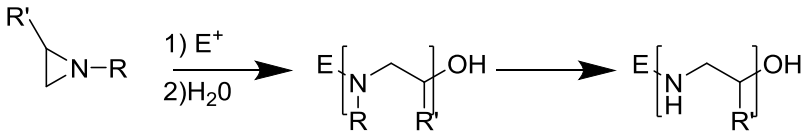

Scheme 1-2 Ring opening polymerisation of substituted aziridine and subsequent deprotection obtaining L-PEI

The best method to obtain linear PEI is still the full hydrolysis of PAOx under either basic or acidic conditions. During the acid hydrolysis the amides are activated by the protonation of the carbonyl functionality and the formed amines are protonated, which heavily influences the reaction speed and the cleavage of the side chain. The protonation of the PEI units plays an important role because this influences the hydrolysis and solubility in water. Under acidic hydrolysis conditions, the amides of the starting polymer are protonated due to the high acid concentration.[89] The influence of the PEI units was examined on a 25% hydrolysed PAOx showing a change in dielectric constant during titration.[90] This was ascribed to the presence of the side chain which influences the protonation in two ways. First, there is a reducing effect as the electrostatic repulsion decreases, which increases the chance of protonation. The second weaker effect, being the electron withdrawing effect of the amide, reduces the protonation, the reduction of electrostatic repulsion dominates and hence the amide side chains promotes the protonation. The

article implied that the average distance between two amines in a partially hydrolysed PEtOx (25% PEI) is lower than 8 atoms and it could be assumed that the formed PEI units are neighbouring groups.[90,91]

Two types of L-PEI can be found depending on the presence of a counter-ion. The first type is protonated as the Cl^--ions are still present, hence the PEI units are protonated and the L-PEI is water soluble. The second type, which is called the free base, is not protonated and can be obtained by boiling the polymer in NaOH. To dissolve the free base linear PEI in water, the temperature has to be higher than its melting temperature (50-68°C) because the PEI forms stable crystalline domains.[92] The free base form is insoluble in water at room and body temperature while the protonated form is water soluble at those temperatures. This protonation is of importance as it heavily influences the different applications of PEI. The PEI solubilised in water acts as a poly-base due to the secondary amine groups. However, no straightforward description of the pKa value of the polymer can be found as the large amount of amine groups heavily influence each other's protonation leading to a broad pKa range. This situation is different compared to small molecules, in dilute conditions small molecules have a discrete pKa and the protonation is only influenced by the acidity of the fluid. For PEI this is more complex. A description of the complexity can be given with three neighbouring PEI units. Protonation of the first amino group will be straightforward with a pKa of 9.5. However, due to the presence of this first positive charge there will be charge repulsion, which lowers the pKa down to 7 for the second protonation. The protonation of the third part will be even more difficult with an associated pKa of less than 7.[93] In the case of PEI, both branched and linear, all amines are chemically correlated as they are always at a two atom distance. Therefore PEI is called a weak polyelectrolyte. In the case of b-PEI the presence of tertiary, secondary and primary amines can further complicate the pKa regime, this will not be discussed. This means that the protonation is not straightforward and difficult to predict as there is a broad pKa regime. Besides the repulsion effect, the charges are present on the backbone and an extra conformational degree comes in to place making it more difficult to predict the protonation.[93] Similar as in small molecules the addition of salt influences the pKa as the addition of salt can change the protonation strength.[94] When an acidic solution of PEI is made basic by titration, Goethals and coworkers observed that the polymer solution becomes turbid and a drop in the pH value is observed at pH 9.4. It was shown that PEI has a pH dependent protonation, this will influence the endosomal escape as the pH in the lysosome is lowered from 7.4 to 5 by an influx of protons as will be further discussed in section 7 of this chapter.

The preparation of L-PEI starts often with PMeOx or PEtOx as parent polymer due to their commercial availability in large quantities, atom economy and good water solubility. The first reported reaction condition were often alkaline (NaOH) at 98°C for 3h.[91,95] In addition to the above mentioned polymers both poly(2-phenyl-2-oxazoline) PPhOx and PiPrOx have been used for the acidic hydrolysis.[96,97] In the following part, the basic and acidic hydrolysis of PAOx are discussed in further detail.

At first the basic hydrolysis will be discussed,(Scheme 1-3) which was reported in different occasions.[98,99] The reaction is second order ($rate = k2[amide][OH^-]$). In the first step the OH^- attacks the carbonyl function and subsequently this tetrahedral intermediate is deprotonated and the carboxylate is released irreversibly.

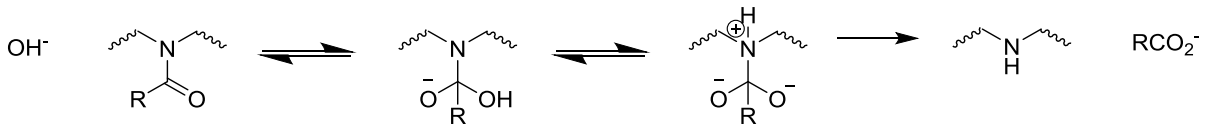

Scheme 1-3 Basic hydrolysis of PAOx: The basic hydrolysis of the PAOx starts with the attack of the OH^- on the amide bond forming the tetrahedral intermediate. After protonation of the nitrogen there is an irreversible release of the carboxylic acid.

Tanaka *et al* reported an attempt for the basis hydrolysis of PPhOx, however they failed.[96] The basic hydrolysis can be controlled by the amount of base added as was shown by Chujo *et al.*[100] A major drawback of this approach is that partial backbone degradation occurs during hydrolysis.[101] In our labs similar observations have been made, yet unpublished. It is, however, unclear how this backbone degradation appears and in which quantity.

The acidic hydrolysis is more promising and the first hydrolysis of PEtOx, PMeOx and PPhOx was shown in 1979 by Kem using HCl (Scheme 1-4).[91] The hydrolysis of PMeOx[91] and PEtOx[102,103] was investigated in a more detailed way. In a first step (Scheme 1-4) the amide is protonated making the attack of water easier, which is the rate determining step. The formed tetrahedral intermediate is promptly converted to the amine under the release of a carboxylic acid. This is accompanied by the corresponding smell of either acetic acid, propionic acid or in the case of PPrOx, butyric acid. As discussed the formed PEI is protonated due to the acidic conditions (pKa ~ 10). When the reaction equilibrium is pushed to the end it is difficult to protonate all the amine groups due to repulsion effects. The acidic hydrolysis of PAOx is an accurate and reproducible method to obtain L-PEI or PAOx-PEI copolymers, which is easily controlled by temperature. The temperature plays a crucial role as the hydrolysis is accelerated when the temperature rises. It was however also shown that at higher temperatures, above 180°C under pressurized conditions, the polymer backbone degrades during acid hydrolysis.[102] Due to the protonation of the formed amines after hydrolysis, there is an effective consumption of protons implying that the overall pH will increase and in this perspective the amount of acid controls the amount of PEI. It may by anticipated that there will still be the possibility to form new PEI units but this will be slow due to the slow exchange of the protons. In normal time frames this will not happen (hours).[102] Next to this discussed hydrolysis mechanism, the acidic hydrolysis maybe accelerated by the formation of seven ring like intermediate with neighboring groups. The proton on the protonated amine gives intramolecular hydrogen bonds which

makes the amide more susceptible to a nucleophilic attack. This was shown by the acceleration at the beginning of the hydrolysis of PEtOx[103] and PPrOx[104] and will be further discussed in chapter 3. The protonation of the formed amine is important and therefore the polyelectrolyte effect is discussed since repulsion of charges can decrease the reaction speed[91] and stretch the polymer chain. This influences the kinetics as it lowers the reaction speed when more amines are protonated, thus with higher hydrolysis degree. This is confirmed with the decrease of the reaction rate at higher hydrolysis degree.[93] The hydrolysis of PEtOx with different chain length showed that the degree of polymerisation (DP) has no influence on the rate of hydrolysis and on the molar mass distribution (*i.e* dispersity) of the resulting polymer. In the same study it was also shown that the PMeOx hydrolyses faster than PEtOx, whereby the kinetics showed that PMeOx had linear kinetics until 80% and PEtOx up to 60% due to the better solubility of the first. The polymer concentration was examined and showed no effect, at least under very acidic conditions where pseudo first order kinetics are achieved.[105] The acid concentration does play a role as protons are consumed during the hydrolysis.[106] The amount of acid controls the amount of PEI units formed in partially hydrolysed copolymers.[102,107] This provides a controlled and robust way to make partially hydrolysed polymers with a certain amount of PEI.

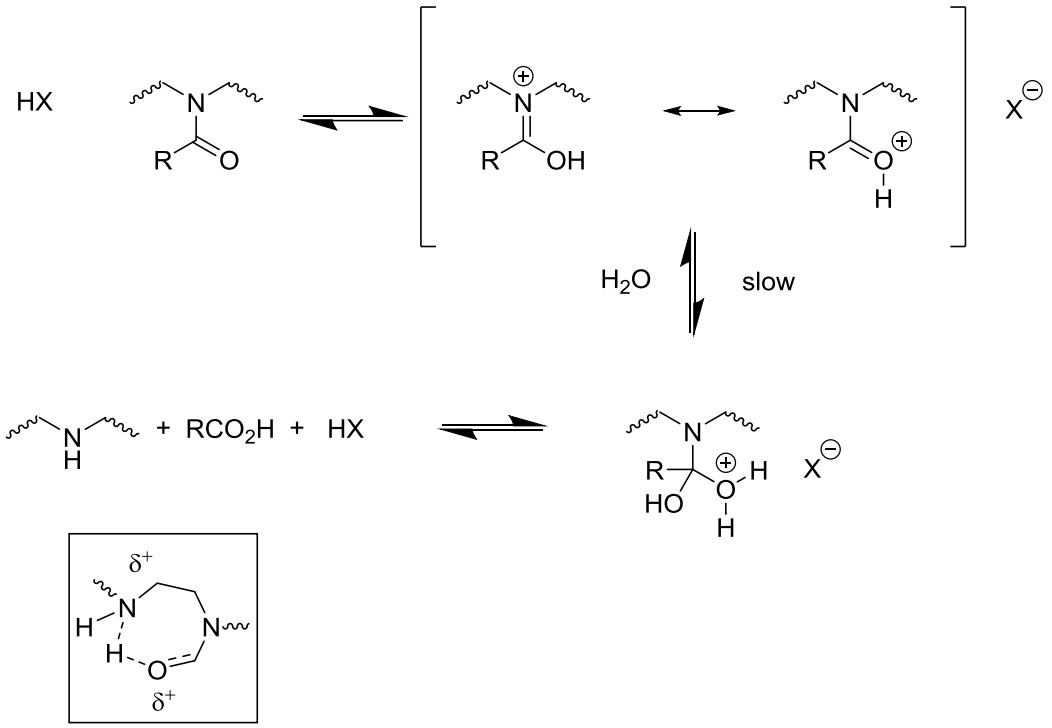

Scheme 1-4 Acid hydrolysis of PAOx: The acid hydrolysis starts with a protonation followed by the formation of the tetrahedral intermediate via water. This step is the rate determining step. The last step removes the carboxylic acid from the polymer obtaining the PEI. In the square at the bottom the seven ring is shown which may facilitate the hydrolysis of a neighbour amide.

The above discussed hydrolysis reactions mainly focused on full hydrolysis of PAOx to obtain L-PEI. The reaction can also be stopped at incomplete conversion to obtain a copolymer with a certain degree of PEI units and the original polymer. Partial hydrolysis was already demonstrated by Kem in 1979 and they assumed that the new polymers could be used in copolymer synthesis.[91] The partial acidic hydrolysis of PEtOx and PPrOx is discussed further on in this PhD work, *cfr*. chapter 3. The obtained PEtOx-PEI copolymers have been demonstrated to be still biocompatible up to 25% hydrolysis.[103]

Partial hydrolysis was also explored with triblock or diblock copolymers aiming to prepare PAOx-b-L-PEI block copolymers. The hydrophobic block was 4-t-butylphenyl-2-oxazoline or 2-undecyl-2-oxazoline and the hydrophilic middle block was PEtOx.[106] Via this method block PEI parts were synthesised due to the selective hydrolysis of the hydrophilic part while only (25%) of the hydrophobic parts were hydrolysed. To obtain a more selective hydrolysis, a lower PEtOx concentration and lower temperatures were used.[106]

Different methods were developed for the synthesis of pure block PEI-PAOx copolymers. The difference in solubility was explored to induce selective hydrolysis. Often a hydrophilic block, PMeOx or PEtOx was

combined with a more hydrophilic block. Both triblocks and diblocks copolymers were used. The triblock copolymers can consist of PPhOx-b-PEtOx-b-PPhOx where the middle block is hydrolysed. Also some efforts have been made to perform acidic hydrolysis in different solvents. Studies have been done on the acidic hydrolysis of PMeOx, PEtOx, PPhOx in 80-20 ethanol water mixtures. The experiment with PMeOx-b-PPhOx and PMeOx-b-PEtOx block copolymers showed that the PMeOx was preferentially hydrolysed although the PPhOx was also partially hydrolysed.[106,108–110] The PMeOx-PEtOx-was less selective although the PMeOx was hydrolysed faster than the PEtOx block. The use of random or block copolymers showed that due to the phase separation of the blocks the methyl block is cleaved off easier.[101]

Application of linear PEI in gene transfection experiments will be discussed in section 7 of this chapter. Here, the application potential of L-PEI in other fields will be briefly discussed. The polymers have often been used to chelate heavy metals[111] such as Hg^{2+},[98,112] Cu^{2+},[84,98,112,113] Cd^{2+},[84,98,112] Co^{2+},[84] Ni^{2+},[84,112] Zn^{2+} [84] and even Ca^{2+},[112]. Further applications include the role as retention aid in paper manufacturing, textile softeners and ion exchange resins. Again in the field of metal chelation partially ethoxylated PEI was applied for filter applications for many heavy metals such as Cu^{2+} and Ni^{2+} and Cd^{2+}. They are applied as electrolytes in batteries as they form polymer-salt complexes with alkali metals ($NaSO_3CF_3$).[114,115] L-PEI was used as a single ion conductor in batteries, increasing the ion conductivity.[116] L-PEI has also been used in gas scrubbers for removal of CO_2 gas out of gas streams however problems with recycling appear, this will be discussed in chapter 4.[117] PEI was also used as a stabilizer for gold nanoparticles. The gold interacting alkene chain was coupled via its acid chloride in a nucleophilic attack of the amine of the L-PEI.[118] SiO_2 was also combined with PEI via an epoxide containing silica groups which where condensed into silica particles an used as a conducter.[119] Finally, applications are found in beauty products for perfume delivery[120] and dermal applications for antibacterial applications.[37]

1.7 Gene therapy and Poly(ethylene imine)

The main application of L-PEI can be found in gene delivery, due to the presence of the positive charges. These charges interact with the negative charged genetic material such as DNA, and RNA. One out of three atoms on the backbone can bear a positive charge creating a high overall charge density along the backbone. Different modification where proposed ensuring better transfection efficiency. A lot of efforts and different adaptions have been done on L-PEI which will be discussed in this section.

As PEI is a key reference for non-viral gene therapy experiments, a brief introduction will be given about this topic. PEI is often used as reference to compare gene transfection efficiency of new vectors. Gene therapy is the treatment of diseases by inducing gene expression of a certain gen of interest. This is done

by using gene carriers to import exogenous nucleic acids into cells. In recent years, a lot of genetic diseases are recognized and potential targets are identified.[121] In gene therapy the cells are provided with genetic information to produce therapeutic proteins thereby overcoming problems with the direct administration of therapeutic proteins, such as degradation. Different types of genetic material can be introduced *e.g.* plasmid DNA, antisense oligonucleotides, shorter interfering RNA, micro RNA and messenger RNA. A gene delivery system is crucial to protect the genes from the harsh conditions in the body and to enhance cell delivery because the nucleic acids are often prone to degradation and do not enter cells. The gene carrier can be viral or non-viral. Still the major contribution is led by viral vectors, almost 70% of the existing gene therapies use genetically modified viruses.[122,123] However, these viruses are not always safe as they can alter the guest genetic code permanently by self-replication leading to severe immune and inflammatory reactions[124,125] and even leukemia. Therefore there is a constant need for alternatives.[126] Viruses such as adenovirus, adeno associated viruses, lentivirus and retro virus have been used.[121,127,128] The viruses are hazardous and the formed complexes are vulnerable during work up obstructing straightforward handling. A major drawback is that only a small amount of genetic material can be used and upscaling is difficult.[123]

Different non-viral systems can be used, but with lower transfection efficiency than viruses. These systems have lower immunogenicity, higher biocompatibility and more scale up potential. Liposomes, cationic lipids[129,130], peptides, polymers and dendrimers (PAMAM) are examples of non-viral gene vectors. They are often biocompatible polymers and have limiting undesired side reactions with proteins and non-targeted cells. Polymeric vectors are based on, *e.g.,* PEG, PPI dendrimers, poly(l-lysine),[131] polymethylacrylate,[132] cyclodextrins,[133,134] PEI-cyclodextrines[135] and polypeptides.[136] The following non-viral vectors are commercial available: Poly(l-lysine),[132,7] L-PEI and polyamidoamine dendrimers (PAMAM).[136,137] The most used L-PEI is the 22 kg/mol PEI as this is used as a benchmark in the majority of *in vivo* genetic experiments.[132,138]

The polymeric vector forms a complex with the nucleic acid and protects the gene from degradation.[139] The nucleic acids are negatively charged therefore polymers with a positive charge are used to condense them. These complexes between nucleic acids and positively charged polymers are referred to as polyplexes.[137] Remarkably, L-PEI is the best of the other polymers vectors as they are still 10^5 less efficient in gene delivery than the viral counterpart.[122,140,141] PEI is better in transfection than many other polymer non-viral vectors because the uptake and release of the genetic material is so efficient. PEI based polyplexes have a better escape from the lysosome and localization in the nucleus.[142] However there is a thin line between the number of cationic charges and the corresponding cytotoxicity. The positive charges induce more interactions with proteins present in the blood and more non-specific interactions. There are problems with injection of PEI polyplexes, such as liver necrosis and (cell)death.[143] The cytotoxicity of

the polymers is depending on the number of positive charges because this increases the tendency to interact with the negatively charged cell membranes.

Partial hydrolysis of PAOx yields copolymers such as PEtOx-PEI, which can be used for gene transfection experiments.[107] They perform better than the b-PEI. When an increased number of PEI units was introduced this induced a higher cytotoxicity. Copolymers of PEI were used as they can lower the cytotoxicity of the PEI by shielding of the positive charges and enhancing the water solubility. In this chapter the end group modifications will be discussed while the grafting will be discussed in the post polymerisation section 8 of this chapter. PEtOx-PEI end capped with a pyridine group was used for tracking the cellular pathway, by adding more positive charges a higher cytotoxicity was observed, whereby 30% of PEI units seems to be the limit.[144] It was shown that with less cationic interacting amines the polymer cannot transfect the genes.[145] In another approach the PEtOx-PEI was used as a macro initiator for the polymerisation of PEtOx herewith obtaining a polymer with (PEtOx-PEI)-b-PEtOx . The polymers were safe for both *in vitro* and *in vivo* use. This approach arise some doubts as the CROP should be nucleophile free while amines are present. Despite this doubt the authors reported low Đ values (between 1.08 and 1.12[146]). A PEtOx-PEI block was formed by coupling the PEtOx and PEI via disulfide bridge at the end group.[147] Not related to the gene transfection part, it was shown that PMeOx-PEI copolymers could be used in the determination of melamine in milk.[148]

Different PAOx could be used in gene transfection such as grafted PEI-g-PPhOx-g-PMeOx, the PEI block was hydrolysed in ethanol:water from PMeOx.[108] PMeOx-s-PEI-b-PTHF-b- PEI-s-PMeOx were made starting from the corresponding PMeOx-b-THF-b-PMeOx however no transfection was observed.[149] A gene transfection PAOx polymer with no PEI is also reported by using PMeOx-P(cationic polyoxazoline)(CPOx). This polymer contained an amine containing positive charge on the side chain. The positive charges make the polymer suitable for gene transfection.[150]

PEG can be coupled to L-PEI to reduce side effects as it will shield the formed polyplexes. PEG-PEI block copolymers were obtained via maleimide NHS coupling combining both end groups.[151] PEI was coupled *via* the terminator end with PEG via an NHS ester or an S-S coupling obtaining a disulphide bridge.[152] Two different polymers containing poly(propylene glycol) (PPG) were synthesised being PEI-b-PPG and PEI-PPG-PEI to see the difference in transfection. The PEI-b-PPG showed efficient plasmid DNA transfection, however no siRNA delivery. The PEI-PPG-PEI behave opposite because of the micelle which is formed.[153] PEI-was also coupled with linear cholesterol, T-shaped or the combination of both. The modification was done on the end-group hydroxyl of the PEI and the secondary amine (linear) or hydroxyl or the amine (T-shaped).[154] PEI with an amine group was coupled to an acrylate modified poly(beta-amino ester).[155] A more complicated construct was made by coupling PEG, poly(l-lysine) and PEI in one construct with an antibody. The coupling between the construct of PEI and PEG-Poly(l-lysine) was done via a degradable disulfide bridge obtaining degradable polyplexes.[156] Poly(l-lysine) grafted with poly(2-methyl-2-oxazoline)

was used for DNA delivery with excellent stability in biological medium.[131] The coupling of chitosan and PEI was shown by using the amine to graft PEI on chitosan, it was however not clear whether this was an end-group modification or a backbone modification.[157,158] PEI-Fe(III) complexes help condensing DNA by reducing the positive charge on the backbone and lowering cytotoxicity.[159]

It is clear that PEI is excellent for gene transfection however sufficient for further *in vivo* use due to its toxicity. Finding new chemical modification is difficult as the amount of new variation become rare. It would be good to change the focus of the field towards different application where the cationic charge can be used.

1.8 Post-polymerisation modification of Linear poly(ethylene imine)

The outstanding chemical versatility of L-PEI initiated a new field where L-PEI was chemically modified. The modifications are straightforward as the amine on the L-PEI can act as a nucleophile. Thereby a new range of polymers is synthesised with a multiplicity of interesting properties. There are different modification routes possible such as, coupling with carboxylic acids, nucleophilic substitution, reductive alkylation/amination, ring opening and Michael addition.

PEI modification can be done on the backbone for enhancing the gene transfection while lowering the toxicity. Despite the unique properties of PEI there are still drawbacks, which makes it difficult to apply as a gene transfection vector in biological systems. To bypass cytotoxicity, aggregation and opsonization problems, post-polymerisation modification reaction can be performed.[160]

1.8.1 Amine modification with carboxylic acids

PEI-g-PEG polymers were made via (1-ethyl-3-(3-dimethylaminopropyl)carbodiimide) (EDC) coupling of PEG with a terminal acid on the secondary amine of L-PEI. The resulting polymers were used in nasal delivery.[161] Dextran modified with a carboxylic acid was also coupled to the amine of L-PEI *via* EDC coupling showing better gene transfection than the dextran coupled *via* reductive amination.[162] The preparation of L-PEI containing nucleic acids was possible by the (*N,N'*-dicyclohexylcarbodiimide) (DCC) coupling of 2-carboxyethyl derivate of the nucleic acid.[163]

1.8.2 Nucleophilic substitution

The Schubert group coupled l-glutathione to L-PEI. L-glutathione enables a better crossing of the blood brain barrier. In the reported methodology, the polymer was partially functionalized with *N*-succinimidyl-4-pentenate, introducing a double bond in the side chain (27%). The double bond was then used in a thiol-ene photo addition reaction. L-PEI was also fully modified with side chains containing the double bond and subsequently a partial modification was done with the glutathione amine group.[164] An imidazole functionalized PEI was obtained *via* the reaction of an excess of 4(5)-(hydroxymethyl)imidazole in the presence of a base. The imidazole act as ribonuclease A mimicking RNA.[165] PEI-dexamethasone was formed by reacting PEI with Trauts reagent (2-iminothiolane) forming a more reactive sulfhydryl group as a side chain. The dexamethasone-21-mesylate was coupled with this sulfhydryl group.[166] Different methods are used to alkylate the amine via nucleophilic substitution of the coupling agent, in this case 4(5)-bromo methylimidazole.[167] The reaction between a bromide mesogenic reagent and subsequent quaternization led to the formation of crystalline polymers.[168] A lot of effort was done in preparing alkylated L-PEI. *via* the nucleophilic substitution with benzyl bromide.[169] PEI was grafted with nucleic acids, in a first attempt a propionic derivate of the nucleic acid was used in a DCC coupling, which was unsuccessful. By using an activated *p*-nitrophenyl ester the reaction was faster due to the better leaving group. A similar coupling was done with nucleic acid containing an acid chloride or bromine containing adenine or thymine.[170–173]

For the synthesis of chelating polymers a styrene-PEI copolymer was carboxylated by using mono chloroacetic acid.[112] With a similar system the mercapto-ethylation was done by the introduction of ethylene sulfide and carbon disulphide.[174] PEI is often used in conducting polymers and was therefore grafted with lithium conductors. The reaction was done with 1,3-propane sulfone.[116]

Hydrogels were made for the capturing of DNA. The PEI was modified with succinimidyl-4-pentenate which reacted with the amine obtaining a polymer with a double bond in the side-chain. The double bond was then used to make hydrogels via thiol-ene chemistry and a diol linker.[54]

A modification of PEI was indirectly shown in industrial gas scrubbers. The amines of PEI are prone to react with CO_2 to form carbamates. It was however shown that these carbamates groups form cyclic urea making the regeneration impossible.[117] This side reaction could be controlled by increasing the gas stream moist.[175]Ferrocene groups were coupled to L-PEI via nucleophilic substitution depending on the required spacer.[176–181]

1.8.3 Reductive Alkylation/amination

One of the first reports on the post polymerisation modification of PEI was reported as the Eschweiler-Clarcke *N*-methylation. In the reaction between an amine and formaldehyde (Scheme 1-5) the methylated PEI is formed.[96,182] More recently Lambermont-Thijs et al described different alkylated products made *via* reductive alkylation.[169]

The amines on the PEI backbone can be modified *via* an oxidation step. The polymers were oxidized with hydroxyl moieties *via* the reaction of the amines with paraformaldehyde (Scheme 1-5), this reaction is an oxidation reaction however when the reaction is pushed an alkylated PEI is obtained. In this article also an epoxide is used to react with the primary alcohol hereby introducing glycidol.[183]

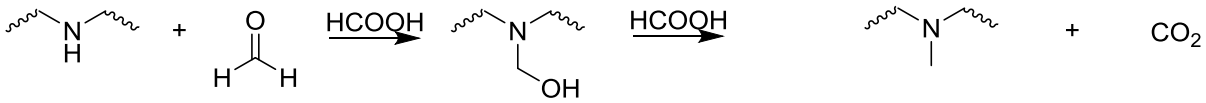

Scheme 1-5 Introduction of formaldehyde on PEI and further reductive alkylation

A similar modification was done by the oxidation of the amine, obtaining PEI-*co*-glycine copolymers. Different oxidizing groups were used obtaining hydroxylamine which is then converted to oxaziridine. Herewith the amide group is located in the backbone giving degradable polymers.[184] The polysaccharide dextran was coupled via reductive amination onto the amines of PEI, but the EDC coupling showed a more efficient gene transfection.[162]

L-PEI was also modified with ferrocene obtaining high current density polymers which can act as anodes in a biosensor. The polymer was cross-linked with a diglycidyl ether. The coupling was done via reductive amination with a ferrocenecarboxyaldehyde.[176–181]

1.8.4 Ring opening epoxide

Alkane modified polymers were made by reacting the amine with an 1,2 epoxydecane.[185] The reaction of PEI with ethylene oxide formed a tertiary amine with an alcohol in the side chain.[87]

1.8.5 Michael addition

PEI-grafted with a methyl ester containing part on the side chain was prepared by Michael addition of methyl methacrylate onto L-PEI. The methacrylate reacted with the amine groups and subsequently, the ester groups could be either amidated or hydrolysed. This approach showed similarities with the

amidation reaction discussed in chapter 6 where methyl ester were formed and used for an amidation reaction[186] In a similar approach the polymer could change its charge by hydrolysing the ester, before hydrolysis the polymer was cationic and afterward it became a partial zwitterion.[187] PEI grafted on polystyrene was used to react with acrylic acid by Michael addition.[112] The coupling of a histidinylated LPEI was achieved by coupling a methacrylate modified histidine.[188]

1.9 Post-polymerisation modification of poly(2-oxazoline)-poly(ethylene imine) copolymers

The copolymers obtained by the partial hydrolysis of PAOx contain the reactive secondary amines with nucleophilic properties. These copolymers can be used in gene transfection however they are valuable precursors in the synthesis of new PAOx copolymers. The use and post-polymerisation modification of copolymers has some great advantages relative to new monomer synthesis. First of all, new monomers have to be synthesised which is a large burden from both synthetic and purification point of view. Often the polymer distribution is not controllable as it can change depending on the reactivity of the monomers and the solubility rate of the new polymers. The introduction of new monomer groups make it difficult to obtain well defined polymers with narrow dispersity. Some groups, especially the nucleophilic groups, need to be protected as they could interfere with the CROP. The polymerisation of EtOx, MeOx and PrOx is highly optimized and these polymers are easily accessible in great quantities, larger MW and low Đ.[189] By submitting these homopolymers to a partial hydrolysis a controlled amount of secondary amino groups can be introduced. This was discussed in the part of the partial hydrolysis of PAOx (chapter 1-6), there is a control of both the amount of PEI and the reaction speed. Difficulties can appear when the reaction is not complete, however this does not occur that often and can prevented by using excess of reagent. Different copolymer of PAOx-PEI are used in a broad range of applications such as hydrogels.

PMeOx-hydrogels were developed by partial hydrolysis followed by the DCC coupling to modify the polymers with an anthracene containing a disulfide bond. A redox and photosensitive gel was formed with a bridged system by coupling of two anthracene moieties (Figure 1-4).[190] The same polymer was also used for the formation of a disulfide containing hydrogel which was formed after reductive gelation, the anthracene was a leaving group to expose the SH groups. The gel formation was induced by the oxidative conditions forming the new S-S bonds out of the SH groups. In the same publication other bifunctional disulfide cross linkers were used: 3,3'dithiodipropanoic acid, the acid chloride of 3,3'dithiodipropanoic

acid and an isocyanate. Due to the presence of the disulfide bridge, reductive conditions such as sodium borohydride or triphenylphosphine were used to degrade the hydrogels and obtain the linear polymers.[191] The same author used the functional group bipyrydyl to modify PAOx, making a thermally and redox reversible hydrogel with either Mn^{2+}, Fe^{2+} or Co^{2+}. The coupling was done *via* the DCC coupling as described before.[192–194] Different types of hydrogels were synthesised by using PMeOx-PEI and react them with hexamethylene diisocyanate or diacid chloride(adipoylchloride) as a cross linker.[100] A hydrogel was also developed by using a coumarin dye which was coupled *via* DCC coupling to the PEI part. The coumarin dye can photo reversibly form a cyclobutane ring with another coumarin dye inducing gelation.[99] From the same authors, hydrogels were reported by the Diels Alder reaction between maleimide modified PMeOx and a furan modified polymer, both were prepared *via* DCC coupling of the reactive moieties onto the L-PEI.[195] Also a DCC coupling onto carbon nanotubes containing carboxylic acids was shown with PMeOx-PEI.[196]

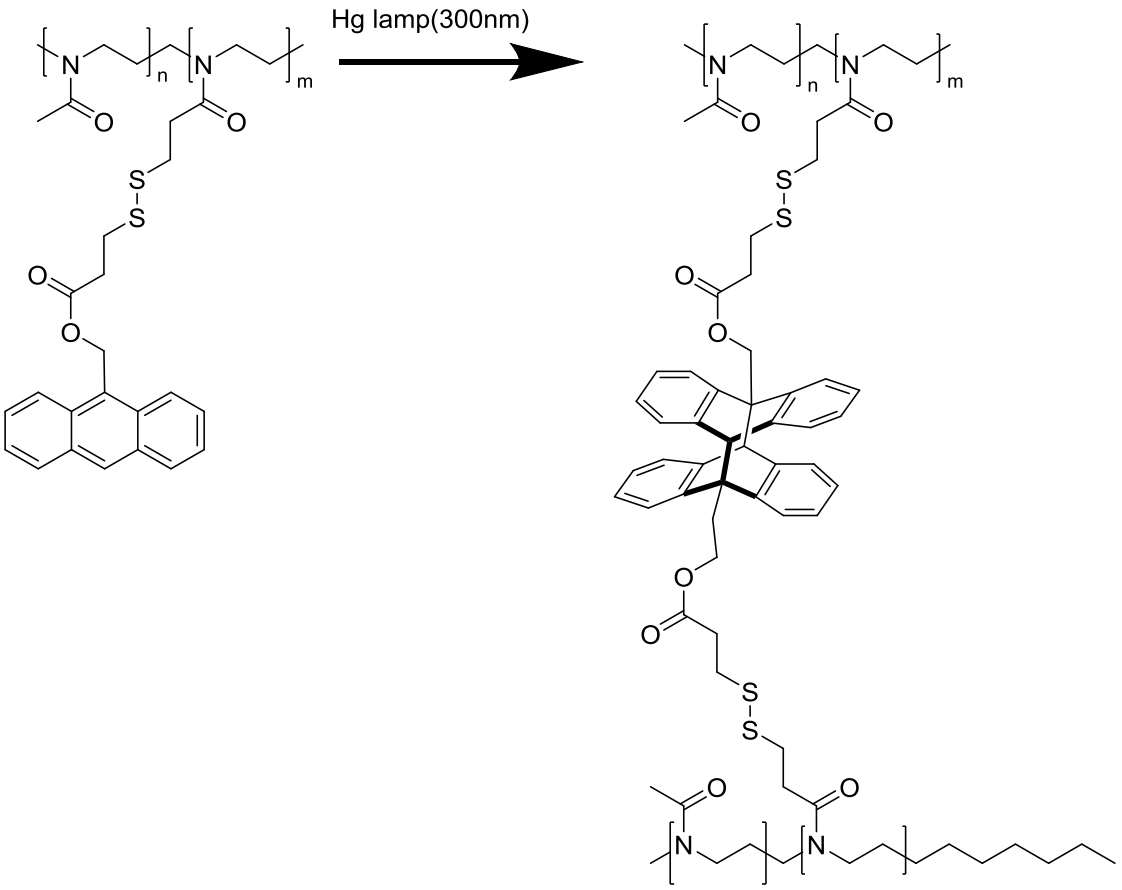

Figure 1-4 Post-polymerisation modification of PMeOx forming an anthracene bridged system

Similar as with PEI homopolymer the amine on the backbone can be used as reactant for coupling of nucleotides for example *via* a DCC coupling of thymine propionic acid.[171] For the synthesis of fluorescent PAOx, pyrene was coupled to both PMeOx and PEtOx. The pyrene contained a carboxyl functionality which was then coupled *via N,N*-diisopropylcarbodiimide (DIC) coupling. In the same publication also gels were made *via* crosslinking with hexamethylene diisocyanate in the presence of (1,8-diazabicycloundec-7-ene) (DBU).[197] Lecommandoux and coworkers found a method for making hydrogels starting from PEtOx-PEI. The cross linker used was a bisglycidyl ether (1,6 hexanediol diglycidyl ether) with two epoxides. These epoxides are attacked by the amine.[198] A similar approach was used for the formation of a degradable hydrogel by using hydroxyethyl disulfide-bis-di-glycidyl ether. These nanogels showed also a dual character as the addition of an acid protonated the PEI present and induced a swelling while the addition of a reductive agent cleaved the nanogel by breaking the S-S bond.[199]

1.10 Goal of the thesis

The use of polymers in biomedical applications shows a huge potential in improving and developing therapeutic strategies.[3,200,201] Three classes of polymers can be distinguished based on size; a macroscopic class, microscopic class and a nanosized class.[2] The polymer itself plays a different role depending on the size. The macroscopic class contains implantable medical devices, artificial organs, prostheses, applications for dentistry, bone repair or hydrogels[202] either as the object itself or as coating[203] against the immune system.[6,204] The micro class includes micro particles, implants for slow release[205] and microgels.[46,206,207] In the nano class, drug delivery plays an important role and polymers can be used as polymer therapeutics. In this class the polymer acts as a vehicle for the drug/active compound making it invisible to the body or improving its solubility in water.[3,21,208] The nano class is highlighted in this thesis as PAOx is mainly involved in this class of polymer therapeutics including polymer-drug conjugates, polymeric micelles and polymer-protein conjugates (Figure 1-1 and Figure 1-3) PEI, that originates from PAOx, plays and important role in gene transfer as it can form polyplexes with genetic material.

The polymer materials used need to be biocompatible, suppress nonspecific protein adsorption and not induce an inflammatory response.[209,210] The stealth behaviour, *i.e* being unrecognized by the immune system, is important as it increases the bioavailability of the bioactive compound and reduces the side effects. This stealth behavior is allied with the specific protein adsorption, which guarantees no immunological responses. The choice of polymers is therefore of vast importance as this affects the properties of the conjugate. PAOx (co)polymers show a great potential in the field of polymer therapeutics as they show stealth effect and are biocompatible, which is similar to PEG while the synthetic and structural versatility of PAOx is much higher.

Next to the biological properties, the biomedical polymers give the possibility for chemical modification. The polymer can act as a platform for the coupling of bioactive molecules, ranging from proteins, drugs, nucleic acids and imaging agents. PAOx was chosen in this doctorate because this class of polymers shows a large chemical modification potential and versatility in potentially coupled groups, including great orthogonality. The PAOx polymers can be modified *via* three different pathways. The first method utilises the end groups to introduce functionalities, both at the initiation and termination side. The second method utilise the polymerisation to introduce functional groups by copolymerisation with functional or alkyl monomers. In the last modification method a post polymerisation modification is possible herewith modifying the side chains of the polymer, the end group or doing a hydrolysis of the side chain. During the hydrolysis amines are introduced on the backbone which can further be modified via numerous reactions. The hydrolysis can either be complete yielding L-PEI or can be partially to obtain the PAOx-PEI. Even though the end group modification and synthesis of new monomers is important however the

focus of this work lays on post polymerisation modification and hydrolysis of PAOx into L-PEI or PAOx-PEI copolymers.

The synthesis of L-PEI is based on either an acid or basic hydrolysis to cleave of the side chain of the PAOx releasing the carboxylic acid. The basic hydrolysis of PAOx is not straightforward as it degrades the backbone partially, therefore the acid hydrolysis was chosen as preferred method.[91,98,195] Next to the full hydrolysis of PAOx the partial hydrolysis of PAOx can be of vast importance for the field. The new polymer obtained after hydrolysis contains two major parts, the first parts still contains the original PAOx with all of its interesting biological properties, the second part is the amine part. This can be used as a gene transfection agent or as a chemical modification platform. Indeed the amines in the PEI units can act as a nucleophile to react with all kinds of chemical functionalities ranging from epoxides, acid chlorides, carboxylic acids, *etc*. Using the hydrolysis approach to introduce functionalities has great benefits relative to a polymerisation approach. First of all the synthesis of the starting PAOx polymers, often PEtOx and PMeOx, is optimized and polymers with narrow Đ and high molecular weight can be found commercially.[189] The multiple purification steps and the need of water free environments makes it hard to introduce the polymerisation of new oxazoline monomers into non specialized labs. This disadvantage is overcome by the straightforward coupling onto the secondary amine of PAOx-PEI. Therefore we further investigated the potential of the PAOx-PEI platform, especially the PEtOx-PEI platform. We focused on the introduction of bioactive functionalities which can then be used in a biomedical context.

To explore the PEtOx-PEI platform, a detailed understanding of the systems is needed. The mechanism and kinetics of the acid hydrolysis were investigated in many occasions,[91,102,103,109] although the copolymer distribution along the chain was never thoroughly investigated. Therefore, in chapter 2 a detailed investigation is reported to unravel the distribution of PEI-units in PAOx-PEI copolymers. This distribution could be randomly or block like and is important as its influences the composition of the new copolymer and its further reactivity. Answering this question will give valuable information for further chemical modification and gene transfection properties. The use of titration would introduce difficulties for unambiguous interpretation and thus a thorough examination via NMR spectroscopy was performed.

Polymers such as PMeOx, PEtOx, and PPhOx are often used in hydrolysis experiments but no description was given for the hydrolysis of PPrOx. The hydrolysis of PPrOx was explored in chapter 3. This polymer is no first choice as it has a Tcp around 25°C. Above this temperature the polymer becomes insoluble and crashes out of solution, which may influence the hydrolysis rate at elevated temperatures. However if the hydrolysis could be successful the introduction of the amine units along the chain could influence the resulting Tcp. The use of viral vectors for gene transfection is still superiorly compared to non-viral gene vectors. Therefore there is a constant search for better non-viral systems. The introduction of PEI units makes it possible for the PPrOx-PEI polymers to interact with DNA to form polyplexes, which will also be discussed in chapter 3.

By fully understanding the copolymer distribution, the chemical toolbox of PEtOx-PEI can be expanded. In chapter 4 carbamates are formed by using the well-known reaction between an amine and CO_2. This reaction forms zwitterionic carbamates with fluorescent properties due to the presence of the lowest unoccupied molecular orbital (LUMO) and highest occupied molecular orbital (HOMO) in proximity on the carbamate. Earlier reports already showed that the b-PEI and CO_2 can react. However the b-PEI has the higher reactive primary amines.[211] Prior, the reaction of L-PEI and CO_2 was explored in the context of gas scrubbers. Exploring this reaction further for making fluorescent PAOx or L-PEI is of great interest as this potentially could expand the toolbox and only a few fluorescent PAOx derivates are known none of which have intrinsic fluorescence.

As mentioned before PAOx could play an important role for polymer therapeutics. The coupling of a bioactive compound onto the polymer is often performed by using "click chemistry". The development of new methods to couple the bioactive molecules onto a platform has to be explored and one of these methods is shown in chapter 5. To ensure a large versatility, four different linkers where chosen to link the polymer and the bioactive molecule. The linker carries on the one hand a part which can react with the amine and on the other hand a methyl ester. This methyl ester is a latent functionality and coupling of the bioactive linker onto the platform can be performed *via* an amidation reaction between the methyl ester and an amine present on the molecule. However the reaction needs to be optimized first and therefore different kind of amines where chosen to react with the ester to form various amides.

In chapter 6 a further expansion of the toolbox is demonstrated for the coupling of carbohydrates. It is needless to say that carbohydrates play a crucial role in all kind of different biological processes and signaling pathways and are thus crucial part of a living organism. Therefore a method was developed which was already successful on b-PEI, the reductive amination. This amination uses the aldehyde on the ring opened version of the carbohydrate to couple to the amine. The reaction is developed for simple carbohydrates such as maltose and glucose. The biological properties and solution behavior are examined and discussed.

1.11 References

(1) Wang, Y.-X.; Robertson, J. L.; Spillman, W. B.; Claus, R. O. *Pharm. Res.* **2004**, *21* (8), 1362.

(2) Duncan, R. *Nat. Rev. Drug Discov.* **2003**, *2* (5), 347.

(3) Duncan, R.; Vicent, M. J. *Adv. Drug Deliv. Rev.* **2013**, *65* (1), 60.

(4) Barz, M.; Luxenhofer, R.; Zentel, R.; Vicent, M. J. *Polym. Chem.* **2011**, *2* (9), 1900.

(5) Qi, Y.; Chilkoti, A. *Curr. Opin. Chem. Biol.* **2015**, *28*, 181.

(6) Merkle, H. P. *Eur. J. Pharm. Biopharm.* **2015**, *97*, 293.

(7) Kwoh, D. Y.; Coffin, C. C.; Lollo, C. P.; Jovenal, J.; Banaszczyk, M. G.; Mullen, P.; Phillips, A.; Amini, A.; Fabrycki, J.; Bartholomew, R. M.; Brostoff, S. W.; Carlo, D. J. *Biochim. Biophys. Acta* **1999**, *1444* (2), 171.

(8) Konradi, R.; Pidhatika, B.; Mühlebach, A.; Textor, M. *Langmuir* **2008**, *24* (3), 613.

(9) Singer, J. W.; Baker, B.; De Vries, P.; Kumar, A.; Shaffer, S.; Vawter, E.; Bolton, M.; Garzone, P. *Adv. Exp. Med. Biol.* **2003**, *519* (L), 81.

(10) Duncan, R. *Nat. Rev. Cancer* **2006**, *6* (9), 688.

(11) Weeratunga, G.; Horne, S. WO2004043995A2, 2004.

(12) Plone, M. A.; Petersen, J. S.; Rosenbaum, D. P.; Burke, S. K. *Clin. Pharmacokinet* **2002**, *41* (7), 517.

(13) Maeda, H.; Ueda, M.; Morinaga, T.; Matsumoto, T. *J. Med. Chem.* **1985**, *28*, 455.

(14) Goel, N.; Stephens, S. *Landes Biosci.* **2014**, *2* (2), 137.

(15) Nowotnik, D. P.; Cvitkovic, E. *Adv. Drug Deliv. Rev.* **2009**, *61* (13), 1214.

(16) Yurkovetskiy, A. V.; Fram, R. J. *Adv. Drug Deliv. Rev.* **2009**, *61* (13), 1193.

(17) Verbraeken, B. K. H. R. In *Encyclopedia of Polymer Science and Technology*; 2014; pp 1–39.

(18) He, Z.; Wan, X.; Schulz, A.; Bludau, H.; Dobrovolskaia, M. A.; Stern, S. T.; Montgomery, S. A.; Yuan, H.; Li, Z.; Alakhova, D.; Sokolsky, M.; Darr, D. B.; Perou, C. M.; Jordan, R.; Luxenhofer, R.; Kabanov, A. V. *Biomaterials* **2016**, *101*, 296.

(19) Koshkina, O.; Lang, T.; Thiermann, R.; Docter, D.; Stauber, R. H.; Secker, C.; Schlaad, H.; Weidner, S.; Mohr, B.; Maskos, M.; Bertin, A. *Langmuir* **2015**, *31* (32), 8873.

(20) Bailon, P.; Won, C. *Expert Opin. Drug Deliv.* **2009**, *6*, 1.

(21) Duncan, R.; Gaspar, R. *Mol. Pharm.* **2011**, *8* (6), 2101.

(22) Schöttler, S.; Becker, G.; Winzen, S.; Steinbach, T.; Mohr, K.; Landfester, K.; Mailänder, V.; Wurm, F. R. *Nat. Nanotechnol.* **2016**, *11* (February), 1.

(23) Armstrong, J. K.; Hempel, G.; Koling, S.; Chan, L. S.; Fisher, T.; Meiselman, H. J.; Garratty, G. *Cancer* **2007**, *110* (1), 103.

(24) Pasut, G.; Veronese, F. M. *Adv. Drug Deliv. Rev.* **2009**, *61* (13), 1177.

(25) Koshkina, O.; Westmeier, D.; Lang, T.; Bantz, C.; Hahlbrock, A.; Würth, C.; Resch-Genger, U.; Braun, U.; Thiermann, R.; Weise, C.; Eravci, M.; Mohr, B.; Schlaad, H.; Stauber, R. H.; Docter, D.; Bertin, A.; Maskos, M. *Macromol. Biosci.* **2016**, No. 16, 1287.

(26) Luxenhofer, R.; Han, Y.; Schulz, A.; Tong, J.; He, Z.; Kabanov, A. V; Jordan, R. *Macromol. Rapid Commun.* **2012**, *33*, 1613.

(27) Luxenhofer, R.; Han, Y.; Schulz, A.; Tong, J.; He, Z.; Kabanov, A. V; Jordan, R. *Macromol. Rapid Commun.* **2012**, *33* (19), 1613.

(28) Luxenhofer, R.; Sahay, G.; Schulz, A.; Alakhova, D.; Bronich, T. K.; Jordan, R.; Kabanov, A. V. *J. Control. Release* **2011**, *153* (1), 73.

(29) Mero, A.; Fang, Z.; Pasut, G.; Veronese, F. M.; Viegas, T. X. *J. Control. Release* **2012**, *159* (3), 353.

(30) Tauhardt, L.; Pretzel, D.; Kempe, K.; Gottschaldt, M.; Pohlers, D.; Schubert, U. S. *Polym. Chem.*

2014, *5* (19), 5751.

(31) Mansfield, E. D. H.; Sillence, K.; Hole, P.; Williams, A. C.; Khutoryanskiy, V. V. *Nanoscale* **2015**, *7* (32), 13671.

(32) Bludau, H.; Czapar, A. E.; Pitek, A. S.; Shukla, S.; Jordan, R.; Steinmetz, N. F. *Eur. Polym. J.* **2016**, 1.

(33) Xili, T.; District, D.; District, H. *Chem. Pharm. Bull. Adv. Publ.* **2013**.

(34) Naka, K.; Nakamura, T.; Ohki, A.; Maeda, S. *Macromol. Chem. Phys.* **1997**, *198* (1), 101.

(35) Donev, R.; Koseva, N.; Petrov, P.; Kowalczuk, A.; Thome, J. *World J. Biol. Psychiatry* **2011**, *12* (S1), 44.

(36) Zhang, N.; Pompe, T.; Amin, I.; Luxenhofer, R.; Werner, C.; Jordan, R. *Macromol. Biosci.* **2012**, *12* (7), 926.

(37) Dworak, A.; Utrata-Wesołek, A.; Oleszko, N.; Wałach, W.; Trzebicka, B.; Anioł, J.; Sieroń, A. L.; Klama-Baryła, A.; Kawecki, M. *J. Mater. Sci. Mater. Med.* **2014**, *25* (4), 1149.

(38) Wang, H.; Li, L.; Tong, Q.; Yan, M. *ACS Appl. Mater. Interfaces* **2011**, *3* (9), 3463.

(39) Pidhatika, B.; Rodenstein, M.; Chen, Y.; Rakhmatullina, E.; Mühlebach, A.; Acikgöz, C.; Textor, M.; Konradi, R. *Biointerphases* **2012**, *7* (1–4).

(40) Zalipsky, S.; Hansen, C. B.; Oaks, J. M.; Allen, T. M. *J. Pharm. Sci.* **1996**, *85* (2), 133.

(41) Waschinski, C. J.; Tiller, J. C. *Biomacromolecules* **2005**, *6* (1), 235.

(42) Correia, V. G.; Bonifácio, V. D. B.; Raje, V. P.; Casimiro, T.; Moutinho, G.; da Silva, C. L.; Pinho, M. G.; Aguiar-Ricardo, A. *Macromol. Biosci.* **2011**, *11* (8), 1128.

(43) Gonzalez-Perez, A.; Feld, K.; Ruso, J. M. *J. Polym. Res.* **2016**, *23* (9), 1.

(44) Bender, J.; Boerman, M. a. TISSUE-ADHESIVE POROUS HAEMOSTATIC, 2016.

(45) Mees, M. A.; Hoogenboom, R. *Macromolecules* **2015**, *48* (11), 3531.

(46) Kelly, A. M.; Wiesbrock, F. *Macromol. Rapid Commun.* **2012**, *33* (19), 1632.

(47) Hartlieb, M.; Kempe, K.; Schubert, U. S. *J. Mater. Chem. B* **2015**, *3* (4), 526.

(48) Dargaville, T. R.; Hollier, B. G.; Shokoohmand, A.; Hoogenboom, R. *Cell Adhes. Migr.* **2014**, *8* (2), 88.

(49) Farrugia, B. L.; Kempe, K.; Schubert, U. S.; Hoogenboom, R.; Dargaville, T. R. *Biomacromolecules* **2013**, *14* (8), 2724.

(50) Wang, X.; Li, X.; Li, Y.; Zhou, Y.; Fan, C.; Li, W.; Ma, S.; Fan, Y.; Huang, Y.; Li, N.; Liu, Y. *Acta Biomater.* **2011**, *7* (12), 4149.

(51) Wang, C. H.; Hwang, Y. S.; Chiang, P. R.; Shen, C. R.; Hong, W. H.; Hsiue, G. H. *Biomacromolecules* **2012**, *13* (1), 40.

(52) Kostova, B.; Ivanova-Mileva, K.; Rachev, D.; Christova, D. *AAPS PharmSciTech* **2013**, *14* (1), 352.

(53) El-Hag Ali, A.; AlArifi, A. S. *J. Appl. Polym. Sci.* **2011**, *120*, 3071.

(54) Hartlieb, M.; Pretzel, D.; Englert, C.; Hentschel, M.; Kempe, K.; Gottschaldt, M.; Schubert, U. S. *Biomacromolecules* **2014**, *15* (6), 1970.

(55) Lück, S.; Schubel, R.; Rüb, J.; Hahn, D.; Mathieu, E.; Zimmermann, H.; Scharnweber, D.; Werner, C.; Pautot, S.; Jordan, R. *Biomaterials* **2016**, *79*, 1.

(56) Eskow Jaunarajs, K. L.; Standaert, D. G.; Viegas, T. X.; Bentley, M. D.; Fang, Z.; Dizman, B.; Yoon, K.; Weimer, R.; Ravenscroft, P.; Johnston, T. H.; Hill, M. P.; Brotchie, J. M.; Moreadith, R. W. *Mov. Disord.* **2013**, *0* (0), 2.

(57) Tong, J.; Luxenhofer, R.; Yi, X.; Jordan, R. *Mol. Pharm.* **2010**, *7* (5), 984.

(58) Velander, W. H.; Madurawe, R. D.; Subramanian, A.; Kumar, G.; Sinai-Zingde, G.; Riffle, J. S.; Orthner, C. L. *Biotechnol. Bioeng.* **1992**, *39* (1992), 1024.

(59) Manzenrieder, F.; Luxenhofer, R.; Retzlaff, M.; Jordan, R.; Finn, M. G. *Angew. Chemie - Int. Ed.* **2011**, *50* (11), 2601.

(60) Broz, P.; Benito, S. M.; Saw, C. L.; Burger, P.; Heider, H.; Pfisterer, M.; Marsch, S.; Meier, W.; Hunziker, P. *J. Control. Release* **2005**, *102* (2), 475.

(61) Farkaš, P.; Korcová, J.; Kronek, J.; Bystrický, S. *Eur. J. Med. Chem.* **2010**, *45* (2), 795.

(62) Broz, P.; Ben-Haim, N.; Grzelakowski, M.; Marsch, S.; Meier, W.; Hunziker, P. *J. Cardiovasc. Pharmacol.* **2008**, *51* (3), 246.

(63) Viegas, T. X.; Bentley, M. D.; Harris, J. M.; Fang, Z.; Yoon, K.; Dizman, B.; Weimer, R.; Mero, A.; Pasut, G.; Veronese, F. M. *Bioconjug. Chem.* **2011**, *22* (5), 976.

(64) Li, J.; Zhou, Y.; Li, C.; Wang, D.; Gao, Y.; Zhang, C.; Zhao, L.; Li, Y.; Liu, Y.; Li, X. *Bioconjug. Chem.* **2015**, *26* (1), 110.

(65) Yi, X.; Kabanov, A. V. *J. Drug Target.* **2013**, *21* (10), 940.

(66) Schulz, A.; Jaksch, S.; Schubel, R.; Wegener, E.; Di, Z.; Han, Y.; Meister, A.; Kabanov, A. V; Luxenhofer, R.; Papadakis, X. C. M.; Jordan, R. *ACS Nano* **2014**, *8* (3), 2686.

(67) Seo, Y.; Schulz, A.; Han, Y.; He, Z.; Bludau, H.; Wan, X.; Tong, J.; Bronich, T. K.; Sokolsky, M.; Luxenhofer, R.; Jordan, R.; Kabanov, A. V. *Polym. Adv. Technol.* **2015**, *26* (7), 837.

(68) Luxenhofer, R.; Schulz, A.; Roques, C.; Li, S.; Bronich, T. K.; Batrakova, E. V.; Jordan, R.; Kabanov, A. V. *Biomaterials* **2010**, *31* (18), 4972.

(69) Han, Y.; He, Z.; Schulz, A.; Bronich, T. K.; Jordan, R.; Luxenhofer, R.; Kabanov, A. V. *Mol. Pharm.* **2012**, *9* (8), 2302.

(70) Schulz, A.; Han, Y.; He, Z.; Bronich, T. K.; Kabanov, A. V.; Luxenhofer, R.; Jordan, R. *Polym. Prepr.* **2012**, *53* (1), 305.

(71) Yan, L.; Qiu, L. *Nanomedicine* **2015**, *10*, 361.

(72) Knop, K.; Pretzel, D.; Urbanek, A.; Rudolph, T.; Scharf, D. H.; Schallon, A.; Wagner, M.; Schubert, S.; Kiehntopf, M.; Brakhage, A. A.; Schacher, F. H.; Schubert, U. S. *Biomacromolecules* **2013**, *14* (8), 2536.

(73) Wang, C. H.; Wang, C. H.; Hsiue, G. H. *J. Control. Release* **2005**, *108* (1), 140.

(74) Hsiue, G. H.; Wang, C. H.; Lo, C. L.; Wang, C. H.; Li, J. P.; Yang, J. L. *Int. J. Pharm.* **2006**, *317* (1), 69.

(75) Lee, S. C.; Kim, C.; Kwon, I. C.; Chung, H.; Jeong, S. Y. *J. Control. Release* **2003**, *89* (3), 437.

(76) Guillerm, B.; Darcos, V.; Lapinte, V.; Monge, S.; Coudane, J.; Robin, J.-J. *Chem. Commun. (Camb).* **2012**, *48* (23), 2879.

(77) Kempe, K.; Vollrath, A.; Schaefer, H. W.; Poehlmann, T. G.; Biskup, C.; Hoogenboom, R.; Hornig, S.; Schubert, U. S. *Macromol. Rapid Commun.* **2010**, *31* (21), 1869.

(78) Kagiya, T.; Maeda, T.; Fukui, K.; Narisawa, S. *Polym. Lett.* **1966**, *4*, 441.

(79) Seeliger, W.; Aufderhaar, E.; Diepers, W.; Feinauer, R.; Nehring, R.; Thier, W.; Hellmann, H. *Angew. Chem. Int. Ed. Engl.* **1966**, *5* (10), 875.

(80) Tomalia, D. a; Sheetz, D. P. *J. Polym. Sci. Part A-1 Polym. Chem.* **1966**, *4* (9), 2253.

(81) Levy, A.; Litt, M. *Polym. Lett.* **1967**, *5*, 881.

(82) Lee, M. S.; Kim, M. G.; Jang, Y. L.; Lee, K.; Kim, T. G.; Kim, S. H.; Park, T. G.; Kim, H. T.; Jeong, J. H. *Macromol. Res.* **2011**, *19* (7), 688.

(83) Kobayashi, S. *Prog. Polym. Sci.* **1990**, *15* (5), 751.

(84) Kobayashi, S.; Hiroishi, K.; Tokunoh, M.; Saegusa, T. *Macromolecules* **1987**, *20*, 1496.

(85) Mannschott, C.; Hockera, H.; Kern, W. *Makromoleculair Chem.* **1981**, *1350*, 1337.

(86) Munir, A.; Goethals, E. J. *Journa Polym. Sci.* **1994**, *19* (1981), 1985.

(87) Kern, W.; Mannschott, C.; H, H. *Makromoleculair Chem.* **1982**, *183*, 1413.

(88) Weyts, K. R.; Goethals, E. J. *Polym. Bull.* **1988**, *19*, 13.

(89) Weyts, K.; Goethals, E. *Die Makromol. Chemie, Rapid Commun.* **1989**, *10*, 299.

(90) Lee, H.; Son, S. H.; Sharma, R.; Won, Y.; Ei-r-eoz, P. P.; Lee, H.; Son, S. H.; Sharma, R.; Won, Y. *J.*

Phys. Chem. B **2011**, *115*, 844.
(91) Kem, K. M. *J. Polym. Sci. Polym. Chem. Ed.* **1979**, *17*, 1977.
(92) Herlem, G.; Lakard, B. *J. Chem. Phys.* **2004**, *120* (19), 9376.
(93) Ziebarth, J. D.; Wang, Y. *Biomacromolecules* **2010**, *11* (1), 29.
(94) Smits, R. G.; Koper, G. J. M.; Mandel, M. *J. Phys. Chem.* **1993**, *97* (21), 5745.
(95) Saegusa, T.; Fujii, H.; Ikeda, H. *Macromolecules* **1972**, *37* (1), 108.
(96) Tanaka, R.; Ueoka, I.; Takaki, Y.; Kataoka, K.; Saito, S. *Macromolecules* **1983**, *16* (2), 849.
(97) Monnery, B. D.; Shaunak, S.; Thanou, M.; Steinke, J. H. G. *Macromolecules* **2015**, *48* (10), 3197.
(98) Saegusa, T.; Kobayashi, S.; Yamada, A. *Macromolecules* **1975**, *8* (4), 390.
(99) Chujo, Y.; Sada, K.; Saegusa, T. *Macromolecules* **1990**, *23* (10), 2693.
(100) Chujo, Y.; Yutaka, Y.; Sada, K.; Saegusa, T. *Macromolecules* **1989**, *22* (3), 1074.
(101) Lambermont-Thijs, H. M. L.; Heuts, J. P. A.; Hoeppener, S.; Hoogenboom, R.; Schubert, U. S. *Polym. Chem.* **2011**, *2* (2), 313.
(102) de la Rosa, V. R.; Bauwens, E.; Monnery, B. D.; De Geest, B. G.; Hoogenboom, R. *Polym. Chem.* **2014**, *5*, 4957.
(103) Van Kuringen, H. P. C.; Lenoir, J.; Adriaens, E.; Bender, J.; De Geest, B. G.; Hoogenboom, R. *Macromol. Biosci.* **2012**, *12* (8), 1114.
(104) Mees, M.; Haladjova, E.; Momekova, D.; Momekov, G.; Shestakova, P. S.; Tsvetanov, C. B.; Hoogenboom, R.; Rangelov, S. *Biomacromolecules* **2016**, *17* (11), 3580.
(105) Lambermont-Thijs, H. M. L.; van der Woerdt, F. S.; Baumgaertel, A.; Bonami, L.; Du Prez, F. E.; Schubert, U. S.; Hoogenboom, R. *Macromolecules* **2010**, *43* (2), 927.
(106) Litt, M. H.; Lin, C. S. *J. Polym. Sci. Part A-1 Polym. Chem.* **1992**, *30*, 779.
(107) Jeong, J. H.; Song, S. H.; Lim, D. W.; Lee, H.; Park, T. G. *J. Control. release* **2001**, *73* (2–3), 391.
(108) Vlassi, E.; Pispas, S. *Macromol. Chem. Phys.* **2015**, *216*, 873.
(109) Van Kuringen, H. P. C.; De La Rosa, V. R.; Fijten, M. W. M.; Heuts, J. P. A.; Hoogenboom, R. *Macromol. Rapid Commun.* **2012**, *33* (9), 827.
(110) Jin, R. H. *ChemPhysChem* **2003**, *4* (10), 1118.
(111) von Zelewsky, A.; Barbosa, L.; Schläpfer, C. W. *Coord. Chem. Rev.* **1993**, *123*, 229.
(112) Saegusa, T.; Kobayashi, S.; Yamada, A. *J. Appl. Polym. Sci.* **1977**, *21*, 2481.
(113) Lazaro-Martinez, J. M.; Rodriguez-Castellon, E.; Vega, D.; Monti, G. A.; Chattah, A. K. *Macromolecules* **2015**, *48* (4), 1115.
(114) Harris, C. S.; Ratner, M. A.; Shriver, D. F. *Macromolecules* **1987**, *20* (17), 1778.
(115) Llanos, J.; Camarillo, R.; Pérez, A.; Canizares, P. *Sep. Purif. Technol.* **2010**, *73* (2), 126.
(116) Doyle, R. P.; Chen, X.; Macrae, M.; Srungavarapu, A.; Smith, L. J.; Gopinadhan, M.; Osuji, C. O.; Granados-Focil, S. *Macromolecules* **2014**, *47* (10), 3401.
(117) Sayari, A.; Heydari-Gorji, A.; Yang, Y. *J. Am. Chem. Soc.* **2012**, *134* (33), 13834.
(118) Tang, Q.; Cheng, F.; Lou, X.-L.; Liu, H.-J.; Chen, Y. *J. Colloid Interface Sci.* **2009**, *337* (2), 485.
(119) Yang, Z.; Coutinho, D. H.; Yang, D. J.; Balkus, K. J.; Ferraris, J. P. *J. Memb. Sci.* **2008**, *313* (1–2), 91.
(120) Bradbury, R.; Penfold, J.; Thomas, R. K.; Tucker, I. M.; Petkov, J. T.; Jones, C. *J. Colloid Interface Sci.* **2016**, *466*, 220.
(121) Mulligan, R. C. *Science (80-.).* **1993**, *260* (5110), 926.
(122) Won, Y. Y.; Sharma, R.; Konieczny, S. F. *J. Control. Release* **2011**, *152* (2), 326.
(123) Sung, L.-Y.; Chen, C.-L.; Lin, S.-Y.; Li, K.-C.; Yeh, C.-L.; Chen, G.-Y.; Lin, C.-Y.; Hu, Y.-C. *Nat. Protoc.* **2014**, *9*, 1882.
(124) Hacein-Bey-Abina, S.; von Kalle, C.; Schmidt, M.; Mccormack, M. P.; Wulfraat, N.; Lebouch, P.; Lim,

A.; Osborne, C. .; PAwliuk, R.; Morillon, E.; Sorensen, R.; Forster, A.; Fraser, P.; Cohen, J. I.; de Saint Basile, G.; Alexander, I.; Wintergerst, U.; Febrourg, T.; Aurias, A.; Stoppa-Lyonnet, D.; Romana; Radford-Weiss, I.; Gross, F.; Valensi, F.; Delabesse, E.; Macintyre, E.; Sigaux, F.; Soulier, J.; Fischer, A.; Cavazzano-Calvo, M. *Science (80-.).* **2003**, *302* (5644), 415.

(125) Raper, S. E.; Chirmule, N.; Lee, F. S.; Wivel, N. A.; Bagg, A.; Gao, G. P.; Wilson, J. M.; Batshaw, M. L. *Mol. Genet. Metab.* **2003**, *80* (1–2), 148.

(126) Check, E. *Nature* **2002**, *420* (6912), 116.

(127) Merten, O. W.; Gaillet, B. *Biochem. Eng. J.* **2016**, *108*, 98.

(128) Konishi, M.; Kawamoto, K.; Izumikawa, M.; Kuriyama, H.; Yamashita, T. *J. Gene Med.* **2008**, *10* (6), 610.

(129) Meyer, O.; Kirpotin, D.; Hong, K.; Sternberg, B.; Park, J. W.; Woodle, M. C.; Papahadjopoulos, D. *J. Biol. Chem.* **1998**, *273* (25), 15621.

(130) Sato, Y.; Hatakeyama, H.; Sakurai, Y.; Hyodo, M.; Akita, H.; Harashima, H. *J. Control. Release* **2012**, 1.

(131) von Erlach, T.; Zwicker, S.; Pidhatika, B.; Konradi, R.; Textor, M.; Hall, H.; Lühmann, T. *Biomaterials* **2011**, *32* (22), 5291.

(132) Mintzer, M. A.; Simanek, E. E. *Chem. Rev.* **2009**, *109* (2), 259.

(133) Chen, Y.; Zhou, L.; Pang, Y.; Huang, W.; Qiu, F.; Jiang, X.; Zhu, X.; Yan, D.; Chen, Q. *Bioconjug. Chem.* **2011**, *22* (6), 1162.

(134) Lai, W.-F. *Biomaterials* **2013**, *35* (1), 401.

(135) Forrest, M. L.; Gabrielson, N.; Pack, D. W. *Biotechnol. Bioeng.* **2005**, *89* (4), 416.

(136) Yue, Y.; Wu, C. *Biomater. Sci.* **2013**, 152.

(137) Rinkenauer, A. C.; Vollrath, A.; Schallon, A.; Tauhardt, L.; Kempe, K.; Schubert, S.; Fischer, D.; Schubert, U. S. *ACS Comb. Sci.* **2013**, *15* (9), 475.

(138) Neuberg, P.; Kichler, A. *Recent developments in nucleic acid delivery with polyethylenimines*; Elsevier, 2014; Vol. 88.

(139) Jäger, M.; Schubert, S.; Ochrimenko, S.; Fischer, D.; Schubert, U. S. *Chem. Soc. Rev.* **2012**, *41* (13), 4755.

(140) Ferrari, S.; Moro, E.; Pettenazzo, A.; Behr, J. P.; Zacchello, F.; Scarpa, M. *Gene Ther.* **1997**, *4* (10), 1100.

(141) Coll, J. L.; Chollet, P.; Brambilla, E.; Desplanques, D.; Behr, J. P.; Favrot, M. *Hum. Gene Ther.* **1999**, *10* (10), 1659.

(142) Boussif, O.; Lezoualc'h, F.; Zanta, M. A.; Mergny, M. D.; Scherman, D.; Demeneix, B.; Behr, J. P. *Proc. Natl. Acad. Sci. U. S. A.* **1995**, *92* (16), 7297.

(143) Chollet, P.; Favrot, M. C.; Hurbin, A.; Coll, J. L. *J. Gene Med.* **2002**, *4* (1), 84.

(144) Shah, R.; Kronekova, Z.; Zahoranová, A.; Roller, L.; Saha, N.; Saha, P.; Kronek, J. *J. Mater. Sci. Mater. Med.* **2015**, *26* (4), 157.

(145) Fernandes, J. C.; Qiu, X.; Winnik, F. M.; Benderdour, M.; Zhang, X.; Dai, K.; Shi, Q. *Int. J. Nanomedicine* **2013**, *8*, 4091.

(146) Lin, C.-P.; Sung, Y.-C.; Hsieu, G.-H. *J. Med. Biol. Eng.* **2012**, *32* (5), 365.

(147) Hsiue, G.-H.; Chiang, H.-Z.; Wang, C.-H.; Juang, T.-M. *Bioconjug. Chem.* **2006**, *17* (3), 781.

(148) Zhang, Y.; Chen, L.; Zhang, C.; Liu, S.; Zhu, H.; Wang, Y. *Talanta* **2016**, *150*, 375.

(149) Rasolonjatovo, B.; Pitard, B.; Guégan, P.; Cheradame, H. *J. Biomater. Nanobiotechnol.* **2014**, *5*, 53.

(150) He, Z.; Miao, L.; Jordan, R.; S-Manickam, D.; Luxenhofer, R.; Kabanov, A. V. *Macromol. Biosci.* **2015**, *15* (7), 1004.

(151) Ogris, M.; Walker, G.; Blessing, T.; Kircheis, R.; Wolschek, M.; Wagner, E. *J. Control. Release* **2003**,

91 (1–2), 173.

(152) Bauhuber, S.; Liebl, R.; Tomasetti, L.; Rachel, R.; Goepferich, A.; Breunig, M. *J. Control. Release* **2012**, *162* (2), 446.

(153) Brissault, B.; Leborgne, C.; Scherman, D.; Guis, C.; Kichler, A. *Macromol. Biosci.* **2011**, *11* (5), 652.

(154) Furgeson, D. Y.; Chan, W. S.; Yockman, J. W.; Kim, S. W. *Bioconjug. Chem.* **2003**, *14* (4), 840.

(155) Zhao, J.; Yang, L.; Huang, P.; Wang, Z. Y.; Tan, Y.; Liu, H.; Pan, J. J.; He, C. Y.; Chen, Z. Y. *J. Colloid Interface Sci.* **2016**, *463*, 93.

(156) Li, J.; Cheng, D.; Yin, T.; Chen, W.; Lin, Y.; Chen, J.; Li, R.; Shuai, X. *Nanoscale* **2014**, *6* (3), 1732.

(157) Lu, H.; Dai, Y.; Lv, L.; Zhao, H. *PLoS One* **2014**, *9* (1).

(158) Jiang, H. L.; Kim, Y. K.; Arote, R.; Nah, J. W.; Cho, M. H.; Choi, Y. J.; Akaike, T.; Cho, C. S. *J. Control. Release* **2007**, *117* (2), 273.

(159) Jorge, A. F.; Morán, M. C.; Vinardell, M. P.; Pereira, J. C.; Dias, R. S.; Pais, A. a. C. C. *Soft Matter* **2013**, *9* (45), 10799.

(160) Pandey, A. P.; Sawant, K. K. *Mater. Sci. Eng. C* **2016**, *68*, 904.

(161) Kichler, A.; Chillon, M.; Leborgne, C.; Danos, O.; Frisch, B. *J. Control. Release* **2002**, *81* (3), 379.

(162) Ochrimenko, S.; Vollrath, A.; Tauhardt, L.; Kempe, K.; Schubert, S.; Schubert, U. S.; Fischer, D. *Carbohydr. Polym.* **2014**, *113*, 597.

(163) Takemoto, K.; Inaki, Y. In *Advances in Polymer Science*; 1981.

(164) Englert, C.; Trützschler, A.-K.; Raasch, M.; Bus, T.; Borchers, P.; Mosig, A. S.; Traeger, A.; Schubert, U. S. *J. Control. Release* **2016**, *241*, 1.

(165) Cheng, L.; Abhilas, K. G.; Breslow, R. *Proc. Natl. Acad. Sci. U. S. A.* **2012**, *109* (32), 12884.

(166) Kim, H.; Bae, Y. M.; Kim, H. A.; Hyun, H.; Yu, G. S.; Choi, J. S.; Lee, M. *J. Cell. Biochem.* **2010**, *110* (3), 743.

(167) Pavlisko, J. A.; Overberger, C. G. *Journa Polym. Sci.* **1981**, *19*, 1621.

(168) Masson, P.; Heinrich, B.; Frère, Y.; Gramain, P. *Macromol. Chem. Phys.* **1994**, *1212*, 1199.

(169) Lambermont-Thijs, H. M. L.; Bonami, L.; Du Prez, F. E.; Hoogenboom, R. *Polym. Chem.* **2010**, *1* (5), 747.

(170) Ludwick, A. G.; Overberger, C. G. *J. Polym. Sci. Polym. Chem. Ed.* **1982**, *20*, 2123.

(171) Ludwick, A. G.; Robinson, K. S.; Mccloud, J. *J. Polym. Sci. Polym. Symp.* **1986**, *74* (1), 55.

(172) Overberger, C. G.; Kikyotani, S. *J. Polym. Sci. Polym. Chem. Ed.* **1983**, *21* (2), 525.

(173) Wada, T.; Inaki, Y.; Takemoto, K. *Polym. J.* **1988**, *20* (1), 1059.

(174) Saegusa, T.; Kobayashi, S.; Yamada, A. *Polym. J.* **1978**, *10* (4), 403.

(175) Sayari, A.; Belmabkhout, Y. *J. Am. Chem. Soc.* **2010**, *132* (18), 6312.

(176) Giffin, G. A.; Castillo, F. Y.; Frech, R.; Glatzhofer, D. T.; Burba, C. M. *Polymer (Guildf).* **2009**, *50* (1), 171.

(177) Glatzhofer, D. T.; Erickson, M. J.; Frech, R.; Yepez, F.; Furneaux, J. E. *Solid State Ionics* **2005**, *176* (39–40), 2861.

(178) Meredith, M. T.; Kao, D.-Y.; Hickey, D.; Schmidtke, D. W.; Glatzhofer, D. T. *J. Electrochem. Soc.* **2011**, *158* (2), B166.

(179) Merchant, S. A.; Iran, T. O.; Meredith, M. T.; Cline, T. C.; Glatzhofer, D. T.; Schmidtke, D. W. *Langmuir* **2009**, *25* (13), 7736.

(180) Merchant, S. A.; Glatzhofer, D. T.; Schmidtke, D. W. *Langmuir* **2007**, *23* (22), 11295.

(181) Merchant, S. A.; Meredith, M. T.; Tran, T. O.; Brunski, D. B.; Johnson, M. B.; Glatzhofer, D. T.; Schmidtke, D. W. *J. Phys. Chem. C* **2010**, *114* (26), 11627.

(182) Fukuda, Y.; Abe, D.; Tanaka, Y.; Uchida, J.; Suzuki, N.; Miyai, T.; Sasanuma, Y. *Polym. J.* **2016**, *48*

(11), 1065.

(183) Englert, C.; Fevre, M.; Wojtecki, R. J.; Cheng, W.; Xu, Q.; Yang, C.; Ke, X.; Hartlieb, M.; Kempe, K.; García, J. M.; Ono, R. J.; Schubert, U. S.; Yang, Y. Y.; Hedrick, J. L. *Polym. Chem.* **2016**, *7* (37), 5862.

(184) Englert, C.; Hartlieb, M.; Bellstedt, P.; Kempe, K.; Yang, C.; Chu, S. K.; Ke, X.; GarcÍa, J. M.; Ono, R. J.; Fevre, M.; Wojtecki, R. J.; Schubert, U. S.; Yang, Y. Y.; Hedrick, J. L. *Macromolecules* **2015**, *48* (20), 7420.

(185) Schroeder, A.; Dahlman, J. E.; Sahay, G.; Love, K. T.; Jiang, S.; Eltoukhy, A. A.; Levins, C. G.; Wang, Y.; Anderson, D. G. *J. Control. Release* **2012**, *160* (2), 172.

(186) Liu, X.; Yang, J. W.; Miller, A. D.; Nack, E. A.; Lynn, D. M. *Macromolecules* **2005**, *38* (19), 7907.

(187) Liu, X.; Yang, J. W.; Lynn, D. M. *Biomacromolecules* **2008**, *9* (7), 2063.

(188) Bertrand, E.; Gonçalves, C.; Billiet, L.; Gomez, J. P.; Pichon, C.; Cheradame, H.; Midoux, P.; Guégan, P. *Chem. Commun. (Camb).* **2011**, *47* (46), 12547.

(189) Hoogenboom, R.; Monnery, B. D. Method for the preparation of uniform, High molar mass cyclic imino ether polymers. WO 2016:008817, 2016.

(190) Chujo, Y.; Sada, K.; Nomura, R.; Naka, A.; Saegusa, T. *Macromolecules* **1993**, *26* (21), 5611.

(191) Chujo, Y.; Sada, K.; Naka, a; Nomura, R.; Saegusa, T. *Macromolecules* **1993**, *26* (5), 883.

(192) Chujo, Y.; Sada, K.; Saegusa, T. *Macromolecules* **1993**, *26* (24), 6320.

(193) Chujo, Y.; Sada, K.; Saegusa, T. *Macromolecules* **1993**, *26* (24), 6315.

(194) Chujo, Y.; Sada, K.; Saegusa, T. *Polym. J.* **1993**, *6*, 599.

(195) Chujo, Y.; Sada, K.; Saegusa, T. *Macromolecules* **1990**, *23*, 2636.

(196) Guo, C.; Zhou, L.; Lv, J. *Polym. Polym. Compos.* **2013**, *21* (7), 449.

(197) Chen, C.-H.; Niko, Y.; Konishi, G. *RSC Adv.* **2016**, *6* (49), 42962.

(198) Legros, C.; Wirotius, A.; Tam, K. C.; Taton, D. *Biomacromolecules* **2014**.

(199) Legros, C.; De Pauw-Gillet, M.-C.; Tam, K. C.; Lecommmandoux, S.; Taton, D. *Polym. Chem.* **2013**, *4* (17), 4801.

(200) Rangelov, S.; Pispas, A. *Polymer and Polymer-Hybrid Nanoparticles: From Synthesis to Biomedical Applications*; 2013.

(201) Bawa, P.; Pillay, V.; Choonara, Y. E.; du Toit, L. C. *Biomed. Mater.* **2009**, *4* (2), 22001.

(202) Navarro, M.; Michiardi, A.; Castaño, O.; Planell, J. A. *J. R. Soc. Interface* **2008**, *5* (27), 1137.

(203) Suwandi, J. S.; Toes, R. E. M.; Nikolic, T.; Roep, B. O. *Wiley, Inter Sci.* **2007**, *33*, 97.

(204) Stevens, M. M.; George, J. H. *Science* **2005**, *310* (November), 1135.

(205) Tayalia, P.; Mooney, D. J. *Adv. Mater.* **2009**, *21* (32–33), 3269.

(206) Miyata, T.; Uragami, T.; Nakamae, K. *Adv. Drug Deliv. Rev.* **2002**, *54* (1), 79.

(207) Van Vlierberghe, S.; Dubruel, P.; Schacht, E. *Biomacromolecules* **2011**, *12* (5), 1387.

(208) Vicent, M. J.; Ringsdorf, H.; Duncan, R. *Adv. Drug Deliv. Rev.* **2009**, *61* (13), 1117.

(209) Chen, H.; Yuan, L.; Song, W.; Wu, Z.; Li, D. *Prog. Polym. Sci.* **2008**, *33* (11), 1059.

(210) Papadimitriou, S. A.; Salinas, Y.; Resmini, M. *Chem. A Eur. J.* **2016**, *22* (11), 3612.

(211) Kanazaki, K.; Sano, K.; Makino, A.; Homma, T.; Ono, M.; Saji, H. *Nat. Sci. Reports* **2016**, *6* (August), 33798.

CHAPTER 1

Chapter 2 : Understanding the partial hydrolysis of poly(2-alkyl-2-oxazolines: Is it random or is it block-like?

Contributors to this chapter:

Prof. José C. Martins, Department of Organic and Macromolecular Chemistry, Ghent University

Dr. Dieter Buyst Department of Organic and Macromolecular Chemistry, Ghent University

Timotee Courtin, Department of Organic and Macromolecular Chemistry, Ghent University

Contributions of the candidate

Synthesis and full characterization of all the polymers

Manuscript submitted

CHAPTER 2

Prologue

The acidic hydrolysis of PAOx is the best known method to obtain L-PEI. The partial hydrolysis of PAOx is also interesting to obtain PAOx-PEI. This copolymer can be used in either gene transfection experiments or as a reaction platform herewith creating new PAOx copolymers. The reaction mechanism for the (partial) hydrolysis of PAOx is described in the introduction. It is, however, unclear what the monomer distribution is along the PAOx-PEI polymer chain. This is of vast importance in the further chapters as this will influence the change in T_{cp} and gene transfection efficiency described in chapter 3. The distribution of different reactive groups along the polymer chain will be important for the post-polymerisation modification procedures as described in chapter 4,5 and 6.

2.1 Introduction

The story of linear poly(ethylene imine) (PEI) and poly(2-alkyl-2-oxazolines) (PAOx) started in 1966.[1–4] The newly discovered PAOx, in this case poly(2-methyl-2-oxazoline) (PMeOx) was hydrolysed under both basic and acidic conditions. The release and corresponding smell of acetic acid after hydrolysis and formation of linear PEI (L-PEI) confirmed that the precursor polymer was indeed PAOx. Like-wise the first post-polymerisation modification reaction of L-PEI was proposed. The hydrolysed L-PEI was reacted with acetic anhydride thereby regenerating the original PMeOx.[1,5] The hydrolysis of PAOx is one of the best methods for obtaining L-PEI[6] next to the ring opening polymerisation of substituted aziridines. [7–11]L-PEI has found applications as a chelating agent for Cu ions[12–14] and other metals[13,14], as charge carrier in electrochemistry [15–17] and as a surfactant in cosmetics.[18–20] However, the most broadly explored application is the use of L-PEI as non-viral gene delivery due to its high positive charge density in the protonated form enabling strong electrostatic interaction with genetic material.[7,21–23] Furthermore the secondary amino groups of L-PEI can also be chemically modified, enhancing the gene transfection efficiency or lowering the cytotoxicity.[7,23–30]

Similarly, copolymers containing L-PEI can be generated through partial hydrolysis of PAOx resulting in PAOx-PEI copolymers that combine the beneficial properties of the parent PAOx, such as low toxicity, non-immunogenic and tuneable physicochemical properties, with those of L-PEI.[23–25,31–35] These partially hydrolysed PAOx-PEI copolymers have been used, e.g., for gene transfection[25,31,35], as a coating material for melamine determination in milk[36] and as a complexation agent for indocyanine green, used as an imaging agent for tumours[37]. The (partial) hydrolysis of PAOx can be performed *via* a hydrolysis reaction

using acidic[33,34,38–42] or basic [1,14,38,39,41,43] conditions. Several PAOx polymers have been used for the hydrolysis namely homo or copolymers of PMeOx[14,38,39,44,45], poly(2-ethyl-2-oxazoline)(PEtOx),[33,34,38] poly(2-propyl-2-oxazoline)(PPrOx)[35] and poly(2-phenyl-2-oxazoline).[1,38–40,46] The acidic hydrolysis is the preferred route as protonation of the formed secondary amino groups keeps the polymer in solution while basic hydrolysis has been reported to lead to partial main chain degradation of the PAOx, which was however not quantified.[38,39] The acidic hydrolysis of PAOx is illustrated in Figure 2-1. The amount of ethylene imine units in partially hydrolysed copolymers can be easily and accurately controlled *via* temperature, time and acid concentration.[33,34,38] The resulting PAOx-PEI copolymers can be utilized as starting materials for further modification reactions with various electrophiles, such as acid chlorides, carboxylic acids (e.g. *via* DCC coupling), isocyanates and alkyl halides.[7] A wide range of functionalities have been introduced into PAOx using such modification reactions of partially hydrolysed PAOx-PEI, including a redox sensitive anthracene group,[45] furan and maleimide polymers for Diels Alder cross linking[47] or methyl ester side chains for further modification with amines through direct amidation.[48] Also bipyrydyl groups have been introduced as a ligand for Co(III) yielding hydrogels upon metal complexation.[49] Likewise hydrogels have been formed by reacting the L-PEI units with bifunctional epoxides as cross linker.[50,51] Moreover, the secondary amines have been used for the introduction of carbohydrates *via* reductive amination.[52]

Despite the numerous studies on the partial acidic hydrolysis of PAOx and the high potential of the resulting polymers for various applications and as reactive platform for making functional PAOx, to date the exact structure of the formed PAOx-PEI is unknown. More specifically, it remains to be established whether hydrolysis of the amide side chains occurs randomly along the PAOx chain or that block-like regions of L-PEI are generated as schematically depicted in Figure 2-1. Insight in the distribution of the L-PEI units is crucial for the use of PAOx-PEI copolymers in gene delivery as the protonation of L-PEI is strongly influenced by neighbouring L-PEI units.[53,54] Furthermore, the distribution of L-PEI units will control the distribution of functional groups upon further reaction, which can significantly alter the properties of such materials, e.g. for cross-linking and hydrogel formation.

Within this work, we took up the challenge to unravel the L-PEI distribution in PAOx-PEI copolymers resulting from partial acidic hydrolysis of PAOx. Therefore, detailed ^{1}H and ^{13}C NMR as well as HMBC and HSQC NMR spectroscopy were performed at high field. Comparative NMR analysis of the parent PEtOx, a partially hydrolysed PEtOx-PEI copolymer and the fully hydrolysed L-PEI was performed enabling us to determine the PEI distribution.

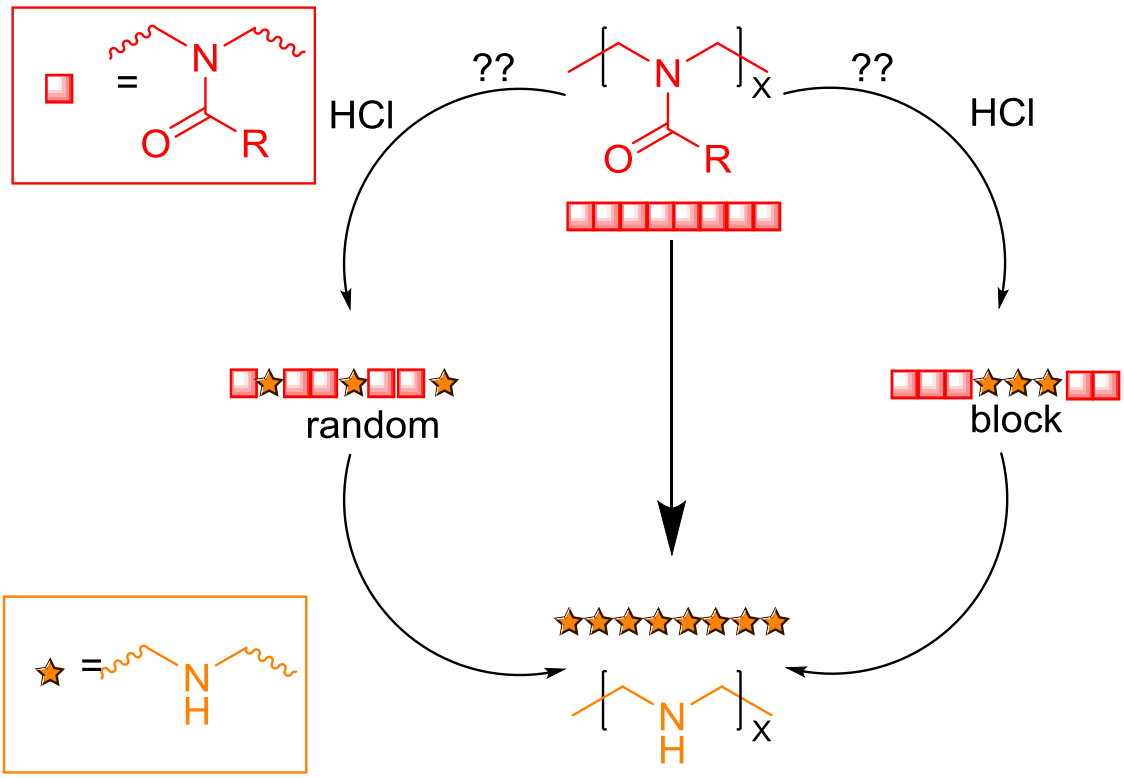

Figure 2-1 Schematic overview of the acidic hydrolysis of PAOx following a random pathway (left) or block-like pathway (right). The red squares represent the amide functionality surrounded by a methylene group on each side and the orange stars represent the amine of the PEI with a methylene group on each side. The formed amines can be protonated in acidic medium. The PEI shown is the free base PEI.

2.2 Materials and methods

2.2.1 Instrumentations

Size exclusion chromatography (SEC) was performed using an Agilent HPLC equipped with a 1260 refractive index detector (RID) a 1,1,1,3,3,3-hexafluoro-2-isopropanol (HFIP) containing 20 mM sodium trifluoroacetate as eluent, which was dried with molecular sieves (3 Å). The flow rate during the measurements was 0.53 mL/min (HFIP-SEC) and polymethylmethacrylate (PMMA) standards were used as standards to calculate the molar mass values. Measurements were performed with a column set consisting of two PSS PFG 300*8Å gel 5 µm MIXED-D columns and a similar guard column (PSS) in series with a molar mass range from 100 - 1 000 000 in a column oven set at 35 °C. Chromatograms were analysed with Agilent Chemstation software using the GPC add-on.

2.2.2 Materials

The synthesis of defined $PEtOx_{400}$ with a degree of polymerisation (DP) of 400 with M_n = 40600 g/mol and Đ = 1.06 has been reported elsewhere.[55] . $PEtOx_{100}$ with a DP of 100 (M_n = 9700 g/mol; Đ = 1.13) was synthesized following a previously reported protocol.[56,57] Poly(2-*n*-propyl-2-oxazoline)s with DP of 75 ($PPrOx_{75}$; M_n 13,000 g/mol, Đ=1.04) was synthesized following the procedure described elsewhere.[20] Hydrogen chloride, sodium hydroxide and dichloromethane (CH_2Cl_2) were obtained from Sigma-Aldrich and used as received. The hydrolysis reactions were performed in a single mode microwave Biotage initiator eight reactor using temperature control based on the IR temperature sensor (Biotage, Uppsala, Sweden). NMR measurements were performed using a Bruker AVANCE II spectrometer operating at 700.13 MHz for ^{1}H and at 176.74 MHz for ^{13}C, except for routine measurements that were performed at 300 MHz using a Bruker AVANCE instrument. All analysis were executed with the Spinworks 4.2 Software.

2.2.3 Procedures

For the detailed NMR study of the partial hydrolysis. 20 mg of polymer was dissolved in 0.6 ml deuterated solvent. Depending on solubility of the polymer an optimum solvent was chosen. $CDCl_3$ for PEtOx and PEtOx-PEI and CD_3OD for the L-PEI. No precipitation was observed in all samples. Other routine measurement samples were prepared by dissolving approximately 10 mg of sample in the deuterated solvent.

Partial hydrolysis of $PEtOx_{400}$ to $PEtOx_{307}$-PEI_{93}

$PEtOx_{400}$ (2 g, DP 400) was dissolved in 7.5 mL of water under stirring. Then, 7.5 mL of a 36 wt% solution of HCl (concentrated HCl) was added and the mixture was heated to 140 °C in the microwave for 40 min. After the hydrolysis reaction, the volatiles were removed on a rotary evaporator. The polymer was basified to pH 10-11 by addition of a 2 M NaOH solution. The solution was then lyophilized and the solid polymer was dissolved in dichloromethane while the formed salts remained in the flask. Next, the organic phase was filtrated and the solvent was removed under reduced pressure to yield a solid white product. The integral ratio between the peaks at 2.56-2.8 ppm (PEI backbone) and 3.15-3.6 ppm (PEtOx backbone) in the ^{1}H-NMR spectrum were used to calculate the degree of hydrolysis revealing 23% hydrolysis.

$PEtOx_{307}$-PEI_{93}: ^{1}H NMR (δ in ppm, $CDCl_3$): δ = 0.9 – 1.25 (m, 3H,CH_2-C<u>H</u>3, 5); 2.1 – 2.50 (m, 2H,CO-C<u>H</u>2-CH_3, 4), 2.56 – 3.0 (m, 4H, NH-C<u>H2,</u> 6); 3.15 – 3.60 (m, 4H,NC<u>H</u>2, 2). ^{13}C NMR (δ in ppm, $CDCl_3$): δ = 9.4 (CH_2-<u>C</u>H3, 5); 25.9 and 26.2 (CO-<u>C</u>H2-CH_3, 4); 43–51 (N-<u>C</u>H2, 6 and 2); 173-175 ppm (N-<u>C</u>=O, 3). SEC: M_n = 33980 g/mol; Đ =1.17.

Full hydrolysis of $PEtOx_{400}$ to PEI_{400}

$PEtOx_{400}$ (2g,DP 400) was dissolved in 7.5 mL of water under stirring. Then, 7.5 mL of a 36 wt% solution of HCl (concentrated HCl) was added and the mixture was heated to 140 °C in the microwave for 3 hr After the hydrolysis, the volatiles were removed on a rotary evaporator. The polymer was basified to pH 10-11 by addition of NaOH pellets and stirring until the polymer was dissolved. After filtration the powder was lyophilized. A white powder was obtained.

^{1}H NMR (δ in ppm, CD_3OD): δ = 2.7-28 (s, 2H, CH_2-NH-C<u>H2</u>,6). ^{13}C NMR (δ in ppm, CD_3OD): δ = 49.7–51 (HN-<u>C</u>H2, 6); SEC: M_n = 41000 g/mol; Đ = 1.07.

Partial hydrolysis of PEtOx (DP = 100, 200 or 400) to PEtOx-PEI with different degrees of hydrolysis. The hydrolysis $PEtOx_{100}$ was performed similar to the previously described partial hydrolysis of $PEtOx_{400}$. However, depending on the sample and desired degree of hydrolysis, either microwave heating, or conventional heating were used. Also different temperature regimes were used (78 °C,100 °C or 140 °C). The work up was similar as described for the partially hydrolysed PEtOx400 for all samples. The integral ratio between the peaks at 2.56-2.8 ppm (PEI backbone) and 3.15-3.6 ppm (PEtOx backbone) in the ^{1}H-NMR spectra were used to calculate the degree of hydrolysis.

$PEtOx_{DP-x}$-PEI_x: ^{1}H NMR (δ in ppm,$CDCl_3$): ^{1}H NMR (δ in ppm, $CDCl_3$): δ = 0.9 – 1.25 (m, 3H, CH_2-C<u>H</u>3, 5); 2.1 – 2.50 (m, 2H, CO-C<u>H</u>2-CH_3, 4), 2.56 – 3.0 (m, 4H, NH-C<u>H2,</u> 6); 3.15 – 3.60 (m, 4H, NC<u>H</u>2, 2). ^{13}C NMR (δ in ppm, $CDCl_3$): δ = 9.4 (CH_2-<u>C</u>H3, 5); 25.9 and 26.2 (CO-<u>C</u>H2-CH_3, 4); 43–51 (N-<u>C</u>H2, 6 and 2); 173-175 ppm (N-<u>C</u>=O, 3).

Partial hydrolysis of $PPrOx_{75}$ to PPrOx-PEI with different degree of hydrolysis

$PPrOx_{75}$ (3 g, DP75) was dissolved in 50 mL of a 6 M HCl solution and subjected to hydrolysis for certain periods of time to obtain the desired degree of hydrolysis according to the kinetic study reported in chapter 3.[35] After the reaction, the solutions were neutralized with NaOH and lyophilized. The copolymers were subsequently extracted with CH_2Cl_2, and after removing the solvent, water was added. A dry powder was obtained after lyophilisation. The integral ratios of the peaks at 2.6-2.8 ppm and 3.2-3.5 ppm were utilized to calculate the degree of hydrolysis. All SEC data can be found in chapter 3.[35]

^{1}H NMR (300 MHz, δ in ppm, $CDCl_3$): 1-1.2 (3 H, CH_2-C<u>H</u>$_3$), (2 H, C<u>H</u>$_2$-CH_3); 2.3-2.5 (2H, C<u>H</u>$_2$-CH_2-CH_3); 2.6-2.8 (4 H, C<u>H</u>$_2$-NH); 3.2-3.5 (4 H, C<u>H</u>$_2$NCH_2).

2.3 Results and discussion

A true understanding of the acidic hydrolysis mechanism of PAOx is crucial to determine the distribution of L-PEI units along the polymer backbone. In Scheme 2-1 the mechanism of the acidic hydrolysis of PAOx is shown. The majority of the carbonyl groups of the amide will be protonated during the reaction due to the high acid concentration (generally ~1-6 M; step 1 in Scheme 2-1). This protonation enhances the electrophilicity of the carbonyl group making it more prone to nucleophilic attack. In the second step of the reaction, water acts as a nucleophile towards the carbonyl group accompanied by an electron shift towards the oxonium creating the tetrahedral intermediate, which is the rate determining step. The tetrahedral intermediate is subsequently deprotonated by water that acts as a base. In this third step, the nitrogen group on the backbone is converted into a good leaving group by protonation. In the fourth step there is a rearrangement of electrons with release of the side chain as carboxylic acid, thereby creating the protonated amine (due to acidic conditions) of PAOx-PEI. The proposed hydrolysis mechanism in Scheme 2-1 is strictly speaking only valid for the first few hydrolysis reactions onto the PAOx chain as it does not take into account the neighbouring amine groups that will be present as hydrolysis proceeds. The protonation of the amine will have an effect at higher hydrolysis degree because more protonated amines are present potentially limiting the formation of more charges on the polymer chain. This effect is observed in the kinetic curve of the hydrolysis because at higher degree of hydrolysis the reaction speed decreases. In principle, two extreme cases may be described for the partial hydrolysis of PAOx, as schematically shown in Figure 2-1. If the presence of an amine on either or both sides of a PAOx do not influence the rates and equilibria during the hydrolysis (left branch in Figure 2-1), the hydrolysis will occur randomly along the chain and the formation of neighbouring L-PEI units will be statistically controlled, i.e. increasing with increasing conversion. Alternatively, the presence of a protonated amine may influence the reaction or shift the equilibria during hydrolysis, thereby facilitating the hydrolysis of PAOx units immediately neighbouring the generated PEI units (right branch in Figure 2-1). Such a rate accelerating neighbouring group effect will, in the extreme case, lead to the formation of growing blocks of L-PEI rather than a randomized distribution for the distribution of PEI-units in PAOx-PEI. This is observed in earlier work of our group, the kinetic curve has an s-shape for both the hydrolysis of PEtOx[34] and PPrOx (chapter 3).[35]

Focusing on individual monomeric units, these two extreme cases should translate in distinctly different environments around the L-PEI units at moderate hydrolysis degrees. In the case of a block-like L-PEI distribution, a particular PEI unit will mostly reside inside a L-PEI block and thus be surrounded by two other PEI units (star) and no PEtOx (squares) causing 'all-star' triads and 'all-triangle' triads (right branch, Figure 2-1) to be the dominant triad forms in the partly hydrolysed PEtOx-PEI. For a random distribution, individual PEI units will mostly be surrounded by PEtOx units and only occasionally by another L-PEI

unit, which will lead to triads containing a L-PEI at the center surrounded by PEtOx units (left branch Figure 2-1). The different constitution of L-PEI containing triads in block-like versus randomly hydrolysed PEtOx copolymers should allow them to be distinguishable by NMR structure analysis, thus allowing to distinguish whether the hydrolysis of PAOx is random or block-like.

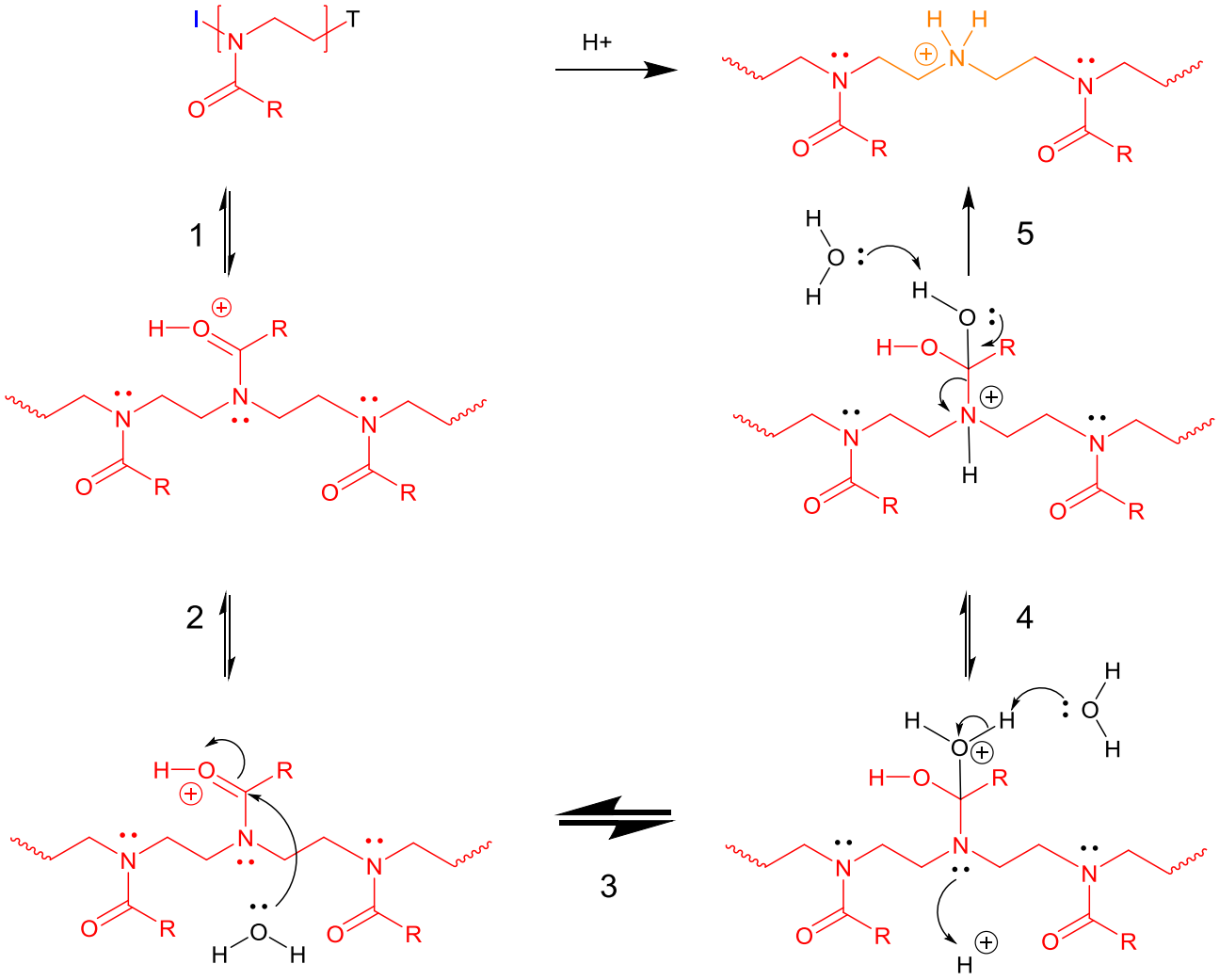

Scheme 2-1 Hydrolysis mechanism of PAOx (1) Protonation of the amide group; (2) nucleophilic attack of water (slow); (3) proton transfer to water; (4) rearrangement and release of the carboxylic acid and protonation of the formed secondary amine due to acid environment yielding a protonated PEI unit.

1D ^{1}H-NMR and ^{13}C-NMR spectroscopy were used as starting points to unravel the PEtOx-PEI copolymer distribution. As a model we used well-defined $PEtOx_{400}$, the partially hydrolysed $PEtOx_{307}$-PEI_{93} (23% hydrolysis) and the fully hydrolysed L-PEI_{400} (100% hydrolysis). Both the L-PEI and PEtOx-PEI are hydrolysis products obtained from the parent $PEtOx_{400}$. Figure 2-2 shows the stacked ^{1}H-NMR spectra of these polymers with the signal assignments. Note that the polymerisation initiator and terminating agent cannot be seen due to the high DP of the utilized polymer. This PEtOx was partially hydrolysed in 6M HCl

solution yielding the $PEtOx_{307}$-PEI_{93} copolymer and the corresponding ^1H NMR spectrum is shown in Figure 2-3, middle plot. Due to removal of the amide side chains the CH2-group of the L-PEI units H(6'and 6") appear at 2.8 ppm. The percentage of PEI is calculated from the integral of the PEI CH2 resonance H(6' and 6") relative to that of all methylene units (i.e. the sum of resonances H(2) and H(6' and 6") revealing a degree of hydrolysis of 23%. The methylene resonance at 2.8 ppm appears to be composed of two, partially overlapping signals, indicating the existence of two distinct chemical environments that we will refer to these as H(6') and H(6"). The ^1H NMR spectrum of the fully hydrolysed PEI_{400} is shown in Figure 2-2, top plot. Only one peak is present at 2.8 ppm (see also the zoom in Figure 2-3) corresponding to the protons of the methylene groups H(6) indicating full hydrolysis of PEtOx.

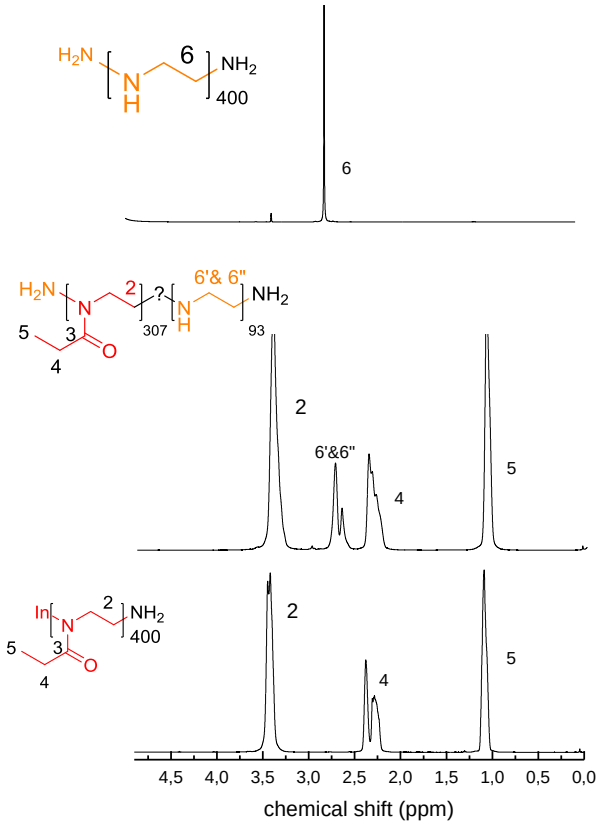

Figure 2-2 Stacked plot of the ^1H-NMR spectra of $PEtOx_{400}$ (bottom, $CDCl_3$), $PEtOx_{307}$-PEI_{93} (middle, $CDCl_3$) and pure PEI_{400} (top, CD_3OD) with assignments;.

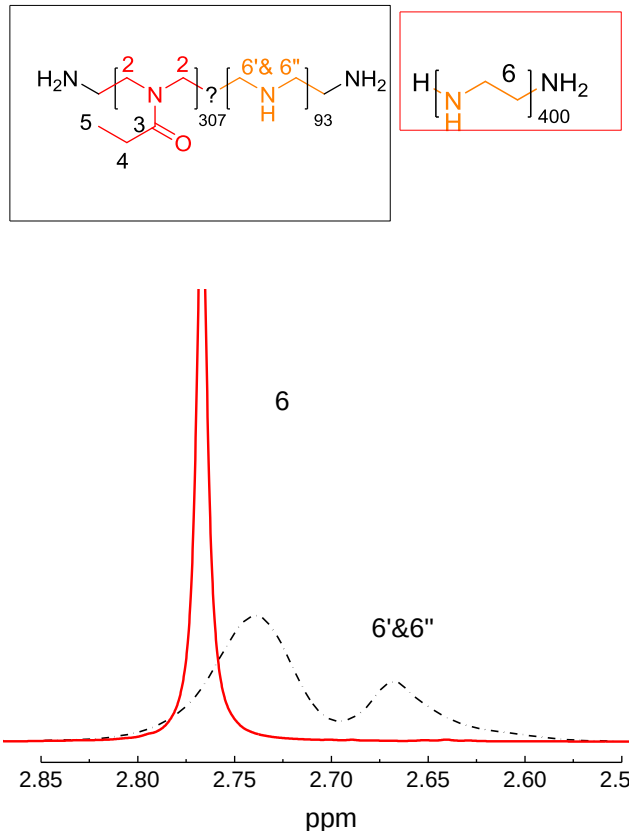

Figure 2-3 : Overlaid zoom of the ^{1}H NMR spectra of $PEtOx_{307}$-PEI_{93} (black) and PEI_{400} (red)

The full, assigned ^{13}C-NMR spectra of the three polymers are shown in Figure 2-4. A zoom of the range from 43 to 50 ppm that shows the main differences between the $PEtOx_{400}$ and the partially hydrolysed PEtOx-PEI, is shown in Figure 2-5. Clearly, additional peaks appear in between 48-50 ppm upon hydrolysis, indicative of the appearance of PEI units. The top spectrum of L-PEI is shown in Figure 2-4 shows that upon complete hydrolysis, the convoluted methylene region simplifies to a single PEI resonance, expectedly showing only one population and thus a single chemical environment for the CH2 groups. Information on the type and distribution of the triads can be extracted from the ^{13}C signature of the methylene area, provided the latter can be deconvoluted into the contributions from individual structures and triads, this allowing the elucidation of the distribution of L-PEI units in the PEtOx-PEI copolymer.

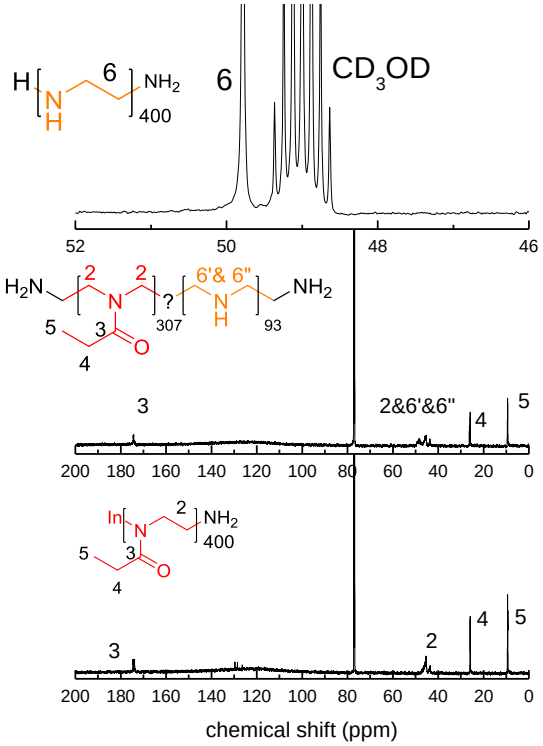

Figure 2-4 ^{13}C-NMR spectra of $PEtOx_{400}$(bottom) ($CDCl_3$); $PEtOx_{307}$-PEI_{93} (middle) ($CDCl_3$ and PEI_{400} (top) (CD_3OD) with assignments.

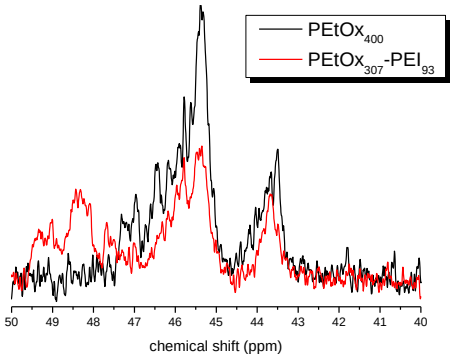

Figure 2-5 Overlay of the ^{13}C-NMR spectra of the CH2-backbone regions of $PEtOx_{400}$(black) and $PEtOx_{307}$-PEI_{93} ($CDCl_3$).

To assign the different methylene resonances in $PEtOx_{307}$-PEI_{97}, 2D ^{1}H-{^{13}C} HSQC and HMBC NMR measurements were performed. The full HSQC spectrum of the $PEtOx_{307}$-PEI_{93} is shown in Figure 2-6 (assignment of cross peaks is given in Table 1), and the area of highest interest is presented in Figure 2-7. In comparison with the HSQC spectrum of the starting polymer $PEtOx_{400}$ (Figure 2-7), the PEtOx-PEI

copolymer shows additional cross peaks connecting the CH2 ^{1}H resonance of the PEtOx copolymer H(2), with carbon resonances in the 47-50 ppm area. The addition of the ^{13}C dimension allows resolution of the mostly featureless ^{1}H resonance H(2) into 3 separate cross peaks. Hence, the formation of 3 types of PEtOx CH2 environments should be considered upon partial hydrolysis. A similar conclusion can be drawn for the CH2 of the PEI backbone H(6' and 6"). Again 3 cross peaks can be observed. Two intense cross peaks connect the H(6') and H(6") resonances to the ^{13}C signals at 49.5 ppm and 48 ppm, respectively. A third, much weaker but discernible cross peak can be found correlating the H(6') ^{1}H resonance with a ^{13}C signal at 53 ppm, which will be referred to as C(6'a). This C(6'a) signal lies below the level of detection in the ^{13}C spectrum, yet becomes visible thanks to the higher signal to noise afforded by ^{1}H excitation and detection in the ^{1}H-{^{13}C}-HSQC setup. The different chemical shifts for the methylene groups of both the PEtOx and PEI units in the copolymer show that distinct chemical environments exist, yet their nature still needs to be established. This was attempted using a ^{1}H-{^{13}C} HMBC experiment, which, in principle, allows to probe the chemical structures immediately surrounding the methylene groups across multiple bonds.

Table 1 Cross peaks identified in the HSQC spectrum of $PEtOx_{307}$-PEI_{93}

Type of CH_2 group	Nr of atom	1H-NMR (ppm)	13C-NMR (ppm)
PEI	6'b	2.76	47.87
PEI	6'a	2.81	52.52
PEI	6"	2.69	49.2
PEtOx	2	3.44	43.77
PEtOx	2	3.43	45.87
PEtOx	2	3.38	48.63

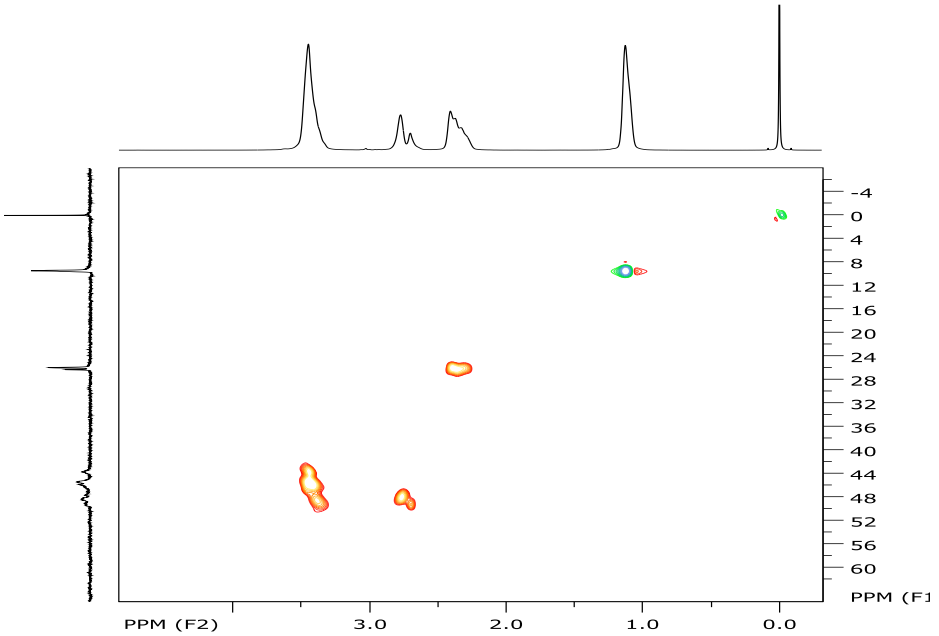

Figure 2-6 HSQC spectrum of $PEtOx_{307}$-PEI_{93} ($CDCl_3$). Red yellow shades indicated CH_2, green blue shades indicate CH/CH_3

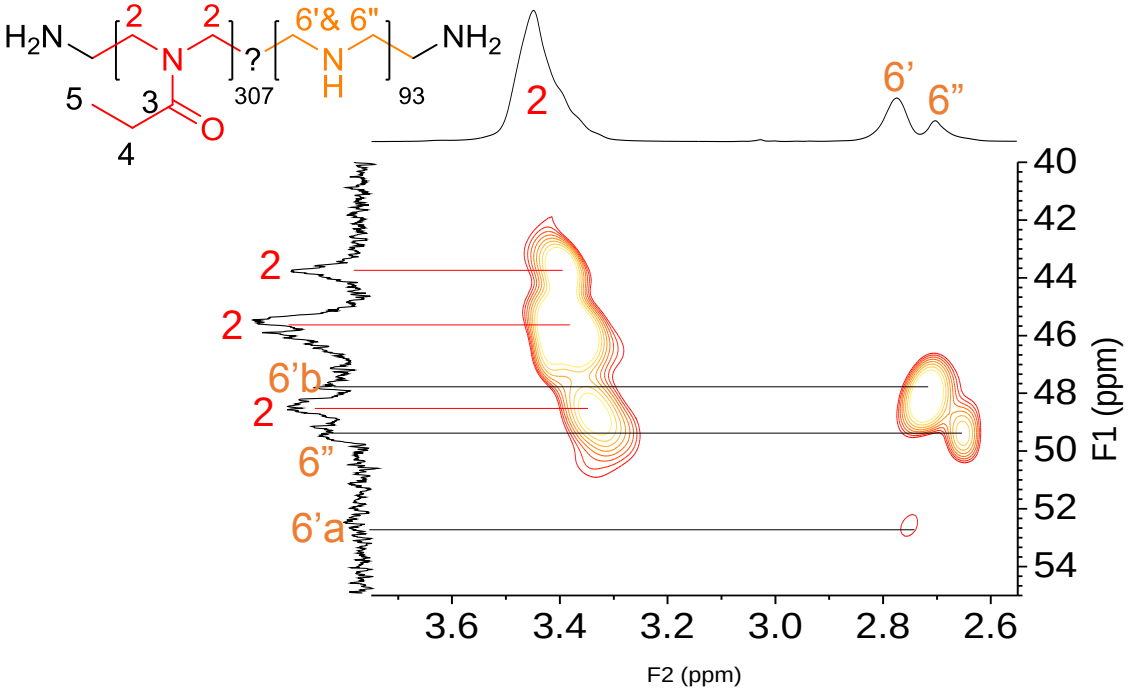

Figure 2-7 HSQC spectrum of $PEtOx_{307}$-PEI_{93} ($CDCl_3$).

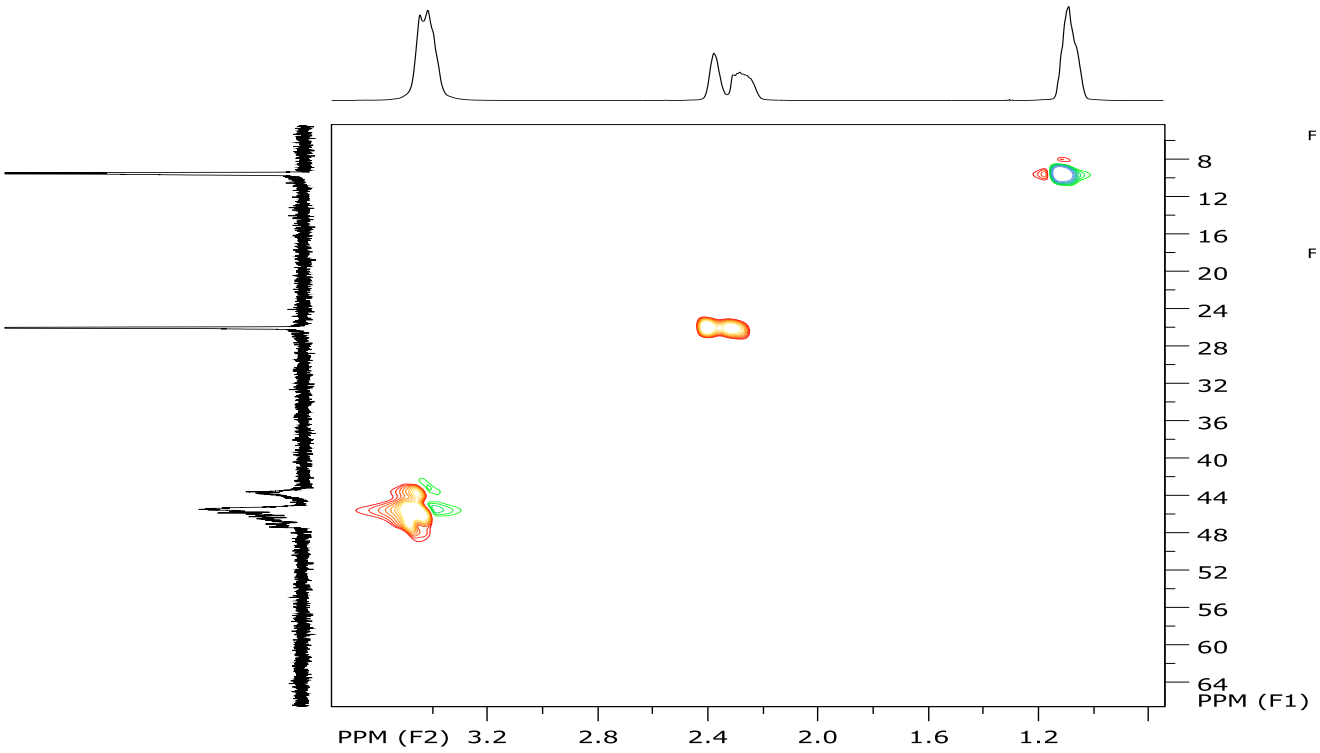

Figure 2-8 HSQC spectrum of $PEtOx_{400}$ ($CDCl_3$).

The full HMBC spectrum of $PEtOx_{307}$-PEI_{93} is shown in Figure 2-9, while details of the areas of highest interest are presented in Figure 2-10 and Figure 2-11. Figure 2-10 shows the area of the CH2 groups of the PEI units of the copolymer. The cross peaks arising from long range $^{n}J_{HC}$ couplings, with n typically 2 or 3 are collected in Table 2. In a partially hydrolysed polymer, cross-peaks in this part of the HMBC spectrum can point to PEI-PEI, PEI-PEtOx or PEtOx-PEI diads. It should be noted that the latter two produce identical HMBC patterns and, therefore, cannot be distinguished. Four cross peaks A to D were observed. Peak A correlates H(6") with C(6") and peak B correlates H(6") with C(6'a) indicating that H(6") is surrounded by two kinds of PEI CH2 groups. However the C(6'a) CH2 is located in another chemical environment. Remark that the difference between C(6'a) and C(6'b) can be made, however the adjacent protons, H(6'a) and H(6'b) can't be distinguished and form a single peak H(6') in the ^{1}H-NMR spectrum. However the C(6'a) CH2 is located in another chemical environment. Two cross peaks(C&D) appear for H(6'), which both correlate with the CH2 of PEtOx C(2) at 45 ppm and 49 ppm. Thus, for the PEI CH2-region we have 3 types of CH2 groups all correlating with different regions. The H(6") and C(6") regions only correlates with other PEI units while C(6'b) only correlates with PEtOx units. The third type, C(6'a) correlates with CH_2 originating from PEI, itself and H(6"). Here it is also clear that for H(6") and C(6") there is no overlap with PEtOx CH2 (2) as no cross peaks can be identified. Also no interaction can be seen between CH_2(6'b) and CH_2(6").

The second region of interest on the HMBC spectrum is in between 3.5 ppm and 3.28 ppm (Figure 2-11) where the CH2 groups of the PEtOx are located. Two cross peaks (E and F) are the cross peaks that were also seen in the HSQC spectrum (PEtOx-PEtOx units), see overlay of HSQC and HMBC in Figure 2-12. The cross peak G shows the correlation between C(6'b) and PEtOx CH2 H(2). The last cross peak correlates C(6'a) with H(2).

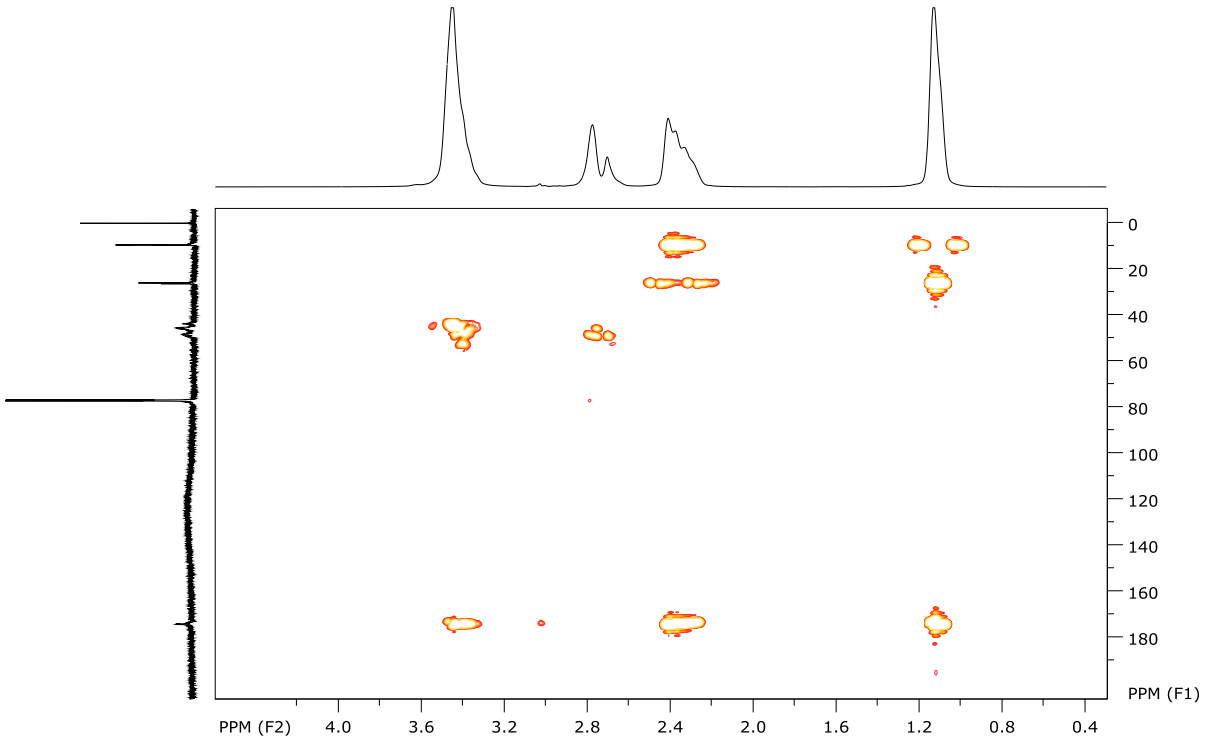

Figure 2-9 HMBC spectrum of PEtOx-PEI_{400} ($CDCl_3$).

Table 2 Cross peaks identified in the HMBC spectrum of $PEtOx_{307}$-PEI_{93}

Cross peak	Type of CH_2 group	CH_2 group (^1H NMR)	CH_2 group (^{13}C NMR)	1H-NMR (ppm)	13C-NMR (ppm)
A	PEI	6"	6"	2.69	49.12
B	PEI	6"	6'a	2.68	52.57
C	PEI	6'b	2	2.75	45.66
D	PEI	6'b	2	2	48.84
E	PEtOx	2	2	3.44	44.55
F	PEtOx	2	2	3.43	48.43
G	PEtOx	2	6'b	3.39	47.95
H	PEtOx	2	6'a	3.40	52.75

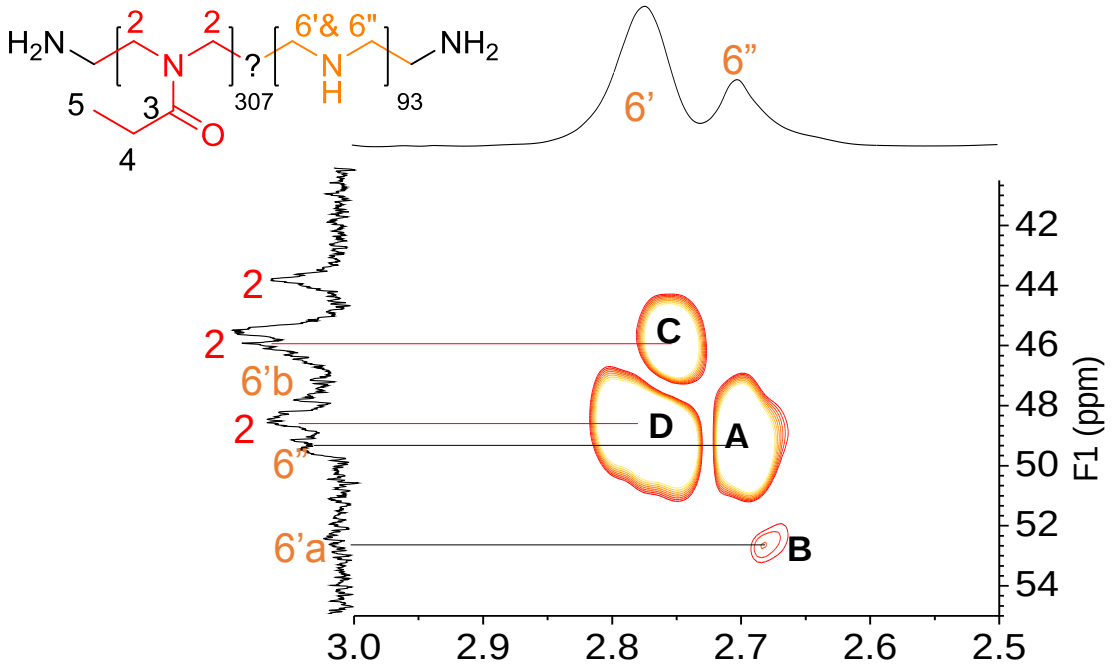

Figure 2-10 Zoom of the HMBC spectrum of $PEtOx_{307}$-PEI_{93} region corresponding to the CH_2 groups of PEI. ($CDCl_3$)

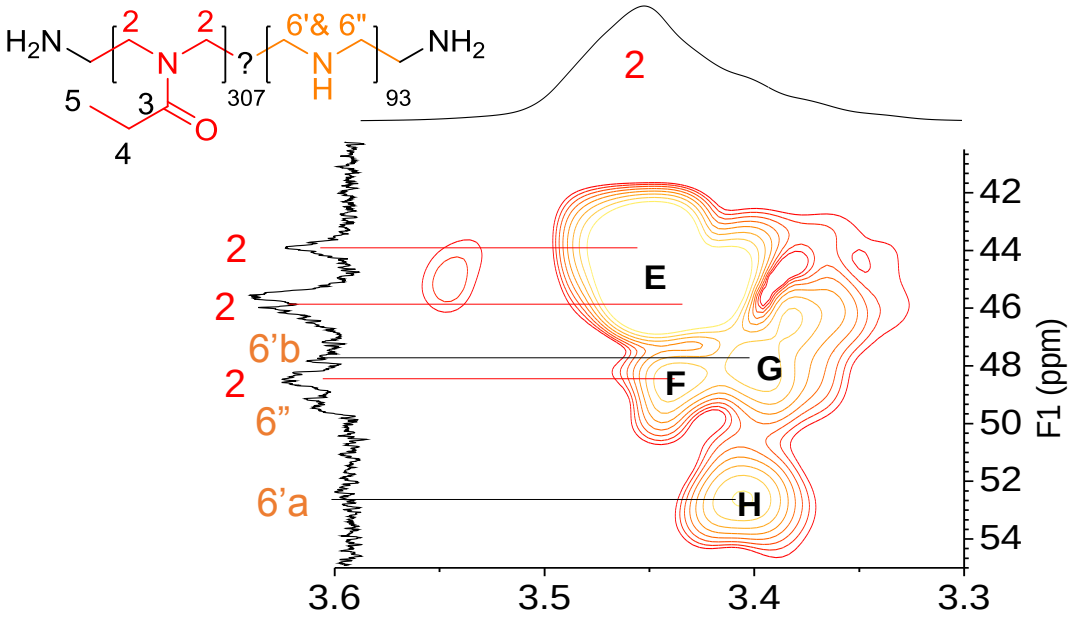

Figure 2-11 Zoom of the HMBC spectrum of $PEtOx_{307}$-PEI_{93} Corresponding to the CH_2 groups of PEtOx.($CDCl_3$)

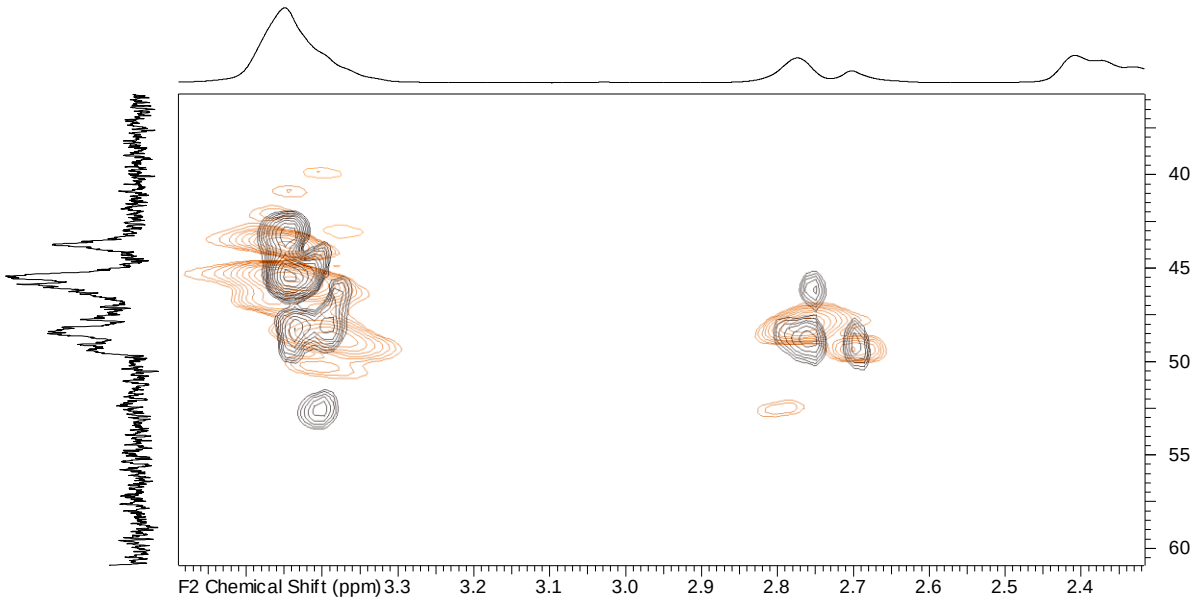

Figure 2-12 Overlay of HMBC(orange) and HSQC (black) spectra of $PEtOx_{307}$-PEI_{93} ($CDCl_3$)

The above discussion reveals that there are 6 types of CH_2 groups. The first type of PEI (6") is surrounded by other PEI (6" and 6'a) units (Figure 2-13). This is the middle star in a 'triple-star' triad indicating block-like L-PEI formation as statistically only very little PEI-triads should be present at 23% hydrolysis. The PEI (6'a) has a connection with the PEI (6") and with PEtOx, which is the transition

between an L-PEI block-like structure and the PEtOx. The last PEI CH_2 group (6'b) is located in between two PEtOx-units which indicates that there is not a perfect block-like hydrolysis, but rather a preferential block-like hydrolysis besides the also occurring random hydrolysis.

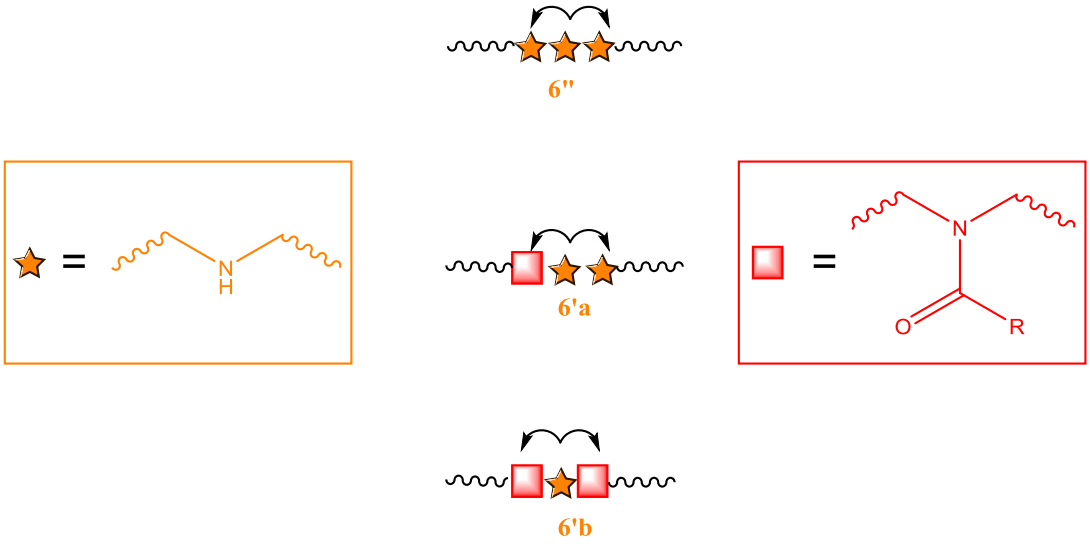

Figure 2-13: Visualisation of the three types of PEI units present in PEtOx-PEI. The star shapes represent PEI units while the red blocks represent the PAOx units.

To further investigate the distribution of L-PEI units in PEtOx-PEI, a range of partially hydrolysed PEtOx samples with different degree of hydrolysis that were available in our laboratory, was analysed by routine ^{1}H NMR spectroscopy (Figure 2-14). Note that all spectra were calibrated against residual solvent signals, but the presence of minor traces of salts induces different chemical shifts. The copolymer characterised by a low % of PEI (3.8%) only shows one broad PEI CH_2 resonance corresponding with a situation expected for random hydrolysis. However, already starting from 10% PEI there is a small sharper peak corresponding to the PEI CH_2 groups with two neighbouring PEI units (6"), which becomes more and more pronounced with increasing degree of hydrolysis. At 41 % hydrolysis the amount of block-like PEI units is larger than the randomly distributed PEI units and at 70% only the signal corresponding to block-like PEI units is present. This probably explains why the reaction mixture becomes milky at higher hydrolysis degree as large PEI block can induce crystallization. To probe the effect of the PAOx side chain on the hydrolysis reaction, we also examined the distribution of both peaks 6' and 6" in a series of partially hydrolysed PPrOx by routine ^{1}H NMR spectroscopy (Figure 2-15).[35] The hydrolysis of PPrOx will be discussed in-depth in chapter 3. Very similar to PEtOx, the sharp signal of block-like PEI units (6") already appears at rather low degree of hydrolysis, namely from 15% hydrolysis onwards.

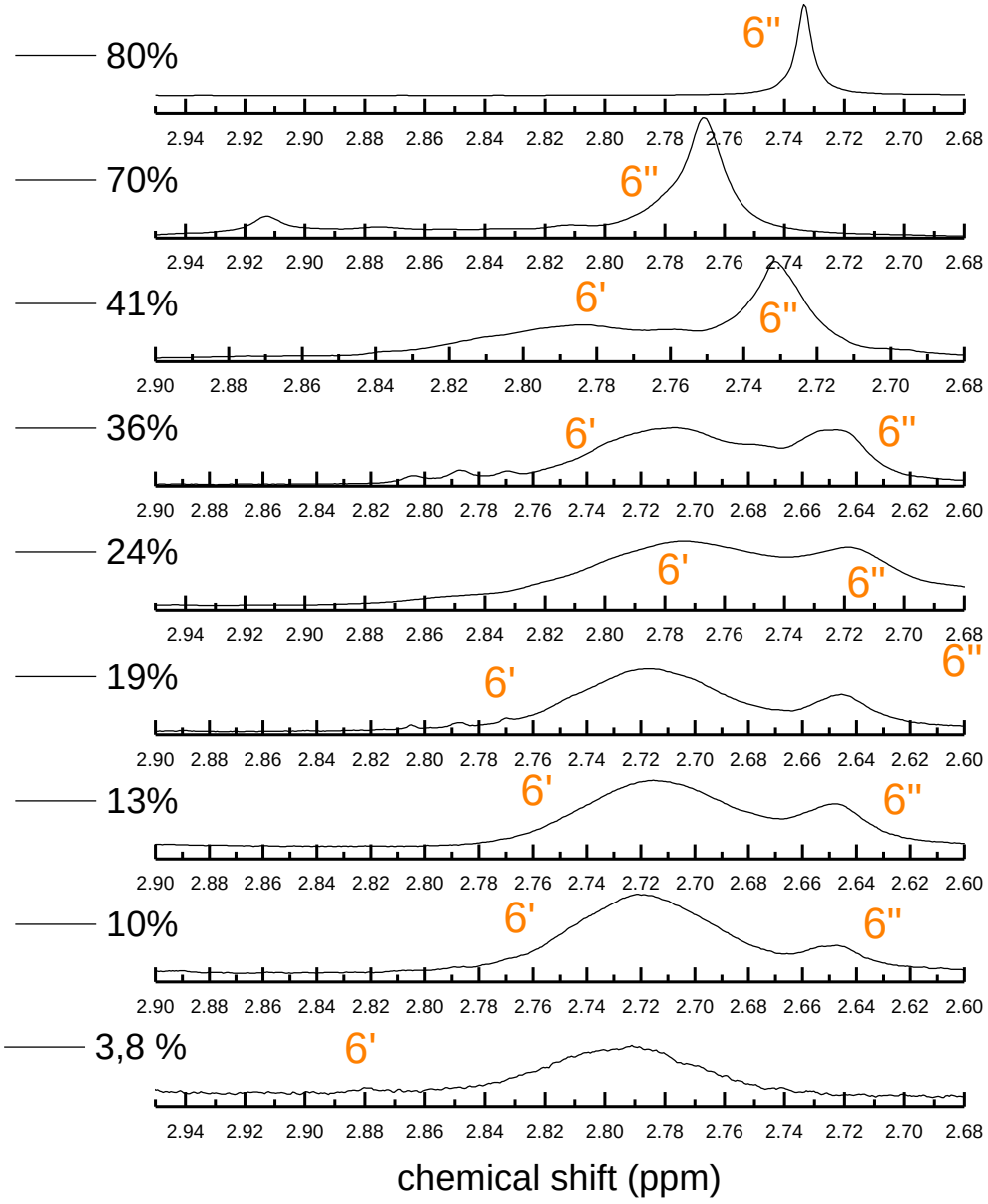

Figure 2-14 Stacked plot of the different ^{1}H-NMR spectra of PEtOx with varying degree of hydrolysis.

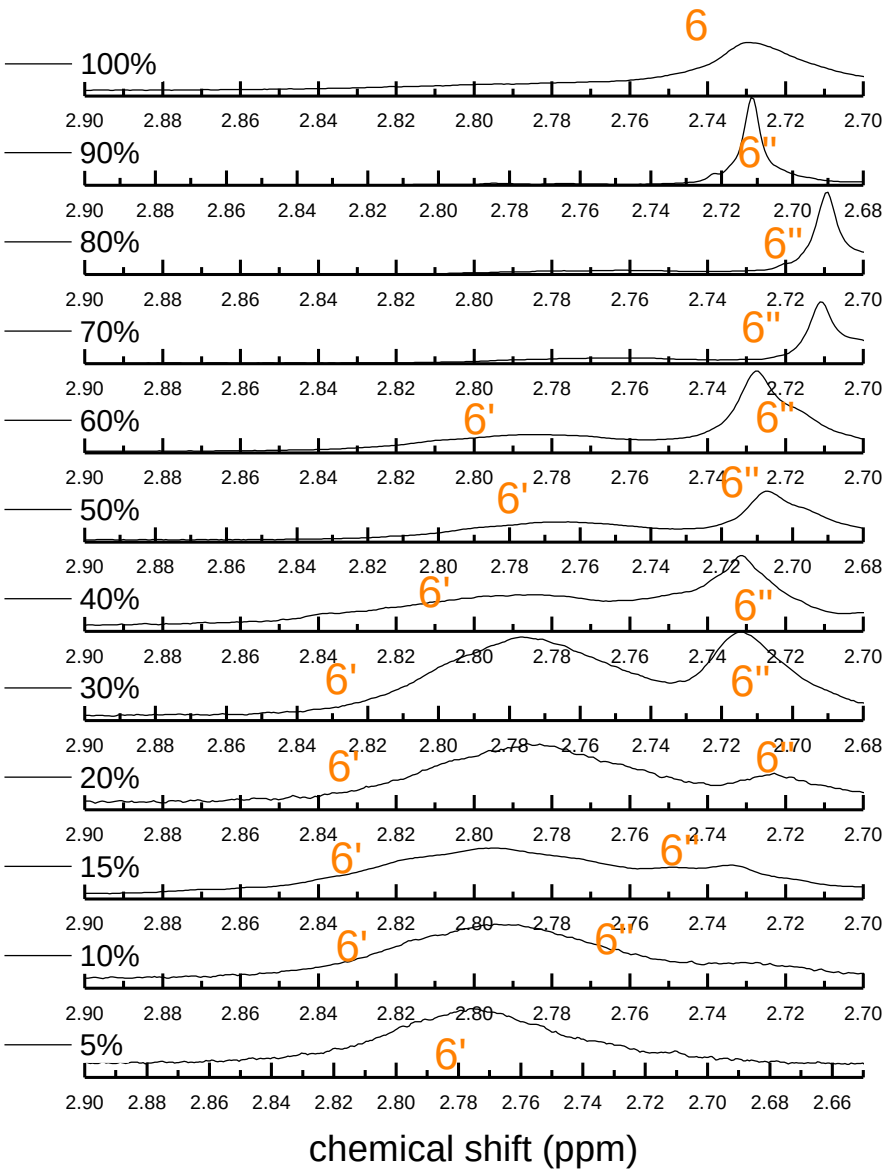

Figure 2-15 Stacked plot of the ^{1}H NMR spectra of different PPrOx-PEI copolymers with varying degree of hydrolysis ($CDCl_3$)

Even though the stack plot of the individual ^{1}H NMR spectra for partially hydrolysed PEtOx already indicates that the hydrolysis occurs in a block-like fashion, a more in-depth statistical analysis is required because during a random hydrolysis process also blocks of PEI units will be formed along the PEtOx chain

at higher degrees of hydrolysis. Therefore, the random distribution of PEI units can be modelled with Bernoulli statistics. This statistical model describes the random process of reaching into a large container containing two types of balls, to take the balls out both balls have equal chance to be taken. There is no influence on what happened in the past.[58–60] Applying these statistics to the hydrolysis of PEtOx, means that the potential neighbouring group effects and steric effects are neglected, thereby describing the random hydrolysis model (Figure 2-1, left). If the experimental data show more pronounced formation of block-like distribution of L-PEI units than the Bernoulli statistical model, it can be concluded that hydrolysis occurs more in a block-like fashion.

In the Bernoulli model the hydrolysis of a PEtOx unit is independent of the neighbouring group. The chance that a PEtOx units is hydrolysed into PEI is defined as P(PEI), while the formation of a block-like PEI containing three PEI units in a row is defined as P^3(PEI) representing the PEI-triad. The blue plot in Figure 2-16 shows the formation of P^3(PEI) as function of the hydrolysis degree following the random Bernoulli statistics. From the spectra in Figure 2-14 and 2-15, the experimental ratio between the peak containing the CH_2 of the triad PEI (no PEtOx/PPrOx interaction; 6") and the CH_2 of the random PEI units (with PEtOx-interaction; 6') can be calculated. As such, the amount of PEI CH_2 groups that have no contact with PEtOx, *i.e.* are present in block-like PEI, can be determined. It should be noted that this does not provide information on the length and number of PEI-blocks, but merely the amount of PEI CH_2 units present in all PEI triads representing the L-PEI block-like structures. From Figure 2-16 it is clear that at low degree of hydrolysis the blue curve and black/red curves are distinctly different. This means that the formation of block-like PEI units is more pronounced in the experimental data than in the random hydrolysis model, providing direct proof that the hydrolysis takes place in a more block-like fashion and the distribution of the L-PEI units in PEtOx-PEI is block-like. Similarly, the hydrolysis of PPrOx also occurs in a more block-like fashion compared to the random hydrolysis Bernoulli model as a similar deviation from Bernoulli statistics was obtained for PEtOx and PPrOx(Figure 2-16 black line). Both the black and red curve are obtained from integration of the ^{1}H-NMR spectra in Figure 2-14 and Figure 2-15, the difference between both curves lays within the standard deviation of the integration. This indicates that there is no significant difference in the distribution of PEI units in partially hydrolysed PEtOx-PEI and PPrOx-PEI.

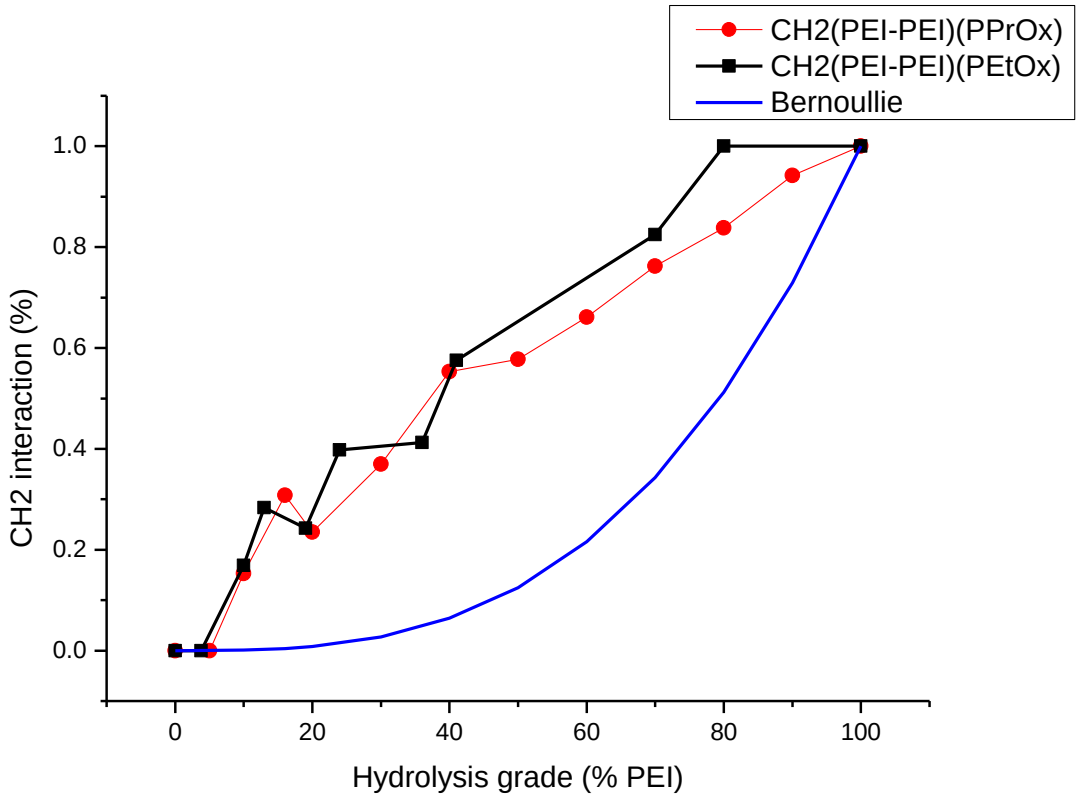

Figure 2-16 Plot of the hydrolysis degree versus the amount of CH_2 interaction within a PEI triad. The blue plot gives the theoretical amount of CH_2 interaction in all PEI triads for a random Bernoulli distribution. The black plot gives the experimental data obtained from Figure 2-14 for PEtOx. The red plot gives the experimental data obtained from fig 2-15 for PPrOx.

Even though we have not determined the exact underlying mechanism that favors the block-like hydrolysis of PEtOx and PPrOx, it may be speculated that it is either related to steric effects or electronic effects. Sterically, the presence of a PEI-unit may enhance the accessibility of the neighbouring amide groups making them more prone to hydrolysis. The occurrence of such steric effects would, however, lead to more pronounced block-like hydrolysis for PPrOx compared to PEtOx. As it was experimentally found that PEtOx and PPrOx show very similar block formation (Figure 2-16) it is unlikely that steric effects are the major driving factor for the observed neighbouring group effect during acidic hydrolysis. Hence, electronic effects may be at the basis of the neighbouring group effect. As previously pointed out by Kem *et al*[38] this neighbouring group effect may be ascribed to the formation of a seven-membered ring like structure. The interaction of the protonated secondary amine group of L-PEI with the neighbouring carbonyl group of the amide is shown in Scheme 2-2. As such, the carbonyl is activated for attack of water favoring the block-like hydrolysis This mechanism should lead to acceleration of the hydrolysis at the beginning of the reaction, the formation of the first PEI units will have an autocatalytic effect. This acceleration was observed in earlier work of our group for the hydrolysis of PEtOx.[34] In Chapter 3 such an

acceleration is also observed in Figure 3-2 showing the effect of the neighbouring group. The acceleration is undo at higher hydrolysis degrees due to the electrostatic repulsion of the protonated amines. This will decrease the reaction speed by charge repulsion effects and results in an overall s-shaped kinetic curve for the hydrolysis which has been observed in older work[34] and in chapter 3 Figure 3-2.

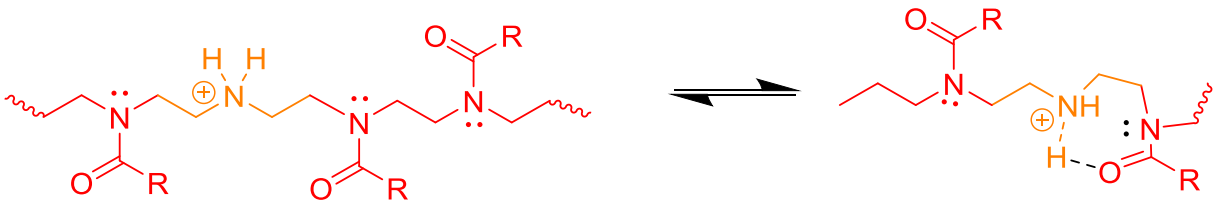

Scheme 2-2 Schematic representation of the seven-membered ring formation as possible mechanism for the observed neighbouring group effect during the acidic hydrolysis of PAOx. Valid at lower hydrolysis degrees.

2.4 Conclusion

Driven by the increasing interest for partially hydrolysed PAOx for various applications as well as a reactive platform for making functional PAOx, we have investigated the partial acidic hydrolysis of PEtOx by detailed NMR spectroscopy. This allowed unraveling whether the PEI units are distributed in a random or more block-like fashion along the polymer chain. Therefore, three different polymers where studied having 0%, 23% and 100% of PEI units in the PEtOx-PEI copolymers. The ^{1}H-NMR and ^{13}C-NMR spectra revealed that the PEtOx-PEI showed additional peaks, ascribed to the PEI units. Further in-depth analysis by HSQC and HMBC revealed the presence of 6 different CH_2 groups in PEtOx-PEI, namely 3 different CH_2 groups corresponding to the PEtOx and 3 CH_2 groups for the PEI. Assignment of these CH_2 groups in the $PEtOx_{307}$-PEI_{93} revealed the presence of PEI-CH_2 groups that are connected with two other PEI units, so called all PEI triads. Thereby implying the formation of block-like PEI at this relatively low degree of hydrolysis. This was also demonstrated by analysing a series of PEtOx-PEI and PPrOx-PEI copolymers with different degrees of hydrolysis indicating the formation of block-like PEI units. Comparison with random hydrolysis as described by Bernoulli statistics confirmed that indeed the PEI units are distributed along the chain in a block like fashion and, thus, acidic hydrolysis occurs in a more block-like manner. This may be ascribed to a neighbouring group effect in which the protonated secondary amine interacts and activates the neighbouring amide carbonyl group facilitating its hydrolysis.

This result is of vast importance for the field of PEI and PAOx polymers as it gives detailed information about the copolymer distribution along the chain. These results can help us to understand the hydrolysis of PPrOx in chapter 3 and the obtained data for its use in gene delivery. The functional group distribution of the new copolymer in chapter 4, 5 and 6 is also unraveled, which can be of further importance as the polymers to be used in the biological context require a strict definition.

2.5 References

(1) Tomalia, D. a; Sheetz, D. P. *J. Polym. Sci. Part A-1 Polym. Chem.* **1966**, *4* (9), 2253.
(2) Seeliger, W. H. H.; Aufderhaar, E.; Diepers, W.; Feinauer, R.; Nehring, R.; Their, W.; Hellmann, H. *Polym. Lett.* **1966**, *5* (1), 871.
(3) T, K.; Narisaw, S.; Maeda, T.; Kenichi, F. *Polym. Lett.* **1966**, *4*, 441.
(4) T. G. Bassiri, A. L. andM. L. *Polym. Lett.* **1967**, *5* (1), 871.
(5) Kagiya, T.; Maeda, T.; Fukui, K.; Narisawa, S. *Polym. Lett.* **1966**, *4*, 441.
(6) Saegusa, T.; Fujii, H.; Ikeda, H. *Macromolecules* **1972**, *37* (1), 108.
(7) Jäger, M.; Schubert, S.; Ochrimenko, S.; Fischer, D.; Schubert, U. S. *Chem. Soc. Rev.* **2012**, *41* (13), 4755.
(8) Tsai, L. R.; Chen, M. H.; Chien, C. Te; Chen, M. K.; Lin, F. S.; Lin, K. M. C.; Hwu, Y. K.; Yang, C. S.; Lin, S. Y. *Biomaterials* **2011**, *32* (14), 3647.
(9) Lin, S.-Y.; Lin, F.-S.; Chen, M.-K.; Tsai, L.-R.; Jao, Y.-C.; Lin, H.-Y.; Wang, C.-L.; Hwu, Y.-K.; Yang, C.-S. *Chem. Commun. (Camb).* **2010**, *46* (30), 5554.
(10) Munir, A.; Goethals, E. J. *Journa Polym. Sci.* **1994**, *19* (1981), 1985.
(11) Reisman, L.; Mbarushimana, C. P.; Cassidy, S. J.; Rupar, P. A. *ACS Macro Lett.* **2016**, *5* (10), 1137.
(12) Lazaro-Martinez, J. M.; Rodriguez-Castellon, E.; Vega, D.; Monti, G. A.; Chattah, A. K. *Macromolecules* **2015**, *48* (4), 1115.
(13) Kobayashi, S.; Hiroishi, K.; Tokunoh, M.; Saegusa, T. *Macromolecules* **1987**, *20*, 1496.
(14) Saegusa, T.; Kobayashi, S.; Yamada, A. *Macromolecules* **1975**, *8* (4), 390.
(15) Harris, C. S.; Ratner, M. A.; Shriver, D. F. *Macromolecules* **1987**, *20* (17), 1778.
(16) Doyle, R. P.; Chen, X.; Macrae, M.; Srungavarapu, A.; Smith, L. J.; Gopinadhan, M.; Osuji, C. O.; Granados-Focil, S. *Macromolecules* **2014**, *47* (10), 3401.
(17) Herlem, G.; Lakard, B. *J. Chem. Phys.* **2004**, *120* (19), 9376.
(18) Wiegand, C.; Bauer, M.; Hipler, U. C.; Fischer, D. *Int. J. Pharm.* **2013**, *456* (1), 165.
(19) Bradbury, R.; Penfold, J.; Thomas, R. K.; Tucker, I. M.; Petkov, J. T.; Jones, C. *J. Colloid Interface Sci.* **2016**, *466*, 220.
(20) Halacheva, S. S.; Penfold, J.; Thomas, R. K. *Langmuir* **2012**, *28*, 173331.
(21) Ferrari, S.; Moro, E.; Pettenazzo, A.; Behr, J. P.; Zacchello, F.; Scarpa, M. *Gene Ther.* **1997**, *4* (10), 1100.
(22) Coll, J. L.; Chollet, P.; Brambilla, E.; Desplanques, D.; Behr, J. P.; Favrot, M. *Hum. Gene Ther.* **1999**, *10* (10), 1659.
(23) Lungwitz, U.; Breunig, M.; Blunk, T.; Göpferich, A. *Eur. J. Pharm. Biopharm.* **2005**, *60*, 247.
(24) Bertrand, E.; Gonçalves, C.; Billiet, L.; Gomez, J. P.; Pichon, C.; Cheradame, H.; Midoux, P.; Guégan, P. *Chem. Commun. (Camb).* **2011**, *47* (46), 12547.
(25) Brissault, B.; Kichler, A.; Guis, C.; Leborgne, C.; Danos, O.; Cheradame, H. *Bioconjug. Chem.* **2003**, *14* (3), 581.
(26) Guis, C.; Cheradame, H. *Eur. Polym. J.* **2000**, *36* (12), 2581.
(27) Halacheva, S.; Price, G. J.; Garamus, V. M. *Macromolecules* **2011**, *44* (18), 7394.
(28) Ludwick, A. G.; Robinson, K. S.; Mccloud, J. *J. Polym. Sci. Polym. Symp.* **1986**, *74* (1), 55.
(29) Glatzhofer, D. T.; Erickson, M. J.; Frech, R.; Yepez, F.; Furneaux, J. E. *Solid State Ionics* **2005**, *176* (39–40), 2861.
(30) Lambermont-Thijs, H. M. L.; Bonami, L.; Du Prez, F. E.; Hoogenboom, R. *Polym. Chem.* **2010**, *1* (5), 747.
(31) Jeong, J. H.; Song, S. H.; Lim, D. W.; Lee, H.; Park, T. G. *J. Control. release* **2001**, *73* (2–3), 391.
(32) Fernandes, J. C.; Qiu, X.; Winnik, F. M.; Benderdour, M.; Zhang, X.; Dai, K.; Shi, Q. *Int. J. Nanomedicine* **2013**, *8*, 4091.
(33) de la Rosa, V. R.; Bauwens, E.; Monnery, B. D.; De Geest, B. G.; Hoogenboom, R. *Polym. Chem.* **2014**, *5*, 4957.
(34) Van Kuringen, H. P. C.; Lenoir, J.; Adriaens, E.; Bender, J.; De Geest, B. G.; Hoogenboom, R. *Macromol. Biosci.* **2012**, *12* (8), 1114.

(35) Mees, M.; Haladjova, E.; Momekova, D.; Momekov, G.; Shestakova, P. S.; Tsvetanov, C. B.; Hoogenboom, R.; Rangelov, S. *Biomacromolecules* **2016**, *17* (11), 3580.
(36) Zhang, Y.; Chen, L.; Zhang, C.; Liu, S.; Zhu, H.; Wang, Y. *Talanta* **2016**, *150*, 375.
(37) Kanazaki, K.; Sano, K.; Makino, A.; Homma, T.; Ono, M.; Saji, H. *Nat. Sci. Reports* **2016**, *6* (August), 33798.
(38) Kem, K. M. *J. Polym. Sci. Polym. Chem. Ed.* **1979**, *17*, 1977.
(39) Lambermont-Thijs, H. M. L.; Heuts, J. P. A.; Hoeppener, S.; Hoogenboom, R.; Schubert, U. S. *Polym. Chem.* **2011**, *2* (2), 313.
(40) Litt, M. H.; Lin, C. S. *J. Polym. Sci. Part A-1 Polym. Chem.* **1992**, *30*, 779.
(41) Tomalia, D. a.; Sheetz, D. P.; Kagiya, T.; Maeda, T.; Fukui, K.; Narisawa, S. *J. Polym. Sci. Part A-1 Polym. Chem.* **1966**, *4* (9), 2253.
(42) Lambermont-Thijs, H. M. L.; van der Woerdt, F. S.; Baumgaertel, A.; Bonami, L.; Du Prez, F. E.; Schubert, U. S.; Hoogenboom, R. *Macromolecules* **2010**, *43* (2), 927.
(43) Chujo, Y.; Yutaka, Y.; Sada, K.; Saegusa, T. *Macromolecules* **1989**, *22* (3), 1074.
(44) Seeliger, W.; Aufderhaar, E.; Diepers, W.; Feinauer, R.; Nehring, R.; Thier, W.; Hellmann, H. *Angew. Chem. Int. Ed. Engl.* **1966**, *5* (10), 875.
(45) Chujo, Y.; Sada, K.; Naka, a; Nomura, R.; Saegusa, T. *Macromolecules* **1993**, *26* (5), 883.
(46) Tanaka, R.; Ueoka, I.; Takaki, Y.; Kataoka, K.; Saito, S. *Macromolecules* **1983**, *16* (2), 849.
(47) Chujo, Y.; Sada, K.; Saegusa, T. *Macromolecules* **1990**, *23*, 2636.
(48) Mees, M. A.; Hoogenboom, R. *Macromolecules* **2015**, *48* (11), 3531.
(49) Chujo, Y.; Sada, K.; Saegusa, T. *Macromolecules* **1993**, *26* (24), 6320.
(50) Legros, C.; De Pauw-Gillet, M.-C.; Tam, K. C.; Lecommandoux, S.; Taton, D. *Eur. Polym. J.* **2015**, *62*, 322.
(51) Legros, C.; Wirotius, A.; Tam, K. C.; Taton, D. *Biomacromolecules* **2014**.
(52) Mees, M. A.; Effenberg, C.; Appelhans, D.; Hoogenboom, R. *Biomacromolecules* **2016**, *17* (12), 4027.
(53) Suh, J.; Paik, H.-J.; Hwang, B. K. *Bioorganic Chemistry*. 1994, pp 318–327.
(54) Lee, H.; Son, S. H.; Sharma, R.; Won, Y. *J. Phys. Chem. B* **2011**, *115*, 844.
(55) Stubbe, B.; Li, Y.; Vergaelen, M.; Van Vlierberghe, S.; Dubruel, P.; De Clerck, K.; Hoogenboom, R. *Eur. Polym. J.* **2016**.
(56) Hoogenboom, R.; Paulus, R. M.; Pilotti, Å.; Schubert, U. S. *Macromol. Rapid Commun.* **2006**, *27* (18), 1556.
(57) Glassner, M.; D'Hooge, D. R.; Young Park, J.; Van Steenberge, P. H. M.; Monnery, B. D.; Reyniers, M. F. F.; Hoogenboom, R. *Eur. Polym. J.* **2015**, *65*, 298.
(58) Frisch, H. L.; Mallows, C. L.; Bovey, F. a. *J. Chem. Phys.* **1966**, *45* (5), 1565.
(59) Bovey, F. A.; Hill, M.; Cleland, R. L.; Allcock, H. R.; Flory, P. J.; Goodman, M.; Overberger, C. G.; Starkweather, H. W.; Vogl, O.; Bowen, D. H. M. 7974.
(60) Bovey, F. A. *Pure Appl. Chem.* **1967**, *15* (3–4), 349.

CHAPTER 2

Chapter 3 : Partially hydrolysed poly(n-propyl-2-oxazoline): synthesis, aqueous solution properties and preparation of gene delivery systems

Contributors to this chapter:

Prof. Stanislav Rangelov, Institute of Polymers, Bulgarian Academia of Science

Dr.Emi Haladjova, Institute of Polymers, Bulgarian Academia of Science

Christo B. Tsvetanov Institute of Polymers, Bulgarian Academia of Science

Denitsa Momekova, Faculty of Pharmacy, Medical University of Sofia

Georgi Momekov, Faculty of Pharmacy, Medical University of Sofia

Pavletta S. Shestakova, NMR Centre, Bulgarian Academy of Sciences

Contributions of the candidate

Synthesis start polymers, hydrolysis experiments and DLS investigations

This work was integrally published as

Biomacromolecules,2016,*17*(11), pp 3580–3590

CHAPTER 3

Prologue

The mechanism for the partial hydrolysis of PAOx and the resulting distribution of PEI units along the polymer chain was thoroughly examined in chapter 2. This revealed a similar block-like distribution of the PEI units in both partially hydrolysed PEtOx and PPrOx. In this chapter the kinetics of the hydrolysis of PPrOx will be examined and the effect of the PEI units upon the T_{cp} will be screened in different conditions. PEI is a well-known gene transfer agent and the copolymers of PPrOx-PEI will be examined for their DNA binding ability. It has been shown that polymers with a Tcp form well defined cationically charged particles at elevated temperatures that form polyplexes with DNA. These polyplex particles can act as a template for coating with poly(N-isopropylacrylamide) via free radical polymerization resulting in stable polyplexes.

3.1 Introduction

Gene therapy is a modern approach for treating diseases in which biological molecules, such as nucleic acids (i.e., plasmid DNA, antisense oligonucleotides, therapeutic RNAs, and siRNA), are used as active components. These molecules are delivered to the nucleus of diseased cells, where they change the gene expression of the cell. A key element in gene therapy is the delivery of nucleic acids. This delivery is achieved using a carrier because the naked nucleic acid would be biodegraded before reaching its target and it wouldn't be taken up by cells. The carrier plays a crucial role in the delivery and expression of DNA in the cell because it prevents the degradation of the nucleic acid by nucleases in the blood. In addition, the desired cell can be targeted and penetrated.[1] Once internalized, a number of barriers and obstacles, such as escape from the endolysosomal pathway, trafficking through the cytosol and gaining nuclear entry,[2] must be overcome.

Two types of carriers can be used: viral and non-viral. The viral carriers are highly efficient and can deliver nucleic acids to a specific cell type. However, they tend to make the DNA modification of the guest permanent, inducing mutagenic and immunogenic responses.[3] The non-viral carriers consist of lipids, peptides or polymers. These are more advantageous than the viral carriers because they are safer and cheaper and exhibit a high loading capacity. In addition, these carriers can be produced in large quantities. The main disadvantage of non-viral carriers is the lower efficiency of nucleic acids delivery to cells, especially to the nucleus.[3,4] Polymethacrylates,[5] carbohydrate-based polymers[5,6] and poly(L-lysine)[7,8] are often used in this context but the most extensively studied systems include both branched (b-PEI) and linear polyethylenimines (L-PEI). b-PEI can be synthesized *via* acid catalyzed ring-opening polymerisation of aziridine,[1] while L-PEI can be prepared by acidic or basic hydrolysis of poly(2-alkyl-2-oxazoline)s (PAOx), such as poly(2-ethyl-2-oxazoline) (PEtOx) or poly(2-methyl-2-oxazoline) (PMeOx).[9] The PEI

polymers carry a positive charge on the amino functionalities (primary, secondary and tertiary for b-PEI and only secondary for L-PEI) that can interact with the negatively charged nucleic acid to form polyelectrolyte complexes known as *polyplexes*. For the design of new carriers, the toxicity must be reduced, and specific cell types must be targeted to create a more efficient vector. Therefore, the choice of a biocompatible, chemically versatile polymer such as PAOx is logical.[10–12] The biggest advantage of PAOx is its high chemical versatility, which allows the introduction of chemical functionalities *via* the end groups, side chain or post-polymerisation modification.[13–17] Previous studies have demonstrated that full hydrolysis is not mandatory, and copolymers containing the original polymer moieties (i.e., PEtOx and PEI) can be synthesized in a controlled manner.[18,10] This approach is advantageous due to a combination of the nucleic acid interacting moieties and other moieties that preserve most of the properties of the original polymer.

The precursors for L-PEIs, namely PAOx represent polymers that are synthesized *via* cationic ring-opening polymerisation (CROP) and exhibit huge potential for biomedical applications. In the development of carriers many other factors besides the nucleic acid binding ability are important. These factors include providing colloidal stability, long-circulation time, introduction of ligands targeting specific cells, reduced (or absence of) cytotoxicity and immunogenicity as well as improved biocompatibility. The PAOx polymers exhibit most of these properties. In addition to the chemical advantages, the PAOx family possesses interesting solution behavior. For example, PMeOx is water soluble, and by adding an extra carbon to the side chain resulting in PEtOx, a lower critical solution temperature (LCST) of 65 °C can be achieved depending on the chain length and concentration.[19,20] Upon addition of another carbon (i.e. poly(2-*n*-propyl-2-oxazoline) (PPrOx)), the LCST shifts to 25 °C.[19,21] Above the specific LCST, the polymer chains undergo reorganization due to dehydration, which under specific conditions can lead to the formation of colloidally stable nanosized particles that are referred to as mesoglobules.[22] The combination of PEI moieties (nucleic acid binding properties) and biologically tolerant moieties exhibiting LCST properties into a single copolymer chain may be a promising approach for the design of effective and biocompatible carriers for delivery of oligo- and polynucleotides as recently shown by Vlassi and Pispas for amphiphilic copolymers obtained by partial hydrolysis of 2-methyl-2-oxazoline/2-phenyl-2-oxazoline gradient copolymers.[23]

In this study, a series of random copolymers of *n*-propyl-2-oxazoline and ethylenimine was synthesized by partial acidic hydrolysis of PPrOx and the resulting materials were fully characterized. Polyplexes with DNA in a wide range of amino to phosphate group (N/P) ratios were prepared and their structure, stability, and cytotoxicity were studied under various experimental conditions. Some of the polyplexes were stabilized by the formation of a cross-linked polymer shell on their surface that acted as a physical barrier keeping the initial particles tight and preventing substantial swelling and eventual disintegration.

3.2 Materials and methods

3.2.1 Instrumentations

Size-exclusion chromatography (SEC). SEC was performed on an Agilent HPLC with a 1260 refractive index detector (RID) using dimethylacetamide containing 50 mM LiCl as an eluent at a flow rate of 0.6 $mL.min^{-1}$. Polymethylmethacrylate (PMMA) standards were used to calculate the molar mass values. The column set consisted of two PLgel 5 µm mixed D columns at 40 °C and a similar guard column (Agilent) in series. The chromatograms were analyzed using the Agilent Chemstation software with the GPC module. The copolymers obtained from hydrolysis were analyzed by size-exclusion chromatography (HFIP-SEC) using an Agilent HPLC that was equipped with a 1260 refractive index detector (RID). The eluent was hexafluoro-2-isopropanol (HFIP) containing 20 mM sodium trifluoroacetate at a flow rate of 0.426 $mL.min^{-1}$. PMMA standards were used to calculate the molar mass values. The column set consisted of two PSS PFG 100Å gel 5 µm mixed D columns and a similar guard column (Agilent) at 35 °C in series. The chromatograms were analyzed using the Agilent Chemstation software with the GPC module.

Nuclear magnetic resonance (NMR). The ^{1}H NMR and ^{13}C NMR spectra were recorded in $CDCl_3$ or DMSO-d_6 on a Bruker Avance 300 MHz or 500 MHz spectrometer. *Diffusion-ordered NMR spectroscopy (DOSY).* The DOSY measurements were performed on a Bruker Avance II+ 600 NMR spectrometer, equipped with a 5 mm dual $^{1}H/^{31}P$ Diff30 probe and a 40 A gradient amplifier, providing a maximum gradient strength of 11.8 $T.m^{-1}$. The experiments were performed at 25 and 37 °C, below and above cloud point temperature (T_{CP}) respectively. The DOSY spectra were acquired with the Diff suite package integrated in Topspin 3.2 by using a double-stimulated echo pulse sequence to compensate for possible convection during the measurements. The diffusion delay (Δ) was set to 50 ms (the relatively short value of the diffusion time was chosen to avoid loss of magnetization due to fast relaxation typical for large particles), sine shaped gradient pulses (δ) of 1.5 ms were applied. A gradient ramp of 24 linearly distributed gradient amplitude values was used. The starting and final gradient amplitudes were adjusted to ensure optimal signal attenuation, typically from 24 to 419 $G.cm^{-1}$ for the measurements at 37 °C and from 16 to 300 $G.cm^{-1}$ for the experiments at 25 °C. All spectra were recorded without sample spinning with 16k time-domain data points in the t2 dimension, 128 transients for each gradient increment, and a relaxation delay of 2 s. The DOSY spectra were measured using the following heating protocol: The sample temperature was equilibrated directly in the magnet using the water-cooling system of the Diff30 probe (BCU-20 variable temperature unit) to set and maintain the selected temperature (25 or 37 °C). First the experiments at 25 °C were performed and then the temperature was set at 37 °C for the measurements above the T_{CP}. The selected temperature was achieved and stabilized within max 20 min after setting the value (according to the reading of the BCU temperature unit). Since the quality of DOSY spectra is very

sensitive to any temperature drift or instabilities the experiments were started one hour after setting the temperature to ensure complete temperature stabilization within the sample volume. The spectra were processed with an exponential window function (line broadening factor 5), 32k data points in the F2 dimension, and 256 data points in the diffusion dimension, by using the fitting routine integrated in TopSpin 3.2 package. The diffusion coefficients were calculated by fitting the sum of the columns along the chemical shift of each signal in the DOSY spectrum with a variant of Stejskal-Tanner equation adapted for the particular pulse sequence used. Additional processing using CONTIN algorithm was also applied.

Dynamic and electrophoretic light scattering. To determine the T_{CP} of the polymers, dynamic light scattering (DLS) measurements were performed in disposable cuvettes at a concentration of 10 mg.mL^{-1} unless otherwise noted. The heating rate was 2 °C.min^{-1} with an equilibration time of 300 s starting at 10 °C and ending at 80 °C. The T_{CP} was taken as the onset of polymer aggregation using both the volume and intensity plots.

The hydrodynamic radii (R_h)of the polyplexes were determined at 65, 37 and 25 ºC on a Zetasizer Nano-ZS instrument (Malvern Instruments) that was equipped with a He-Ne laser (λ = 633 nm) and a non-invasive backscatter system, allowing for measurement of the scattered light at a scattering angle of 173º according the Stokes-Einstein equation:

$$R_h = kT/(6\pi\eta D)$$

where k is the Boltzmann constant, η is the solvent viscosity at temperature T in Kelvin and D is the diffusion coefficient. Each measurement was performed in triplicate.

The ζ potentials of the polyplexes were calculated from the obtained electrophoretic mobility at 37 and 25 ºC using the Smoluchowski equation:

$$\zeta = 4\pi\eta\upsilon/\varepsilon$$

where η is the solvent viscosity, υ is the electrophoretic mobility, and ε is the dielectric constant of the solvent.

3.2.2 Materials

HCl, NaOH, dichloromethane, *N*-isopropylacrylamide (NIPAM), *N,N*-methylenebis(acrylamide) (BIS), 2,2'-azobis(2-methylpropionamidine) dihydrochloride and polyethylenimine (M_w = 25000 Da) were obtained from Sigma-Aldrich and used as received. Salmon sperm DNA (D-1626, 2000 bp, corresponding to a molar mass of 1.32x10^6 Da) were also obtained from Sigma-Aldrich. PPrOx with different degrees of polymerisation (DPs) [i.e., $PPrOx_{75}$ (M_n 1.3x10^4 Da, Đ=1.04), $PPrOx_{160}$ (M_n 1.7x10^4 Da, Đ=1.2), $PPrOx_{200}$ (M_n 1.9x10^4 Da, Đ=1.4)] were synthesized according to a previously reported procedure.[24] DPs values were based on the monomer feed and NMR data, whereas M_n and Đ were determined by SEC (see below). All

of the polymerisation mixtures were prepared in a Vigor glove box and the polymerisation were performed at 140 °C for 32 min, except for $PPrOx_{75}$, which was synthesized at 85 °C for 7 hours. To prepare the polyplexes, a 100 $\mu g.mL^{-1}$ stock solution in ultrapure water (> 18 MΩ.cm) was used.

Cell lines and culture conditions

The HL-60 (acute promyelocyte leukemia) and RPMI-8226 (multiple myeloma) cell lines were supplied by DSMZ GmbH, Germany. The urinary bladder carcinoma EJ was obtained from American Type Cell Culture, USA. In general, the cells were cultured in a controlled environment (i.e., 37 °C in 5% CO_2 humidified atmosphere). The cell lines were maintained in RPMI 1640 supplemented with 2 mM L-glutamine and 10% fetal calf serum. These cell lines were also subcultured twice weekly to maintain continuous logarithmic growth. The EJ cells were used prior to the seventh passage.

3.2.3 Procedures

Kinetics of hydrolysis of poly(n-propyl-2-oxazoline).

A stock solution of $PPrOx_{75}$ (M_n 1.3x10^4, corresponding to DP 75, Đ = 1.04) was prepared by dissolving 3 g in 50 mL of a 6 M HCl solution. 15 mL of the polymer stock solution was added to closed microwave *via*ls and heated to 100 °C (internal temperature) in dry sin blocks. At various time intervals, a sample was removed and neutralized by the addition of a NaOH solution to calculate the degree of hydrolysis based on ^{1}H NMR spectroscopic analysis. *^{1}H NMR (300 MHz, δ in ppm, $CDCl_3$): 1-1.2 (3 H,CH_2-C$\underline{H}_3$), (2 H,C$\underline{H}_2$-CH_3); 2.3-2.5 (2H,C$\underline{H}_2$-CH_2-CH_3); 2.6-2.8 (4 H,C$\underline{H}_2$-NH); 3.2-3.5 (4 H,C$\underline{H}_2$NCH_2)*. The integral ratios of the peaks at 2.6-2.8 ppm and 3.2-3.5 ppm were utilized to calculate the degree of hydrolysis.

Preparation of the PPrOx-PEI copolymers.

3 g of PPrOx with various DPs (DP 75, 160, or 200) were dissolved in 50 mL of a 6 M HCl solution and subjected to hydrolysis for certain periods of time to obtain the desired degree of hydrolysis according to the kinetic study. The solutions were neutralized with NaOH and freeze-dried. The copolymers were extracted with CH_2Cl_2, and after removing the solvent, water was added. A dry powder was obtained after freeze-drying. The codes, DPs, PEI contents, total molecular weight and dispersity of the resulting copolymers are provided in Table 1.

Table 1. Molecular weight characterization data and PEI contents of PPrOx-PEI copolymers obtained by acidic hydrolysis of PPrOx homopolymers of different degrees of polymerisation.

Code	DP[a]	PEI,[b] %	M_n,[c] Da	Đ[c]
$PPrOx_{71}$-PEI_4	75	5	10 100	1.4
$PPrOx_{68}$-PEI_7	75	10	12 500	1.2
$PPrOx_{149}$-PEI_{11}	160	7	21 200	1.3
$PPrOx_{146}$-PEI_{14}	160	8.5	18 900	1.3
$PPrOx_{186}$-PEI_{14}	200	7	24 600	1.4
$PPrOx_{182}$-PEI_{18}	200	9	34 000	1.2

[a] based on monomer feed and ^{1}H NMR; [b] based on ^{1}H NMR; [c] obtained by SEC

Formation of polyplexes. The polyplexes were formed by dropwise addition of appropriate amounts of DNA (100 μg.mL^{-1}) into an aqueous solution of the copolymer (0.5 mg.mL^{-1}) at 65 °C under vigorous stirring. The polyplexes were prepared in amine to phosphate group ratios (N/P) in the 0.5-10 range.

Coating of polyplex nanoparticles. To form a cross-linked polymer shell around the polyplex particles, seeded radical polymerisation of NIPAM was employed. The cross-linking reaction was carried out in aqueous media under mild conditions according to a previously published procedure.[25,26] NIPAM (5 mmol.L^{-1}) and BIS cross-linker (0.26 mmol.L^{-1}) were dissolved in water, and the mixture was added to the polyplex dispersion at 65 °C under a nitrogen atmosphere with vigorous stirring. After 30 min, 2,2'-azobis(2-methylpropionamidine) dihydrochloride (1 mmol.L^{-1}) was introduced to initiate the copolymerisation of NIPAM and BIS. The cross-linking reaction was allowed to proceed at 65 °C for 5 h.

Cytotoxicity assay. The cytotoxicity of the tested polymers and their polyplexes with DNA was assessed using the MTT-dye reduction assay. This method is based on the ability of vital cells to metabolize a yellow tetrazolium salt to the violet formazan product, which is spectrophotometrically quantified. The assay was performed according to a previously described protocol[27] with slight modifications.[28] Exponentially growing cells were plated in 96-well sterile plates at a density of 10^4 cells/well in 100 μL of medium and incubated for 24 h. Then, the tested polymers or polyplexes were applied to the cells in a concentration range of 5-40 μg.mL^{-1} or 2.5 -14 μg.mL^{-1}, respectively, for 72 h. For each concentration, a set of 8 wells was used. After a 72 h of continuous exposure, 10 μL aliquots of the MTT solution (5 mg.mL^{-1}) were added to each well, and the plates were incubated for additional 4 h at 37 °C in a humidified 5 % CO_2 atmosphere. The produced formazan crystals were solubilized by addition of HCOOH (5 %) acidified isopropanol. The

MTT-formazan absorbance was determined on a microprocessor-controlled multiplate reader (Labexim LMR-1).

3.3 Results and discussion

3.3.1 Hydrolysis of PPrOx

The hydrolysis or PPrOx was investigated under acidic conditions in 6 M HCl at 100 °C. The hydrolysis kinetics was determined by taking samples at different times and the degree of hydrolysis (i.e. the copolymer compositions) of these samples was determined *via* ^{1}H NMR spectroscopy from the signals at 2.6-2.8 ppm and 3.2-3.5 ppm (Figure 3-1). It was observed that during the initial stage of the reaction, white milky dispersions were formed that sometimes contained macroscopic flocks, which can be ascribed to performing the reaction at a temperature well above the T_{CP} of the starting PPrOx. During hydrolysis, the side chains of PPrOx are cleaved, resulting in the formation of ethylenimine units while butyric acid is released. The appearance of a signal corresponding to the methylene protons adjacent to NH at 2.8 ppm (Figure 3-1) as well as its increase in intensity with reaction time quantitatively confirmed the progress of hydrolysis.

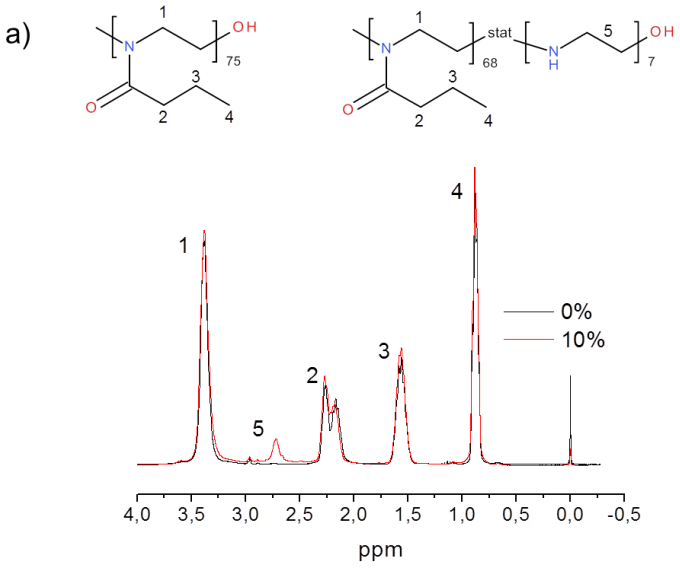

Figure 3-1 ^{1}H NMR spectra of the initial PPrOx (black line) and the resulting PPrOx-PEI copolymer with 10 % PEI content (red line).

The conversion, which is expressed as the degree of hydrolysis as a function of reaction time, is shown in Figure 3-2. The hydrolysis is slow during the initial stage of the reaction, which is most likely due to the hydrophobicity of the polymer at temperatures above its T_{CP} of 25 °C. Nonetheless, even under these reaction conditions, H_3O^+ can slowly reach the side chains and cleave them off. With the slow progress of the hydrolysis in the initial stage, the polymer chains become more soluble, which accelerates the hydrolysis (Figure 3-2, linear increase of conversion). The conversion reached a plateau at about 90 % after ca. 2 hours. In comparison to the previously investigated hydrolysis of PEtOx, the hydrolysis of PPrOx is much slower ascribed to the higher hydrophobicity of PPrOx.[11] The hydrolysis of PEtOx was already 50% after 40 minutes (DP 100) while the PPrOx (DP 75) barely reaches 20% hydrolysis.

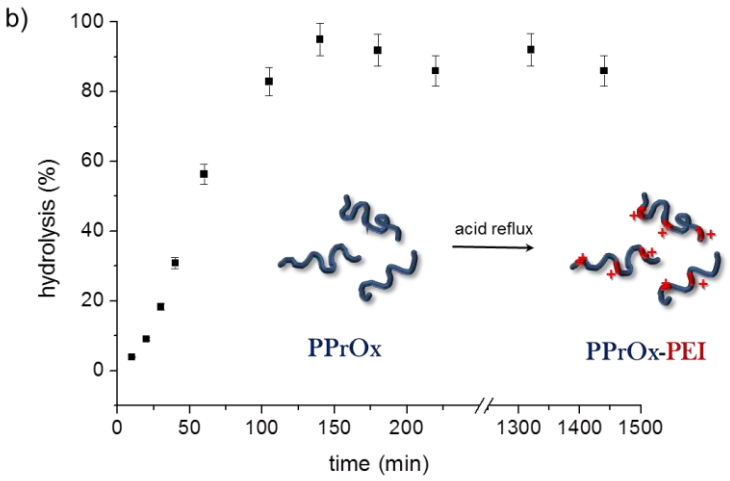

Figure 3-2 Degree of hydrolysis (%)of $PPrOx_{75}$ as a function of the reaction time. Each point was measured in triplicate.

It is important to note that after hydrolysis the copolymers maintained their narrow Đ (Figure 3-3), which implied that the polymer backbone was not cleaved during the reaction and well-defined PPrOx-PEI copolymers were obtained. Minor variation in elution time during HFIP SEC can result from variation in HFIP water content obstructing hard conclusions on molar mass from SEC. Nonetheless, the SEC traces clearly show that the molar mass distribution remains intact during hydrolysis.

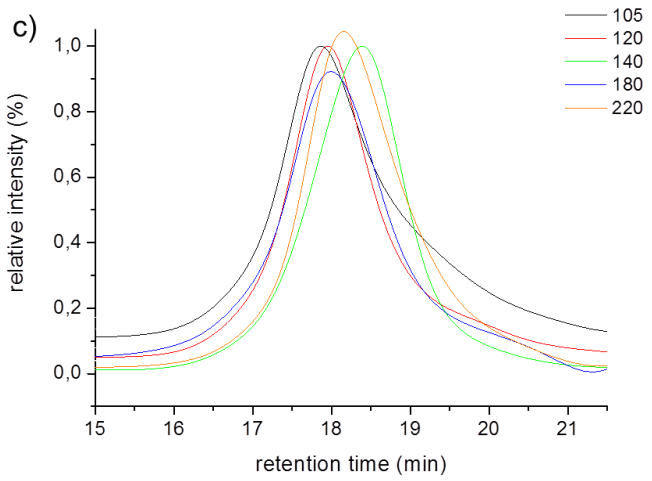

Figure 3-3 SEC traces in HFIP of selected samples taken at different time intervals (min) during the process of hydrolysis.

3.3.2 Effect of PEI-units on T_{cp} of PAOx-PEI

The phase separation of an aqueous solution of PPrOx upon crossing the T_{CP} is driven by entropic dehydration of the side chains leading to release of the hydrating water molecules to the bulk water. Upon hydrolysis of PPrOx, an amine functionality is introduced into the backbone, which can influence the LCST properties of the resulting copolymers. A set of copolymers based on $PPrOx_{75}$ with PEI contents ranging from 3 to 65 % were synthesized based on the determined hydrolysis kinetics. The T_{CP} of these copolymers was determined using DLS under various experimental conditions: in water, at different pH, and in presence of bovine serum albumin (BSA) and KSCN. DLS was utilized to determine the T_{CP} as turbidimetry was found to be inaccurate possibly due to sticking of the copolymer material to the glass as well as formation of low scattering small aggregates. The T_{CP} was taken as the onset of polymer aggregation from DLS. The results are summarized in Table 2.

In water, the T_{CP} of $PPrOx_{75}$ was found to be 24°C. Upon increasing the PEI content to 16 %, a rather small increase of T_{CP} was observed with maximal 8 °C increase up to a T_{CP} of 32 °C. This rather small increase in T_{CP} may be ascribed to only partial protonation of the PEI units in water as well as potential shielding of the (charged) PEI units by the rather hydrophobic PPrOx units. Suh et al.[29] demonstrated that about 77-85 % of the amines in PEI were unprotonated at neutral pH. The 16% showed that around 30% is of the CH2 is located in PEI, this means if we assume that we have block with three PEI units this means that 90% of the PEI is located in a block distribution. Further increasing the PEI content led to the observation of a plateau in T_{CP} around 50 °C for a PEI content of 35 to 65 %. In chapter 2 we discussed that the polymers show a block-like distribution of PEI units along the chain. This means that it would be

difficult to protonate all of the amines and in the block not all of them are protonated. This also means that the charge present is enough to induce repulsion between the chains. Because the pH value of the solution plays an important role in the protonation of the PEI units, the T_{CP} of the copolymers was also determined at pH of 5 and 11 where the PEI units are expected to be fully protonated and deprotonated, respectively. Unexpectedly, the T_{CP} results at both pH values are the same confirming that the PEI units are rather shielded and do not have a strong influence on the solubility behavior of the PPrOx-PEI copolymers. Instead, the minor decrease in T_{CP} at pH 5 and 11 may be ascribed to salting out effects. The next step involved the addition of a strong "salting-in" salt, namely KSCN that is known in the Hofmeister series to increase the solubility of non-polar molecules and decrease the order in the water shell. The addition of this salt resulted as expected in a significant increase in T_{CP} as previously also shown for PPrOx.[29] The general trend that more PEI units increase the T_{CP} was retained in this series. Finally, the effect of the presence of a negatively charged protein, namely BSA, was studied. By adding the BSA the positive charges were shielded and this could potentially have an effect on the T_{CP}. This means that there is a strong interaction with the negatively charged protein. The T_{CP} of PPrOx-PEI copolymers with a hydrolysis degree lower than 16 was not affected by the presence of BSA. The PPrOx-PEI copolymers with higher PEI content revealed a significant increase in T_{CP} indicating that the polymer interacts with BSA, which suppresses aggregation providing a first indication that these copolymers may be used for the formation of polyplexes with negatively charged nucleic acids.

Table 2. T_{CP} values (°C) for a series of PPrOx-PEI copolymers with increasing PEI content from 0 to 65 % and total DP of 75. The copolymer concentration was 10 mg.mL^{-1}. The T_{CP} values were determined as the onset of aggregation from DLS.

% PEI	Water	BSA[a]	pH 11	pH 5	KSCN[b]
0	24.0	22.0	21.0	24.0	40.0
3	24.0	24.0	22.0	21.0	47.5
5	30.0	30.0	24.0	21.0	42.5
11	30.0	30.0	24.0	23.0	45.0
16	32.0	34.0	24.0	26.0	50.0
35	55.0	60.0	40.0	39.0	57.5
58	50.0	69.0	48.0	48.0	67.5
65	48.0	-	49.0	48.0	65.0

3.3.3 DOSY and ζ-potential measurements of PPrOx-PEI

As mentioned in the previous section, upon the introduction of the ethyleneimine functionality, the partially hydrolysed copolymers preserved their thermoresponsive behavior. Next, the effect of the temperature induced phase transition of the PPrOx-PEI copolymers, shown in Table 3, on the physicochemical properties was investigated to evaluate their potential to interact with DNA. The copolymers in this set exhibit various total DPs (from 75 to 200) and are characterized by their PEI contents (i.e., 5 – 10 % range). The increasing PEI content shifted the transition (T_{CP}) to temperatures that were substantially higher than the physiological temperature, as mentioned in the previous section. In addition, a substantial increase in the cytotoxicity can be anticipated for the copolymers with a higher PEI content. Therefore, the latter were not further studied.

Table 3. ζ-potential of a series of PPrOx-PEI copolymers in aqueous solution measured at 25 and 37 °C.

Copolymer	ζ-potential (mV)	
	25 °C	37 °C
$PPrOx_{71}$-PEI_4	-2.6 ± 5.3	25.5 ± 6.5
$PPrOx_{68}$-PEI_7	-6.3 ± 3.1	31.8 ± 8.4
$PPrOx_{149}$-PEI_{11}	-5.0 ± 4.4	19.6 ± 5.6
$PPrOx_{146}$-PEI_{14}	-6.1 ± 4.7	34.2 ± 6.7
$PPrOx_{182}$-PEI_{18}	-6.1 ± 4.2	19.0 ± 6.9

DOSY has been developed as a valuable tool for complex mixture analysis. The DOSY spectra typically represent a two-dimensional matrix that correlates the chemical shifts of the signals (the horizontal scale) with the diffusion coefficients (the vertical scale). The method exploits the differences in the diffusion coefficients, which are related to particle sizes, to spectroscopically discriminate between components in a solution mixture. Figure 3-4 shows the DOSY spectra of a 1 $mg.mL^{-1}$ solution of the $PPrOx_{68}$-PEI_7 copolymer (corresponding to 10% PEI content) recorded at 25 and 37 °C, which is below and above the T_{CP}, respectively. At 25 °C, the signals are very well resolved, and their chemical shifts are correlated with one population of particles with a diffusion coefficient of 6.0 x 10^{-11} $m^2.s^{-1}$ (Figure 3-4a), corresponding to a hydrodynamic radius of approximately 3.3 nm representing molecularly dissolved copolymer chains. The signals changed drastically at 37 °C (Figure 3-4b) and their hyperfine structure disappeared, which

may be due to reduced mobility resulting from formation of large aggregates, presumably mesoglobules. Indeed, the DOSY spectrum measured at 37 °C shows the existence of a second population of slow moving particles with a diffusion coefficient of approximately 0.5 x 10^{-11} $m^2.s^{-1}$, corresponding to a hydrodynamic radius of ≈ 50 nm, when assuming spherical shape. The additional treatment of the diffusion profiles with CONTIN (Figure 3-4b) indicated the presence of even larger particles with broad size distribution (170–260 nm), which are most likely clusters of mesoglobules.

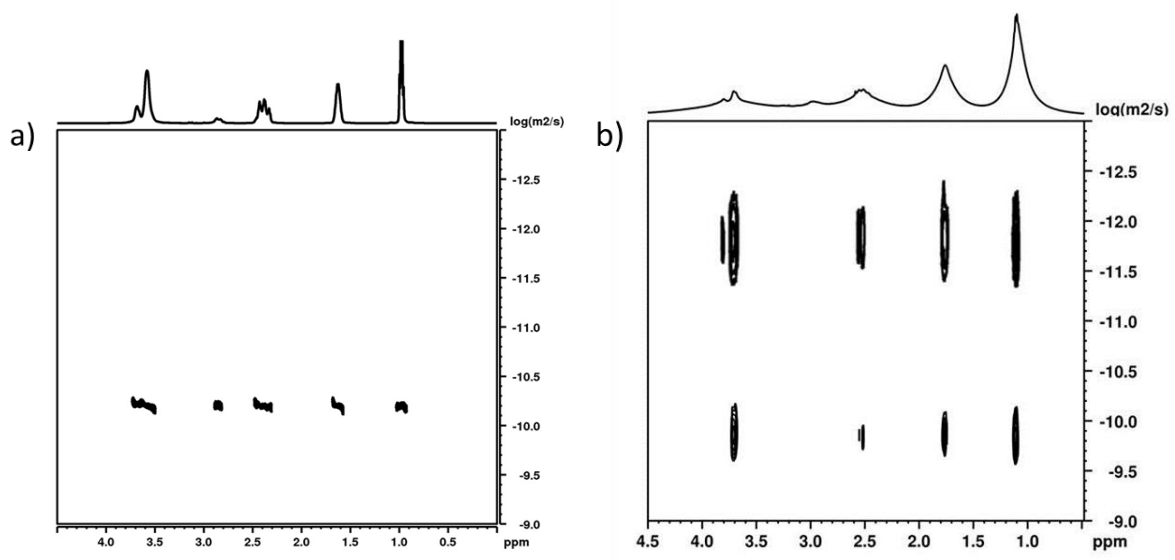

Figure 3-4 DOSY spectra of a 1 $mg.mL^{-1}$ solution of $PPrOx_{68}$-PEI_7 recorded at 25 (a) and 37 (b) °C.

Dynamic light scattering, which is an independent method for determining the particle size, confirmed the formation of large (R_h up to 120 nm) particles (mesoglobules) upon heating above the transition temperature. The differences in the mesoglobule size may be due to the different heating protocols, which are known to greatly influence their size and size distribution.[30,31] Thus, the fast heating (temperature jump) leads to fast phase separation and formation of small kinetically frozen mesoglobules while the slow (gradual) heating allows the growth of the particles.

Very interesting results were obtained from the electrophoretic light scattering (Table 3). At 25 °C, when the copolymers were molecularly dissolved, the ζ-potential was close to zero/slightly negative, which is in agreement with the small number of ethylenimine units, only part of which are charged.[32] The, insignificant in magnitude, negative values of the ζ-potential most probably derive from special arrangement of the hydration layer around the copolymers and strongly suggest that the charged ethylenimine units are shielded by the PPrOx moieties so that the copolymers at those conditions behave as non-ionic species. At 37 °C, however, the ζ-potential became strongly positive, implying that aggregation induced relocation of the positive charges to the outermost surface of the mesoglobules occurred simultaneously with the polymer phase transition. The rearrangement is schematically

represented in Figure 3-5 and could be considered beneficial since it would increase the accessibility of the positive charges and, in turn, favor the interactions with DNA and formation of better defined polyplexes. Besides the relocalization effect, we can speculate on lowering of pK_a due to the collapse of PPrOx and more effective protection of the amino groups as reported elsewhere for other systems.[33–35]

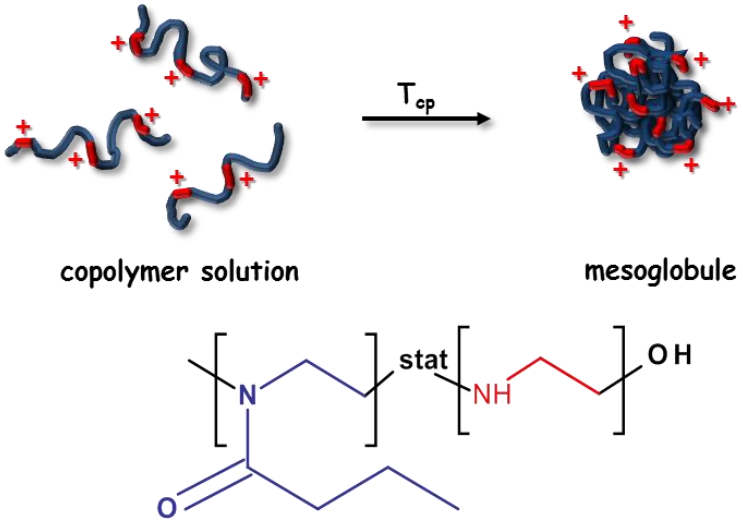

Figure 3-5 Schematic representation of the formation of mesoglobules from PPrOx-PEI copolymers in aqueous solution as well as the proposed rearrangement of the positive charges.

3.3.4 Complexation of PPrOx-PEI with DNA

The picture, derived from the previous section, illustrates that well-defined nanosized particles (mesoglobules) are formed at elevated (invariably above the T_{CP}) temperatures that are composed of a large hydrophobic core of collapsed PPrOx and a thin positively charged shell with amino groups accessible for complexation with oppositely charged nucleic acids. This structure of the charged mesoglobules mimicks the structure of the globular proteins to a great extent. One can anticipate that with a further increase of temperature those features would become more pronounced, i.e., the core would become more tight and compact due to further dehydration and the positively charged groups would become more accessible, which would favor the polyplex formation. Therefore, the complexation with DNA was performed at temperatures well above the LCST of the PPrOx-PEI copolymers by drop-wise addition of an aqueous solution of DNA to a heated to 65 °C copolymer dispersion under vigorous stirring.

Polyplexes were obtained at N/P ratios in the 0.5 – 10 range. At 65 °C, the polyplex particles were relatively small with hydrodynamic radii as determined by DLS typically less than 100 nm (Figure 3-6). The three studied copolymers contained the same amount of PEI (8.5 – 10 %) but a different total DP. However, no noticeable effect of the DP on the particle size was observed with the exception of the copolymer with the lowest DP, which exhibited a slight increase in R_h, to approximately 200 nm only at

the highest N/P ratios (Figure 3-6a). Lowering the temperature to 25 °C had a dramatic effect on the particle sizes because a 5- to 10-fold increase in R_h at a N/P ≥ 2 was observed (Figure 3-6). The increase was significantly smaller at N/P < 2 and the size of the resulting particles was still appropriate for intravascular administration. After a further increase in temperature to the physiological value of 37 °C, the behavior of the systems did not change and the R_h vs. N/P curve patterns generally followed those at 25 °C.

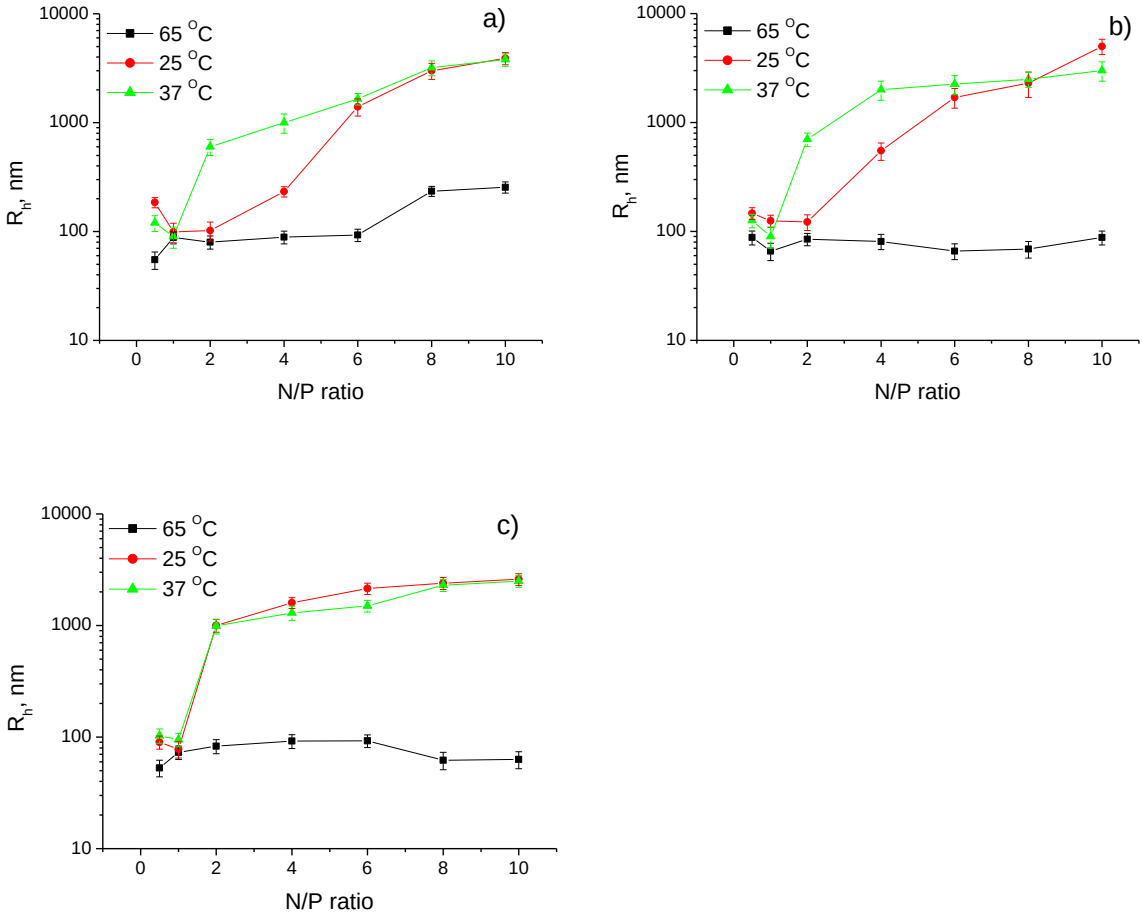

Figure 3-6 Influence of the N/P ratio on the hydrodynamic radii (R_h) of the polyplexes obtained with the $PPrOx_{68}$-PEI_7 (a), $PPrOx_{146}$-PEI_{14} (b), and $PPrOx_{182}$-PEI_{18} (c) copolymers. The polyplexes were prepared at 65 °C, then cooled to 25 °C and heated again to the physiologically relevant 37 °C. The hydrodynamic radii were determined by DLS.

Upon decreasing temperature to 25 °C, disintegration of the PPrOx core and transition to a molecularly dissolved state were initiated. However, the DNA remained bound to the PEI moieties and at N/P ratios ≥ 2, the DNA acted as a physical cross-linking agent. As a result, enormously swollen microgel particles that tended to further aggregate due to the low ζ-potential (Figure 3-7) were formed. The rearrangement is schematically represented in Figure 3-8. At lower N/P ratios (< 2), the role of DNA, which was in excess,

was no longer as a cross-linking agent. Instead, the layer that it formed on the surface of the mesoglobules by binding to the PEI moieties probably provided a barrier function similar to that of a membrane, which strongly reduced the mobility of the PPrOx moieties and prevented the latter from leaving the initial polyplex particles. Furthermore, the strongly negative ζ-potential (Figure 3-7) contributed to the colloidal stability of the particles and inhibited aggregation. The overall size of the particles increased only slightly, which can be ascribed to swelling of the PPrOx core. The rearrangement that occurred upon cooling affected only the PPrOx cores, which transformed from dense and compact to swollen and loose.

The expected restoration process of the initial structure of the polyplex particles at N/P ≥ 2 did not take place upon heating to 37 °C, though this temperature was above the T_{CP}. The values of the ζ-potential were restored (Figure 3-7), but the R_h values were not (Figure 3-6). To explain this result, it is important to recall the restricted mobility of the copolymer chains that are fixed to the large DNA molecules *via* numerous cross-linking centers/junctions (Figure 3-8). This limited freedom prevented the re-formation of the initial structures. Instead, small in volume but large in number PPrOx domains, interconnected *via* DNA, were presumably formed (Figure 3-8). With this rearrangement, the PEI moieties that were not involved in interactions with DNA (note that at N/P ≥ 2, the copolymer is in excess) preferentially migrated to the surface of the microgel particles, whereas DNA remained mainly in their interior, which explains the restoration of the ζ-potential values.

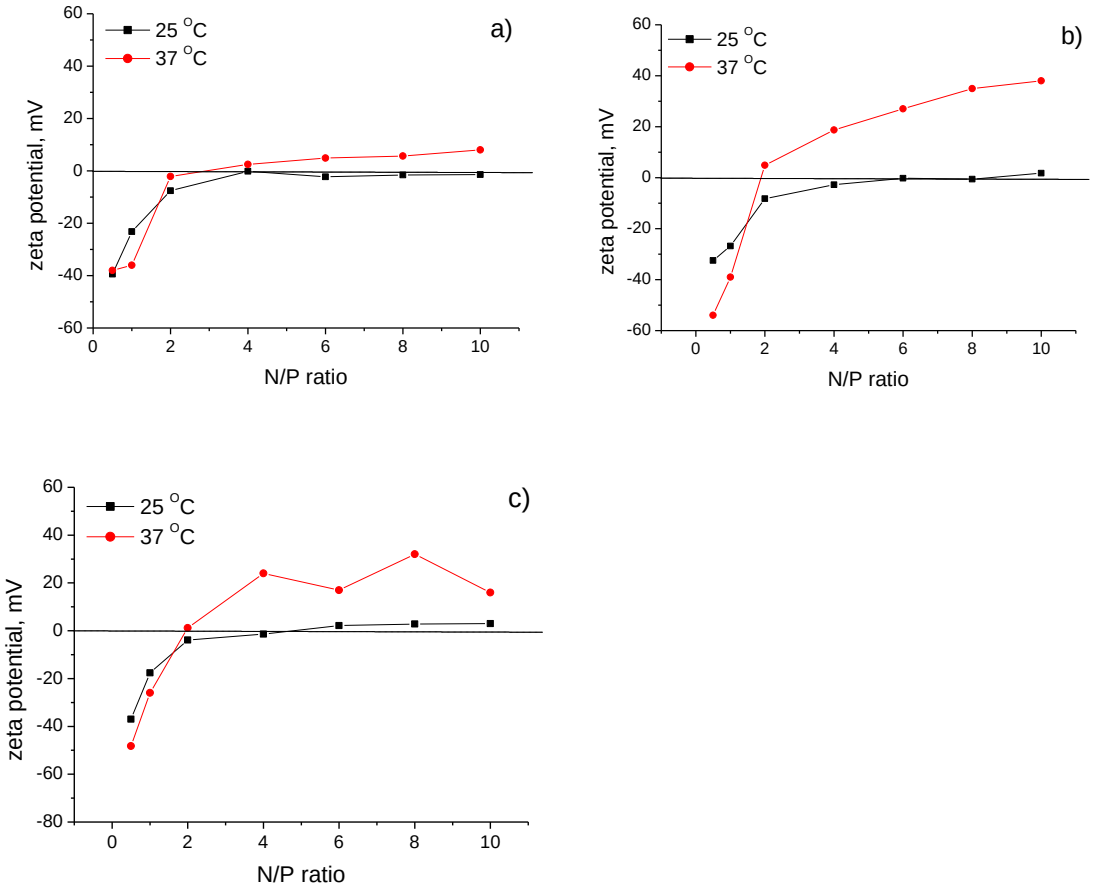

Figure 3-7 Variations of ζ-potential of polyplexes formed from $PPrOx_{68}$-PEI_7 (a), $PPrOx_{146}$-PEI_{14} (b), and $PPrOx_{182}$-PEI_{18} (c) copolymers with the N/P ratio at 25 and 37 °C.

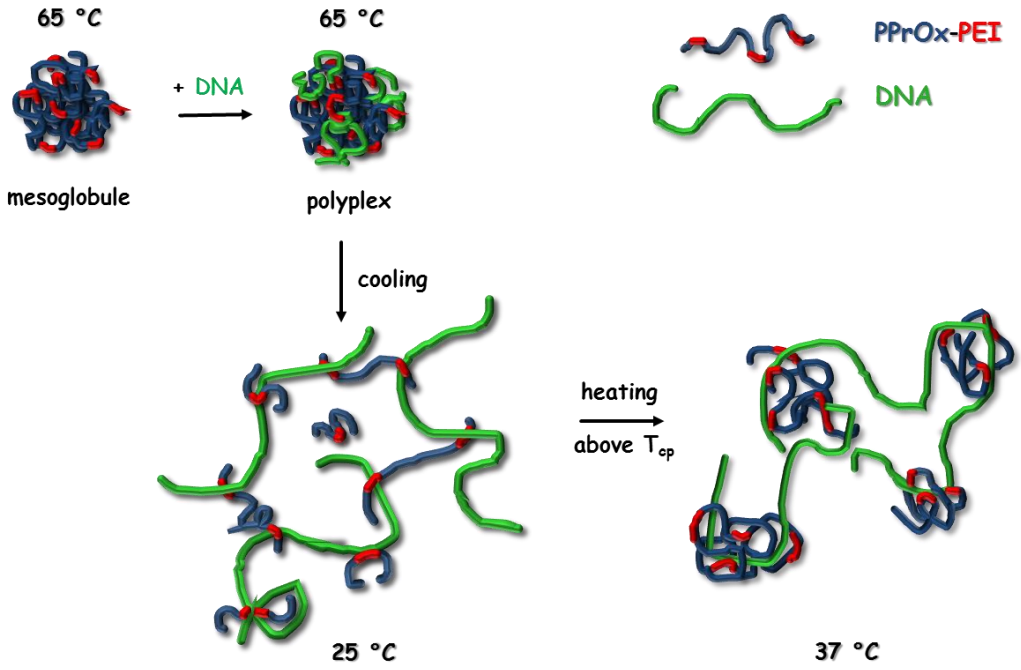

Figure 3-8 General scheme of the rearrangements of the structures formed from PPrOx-PEI copolymers and DNA at N/P ≥ 2 due to temperature variations. Up: formation of mesoglobules and polyplex particles at elevated temperatures. Down: schematic representation of part of the interior of the enormously swollen polyplex particles at lower temperatures and their rearrangement upon heating from 25 to 37 °C. Interparticle aggregation may also contribute to dimensional changes. Structures are not drawn to scale.

3.3.5 Coating of the polyplex particles

In summary, the results discussed in the previous section indicate that upon cooling from 65 to 25 °C followed by heating to a physiologically relevant temperature, the polyplex nanoparticles at N/P ≥ 2 underwent unfavorable rearrangement, which was associated with a tremendous increase in the size and formation of microgel particles. The particles at N/P < 2 typically preserved their initial dimensions. However, these particles were negatively charged, which might also influence unfavorably the interactions with cell membranes and, in turn, the cellular uptake. To avoid undesirable rearrangement into large microgel particles, the initial polyplex nanoparticles were stabilized by coating them with a cross-linked polymeric shell. A similar approach has recently been employed to prepare polymeric nanocapsules[36] and cover complexes of DNA and cationic copolymers.[25,26,37] This method employs heterophase radical copolymerisation that occurs on the surface of the (polyplex) particles. The resulting shell acts as an envelope (i.e., a physical barrier) that provides mechanical strength and keeps the initial particles tight, preventing substantial swelling and eventual disintegration. In addition, stealth properties, targeting, and membrane functions can be imparted to the more sophisticated constructions.[30]

The polyplex nanoparticles that were prepared from the $PPrOx_{182}$-PEI_{18} copolymer at N/P = 4 were coated *via* heterophase (seeded) copolymerisation of Poly(N-isopropylacrylamide) NIPAM and NN-methylenbisacrylamide (BIS). The latter acted as a cross-linking agent and the polymerisation was initiated by 2,2'-azobis(2-methylpropionamidine) dihydrochloride. Note that this is a model system for proof of concept and for future continuation of this work towards gene delivery a degradable crosslinker will be introduced.

The construction of the coating was performed immediately after formation of the polyplex nanoparticles at 65 °C. The monomer and initiator amounts as well as the polyplex concentration were selected to obtain a shell thickness of approximately 30 nm. The consecutive steps for shell formation and cooling to 25 °C as well as the corresponding variations in hydrodynamic radii are shown in Figure 3-9. The construction of the shell was associated with a slight increase in Rh from 93 to 125 nm. The shell thickness was calculated from the difference between the hydrodynamic radii of the initial polyplex and the coated polyplex particles. In particular, the shell thickness for the system based on $PPrOx_{182}$-PEI_{18} was 32 nm, which was in very good agreement with the theoretical value. This result indicates precise and effective control during the coating procedure. Upon cooling to 25 °C, the coated polyplex particles slightly increased in size. As previously suggested,[38] the shell, which is based on PNIPAM, acts as water-permeable elastic and flexible protective outer layer, possessing properties of a thermoresponsive hydrogel that allows for swelling upon cooling and deswelling (shrinking) upon heating. Note that the LCST of PNIPAM is 32 °C and upon cooling from 65 to 25 °C this critical temperature is crossed. A 50 % increase in the particle dimensions was observed for the systems based on $PPrOx_{182}$-PEI_{18} (Figure 3-7). The increase was even smaller (below 22 %) for the systems based on copolymers with lower degrees of polymerisation (data not shown). Assuming that the shells were constructed following the same procedure, which implied the same cross-linking density, one may conclude that not only the PNIPAM shell but the copolymer molar mass has a substantial role in the swelling process. Nevertheless, the size increase of the coated particles upon cooling may be considered insignificant compared to the enormous (5- to 10-fold) increase in the size of non-coated polyplex particles (see above). This approach involving coating of the polyplex particles was successful in terms of retaining their colloidal stability and preserving the initial physicochemical parameters, especially the hydrodynamic dimensions. Other benefits include reduction of the strongly positive (or negative) values of the ζ-potential, which prevents salt-induced aggregation, reduces the protein and cell interactions that lead to extension of the plasma circulation time, modulates the interactions with the cell surface and cellular compartments, and reduces cytotoxicity. Whereas the former are subjects of forthcoming publications, the cytotoxicity evaluation of the copolymers, polyplexes and coated polyplexes is presented in the next section.

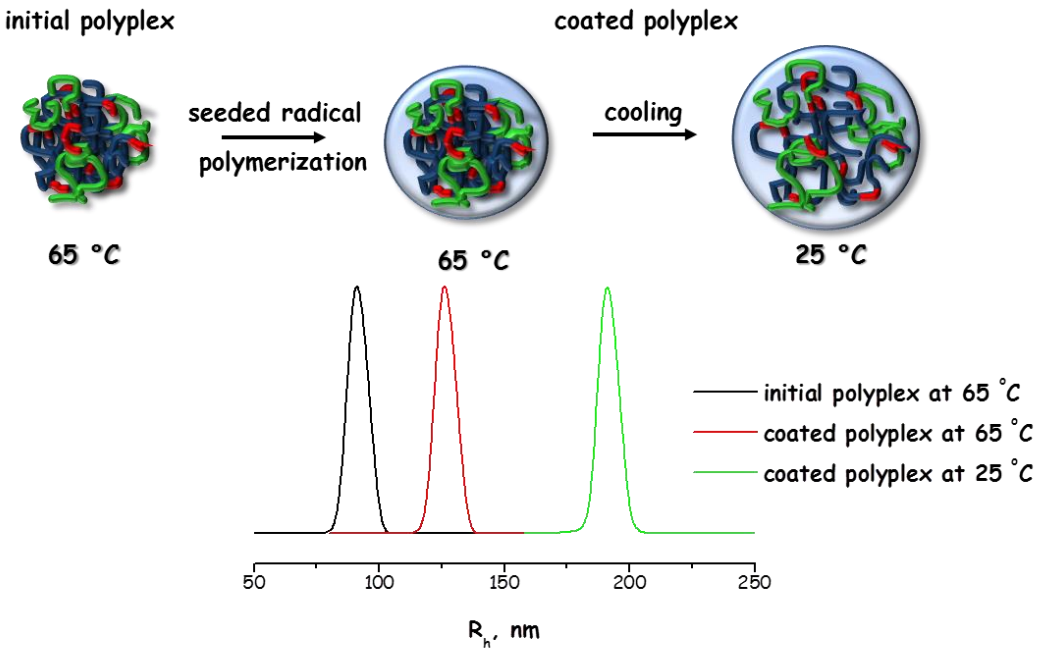

Figure 3-9 Schematic presentation of the approach for coating polyplex nanoparticles and their behavior upon cooling (upper panel). Size and size distribution variations of initial polyplex and coated polyplex, based on $PPrOx_{182}$-PEI_{18} copolymer at N/P = 4 at different temperatures (lower panel). Expansion of both PNIPAM shell and polyplex contribute to the dimensional changes

3.3.6 Cytotoxicity evaluation

The lack of toxicity is an important prerequisite for the excipients used in preparation of drug or gene delivery systems. However, one of the major limitations against broad application of PEI is its prominent cytotoxicity. Therefore, a basic cytotoxicity evaluation of the copolymers and their counterpart polyplexes was performed using a panel of human cell lines with different cell type and origin (RPMI-8226, HL-60, and EJ). The corresponding concentration-response curves are shown in Figure 3-10. As evident from the results, the tested copolymers exhibited strong concentration-dependent cytotoxic effects, causing almost total eradication of viable cells at the highest concentration levels. For the sake of comprehensiveness we also tested the cytotoxicity potential of the reference PEI. Despite of the shown inhibitory effect on the cell proliferation, the tested copolymers are less toxic as compared to PEI which has an IC_{50} values of 10.7 µM (Figure 3-10d). The toxicity increase could be caused by the fact that all positive charges are on the outside of the mesoglobule and thus in direct contact with the organism.

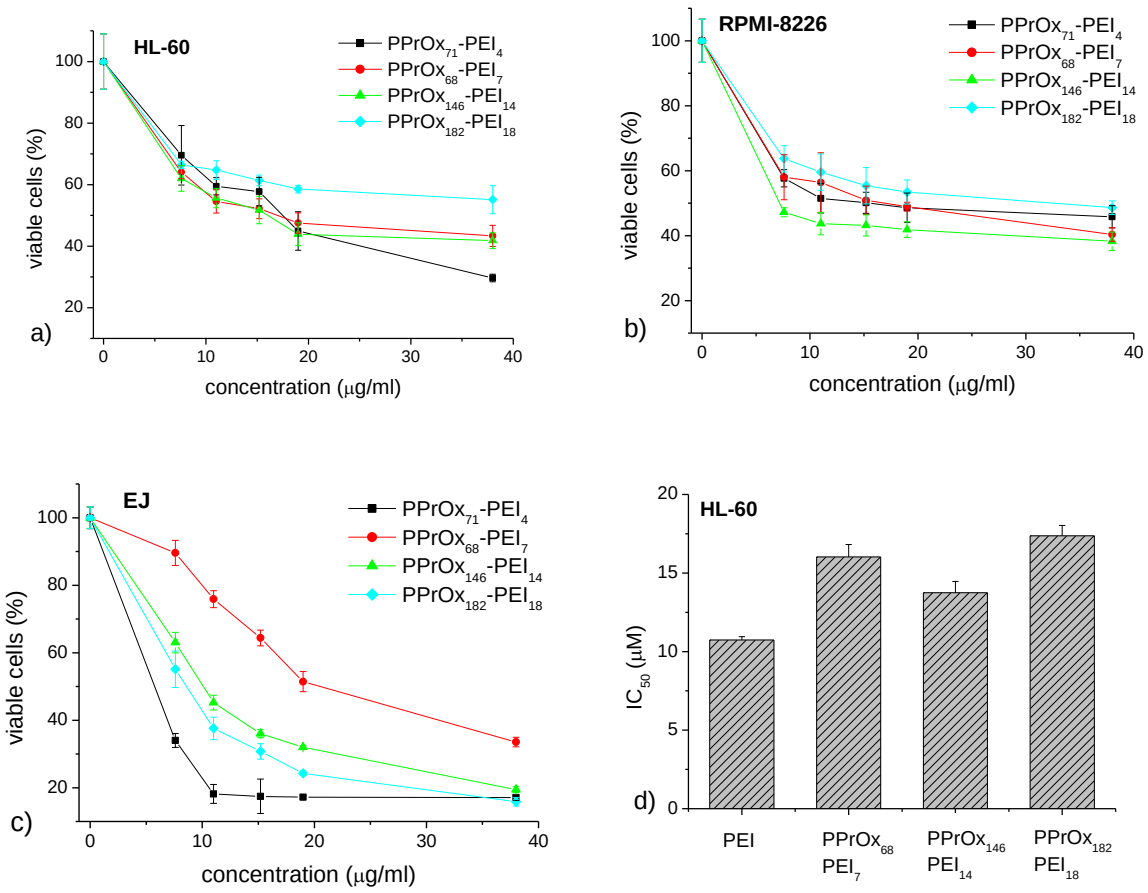

Figure 3-10 (a-c) Cytotoxicity of a series of PPrOx-PEI copolymers determined by the MTT-dye reduction assay after 72 h of continuous exposure towards a panel of human cell lines. Each data point represents the arithmetic mean ± SD of 8 separate experiments. (d) IC_{50} values of selected PPrOx-PEI copolymers and referent PEI towards HL-60.

Considering the proposed utility of tested copolymers for gene delivery vectors, we sought to determine the cytotoxic potential of their non-coated and PNIPAM-coated polyplexes after 72 h exposure (Figure 3-9). In contrast to the cytotoxicity of the free copolymers, the polyplexes are characterized with far less prominent inhibitory effects on cell viability (cf. Figure 3-8 a-c with left panel of Figure 3-9). Even at the highest concentrations the inhibitory effect on cell viability was not more than 30 % as compared to the untreated control. This lower cytotoxicity of the polyplexes is probably due to shielding the positive charges of PEI resulting from the complexation with the DNA. The coating of the polyplexes with PNIPAM contributed to further loss of cytotoxic effects (Figure 3-9) and rendered them practically devoid of cytotoxicity. The favorable effect is better pronounced for HL-60 and RPMI-8226. Obviously, the additional diffusion steric barrier afforded by the coating hampered the accessibility of the toxic cationic surface groups of the PPrOx-PEI to the biological targets, mediating their cytotoxicity.

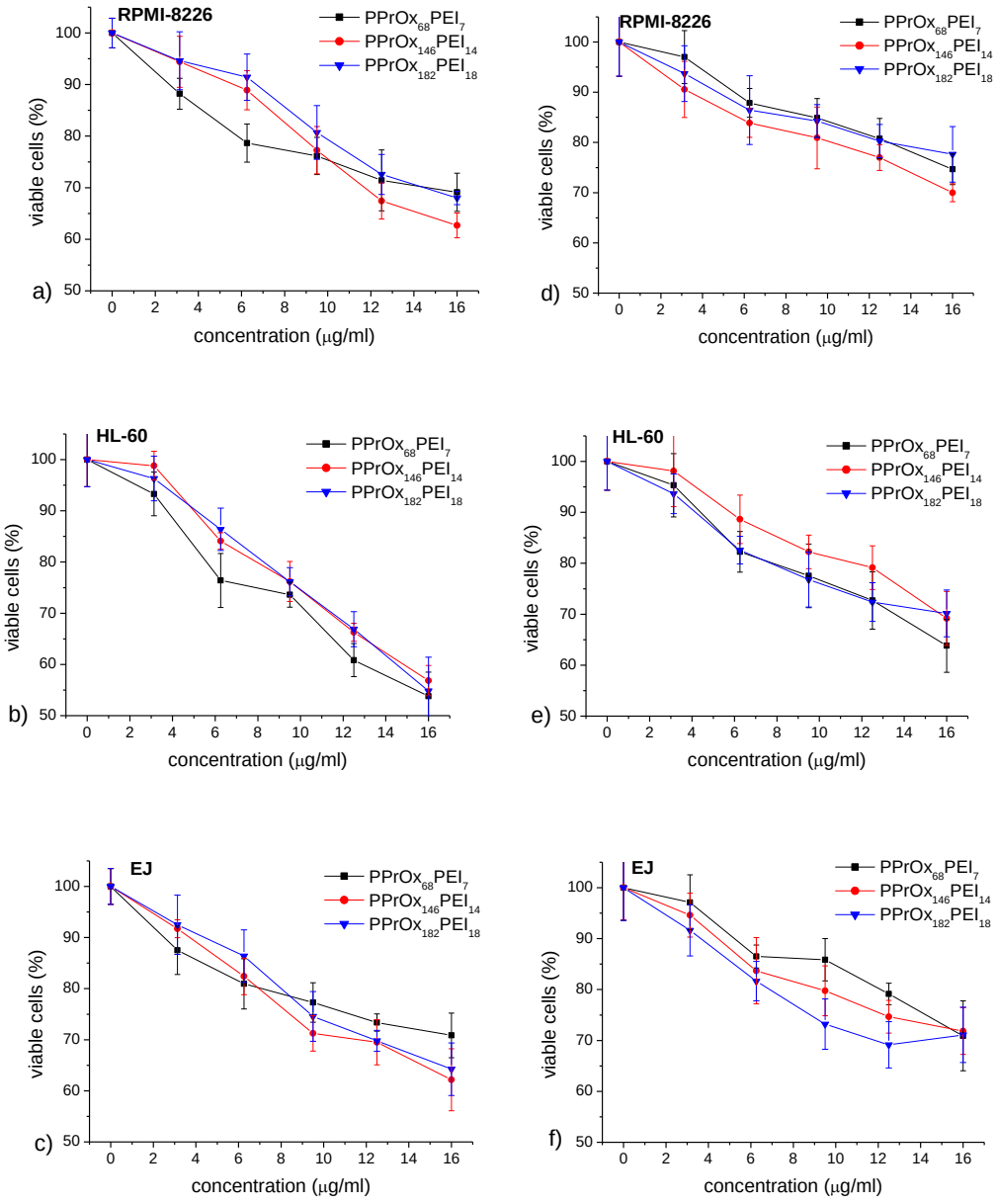

Figure 3-11 Cytotoxicity of non-coated (a – c, left panel) and the corresponding PNIPAM-coated (d – e, right panel) polyplexes at N/P = 4, determined by the MTT-dye reduction assay after 72-h continuous exposure. Each data point represents the arithmetic mean ± SD of 8 separate experiments

3.3.7 Transfection experiments

After the formation the polyplexes of DNA with $PPrOx_{182}$-PEI_{18}, the (non-coated) particles were tested in an *in vitro* cell transfection experiment. The test was performed on two human cell lines, non-malignant HEK-293 (human kidney embryonal cells) and malignant REH (acute leukemia), by using flow cytometry. By using cationic polymers genetic information is introduced into the cell whereby a fluorescent protein is expressed, such that the flow cytometer can detect these cells. The b-PEI was used as a reference transfection agent. The non-coated polyplexes showed a 65% transfection efficiency as compared to the b-PEI. The particles with the PNIPAM shell had only 45%.

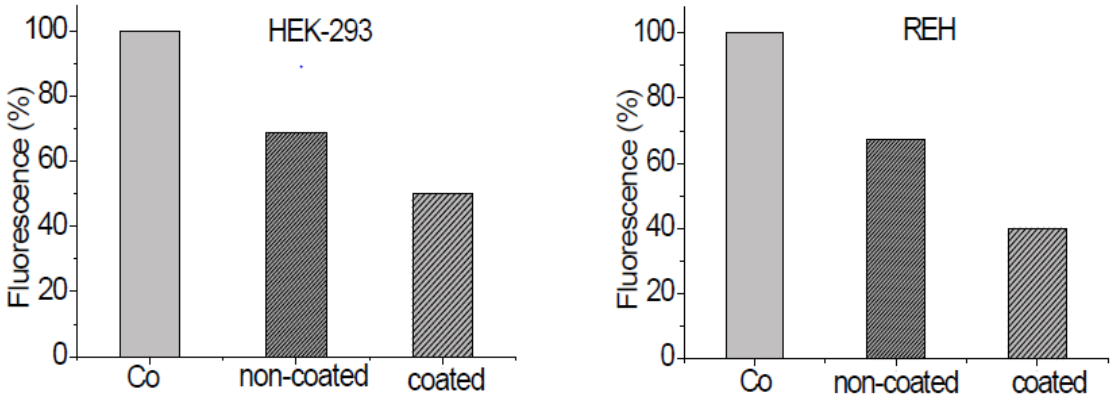

Figure 3-12 Transfection efficiency of non-coated and coated PPrOx-PEI polyplexes at N/P 4 expressed as % relative to fluorescence of b-PEI-polyplexes taken as 100%.

3.4 Conclusions

PPrOx-PEI copolymers were prepared by acidic hydrolysis of PPrOx at 100 °C in 6 M HCl. Kinetic studies revealed a slow initial phase of hydrolysis and a plateau at around 90 % conversion. The hydrolysis of PPrOx was a substantially slower process compared to that of PEtOx due to the higher hydrophobicity of PPrOx. The partial hydrolysis kinetics and procedure was then applied for the preparation of a series of PPrOx-PEI copolymers yielding well-defined copolymers.

The introduction of PEI moieties distributed along the PPrOx chain gradually increased the T_{CP} in water from 24 °C for the $PPrOx_{75}$ to 32 °C for PPrOx-PEI with 16% PEI. Copolymers with 35% to 65% PEI all had a T_{CP} around 50 °C. The T_{CP} values were found to mildly decrease when the solution pH was adjusted to either 5 or 11 indicating that the protonation state of the PEI moieties has little influence, ascribed to their shielding by the PPrOx moieties. Finally, the T_{CP} shifted to higher temperatures upon addition of KSCN due to the salting-in effect and by specific interaction with BSA as indicated by the clear dependence of the effect of BSA on the PEI content of the copolymers.

At elevated (above T_{CP}) temperatures, the DOSY NMR and electrophoretic light scattering results revealed formation of well-defined nanosized particles (mesoglobules) composed of a PPrOx core and a thin shell with numerous positively charged amino groups that are accessible for complexation with oppositely charged nucleic acids. A series of copolymers that varied in their total degree of polymerisation and PEI content (i.e., 5–10 % range) was evaluated as DNA delivery carriers. Polyplex particles with R_h typically less than 100 nm were obtained at N/P ratios in the 0.5 – 10 range at 65 °C. Upon lowering the temperature to 25 °C (below T_{CP}) followed by an increase to a physiologically relevant temperature (i.e., 37 °C, above T_{CP}), the polyplex particles at $N/P < 2$ underwent minor changes in their dimensions ascribed to the formation of a surface layer of DNA, which was in excess, that acted as a barrier and prevented swelling and disintegration of the initial particles. The polyplex particles at $N/P \geq 2$ dramatically rearranged upon cooling below the T_{CP} into strongly swollen microgel particles, in which the PPrOx core disintegrated and the individual copolymer chains were proposedly fixed to the DNA molecules *via* numerous junctions with ethylenimine units (Figure 3-8). Additional rearrangement consisting of the formation of numerous small PPrOx domains that were interconnected *via* DNA (Figure 3-8) occurred upon heating to 37 °C. However, the initial arrangement of the particles was not restored. This rearrangement of the polyplexes upon cooling could be overcome by coating of the initial polyplex nanoparticles with a cross-linked polymeric shell. The resulting outer layer acted as a physical barrier that prevented strong swelling and disintegration of the initial particles upon cooling.

The bioassay clearly showed that the complexation and then in turn the outer coating each afforded for progressive loss of cytotoxicity as compared to the free PPrOx-PEI copolymers. Thus, besides the steric

stabilization, the outer coating is associated with a potential bypass of the safety issues of polyplexes as non-viral vectors for gene delivery.

This chapter showed that besides PEtOx and PMeOx, the PPrOx is another valuable candidate as precursor for L-PEI. The partial hydrolysis of PPrOx, which was used in chapter 2 for the confirmation of the block like acidic hydrolysis, was further investigated to determine the hydrolysis kinetics. This opens up a new polymer toolbox that allows the preparation of biocompatible thermoresponsive polymers. The partially hydrolysed PPrOx-PEI polymers contain amines, which can be used as a reactive handle to couple bioactive molecules. The use in gene transfection is just one possible application that opens up new opportunities for thermoresponsive polymers in gene delivery. The chemical modifications proposed in the following chapters can of course also be applied on these PPrOx-PEI copolymers to make functional derivatives.

3.5 References

(1) Jäger, M.; Schubert, S.; Ochrimenko, S.; Fischer, D.; Schubert, U. S. *Chem. Soc. Rev.* **2012**, *41* (13), 4755.
(2) Rangelov, S.; Pispas, A. **2013**, 499.
(3) Dinçer, S.; Türk, M.; Pişkin, E. *Gene Ther.* **2005**, *12 Suppl 1*, S139.
(4) Ahmed, M.; Wattanaarsakit, P.; Narain, R. *Eur. Polym. J.* **2013**, *49* (10), 3010.
(5) Twaites, B. R.; de las Heras Alarcón, C.; Cunliffe, D.; Lavigne, M.; Pennadam, S.; Smith, J. R.; Górecki, D. C.; Alexander, C. *J. Control. Release* **2004**, *97* (3), 551.
(6) Qin, Z.; Liu, W.; Li, L.; Guo, L.; Yao, C.; Li, X. *Bioconjug. Chem.* **2011**, *22* (8), 1503.
(7) Kwoh, D. Y.; Coffin, C. C.; Lollo, C. P.; Jovenal, J.; Banaszczyk, M. G.; Mullen, P.; Phillips, A.; Amini, A.; Fabrycki, J.; Bartholomew, R. M.; Brostoff, S. W.; Carlo, D. J. *Biochim. Biophys. Acta* **1999**, *1444* (2), 171.
(8) Schaffer, D. V.; Fidelman, N. a.; Dan, N.; Lauffenburger, D. a. *Biotechnol. Bioeng.* **2000**, *67* (5), 598.
(9) Lambermont-Thijs, H. M. L.; Bonami, L.; Du Prez, F. E.; Hoogenboom, R. *Polym. Chem.* **2010**, *1* (5), 747.
(10) Van Kuringen, H. P. C.; Lenoir, J.; Adriaens, E.; Bender, J.; De Geest, B. G.; Hoogenboom, R. *Macromol. Biosci.* **2012**, *12* (8), 1114.
(11) Hoogenboom, R. *Angew. Chem. Int. Ed. Engl.* **2009**, *48* (43), 7978.
(12) Sedlacek, O.; Monnery, B. D.; Filippov, S. K.; Hoogenboom, R.; Hruby, M. *Macromol. Rapid Commun.* **2012**, *33* (19), 1648.
(13) Bertrand, E.; Gonçalves, C.; Billiet, L.; Gomez, J. P.; Pichon, C.; Cheradame, H.; Midoux, P.; Guégan, P. *Chem. Commun. (Camb).* **2011**, *47* (46), 12547.
(14) Legros, C.; De Pauw-Gillet, M.-C.; Tam, K. C.; Lecommandoux, S.; Taton, D. *Eur. Polym. J.* **2015**, *62*, 322.
(15) Guillerm, B.; Monge, S.; Lapinte, V.; Robin, J.-J. *Macromol. Rapid Commun.* **2012**, *33* (19), 1600.
(16) Rossegger, E.; Schenk, V.; Wiesbrock, F. *Polymers (Basel).* **2013**, *5* (3), 956.
(17) Lava, K.; Verbraeken, B.; Hoogenboom, R. *Eur. Polym. J.* **2015**, *65*, 98.
(18) de la Rosa, V. R.; Bauwens, E.; Monnery, B. D.; De Geest, B. G.; Hoogenboom, R. *Polym. Chem.* **2014**, *5*, 4957.
(19) Hoogenboom, R.; Thijs, H. M. L.; Jochems, M. J. H. C.; van Lankvelt, B. M.; Fijten, M. W. M.; Schubert, U. S. *Chem. Commun.* **2008**, No. 44, 5758.
(20) Lin, P.; Clash, C.; Pearce, E. M.; Kwei, T. K.; Aponte, M. A. *J. Polym. Sci. Part B Polym. Phys.* **1988**, *26* (3), 603.
(21) Park, J. S.; Kataoka, K. *Macromolecules* **2007**, *40* (10), 3599.
(22) Toncheva, N.; Tsvetanov, C.; Rangelov, S.; Trzebicka, B.; Dworak, A. *Polym. (United Kingdom)* **2013**, *54* (19), 5166.
(23) Vlassi, E.; Pispas, S. *Macromol. Chem. Phys.* **2015**, *216*, 873.
(24) Wiesbrock, F.; Hoogenboom, R.; Leenen, M. A. M.; Meier, M. A. R.; Schubert, U. S. *Macromolecules* **2005**, *38* (12), 5025.
(25) Dimitrov, I. V.; Petrova, E. B.; Kozarova, R. G.; Apostolova, M. D.; Tsvetanov, C. B. *Soft Matter* **2011**, *7* (18), 8002.
(26) Haladjova, E.; Rangelov, S.; Tsvetanov, C. B.; Pispas, S. *Soft Matter* **2012**, *8*, 2884.
(27) Mosmann, T. *J. Immunol. Methods* **1983**, *65* (1–2), 55.
(28) Kostova, B.; Ivanova-Mileva, K.; Rachev, D.; Christova, D. *AAPS PharmSciTech* **2013**, *14* (1), 352.
(29) Bloksma, M. M.; Bakker, J.; Weber, C.; Hoogenboom, R.; Schubert, U. S. **2010**, 724.
(30) Haladjova, E.; Toncheva-Moncheva, N.; Apostolova, M. D.; Trzebicka, B.; Dworak, A.; Petrov, P.; Dimitrov, I.; Rangelov, S.; Tsvetanov, C. B. *Biomacromolecules* **2014**, *15* (12), 4377.
(31) Zhang, Q.; Voorhaar, L.; Filippov, S. K.; Yesil, B. F.; Hoogenboom, R. *J. Phys. Chem. B* **2016**, acs. jpcb.6b03414.
(32) Suh, J.; Paik, H.-J.; Hwang, B. K. *Bioorganic Chemistry*. 1994, pp 318–327.
(33) Isom, D. G.; Castañeda, C. A.; Cannon, B. R.; García-Moreno, B. *Proc. Natl. Acad. Sci. U. S. A.* **2011**,

108 (13), 5260.
(34) Cotanda, P.; Wright, D. B.; Tyler, M.; O'Reilly, R. K. *J. Polym. Sci. Part A Polym. Chem.* **2013**, *51* (16), 3333.
(35) Custers, J. P. A.; van Nispen, S. F. G. M.; Can, A.; de La Rosa, V. R.; Maji, S.; Schubert, U. S.; Keurentjes, J. T. F.; Hoogenboom, R. *Angew. Chemie Int. Ed.* **2015**, *54* (47), 14085.
(36) Weda, P.; Trzebicka, B.; Dworak, A.; Tsvetanov, C. B. *Polymer (Guildf).* **2008**, *49* (6), 1467.
(37) Online, V. A.; Petrov, P. D.; Ivanova, N. I.; Apostolova, M. D.; Tsvetanov, B. *RSC Adv.* **2013**, *3* (11), 3508.
(38) Trzebicka, B.; Haladjova, E.; Otulakowski, Ł.; Oleszko, N.; Wałach, W.; Libera, M.; Rangelov, S.; Dworak, A. *Polymer (Guildf).* **2015**, *68*, 65.

Chapter 4 :
The plunge of PEI into Supercritical CO_2

Contributors to this chapter:

Prof. Steve Howdle, School of Chemistry, The University of Nottingham

Thomas McAllister School of Chemistry, The University of Nottingham

Silvio Curia, School of Chemistry, The University of Nottingham

Contributions of the candidate

Synthesis of the start polymers and full analysis

CHAPTER 4

Prologue

Next to its DNA binding ability the L-PEI units can act as a reaction platform to introduce new functionalities. This gives the possibility to make different types of copolymers without the burden of new monomer synthesis. In this chapter the modification of PEI units in either a pure L-PEI polymer or in a PEtOx-PEI copolymer, yielding a copolymer of L-PEI and a copolymer of PEtOx respectively. The reaction we explored was the reaction between an amine and CO_2 resulting in a carbamate. This fluorescent zwitterion is introduced on L-PEI or PEtOx, obtaining either a fluorescent L-PEI as a potential gene transfection agent and a fluorescent biocompatible polymer as such expanding the chemical toolbox of both polymers.

4.1 Introduction

Poly(2-alkyl-2-oxazoline)s (PAOx) are a class of polymers with many applications in the biomedical field due to their excellent biocompatibility.[1–3] The polymers can be seen as a competitor for the current gold standard PEG.[4] Both polymers have similar behavior in biological media,[5] although the PAOx polymer class is superior when it comes to chemical versatility[6]. Chemical functionalities on the PAOx polymer can be introduced through end groups[6], through functional monomers[6–8] or via post-polymerisation modification.[9] The main example of post-polymerisation modification of PAOx is the (partial) hydrolysis of PAOx into linear poly(ethylene imine) L-PEI.[10] The L-PEI is the key reference in gene transfection experiments.[11,12] The amines on the backbone of L-PEI can not only be used as a charge carrier but also for a broad range of reactions to introduce chemical functionalities along the backbone.[13] These reactions can be applied on the fully hydrolysed L-PEI and on the partially hydrolysed PAOx-L-PEI.[14,15] As such the post-polymerisation modification can be used to introduce different kind of functionalities, which broaden the application field of the PAOx polymer class and broaden the chemical toolbox. The introduced functionalities are often bioactive molecules but it is also possible to prepare fluorescent polymers.

Remarkably there are not a lot of fluorescent poly(2-alkyl-2-oxazoline)s published.[16–18] The first example was reported by Kanazaki *et al*[16] and showed the coupling of a indiocyanine green molecule to a partially hydrolysed PEtOx. The group of Ana Aguiar-Ricardo synthesized PAOx polymers in $scCO_2$ and observed that they exhibited a blue fluorescence, which originates from the carbamic acid that was formed during the initiation.[19] This origin of fluorescence was proven by comparing it to the small model molecule tris(2-aminoethyl) carbamic acid.[20] These carbamic acid containing PEtOx were further used as a tag for bacterial cell membranes, when the PAOx was end capped with quaternary amines.[21–23] The initiator based method is advantageous because it allows to orthogonally alter the side chain and terminator end. The same group also showed the development of a dendrimeric theranostic based on polyurea and a fluorescent poly(2-methyl-2-oxazoline) (PMeOx) and PEtOx. As model drug, paclitaxel was loaded into

the dendrimer. However, this polymer only contains one carbamate per polymer chain limiting the achievable fluorescence intensity. A combination of the biocompatible PEtOx or PMeOx with fluorescent carbamate groups in the side chains would make a powerful tool in fluorescent imaging.

Fluorescent imaging is crucial for the understanding of dynamic biological processes and detection and diagnosis of diseases. The chromophore visualizes the site of interest without being invasive hence not interfering.[24] The fluorescent chromophores can have an organic, inorganic or hybrid nature.[25,26] Fluorescent organic molecules[24] are often bulky proteins[27–30] such as GFP[31] or conjugated dyes e.g. rhodamines[32]. These organic molecules often show low sensitivity due to low absorption and photo bleaching. Quantum dots[33,34] are an example of fluorescent inorganic materials, besides other inorganic particles such as metal nanoparticles or silica nanoparticles.[24,33,35,36] Some of the organic and inorganic dyes suffer from inherent toxicity, which is problematic in a biological context.[29,34,37,38] The overall biological properties of fluorescent materials can be improved by combining them with biocompatible polymers. Polymers can act as a stabilizer and ensure better solubility of fluorescent materials while also expanding the chemical modification potential. Which can be used to incorporate selective targeting, or coupling of bioactive molecules. Thereby theranostic polymers can also be developed by coupling drugs or reactive molecules to the fluorescent polymer.[37] The polymer needs to be non-toxic while both short and long term protecting the chromophore from the harsh biological environment preventing leakage and degradation for which PAOx are very promising. Higher intensities are achieved by multiple fluorescent dye loading, to increase the local concentration and thereby resulting in brighter signals.

Different methods can be applied for the synthesis of fluorescent polymers, either through polymerisation or a post-polymerisation modification.[37,39] During the polymerisation a fluorescent moiety can be used as an initiator[40] or terminator or covalently bound to a monomer that is polymerised.[39] The post-polymerisation modification method uses reactive groups on the polymer to couple the fluorescent dye on one or both of the terminal groups[41] or the side chains.[42,43] Besides fluorescently labelled polymers, intrinsically fluorescent polymers can also be used for imaging, mostly conjugated polymers.[44–47]

Intrinsically fluorescent polymers that lack extended π-conjugated systems are rare, but can be obtained when the electron hole (LUMO) and excited electron (HOMO) are in close proximity, both electronically and spatially. In the case of amino containing dendrimers the coexistence of carboxylic acids and tertiary amines have been reported to induce fluorescence.[48–50] The fluorescence intensity increased upon oxidation of the amine groups.[49–53] In some cases the protonation is important which was shown when poly(amido amine) (PAMA) dendrimers containing urea bonds had intrinsic pH dependent fluorescence.[48] The role of the polymer branching on the recombination of the electron with its hole was examined by comparison of branched and linear poly(ethylene imine) (b-PEI and L-PEI) were compared, both showing blue emission.[54] The complex with oxygen and the electron lone pair of the amine plays a crucial role as it induces an electron hole recombination process which causes the emission.[54] This was

demonstrated by an increase in fluorescence upon oxidation. Note that the fluorescence was measured in methanol as L-PEI in its free base form, is not soluble in water. b-PEI, which is water soluble, shows increased fluorescence after reaction with CO_2. The origin of the fluorescence of PEI is the formation of conjugated system when the lone electron pair of the nitrogen forms a conjugated system with the deprotonated carbamate.[55] The last examples showed that it could be possible to synthesise PEI with a fluorescent label by the reaction with CO_2.

The primary amines in b-PEI can react with ambient CO_2[56] leading to the formation of zwitterionic carbamates.[57,58] CO_2 is at first sight a simple linear non polar molecule, however with complex chemistry. Due to the charge distribution the central carbon atom is prone to nucleophilic attack.[57,59] The attack of a amine, Scheme 4-1, yields a carbamate that is immediate deprotonated by non-reacted amines. This acid base equilibrium results in the formation of a stable zwitterion as shown in Scheme 4-1.[55,57,59,60] As a consequence half of the amines react with the CO_2 while the other half acts as a base and is protonated.[61] The nature of the amine is crucial as secondary amines react much slower with CO2 than primary amines due to enhanced steric hindrance.[62] This reaction is reversible, whereby the amine is formed and CO_2 is released in the reversed reaction.[23]

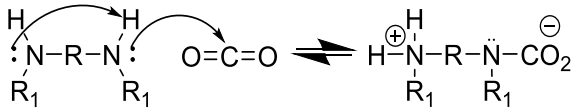

Scheme 4-1 Formation of the zwitterionic carbamate from a secondary amine (one step process, equilibrium).[62,63] The nucleophilic attack of the first amine onto the carbon of CO_2 forms a carbamate, the second amine acts as a base and deprotonates the carbamate resulting in the zwitterionic carbamate.

This reversible reaction could be advantageous in industrial applications to filter CO_2 out of waste streams via the formation of carbamates. Therefore b-PEI and L-PEI have been applied in CO_2 scrubbers.[64] However, upon reversible cycling, heating of the material, a loss in CO_2 capture ability was observed, which has been ascribed to the irreversible formation of cyclic imidazolidinone. This reaction proceeds slower than the carbamate formation but can be accelerated at elevated temperatures (Figure 4-1, bottom).[65] When two amines are in close proximity they form a cyclic urea while locking the CO_2 on the diamine. The humidity of the gas stream plays a crucial role for this side reaction because wet gas was proposed to suppress the cyclic urea formation as during the ring closure water is released.[64,66]

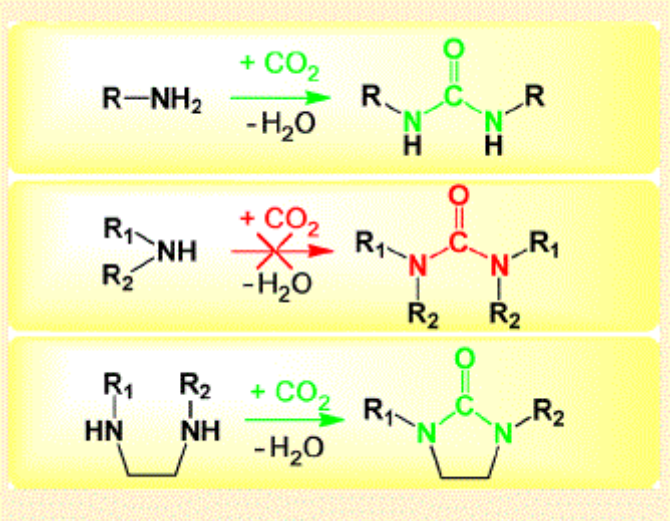

Figure 4-1: Side reactions in amine-containing CO_2 adsorbents: The reversible reaction between two primary amine forms an urea (top), the reaction of a secondary amine and CO_2 is impossible due to steric hindrance(middle), the reaction of two connected secondary amines with CO_2 forms a cyclic urea (bottom) [64]

By combining amine containing polymers and CO_2, the formation of the carbamate functionality can lead to fluorescent polymers. The high amine concentration in L-PEI is of high interest for this reaction, because it could lead to fluorescent L-PEI as a gene transfection vector.[11,12] Due to the nature of the reaction with CO_2 only a part of amines will be functionalised. The first amine will react with the CO_2 while the second amine will act as a base by deprotonating the carbamate. The combination of the fluorescent label and the qualities of L-PEI in gene transfection, will lead to a fluorescent non-viral vector. Next to the fully hydrolysed polymers, the partial hydrolysed PAOx polymers can be applied. The PAOx-PEI is a reaction platform and can be seen as a chemical handle for the introduction of different kind of functionalities. The amines of the PAOx-PEI polymers can react with CO_2 to form carbamates. This enables the formation of intrinsically fluorescent PAOx containing polymers showing 'stealth behavior upon injection in the body.[67] The earlier reports showed that the more reactive primary amine of b-PEI reacted with ambient CO_2 and that only at elevated temperatures the secondary amines of L-PEI react with CO_2. The latter is caused by the steric hindrance induced by the secondary amines.

To overcome the lower reactivity of the secondary amine of L-PEI, $scCO_2$ was used for the modification of L-PEI in this study. This could increase the reaction rate and due to the non-solvent character no solubility problems should arise. Earlier reports showed that ambient CO_2 reacts with the primary amines in b-PEI, however not with the secondary amines.[56] As illustrated in Scheme 4-2, the reaction between the amine and $scCO_2$ is anticipated to reversibly form deprotonated carbamates and protonated amines. However we have to keep in mind that the irreversible formation of cyclic urea could also be possible, which could induce cross linking. Therefore, lower temperatures will be investigated and as well as the

presence of water to suppress cyclic urea formation. The reaction of the L-PEI with $scCO_2$ was investigated for different reaction times to study the progress of the reaction and determine the optimal exposure time.

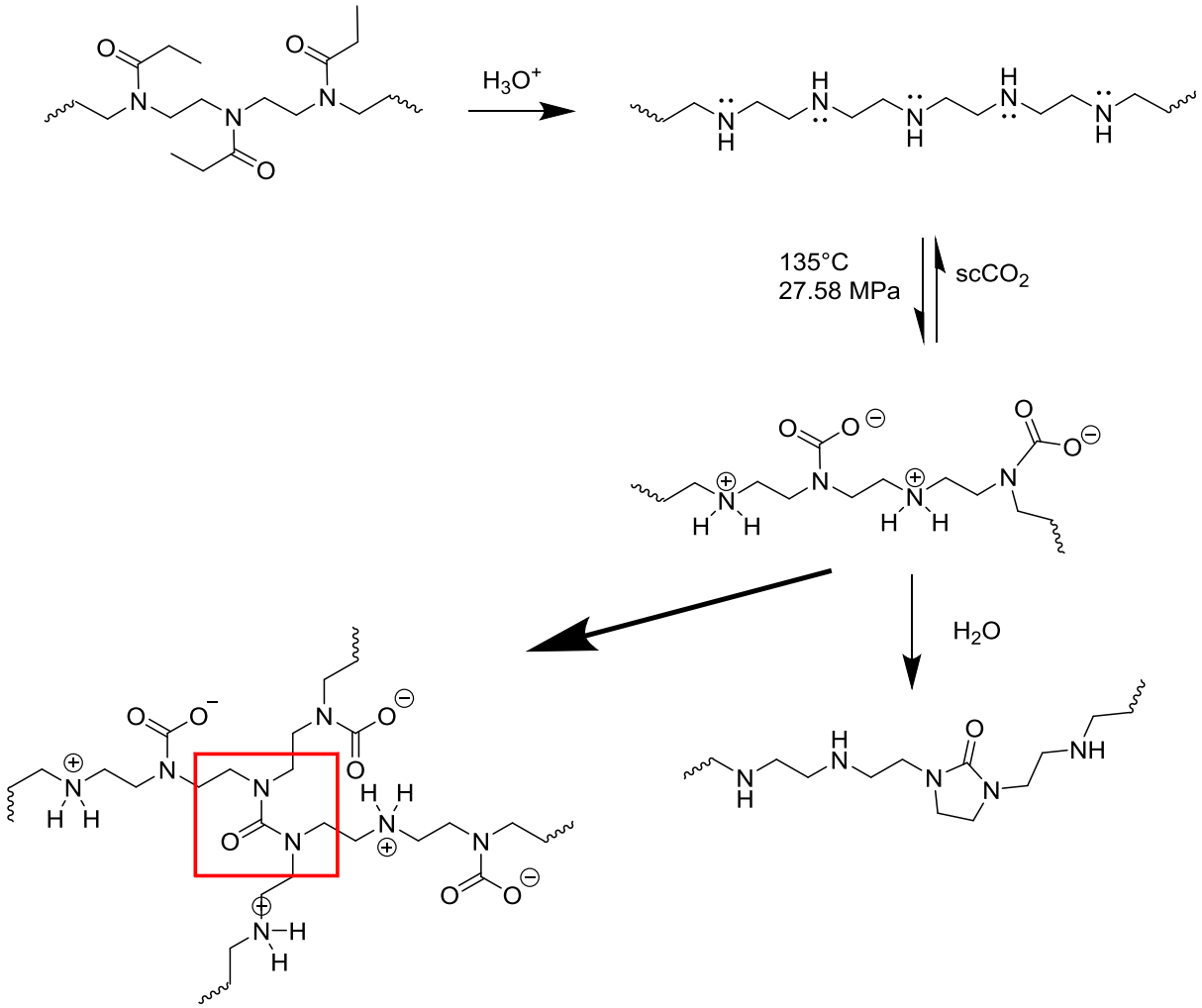

Scheme 4-2 Reaction of the L-PEI with $scCO_2$ forming carbamates. The scheme (from top to bottom) shows the hydrolysis of the PEtOx into a fully hydrolysed L-PEI. During the reaction of L-PEI with $scCO_2$, carbamates are formed by the nucleophilic attack of the amine of the L-PEI on the CO_2, the neighbouring amine on the PEI acts as a base yielding the carbamate zwitterion. Cyclic urea can be irreversibly formed thereby water is released. The formation of this bond leads to crosslinking (red square).

The second part of this chapter focuses on the reaction of a PEtOx-PEI copolymer with $scCO_2$. This polymer was synthesised by the partial acidic hydrolysis of PEtOx, yielding a polymer with a block-like distribution of blocks of L-PEI present along the backbone, which was shown in chapter 2. The amines of the PEI parts can react with the $scCO_2$ yielding the carbamates (Scheme 4-3). The remaining PEtOx remains unmodified and will yield a biocompatible polymer. This methodology gives the opportunity to obtain multiple carbamate units on one polymer chain proposed leading to a higher fluorescence

intensity. This is quite different from the earlier reported PEtOx containing carbamates end-groups prepared in $scCO_2$. (Figure 4-2). As shown in Figure 4.2 these polymers with a single carbamate end-group could already be used as a tag for the cell wall. We will obtain a polymer with a much higher carbamate loading hence a much higher fluorescence potentially allowing their use for fluorescence imaging at much lower concentration.

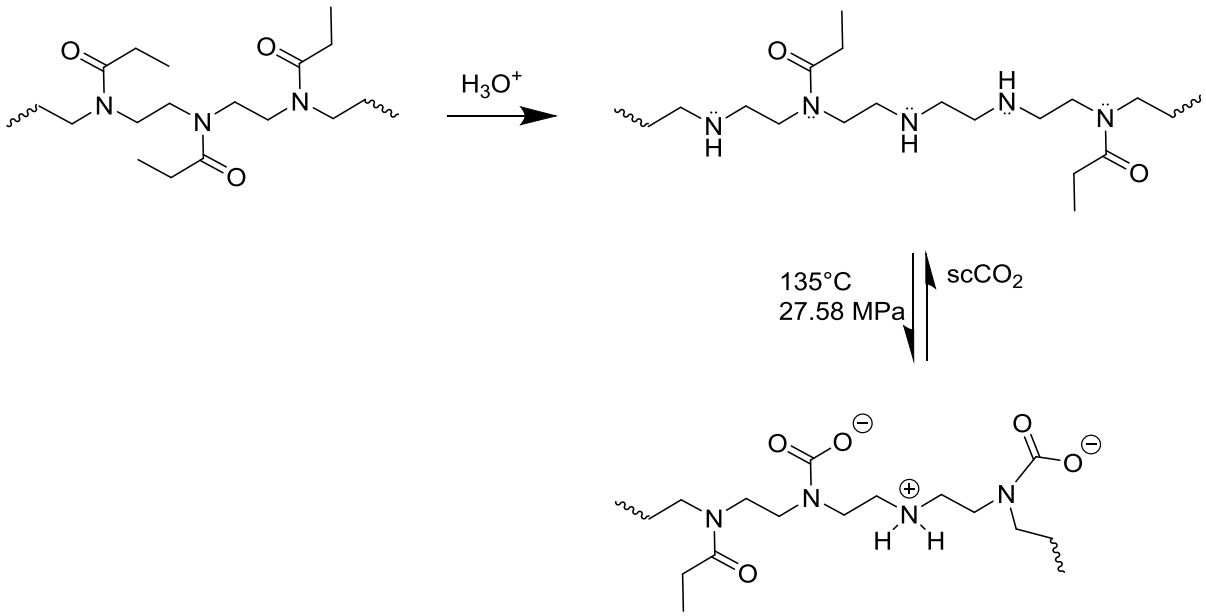

Scheme 4-3 Reaction of the PAOx-PEI with $scCO_2$ forming carbamates. This scheme (from top to bottom) shows the partial hydrolysis of the PEtOx into PEtOx-PEI polymer. During the reaction with $scCO_2$, carbamates are formed by the nucleophilic attack of the amine on the CO_2, the neighbouring amine on the PEI acts as a base to deprotonate the formed carbamate.

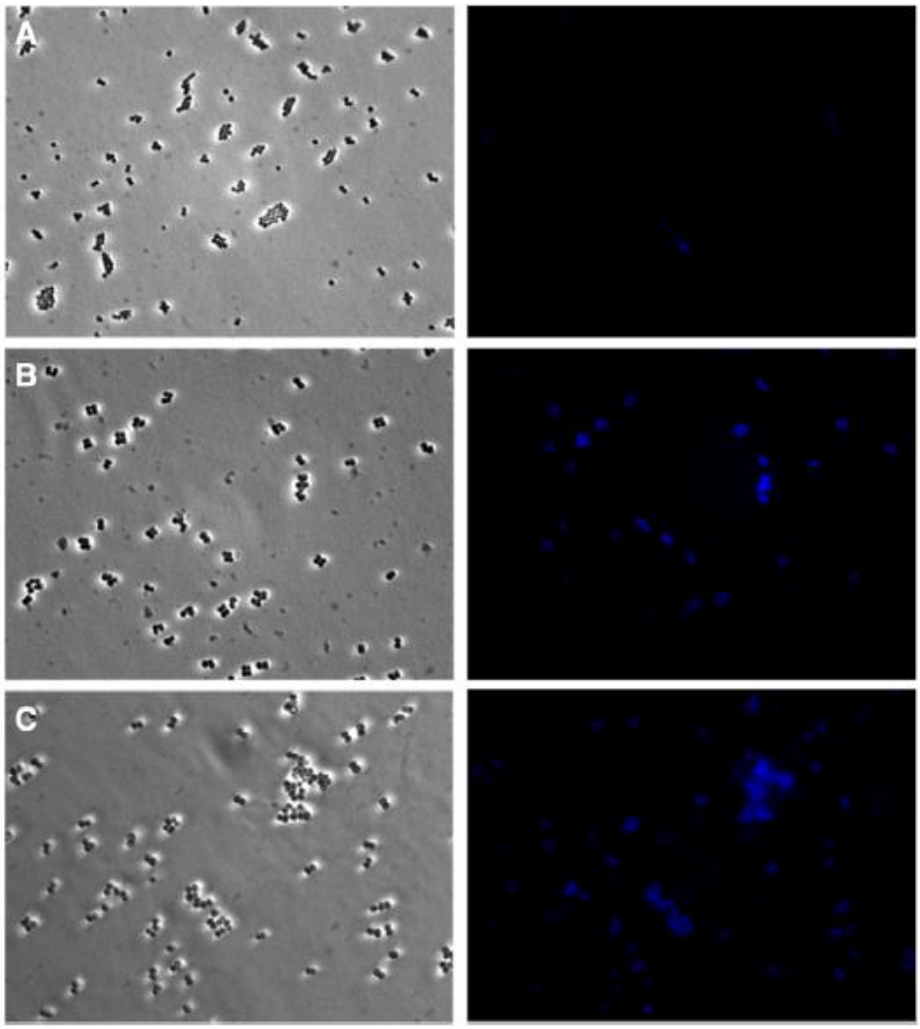

Figure 4-2 Fluoresence labelling of *S. Aureus* using carbamate containing oligo(2-methyl-2-oxazoline) terminated with N,N-dimethyldodecylamine. Bacterial cells visualized by phase contrast (left panels) and cells visualized by fluorescence microscopy using DAPI filters (right panels). (A) cells in the absence of oligomer and cells in the presence of oligomer with low carbamic acid (B)and high end group functionalisation degree, (C).[20]

4.2 Materials and methods

4.2.1 Instrumentations

Size exclusion chromatography (SEC) was performed using an Agilent HPLC equipped with a 1260 refractive index detector (RID) and UV-VIS detector with detector set on 375 nm. Using 1,1,1,3,3,3-hexafluoro-2-isopropanol (HFIP) containing 20 mM sodium trifluoroacetate as eluent, which was dried with molecular sieves (3 Å). The flow rate was 0.53 mL/min (HFIP-SEC). Polymethylmethacrylate (PMMA) standards were used to calculate the molar mass values. The column set consisted of two PSS PFG 300*8Å gel 5 µm MIXED-D columns and a similar guard column (PSS) in series with a molar mass range from 100-1 000 000 at 35 °C. Chromatograms were analyzed with Agilent Chemstation software using the GPC add-on. The hydrolysis reactions were done in a single mode microwave Biotage initiator eight using temperature control (IR temperature sensor) (Biotage, Uppsala, Sweden). NMR measurements were done using a Bruker AVANCE II spectrometer operating at 400.12 MHz for ^{1}H and at 100.61 MHz for ^{13}C. All analysis were done with the Spinworks 4.2 Software and chemical shifts are given in ppm. The exposure of the polymers to supercritical CO_2 was done in a house built autoclave, clamp sealed, Mk.III stainless steel autoclave. DSC measurements were performed on a Q2000 from TA Instruments from -50 to 200 degrees and for the modulated DSC samples the temperature was modulated by ± 1°C every 60 s with an overall heating rate of 3 °C/minute. The fluorescence measurements were done in a Varian Cary Eclipse spectrophotometer equipped with a Cary temperature and stir control.

4.2.2 Materials

PEtOx with a degree of polymerisation (DP) of 400 was synthesized as reported elsewhere (M_n =40600 ; Đ = 1.06).[68] Hydrogen chloride, sodium hydroxide and dichloromethane where obtained from Sigma-Aldrich and used as received.

4.2.3 Procedures

Partial hydrolysis of PEtOx to $PEtOx_{307}$-PEI_{93}

PEtOx (2 g, DP 400) was dissolved in 7.5 mL of water under stirring. Then, 7.5 mL of a 36 wt% solution of concentrated HCl was added and the mixture was heated to 140 °C in the microwave for 40 min. After the hydrolysis, the volatiles were removed on a rotary evaporator. The polymer solution was basified to pH 10-11 by addition of a 2 M NaOH solution. The solution was then lyophilized and the solid was dissolved in dichloromethane while the salts remained as solids in the flask. Next, the organic phase was filtered and concentrated under reduced pressure to yield a solid white product. The integral ratio between the peaks at 2.56-2.8 ppm (PEI backbone) and 3.15-3.6 ppm (PEtOx backbone) in the ^{1}H-NMR spectrum are used to calculate the degree of hydrolysis (23%).

$PEtOx_{307}$-PEI_{93}: ^{1}H NMR ($CDCl_3$): δ = 0.9 – 1.25 (m, 3H, 5); 2.1 – 2.50 (m, 2H, 4), 2.56 – 3.0 (m, 4H, 6); 3.15 – 3.60 ppm (m, 4H, 2). ^{13}C NMR ($CDCl_3$): δ = 9.4 (CH_3, 5); 25.9 and 26.2 (CH_2, 4); 43 – 51 (CH_2, 6 and 2); 175-173 ppm (C=O, 3). (M_n = 33980 g/mol; Đ = 1.1).

Full hydrolysis of $PEtOx_{400}$ to PEI_{400}

PEtOx (2 g, DP 400) was dissolved in 7.5 mL of water under stirring. Then, 7,5 mL of a 36 wt% solution of HCl (concentrated HCl) was added and the mixture was heated to 140 °C in the microwave for 3 hr. After the hydrolysis, the volatiles were removed on a rotary evaporator. The polymer solution was basified to a pH 10-11 by addition of NaOH pellets and stirring while heating until the polymer was dissolved. When the solution was cooled the polymer precipitated. After filtration the powder was lyophilized. A white powder was obtained.

PEI_{400} (1&3)^{1}H NMR (CD_3OD): δ = 2.7-28(s,CH_2,6). ^{13}C NMR (CD_3OD): δ = 9.4 (CH_3, 5); 25.9 and 26.2 (CH_2, 4); 49.7 – 51 (CH_2, 6); PEI-1 (M_n = 87000 g/mol; Đ = 1.13) and PEI-2(M_n = 84000 g/mol;Đ = 1.23)

Modification of the polymers with supercritical CO_2

The polymer, typical 100 mg, was transferred into a small glass *via*l that was placed in the autoclave. Secondly the autoclave was heated to 135°C, except PEI_{400} (24C), which was done at 40°C. The CO_2 pressure was raised up to 27.58 MPa. After the desired reaction time the autoclave was vented. NMR samples were prepared by dissolving the polymer in D_2O.

Three start polymers, PEI-1 (DP 400); PEtOx-PEI-2 (DP 400) and PEI-3 (DP400) were used and were reacted simultaneous in the autoclave. The yield of the reaction between the amine of the polymer and CO_2 was calculated *via* ^{1}H-NMR spectroscopy by using the values of integration of the CH_2 (peak 5&6&7)next to the formed carbamic acid functionality, divided by the total CH_2 protons(peak 1-7)

Data of the PEI-1(x) polymers

PEI-1(0.5) ^{1}H NMR (D2O): δ = 2.7-2.8(m,CH2,1); 3.0 (m,CH2,2);3.01 (m,CH2,3);3.14 (CH2,m,4);3.24-3.35 (CH2,s,5); 3,4. (CH2,m,6); 3.49(CH2,s,7) . ^{13}C NMR (D2O): δ = 44.77 (CH2, 7 and 1); 46.49(CH2,5); 46.85 (CH2, 3);47.44 (CH2, 4); 160.34 (CO, 9); 163.6-164.40 (NCO)(M_n = 13700 g/mol; Đ = 1.3)

PEI-1(1) ^{1}H NMR (D2O): δ = 2.7-2.8 (m,CH2,1); 3.0 (m, CH2,2); 3.01 (m, CH2, 3); 3.16 (CH2, m, 4);3.32-3.35 (CH2, s, 5); 3,40. (CH2, m, 6); 3.48(CH2,s,7) . ^{13}C NMR (D2O): δ = 44.84 (CH2, 7 and 1); 46.43(CH2, 5); 46.82 (CH2, 3);47.44 (CH2, 4); 160.34 (CO, 9); 163.6-164. (NCO)(M_n = 75000 g/mol Đ = 1.3)

PEI-1(2) ^{1}H NMR (D2O): δ = 2.7-2.8 (m,CH2,1); 3.1 (m, CH2, 3);3.18 (CH2, m, 4);3.23-3.31 (CH2, s, 5); 3,42. (CH2, m, 6); 3.5 (CH2,s,7) . ^{13}C NMR (D2O): δ = 44.43 (CH2, 7); 44.68 (CH2, 1), 46.49(CH2,5); 46.92 (CH2, 3);47.48 (CH2, 4); 160.26 (CO, 9); 163.6-164.19 (NCO) (M_n =47000 g/mol; Đ =1.76)

PEI-1(2large) ^{1}H NMR (D2O): δ = 2.7-2.8 (m, CH2, 1); 3.1 (m, CH2, 3);3.18 (CH2, m, 4);3.23-3.31 (CH2, s, 5); 3,42. (CH2, m, 6); 3.49(CH2, s, 7) . ^{13}C NMR (D2O): δ = 44.76 (CH2, 1&7), 46.49 (CH2,5); 46.92 (CH2, 3);47.48 (CH2, 4); 160.26 (CO, 9); 163.6-164.19 (NCO) (M_n = 23295 g/mol; Đ = 1.65)

PEI-1(24) ^{1}H NMR (D2O): δ = 2.7-2.8 (m, CH2, 1); 3.0 (m, CH2, 2);3.08 (m, CH2, 3);3.15 (CH2, m, 4);3.21-3.31 (CH2, s, 5); 3,4. (CH2, m, 6); 3.49 (CH2, s, 7) . ^{13}C NMR (D2O): δ = 44.44 (CH2, 7); 44.76 (CH2, 1); 46.49 (CH2, 5); 46.88 (CH2, 3);47.46 (CH2, 4); 160.34 (CO, 9); 163.6-164.19 (NCO) (M_n =28000 g/mol; Đ = 4.5)

PEI-1(24C) ^{1}H NMR (D2O): δ = 2.7-2.8 (m,CH2,1); 3.0 (m,CH2,2);3.08 (m,CH2,3);3.16 (CH2,m,4);3.25-3.34 (CH2,s,5); 3,4. (CH2,m,6); 3.49(CH2,s,7) . ^{13}C NMR (D2O): δ = 44.80 (CH2, 7 and 1); 46.48(CH2,5); 46.83 (CH2, 3);47.51 (CH2, 4); 160.38 (CO,9); 163.6-164.40 (NCO)(M_n = 33000 g/mol; Đ = 1.55)

PEI-1(48) ^{1}H NMR (D2O): δ = 2.7-2.8 (m, CH2, 1); 3.10 (m, CH2, 3); 3.14 (CH2, m, 4);3.28 (CH2, s, 5); 3.43. (CH2,m,6); 3.48(CH2,s,7) . ^{13}C NMR (D2O): δ = 42.42(CH2,6"); 43.01 (CH2,5); 44.90 (CH2, 7 and 1); 45.48 (CH2,5); 46.83 (CH2, 3);47.51 (CH2, 4); 160.44 (CO, 9); 162.6 (NCO)-164. (NCO)(M_n =9105 g/mol; Đ = 11)

Table 1. Selected data of the PEI-1(x) copolymers obtained after reaction with scCO2

Polymer	Reaction time (h)	Amine conversion (%)*	T_m (DSC) (°C)	% loss (100-150°C) (TGA)
PEI-1	0	0	68.8	/
PEI-1(0.16)	10 min	Insoluble*	68.3	4.8
PEI-1(0.5)	0.5	36.9	65.2	32.4
PEI-1(1)	1	36.5	65.2	32.2
PEI-1(2)	2	39.9	53.2	40.5
PEI-1(24)	24	41.6	40.7	28.4
PEI-1(24C)	24 (40°C)	34.1	86.2	31.7
PEI-1(48)	48	52.9	T_g (-21)	28.4
PEI-1(2Large)	2 (0.5g)	34.8	63.7	36.0

* From ^{1}H NMR spectroscopy. (* not determined)

Data of the PEtOx-PEI-2(x) polymers

PEtOx-PEI-2(0.16)) ^{1}H NMR (D2O): δ = 0.9 – 1.25 (m, 3H, 5); 2.2 – 2.50 (m, 2H, 4), 2.65 – 2.88 (m, 4H, 6); 3.20 – 3.60 ppm (m, 4H, 2,7,8). ^{13}C NMR (D2O): δ = 9.11 (CH3, 5); 25.99 (CH2, 4); 43 – 51 (CH2, 6,2,7 and 8); 163.1 (NC=O,7 and 8),177 ppm (NC=O, 3). (SEC, not soluble in eluent)

PEtOx-PEI-2(0.5) ^{1}H NMR (D2O):δ = 0.9 – 1.10 (m, 3H, 5); 2.13 – 2.50 (m, 2H, 4), 2.73 – 2.90 (m, 4H, 6); 3.20 – 3.73 ppm (m, 4H, 2,7,8). ^{13}C NMR (D2O): δ = 9.11 (CH3, 5); 25.99 (CH2, 4); 43 – 51 (CH2, 6,2,7 and 8); 163.1 (NC=O,7 and 8),177 ppm (NC=O, 3). (M_n = 102000 g/mol; Đ = 1.30)

PEtOx-PEI-2(1) ^{1}H NMR (D2O):δ = 0.91 – 1.10 (m, 3H, 5); 2.20 – 2.48 (m, 2H, 4), 2.73 – 2.93 (m, 4H, 6); 3.20 – 3.78 ppm (m, 4H, 2,7,8). ^{13}C NMR (D2O): δ = 8.9 (CH3, 5); 25.80 (CH2, 4); 42.4 – 48.04 (CH2, 6,2,7 and 8); 160.4 (C=O);177 ppm (C=O, 3). (M_n = 35000 g/mol; Đ =1.36)

PEtOx-PEI-2(2) ^{1}H NMR (D2O):δ = 0.85 – 1.30 (m, 3H, 5); 2.13 – 2.50 (m, 2H, 4), 2.73 – 3.02 (m, 4H, 6); 3.20 – 3.73 ppm (m, 4H, 2,7,8). ^{13}C NMR (D2O): δ = 9.11 (CH3, 5); 25.99 (CH2, 4); 42.4 – 47 (CH2, 6,2,7 and 8); 160.4 (C=O); 163.1 (NC=O,7 and 8),177 ppm (C=O, 3). (M_n = 132000 g/mol; Đ = 1.18)

PEtOx-PEI-2(2large)) ^{1}H NMR (D2O):δ = 0.85 – 1.10 (m, 3H, 5); 2.11 – 2.45 (m, 2H, 4), 2.74 – 2.95 (m, 4H, 6); 3.20 – 3.80 ppm (m, 4H, 2,7,8). ^{13}C NMR (D2O): δ = 8.73 (CH3, 5); 25.4 (CH2, 4); 42.4 – 48 (CH2, 6,2,7 and 8); 160.4 (C=O);177 ppm (C=O, 3). (SEC not recorded)

PEtOx-PEI-2(24C) ^{1}H NMR (D2O):δ = 0.90 – 1.18 (m, 3H, 5); 2.21 – 2.47 (m, 2H, 4), 2.65 – 3.07 (m, 4H, 6); 3.20 – 3.80 ppm (m, 4H, 2,7,8). ^{13}C NMR (D2O): δ = 8.9 (CH3, 5); 25.6 (CH2, 4); 41.2 – 49 (CH2, 6,2,7 and 8); 160.59 (C=O);177 ppm (C=O, 3). (SEC not recorded)

PEtOx-PEI-2(24)) ^{1}H NMR (D2O):δ = 0.91 – 1.12 (m, 3H, 5); 2.12 – 2.47 (m, 2H, 4), 3.17 – 3.86 ppm (m, 4H, 2,7,8). ^{13}C NMR (D2O): δ = 8.9 (CH3, 5); 25.6 (CH2, 4); 41.2 – 49 (CH2, 6,2,7 and 8); 160.59 (C=O);177 ppm (C=O, 3). (M_n = 21753 g/mol; Đ = 2.82)

PEtOx-PEI-2(48)^{1}H NMR (D2O):δ = 0.93 – 1.15 (m, 3H, 5); 2.12 – 2.475(m, 2H, 4), 3.20 – 3.74 ppm (m, 4H, 2,7,8). ^{13}C NMR (D2O): δ = 8.9 (CH3, 5); 25.4 (CH2, 4); 41.7 – 50.53 (CH2, 6,2,7 and 8); 160.59 (C=O);177 ppm (C=O, 3). (M_n = 1791 g/mol; Đ = 8.03)

Table 2 Selected data for PEtOx-PEI-2(x) obtained after reaction with scCO2; Note that amine conversion could not be determined due to overlapping signals

Polymer	Reaction time (h)	T_g (DSC)	% loss (100-150°C) (TGA)
PEtOx-PEI-2	0	35.8	/
PEtOX-PEI-2(0.16)	10 min	24.5	3.5
PEtOx-PEI-2(0.5)	0.5	64.8 (T_m)	9.1
PEtOx-PEI-2(1)	1	67.4	7.3
PEtOx-PEI-2(2)	2	70.7 (T_m)	9.4
PEtOx-PEI-2(24)	24	59.1 (T_m)	8.0
PEtOx-PEI-2(24C)	24/40°C	12.6	4.1
PEtOx-PEI-2(48)	48	49.4	10.7
PEtOx-PEI-2(2L)	2 (0.5g)	42.3	9.4

Data of the PEI-3(x) polymers

PEI-3(0.5) ^{1}H NMR (D2O): δ = 2.80-2.93 (m, CH2, 1); 2.97 (m, CH2, 2); 3.01 (m, CH2, 3); 3.10 (CH2, m, 4); 3.22-3.32 (CH2, s, 5); 3,37 (CH2, m, 6); 3.45 (CH2, s, 7) ^{13}C NMR (D2O): δ = 44.94 (CH2, 7 and 1);45.37 (CH2, 7 and 1); 45.81 (CH2, 7 and 1) 46.40 (CH2,5); 46.65 (CH2, 3);47.399 (CH2, 4); 160.34 (C̲O, 9); 163.6-164.40 (NC̲O) (SEC not recorded)

PEI-3(1) ^{1}H NMR (D2O): δ = 2.75-2.95 (m, CH2, 1); 2.99 (m, CH2, 2); 3.03 (m, CH2, 3); 3.13 (CH2, m, 4); 3.22-3.33 (CH2, s, 5); 3,40. (CH2, m, 6); 3.47 (CH2, s, 7) ^{13}C NMR (D2O): δ = 44.82 (CH2, 7 and 1); 45.22 (CH2,7 and 1); 45.66 (CH2, 7 and 1) 46.43 (CH2, 5); 46.61 (CH2, 3); 47,43 (CH2, 4); 160.39 (C̲O,9); 163.6-164.40 (NC̲O) (M_n = 66000 g/mol; Đ = 1.3)

PEI-3(2) ^{1}H NMR (D2O): δ = 2.75-2.95 (m, CH2, 1); 2.96 (m, CH2, 2);3.03 (m, CH2, 3);3.10 (CH2, m, 4); 3.22-3.33 (CH2, s, 5); 3,37. (CH2, m, 6); 3.45(CH2, s, 7) ^{13}C NMR (D2O): δ = 44.97 (CH2, 7 and 1); 45.40 (CH2,7 and 1); 45.79 (CH2,7 and 1) 46.45 (CH2, 5); 46.76 (CH2, 3);47,42 (CH2, 4); 160.56 (C̲O, 9); 163.6-164.45 (NC̲O) (SEC not recorded)

PEI-3(24) ^{1}H NMR (D2O): δ = 2.78-2.98 (m, CH2, 1); 3.08 (m, CH2, 3);3.15 (CH2, m, 4);3.22-3.31 (CH2, s, 5); 3,41. (CH2, m, 6); 3.48 (CH2, s, 7) ^{13}C NMR (D2O): δ =42.97 (CH2,not determined); 44.70 (CH2, 7 and 1);45.41(CH2,7 and 1); 46.43(CH2,5); 46.88 (CH2, 3); 47,47 (CH2, 4); 160.28 (C̲O,9); 163.52-164.49 (NC̲O) (SEC not recorded)

PEI-3(24C) ^{1}H NMR (D2O): δ = 2.86 (m, CH2, 1); 2.95 (m, CH2, 2); 3.29 (CH2, s, 5); 3,42. (CH2, m, 6&7); ^{13}C NMR (D2O): δ = 44.09 (CH2, 7 and 1); 45.51 (CH2, 7&1); 46.59 (CH2, 5); 46.76 (CH2, 3);47,41 (CH2, 4); 160.57 (C̲O, 9); 163.78-164.25 (NC̲O) (SEC not recorded)

PEI-3(48) ^{1}H NMR (D2O): δ = 2.80 (m, CH2, 1); 2.92 (m, CH2, 3); 3.27(CH2, s, 5); 3,40. (CH2, m, 6); ^{13}C NMR (D2O): δ =41.13 (CH2, 5'); 42.37 (CH2, 6),42.88 (CH2, 5); 45.29 (CH2, 6); 47,37 (CH2, 1); 160.28 (C̲O,9); 162.59-164.49 (NC̲O)(M_n = 18000 g/mol; Đ = 2.1)

Table 3 selected data for PEI-3(x) obtained after reaction with sCO_2

Polymer	Reaction time (h)	Amine conversion (%)*	T_m (°C)(DSC)	% loss (100-150°C) (TGA)
PEI-3-(0)	0	0	68.3	/
PEI-3(0.16)	10 min	ns	55.9	30.9
PEI-3(0.5)	0.5	36.8	35.7	31.3
PEI-3(1)	1	32.1	63.1	35.3
PEI-3(2)	2	31.6	56.5	30.9
PEI-3(24)	24	44.4	45.3/T_g (35.0)	27.3
PEI-3(24C)	24/40°C	23.5	61.8	10.9
PEI-3(48)	48	55.0	-19.0	25

4.3 Results and discussion

The work of Pan et al[56] on the modification of b-PEI and L-PEI with ambient CO_2 demonstrated that the more reactive primary amines on b-PEI reacts to form fluorescent carbamates. Moreover, fluorescent poly(2-oxazoline)s were synthesized in the group of Aguiar-Ricardo by using scCO2 as a polymerisation medium, whereby a fluorescent carbamate was introduced at the initiator site.[22,23,69] Intrigued by those literature examples and the fluorescence of carbamate functional polymers, we have explored the modification of the secondary amine group of L-PEI and PEtOx-PEI with $scCO_2$. This chapter is divided in two parts, in the first part we will focus on the reaction between L-PEI and scCO2, which will give us information about the reaction and help us to identify different species. Furthermore, the resulting fluorescent L-PEI may be interesting as intrinsically fluorescent gene transfection vector. Secondly, the treatment of a copolymer containing PEI and PEtOx with $scCO_2$ will be investigated for the preparation of biocompatible fluorescent polymers.

4.3.1 Polymer synthesis with L-PEI

The L-PEI was obtained by the full hydrolysis of well-defined PEtOx (DP 400), which was used in Chapter 2. Two L-PEI polymers were used, referred to as PEI-1 and PEI-3. While the synthesis of both polymers was identical, PEI-1 was a freshly prepared sample while PEI-3 had been standing under ambient conditions for 2 months and attracted water from the air. As seen on the TGA (Figure 4-3 left), the PEI-3 loses more weight during heating in the region of 100°C, an indication of the presence of water. The higher water peak in the ^{1}H-NMR spectrum is another indication of the higher water content of PEI-3. This was further examined with modular DSC (Figure 4-3, right). The modulated method uses small steps of heating and equilibrating to distinguish polymer peaks from non-polymer peaks and can thus be used to identify solvent evaporation peaks. The solid lines of PEI-1 shows that no solvent is present as the reversible and non-reversible cycles are identical both showing the melting point of L-PEI. However for the PEI-3 (dashed lines) an extra peak appears in the non-reversible mode, which is not present in the reversible mode. This weight loss around 120°C is non reversible. This shows that this peak is not related to the polymer and is presumably caused by the evaporation of a solvent, in our case water. The main reason why wet and dry L-PEI were chosen for treatment with $scCO_2$ was to observe if an influence of water could be recognized.[64]

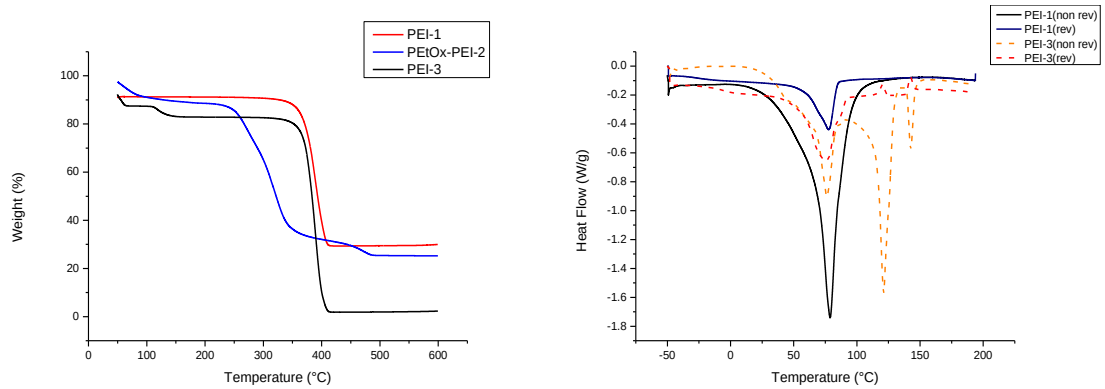

Figure 4-3 TGA (left) and modulated DSC (right) of the starting polymers PEI-1 and PEI-3.

Both L-PEI polymers were exposed to $scCO_2$ in a closed autoclave at 135°C and with a pressure of 27.58 MPa. The secondary amine is expected to react with $scCO_2$ resulting in the formation of carbamates. The advantage of the $scCO_2$ is that it has both liquid and gas properties enabling good penetration into the solid polymer. The reaction times were altered to monitor the progress of the reaction and to spot eventual side reactions. The first change in properties that was observed was the water solubility of the resulting samples as the starting product, the free base L-PEI is not water soluble at room temperature. Also the polymer became bright yellow and even brown for longer reaction times. The texture of the polymer changed from a soft and powder like for the staring materials to a hard and brittle product. The TGA of both the PEI-1 and PEI-3 after exposure to $scCO_2$ for different times are shown in Figure 4-4. The starting polymers start to degrade around 370 °C and are fully degraded at 405°C. This degradation step is also present for the modified polymers, but they reveal a second degradation step between 100°C and 150°C. This mass loss is an indication of the release of CO_2 from the formed carbamates, which happens around 135°C.[65] The PEI-1(0.16) that was reacted for only 10 min with $scCO_2$ has a weight loss of 4.8% in this region. While the PEI-1(0.5) and PEI-1(2) have a weight loss of 32% and 40.5%, respectively, showing that the addition of CO_2 on the polymer has significantly increased. We hypothesized that after 24h and 48h the weight loss would further increase. However, this is not the case as the weight loss of CO_2 drops to ~30%. This observation indicates that the reversibility of the reaction is partially lost upon extended exposure times and that side reactions may occur that lock the CO_2 on the polymer chain.

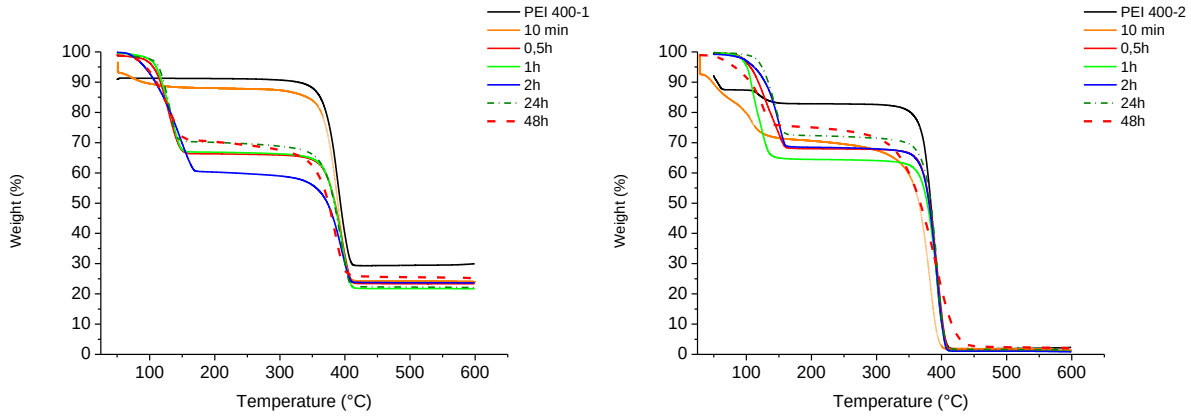

Figure 4-4 TGA of PEI400-1 (left) and PEI400-3 (right) before and after treatment with $scCO_2$for different reaction times.

The PEI-3(x) polymers, Figure 4-4(right), show a similar trend, although the maximum CO_2 loading of 35% is already reached after 1 h. The general weight loss is slightly decreased compared to PEI-1. The weight loss of the 10 min sample probably due to the water present. However in the PEI-3(x) samples it seems that the ring formation happens faster and in this case water helps the ring formation rather than blocking it. Nonetheless, for both polymers it is shown that after a short time, the loss of CO_2 is maximised and with longer reaction times this loss decreases due to side reactions locking the carbamates on the chain. We obtained a maximum of 40% loading of CO_2 while, as stated before, the maximum loading is 50% on L-PEI due to the formation of a zwitterionic carbamate.

To further evaluate the effect of $scCO_2$ treatment on the residual polymer after heating and CO_2 loss, differential scanning calorimetry (DSC) was performed. The first run, not shown, shows a transition around 135°C which is the irreversible release of CO_2, as seen in TGA. Therefore, the second run was evaluated and since all CO_2 should be removed during the first heating run the original L-PEI should be retained if only carbamates are formed. The pure L-PEI has a melting transition at 69,7 °C and for PEI-1(0.16) there is almost no shift in T_m, meaning that the newly formed groups are indeed carbamates. With longer reaction times, a clear shift of the T_m is seen towards lower melting temperatures. For the 2h reacted polymer the T_m is 53°C indicating that the remaining polymer after removal of the carbamate is different than the original PEI and the crystallinity is disturbed. For the 24h reacted polymers, the DSC revealed a glass transition temperature (T_g), followed by a cold crystallization (exotherm) and a melting transition. The 48h reacted polymers no longer have a T_m, but only a T_g indicating the amorphous nature of these polymers.

The TGA and DSC results prove that CO_2 has been chemically bound to the PEI after treatment with $scCO_2$ and is only partially released upon heating the samples. Moreover, the original L-PEI is not recovered for $scCO_2$ longer exposure times and in particular the samples of 24 and 48h exposure indicated

that the carbamates have irreversibly reacted with L-PEI. Based on the literature it may be proposed that the cyclic urea side product is formed.[64,65]

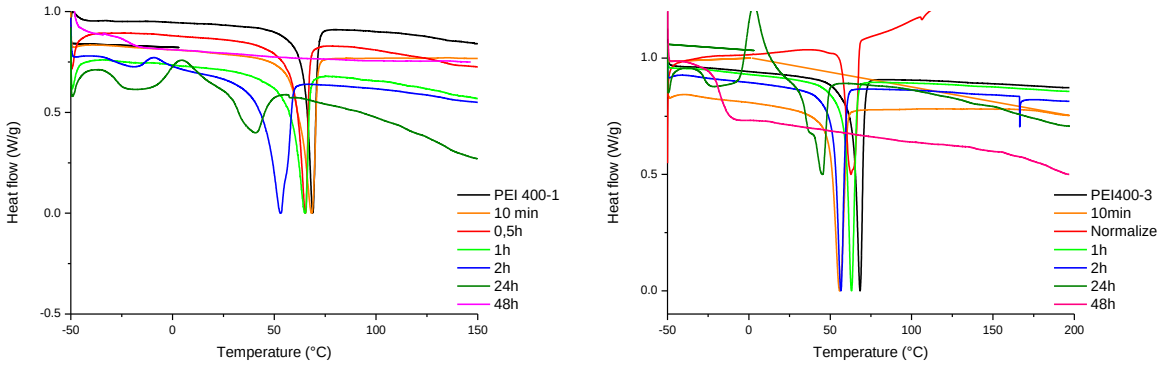

Figure 4-5 DSC of PEI-1(x) (left) and PEI-3(x) (right) before and after treatment with $scCO_2$ for different times.

The ^{1}H-NMR spectra of PEI-1(x) and PEI-3(x) after exposure to $scCO_2$ for different times are shown in Figure 4-6, left. Notice that the 10 min sample is not added as this was found to be insoluble in conventional solvents such as CD_3OD, $CDCl_3$, D_2O, D-DMSO. The single PEI-peak at 2.7-2.8 ppm has disappeared which is a proof of the reaction between the PEI and CO_2 forming the carbamate and inducing a chemical shift of the CH_2 protons. Hereby 3 domains are distinguished, the first domain is found in the region 2.8-3.60 ppm (peaks (1-4)) corresponding to CH_2 protons next to a free amine, these are the unreacted PEI units. The second region contains a single peak (5) at 3.30 ppm. The last domains is located between 3.35-3.55 ppm and contains a both a shoulder (6) and a large peak (7). This domain corresponds with the CH_2 groups next to an amide, probably the carbamate. Important to notice is the rise in intensity of peak (6) with longer reaction times. In PEI-1(48) this peak is as large as peak (7). The peaks of (6) and (5) overlap with longer reaction time. In PEI-1(0.5) this is a single peak but the 48h sample shows a large overlap between (5) and (6). The PEI-3(x) polymers are shown in Figure 4-6, right. The three domains can again be recognized, however peak (1) is larger and the peak (4) remains smaller. The main difference is that (6) seems to be enhanced and is incorporated in (7) rather than being present as a shoulder. The 48h sample shows that peak (1) is similar to the start PEI peak, peak (7) has disappeared and (6) is the single peak. This means that this polymer does not contain any carbamates and only the presumably isolated cyclic urea. In summary, the ^{1}H-NMR spectra show that there are three types of CH_2 groups formed, one related to PEI, one related to a possible carbamic acid and a third unassigned resonance.

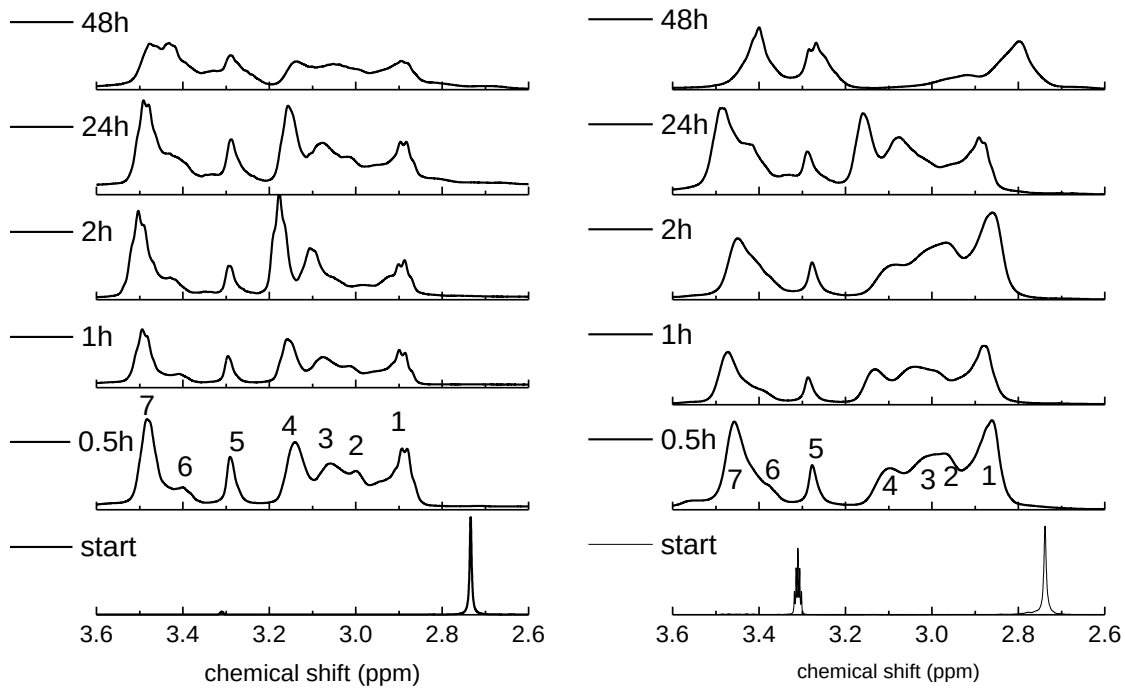

Figure 4-6 Stack plot of the 1H-NMR spectra of PEI-1(x) and PEI-3(x) before and after exposure to $scCO_2$ for different times; measured in D2O except for both start polymers that were measured in CD3OD.

The 2D correlation spectroscopy {^{1}H-^{1}H} (COSY) was used to identify the relation between the different protons. The COSY of four different polymers was measured, namely PEI-1(0.5); PEI-1(2), PEI-1(48) and PEI-3(48). All PEI-1(x) polymers show one cross peak. Therefore, only the COSY spectrum of PEI-1(0.5) is shown in Figure 4-7. The rectangle shows the cross peak between the protons (4) and (7). Hence CH_2 (4) is a direct neighbor of the CH2 (7), which is the CH2 next to the amide. This means that both methylene groups are neighbouring and because the CH_2 (7) is located next to a carbamic acid, the CH_2 (4) will be neighbouring an amine of PEI as indicated in Figure 4.7. The COSY of PEI-3(48) will be discussed further on because this polymer has a different functionality.

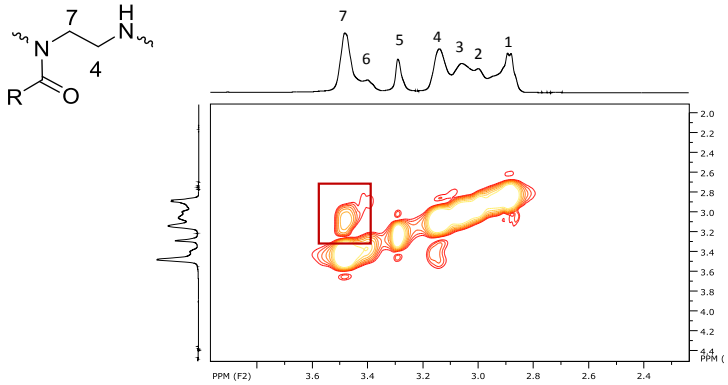

Figure 4-7 COSY spectrum of PEI-1(0.5) in D_2O. The red rectangle shows the cross peak between protons (7) and (4). The chemical structure shows the correct assignment.

To further understand the ^{1}H and ^{13}C-NMR spectra and the corresponding polymer structures, a more detailed study was performed on three different polymers PEI-1(0.5); PEI-1(2) and PEI-1(48). The ^{13}C-NMR spectrum of the PEI-1(0.5) is shown below in Figure 4-8 revealing a range of peaks in the region of 42-50 ppm (CH_2-domain) and above 160 ppm (C=O domain). These extra signals are not present in L-PEI and indicate that the CO_2 is bound on the amines of the L-PEI. The peak at 160 ppm is intriguing as similar observations were reported in an earlier publication.[56] This paper claimed that this peak corresponds to the deprotonated carbamic acid. The HMBC analysis described further will however show this is incorrect. Next to our experimental prove, literature also provides some arguments that contradict this assignment. First, all peaks are broad indicative of polymer signals, except for the signal at 160 ppm. Secondly carbonates are well studied specie by ^{13}C-NMR spectroscopy and a broad range of publications indicate that the 160,1 ppm signal belongs to the CO_3^{2-}/HCO_3^-.[70–73] The carbonate is formed when the carbamate is hydrolysed and produces the bicarbonate and the free amine. This is shown in the reaction below.[70]

$$R_2NCOO^- + H_2O \rightleftarrows HCO_3^- + R_2NH$$

The carbonate is formed due to the solvation of CO_2 in water were the amine acts as a base leading to following equilibrium were B is a base. This explains the presence of the sharp peak at 160 ppm in Figure 4-8.

$$CO_2 + 2H_2O \rightleftarrows HCO_3^- + H_3O^+$$

$$HCO_3^- + BH \rightleftarrows CO_3^{2-} + BH_2^+$$

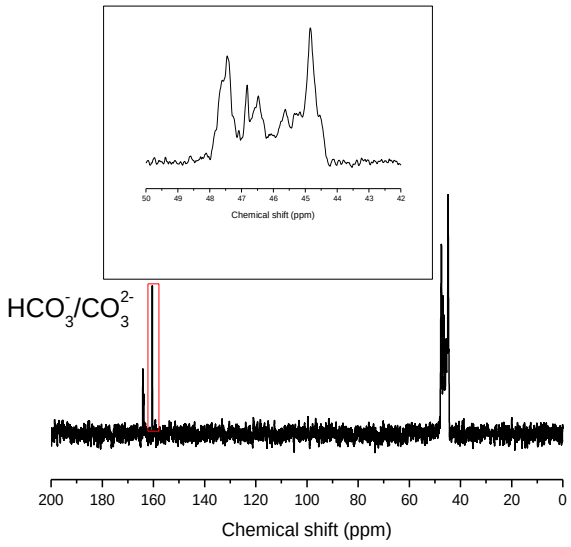

Figure 4-8 ^{13}C-NMR spectrum of PEI-1(0.5h) in D_2O, The inset shows the zoom of the CH_2 region(42-50) ppm.

The assignment of the peaks located between 40-50 ppm on the ^{13}C-NMR will tell us which type of CH_2 groups are present. Therefore an identification of the carbon peaks and the corresponding protons is done *via* the 2D NMR technique, {^{1}H-^{13}C}, heteronuclear single quantum correlations spectroscopy (HSQC). For the PEI-1(0.5) the HSQC spectrum is shown in Figure 4-9, allowing identification of the protons and the corresponding carbon atoms. Carbons (1) and (7) have overlap and cannot be distinguish *via* this technique. The carbon connected to H (2) is not visible and does not form a cross peak on the HSQC, probably caused by the lower abundance of C (2), similar conclusions can be drawn for C (6). Table 4 lists the corresponding coordinates of the cross peaks.

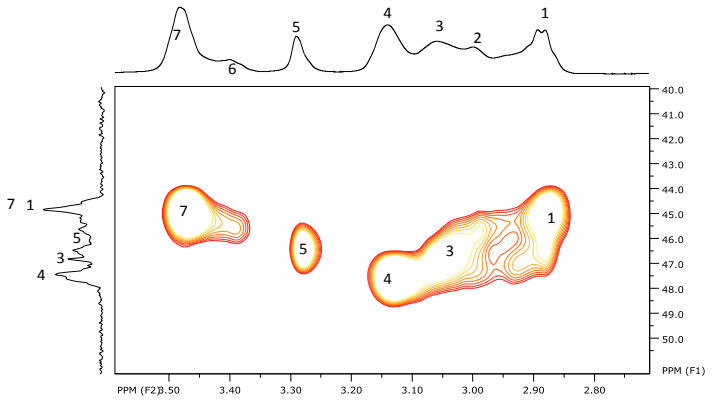

Figure 4-9 HSQC spectrum of PEI-1(0.5) in D2O

Table 4 Cross-peaks present in the HSQC spectrum of PEI-1(0.5); f1(^{13}C-NMR), f2(^{1}HNMR)

CH_2	f1(ppm)	f2(ppm)
1	44.9	2.87
2	/	/
3	46.8	3.07
4	47.6	3.13
5	46.4	3.28
6	/	3.40
7	44.9	3.47

By identifying the neighboring groups of the CH_2 groups, the chemical environment will be unraveled. This can be done via heteronuclear multiple bond correlation (HMBC) spectroscopy. We split the HMBC spectrum in two parts to have a better overview, the first part will focus on the 40-50 ppm region (CH_2) (Figure 4-10) while the second part focus on 155-165 region (quaternary carbons) (Figure 4-11). The cross peaks correlate specific carbon atoms and protons within 2-4 bonds. Table 5 lists the cross peaks and corresponding coordinates. The cross peaks designated with a number are cross peaks that were also present in HSQC spectrum, Table 4. This means that the protons are connected to carbons with a similar chemical environment. The cross peaks (a) and (b) show that CH_2(3) and CH_2(1) are connected, however on COSY (Figure 4-7) no cross peak is observed. This implies that there is an amine group in between both CH2 groups. We propose an amine group in the middle as both CH_2 groups are located in the PEI region and no connection can be found with a carbonyl group. The chemical shift is induced by the change in chemical environment between CH_2(3) and CH_2(1), proposed structure is given in Figure 4-10. Cross peaks (c) and (e) confirm the conclusion obtained from the COSY spectrum, by linking (7) and (4) as neighboring CH_2 groups; the proposed structure can be found in Figure 4-7. The last cross peak is (d), which cannot be assigned due to the overlap of carbons (7) and (1). This means that either C(7) or C(1) are connected to H(5).

The 155-170 region, Figure 4-11, shows the correlation of the quaternary carbons with only two protons H(7) and H(5). This confirms that these peaks are the carbamates of the CH2 groups next to an amide like bond, CH_2 (7) in Figure 4-7. The CH_2 (5) is connected to a amide bond, however the nature of the carbonyl is still unclear (Figure 4-11).The second carbonyl group (160 ppm) does not connect with any protons in

the proximity of three to four bonds. This confirms our assignment of this sharp CO_3^{2-} signal as no protons are connected.

Table 5 Cross peaks present in the HMBC spectrum of PEI-1(0.5).

Cross peak	f1(ppm)	C	f2(ppm)	H
1	44.97	1	2.87	1
a	46.84	3	2.87	1
2	45.75	?	2.98	2
b	44.64	1	3.06	3
c	44.74	7	3.14	4
4	47.6	4	3.13	4
5	46.4	5	3.28	5
d	44.8	7/1	3.29	5
7	44.7	7	3.49	7
e	47.5	4	3.5	7
f	163.9	8	3.28	5
g	164	8	3.48	7

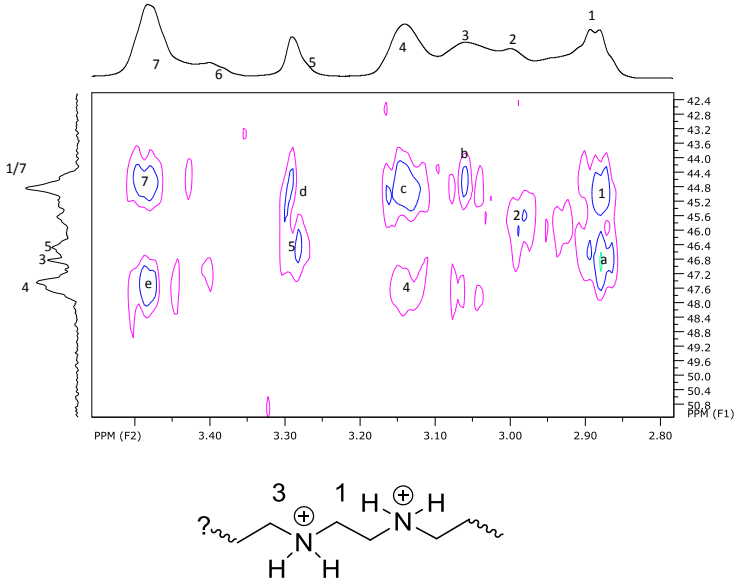

Figure 4-10 Zoom of the HMBC spectrum of PEI-1(0.5) (region 40-51 ppm). The structure below shows a part of the backbone of the modified polymer. CH_2 (1) is connected with CH_2 (3) within two bonds.(D_2O)

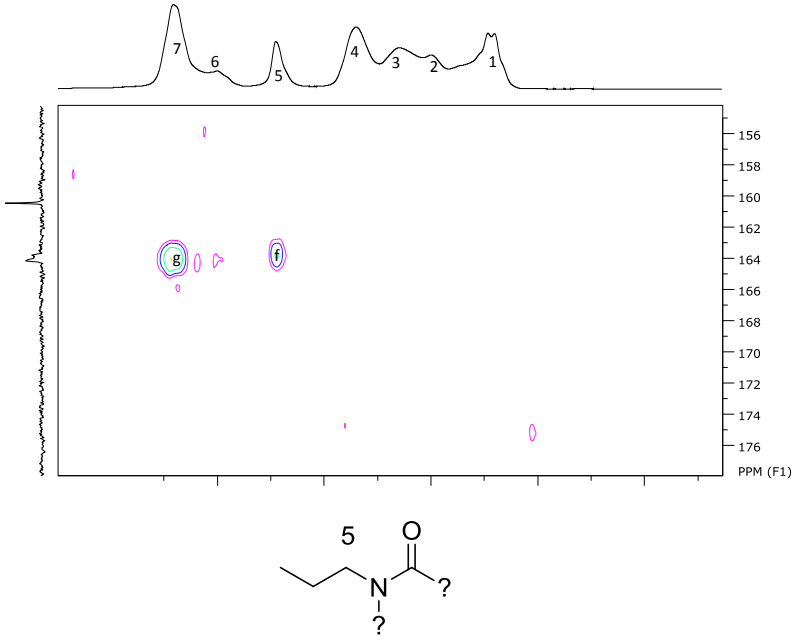

Figure 4-11 Zoom of the HMBC spectrum of PEI-1(0.5) (region 160-150ppm) (D_2O)

To evaluate and understand the polymer structure for the other polymers, a similar NMR analysis was done on the PEI-1(2). As shown in the stack plot in Figure 4-6, peak H(4) and H(6) are slightly increased in PEI-1(2) compared to PEI-1(0.5). As previously mentioned the COSY spectrum of these polymers does not provide extra information. The HSQC is shown in Figure 4-12. A few extra details appear as cross-peaks (1) and (7) in PEI-1(2) are slightly separated. The cross peak of H(6) and C(6) is visible and appears at 45.6 ppm and 3.40 ppm. In the stacked plot (Figure 4-6) H(6) is a shoulder of the H(7), which increases with longer reaction times. In the HMBC spectrum of PEI-1(2) (Figure 4-13) we see similar correlations as for PEI-1(0.5). The cross peaks can be found in Table 7, which however do not provide extra information for the CH_2 area. CH_2(1) and CH_2(3) have a cross peak (a) which was identified in Figure 4-10, CH_2(7) and CH_2(4) have two cross peaks (b) and (d) which was identified to be in Figure 4-7. C(7/1) and CH_2(5) have a cross peak (c), which does not provide further information as C(1) and C(7) are inseparable. The region of the quaternary carbons provides more valuable information. The quaternary carbon (8) does not only have cross-peaks with (5) and (7) ((e) and (f)) but also shows an extra cross-peak (g) with H(6). This means that the CH_2(6) is in close contact with a carbonyl functionality. Via the DSC and TGA we showed that the amount of presumably cyclic urea is increasing with reaction. This is confirmed by the stacked plot where H(6) steadily grows upon time confirming that the CH2(6) is most likely located within the irreversibly formed cyclic urea.

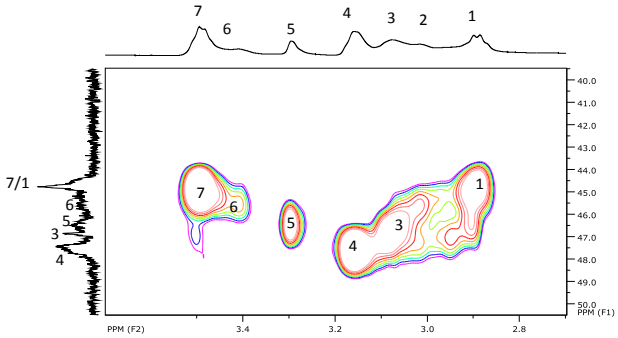

Figure 4-12 The HSQC spectrum of PEI-1(2) in D20

Table 6 HSQC cross peaks present in the spectrum PEI-1(2)

CH_2	f1(ppm)	f2(ppm)
1	44.77	2.87
2	/	/
3	46.9	3.07
4	47.6	3.14
5	46.5	3.29
6	45.6	3.40
7	44.9	3.47

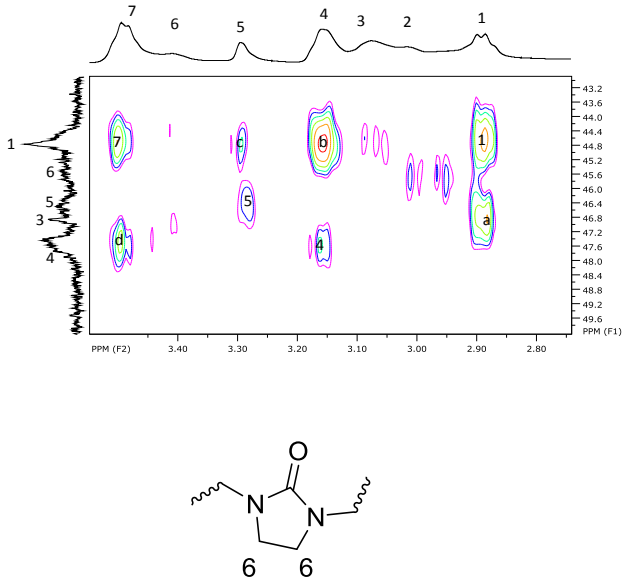

Figure 4-13 HMBC spectrum of PEI-1(2) (D2O). The structure shows that CH_2(6) is located in the cyclic urea.

Table 7 Cross peaks present in the HMBC spectrum of PEI-1(2)

Cross peak	f1(ppm)	C	f2(ppm)	H
1	44.68	1	2.87	1
a	46.91	3	2.87	1
b	44.69	7	3.15	4
4	47.66	4	3.15	4
5	46.48	5	3.28	5
c	44.82	7/1	3.30	5
7	44.77	7	3.50	7
d	47.61	4	3.5	7
e	163.76	8	3.28	5
f	164	8	3.49	7
g	164	8	3.40	6

The polymer which was exposed to $scCO_2$ for 48h was also examined in further detail as this could provide further information about the ring formation. As the TGA showed a decreased in CO_2 loss around 130°C this polymer should contain more irreversibly formed ring structures. This was confirmed by the second run of the DSC, that indicates that the polymer after heating to remove the carbamates is no longer pure L-PEI. The ^{1}H-NMR spectrum of PEI-1(48) shows that the peaks H(6) and H(7) merge into one large domain. On the HSQC spectrum (Figure 4-14) the new appearing peaks on the ^{13}C-NMR spectrum are

assigned. The spectrum shows that the signal of C(1) shifted around 1 ppm on the ^{13}C-NMR spectrum so it's no longer overlapping with C(7). Peaks C(5), C(6) and C(7) remain at the same location, although a few new peaks appear too. There is an extra peak C(5'), which has its carbon at 42.55 ppm, in between C(6') and C(6"). This is a clear indication that the polymer contains different chemical environments compared to L-PEI and PEI-1(2). The HMBC cross peaks are listed in Table 9. Again CH_2(3) and CH_2(1)are connected as well as CH_2(7) and CH_2(4). Due to the deconvolution of C(1) and C(7), it is revealed that CH_2(5) and CH_2(1) have a cross peak. This helps to unravel the problem we had with the PEI-1(0.5) as both (7) and (1) were located at the same chemical shift in the ^{13}C-NMR spectrum. Peaks (6") and (5) are also correlated which could indicate that all kinds of micro domains have arisen. This means that all kind of domains with different neighbouring groups are formed, amines located next a carbamate or ring.

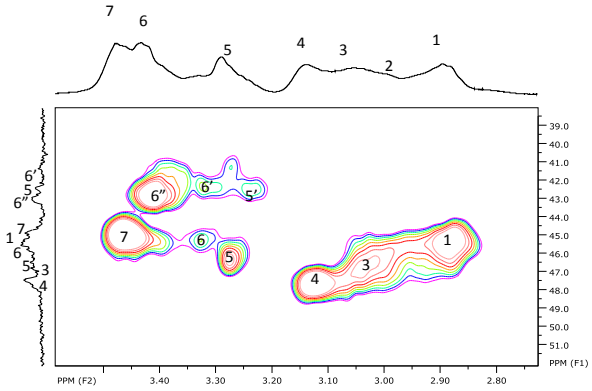

Figure 4-14 HSQC spectrum of PEI-1(48) in D2O.

Table 8 Cross peaks in the HSQC spectrum of the PEI-1(48).

CH_2	f1(ppm)	f2(ppm)
1	45.52	2.91
2	/	/
3	46.60	3.05
4	47.68	3.15
5	46.30	3.30
5'	42.55	3.26
6"	42.81	3.43
6'	42.46	3.34
6	45.36	3.35
7	44.87	3.48

Table 9 Cross peaks in the HMBC spectrum of PEI-1(48)

Cross peak	f1(ppm)	C	f2(ppm)	H
1	44.53	1??	2.83	1
a	46.73	3	2.84	1
b	44.83	7	3.10	4
4	47.66	4	3.15	4
5	46.28	5	3.24	5
c	42.99	6"	3.20	5
d	44.82	1	3.30	5
7	44.83	7	3.45	7
e	47.54	4	3.44	7
f	163.65	8	3.24	5
g	163.84	8	3.29	5
h	164	8	3.44	7
I	162.72	?	3.20	5

When observing the stack plot of PEI-3(x) a similar behaviour is seen as in the PEI-1(x) polymers, except for the PEI-3(48). This polymer gives us an unique opportunity as it contains the highest fraction of cyclic urea rings. The shoulder H(6) is dominant and the H(7) peak seems to have disappeared. The H(4) peak has also disappeared again showing the relation between these two peaks. The peak of the CH_2 correlated with PEI, shows a double distribution H(1&2). The manifold of peaks that was previously present in the other polymer samples has vanished. We further investigated the PEI-3(48) *via* different NMR techniques. Already on the COSY spectrum, Figure 4-15, a remarkably difference is observed. The previous COSY spectra only showed one cross peak between peaks H(4) and H(7), while the PEI-3(48) polymer showed a cross peak connecting H(1) and H(5).

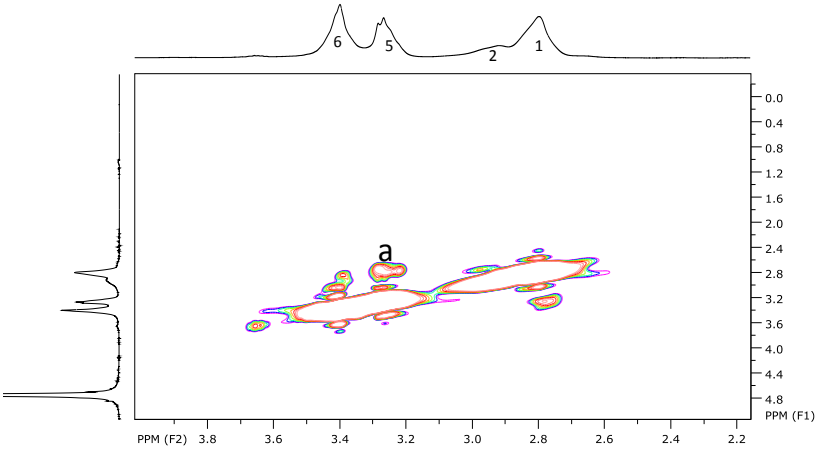

Figure 4-15 ^1H-^1H COSY spectrum of PEI-3(48) in D_2O.

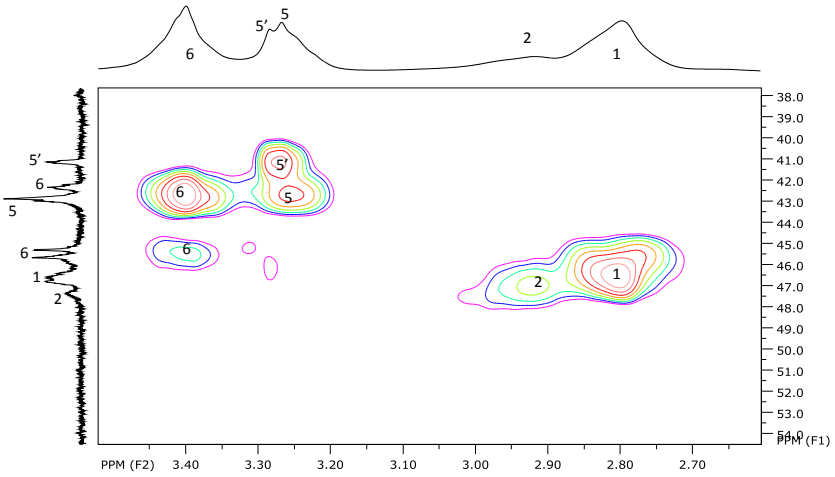

Figure 4-16 HSQC spectrum of PEI-3(48) in D_2O.

Table 10 Cross peaks in the HSQC spectrum of PEI-3(48).

CH_2	f1(ppm)	f2(ppm)
1	46.55	2.80
2	47.93	2.92
5	42.68	3.25
5'	41.12	3.27
6	42.65	3.40
6	45.43	3.40

The identification of the carbon atoms with the corresponding protons is found on the HSQC spectrum, Figure 4-16 and Table 10. Remark that for H(6) and H(5) two types of carbons can be found C(6&6') and C(5&5') respectively. This may be caused by two neighbouring cyclic urea, however this cannot be concluded from the present data. The HMBC spectrum of PEI3-(48), Figure 4-16, gives us valuable information about the interaction with the urea ring. It shows that both H(7) and H(4) are correlated as they both disappeared from the ^{1}H-spectrum. It was already shown that CH_2(7) was correlated to an amide bond. In this polymer no significant carbamates were present, only ring structures. Furthermore, peaks (5) and (1) are also part of the same family. Focusing on (5) we know that is in close contact with a carbonyl functionality, found on the previous HMBC spectrum as it shows a cross peak with a Cq. However the absence of the carbamic acid on this polymer shows that there is also a correlation between CH_2(1) and CH_2(5) which was confirmed on the COSY spectrum. The HMBC spectrum clearly shows that CH_2(6) and CH_2(5) are in proximity. This means that the CH_2(5) is located next to the ring, Figure 4-17.

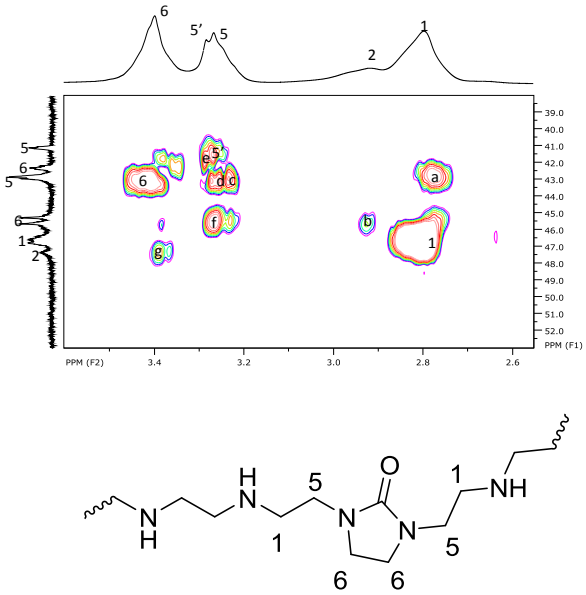

Figure 4-17 HMBC spectrum of the PEI-3(48) in D_2O. Structure showing the urea ring and the assigned peaks.

Table 11 Cross peaks observed in the HMBC PEI-3(48)

Cross peak	f1(ppm)	C	f2(ppm)	H
a	42.86	5	2.78	1
1	46.77	1	2.80	1
b	45.73	5/6	2.93	2
C	43.01	5/6	3.24	5
d	43.10	5/6	3.25	5
5’	41.53	5’	3.27	5‘
e	43.10	5/6	3.27	5’
f	45.47	6	3.27	5’
6	43.04	6	3.42	6
g	47.41	2	3.39	6
H	162.95	Cq	3.25	5
I	162.58	Cq	3.28	5’

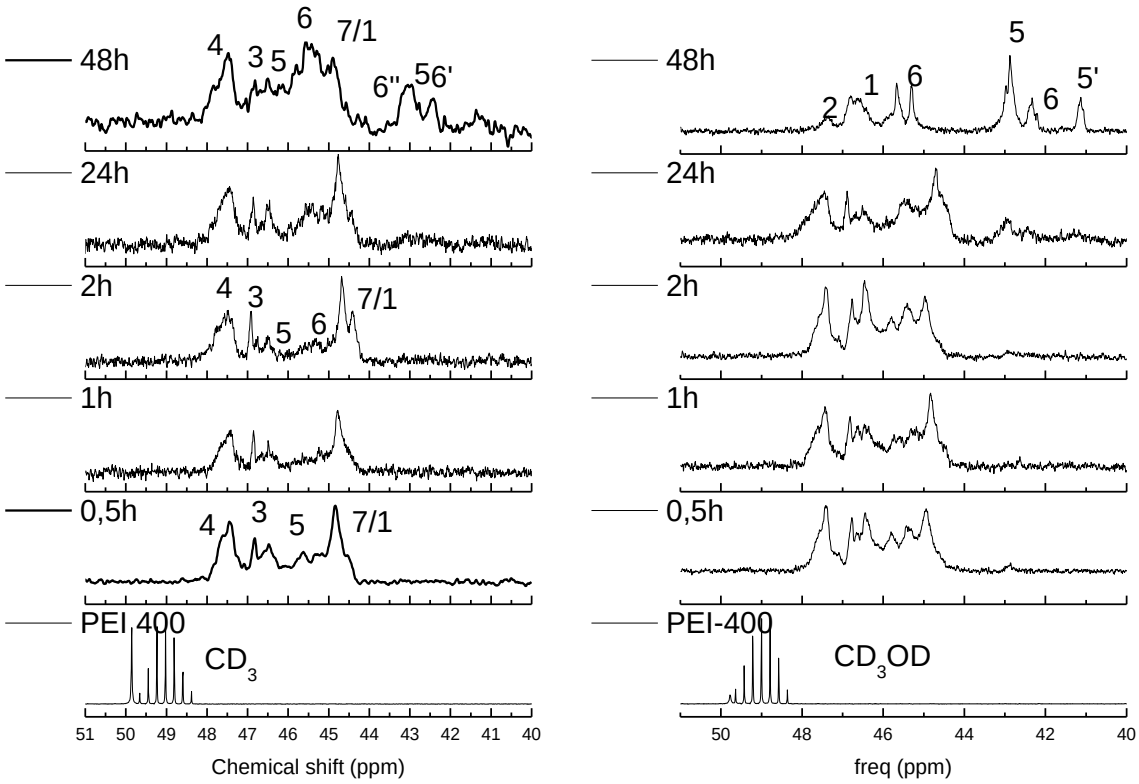

Figure 4-18 ^{13}C-NMR spectra stack plots of the PEI-1(x) (left) and PEI-3(x) (right) in D_2O.

All peaks in both the ^{1}H-NMR and ^{13}C-NMR spectra have now been identified and the assigned peaks and structures are summarized in Figure 4-19. The first group of peaks indeed has no contact with a carbonyl functionality and can be appointed as the CH_2 zone next to PEI, this includes the peaks from (1)-(4). The peak corresponding with (1) is probably the CH_2 group next to the amine, in an amine rich environment. The peak CH_2(4) is located next to peak CH_2(7) in the HMBC and COSY spectra and when (7) disappeared peak (4) also vanished. We can therefore assume that this is the PEI unit in a carbamate rich environment as it shows no correlation with other CH_2 groups of PEI. In the second CH_2 zone the peaks (5), (6) and (7) are located corresponding to CH_2 groups, next to a carbonyl functionality. This is the carbamate zone. During the reaction with $scCO_2$ (6) is steadily growing so it is proposed that this is the CH2 of the cyclic urea. Hence (7) is the CH_2 group next to the carbamate. For CH_2(5) the assignment is complex as it is connected with a carbonyl of an amide and it is in contact with CH_2(1). This can be the CH2 next to the ring structure while still in contact with the CH_2 group of PEI. As the carbamate can't exist as stable species, the formation of a zwitterion plays an important role. Therefore, it may be speculated that all the NH groups located next to the carbamate functions have a positive charge, which alters the chemical shift as observed in peak (4). This is different for the urea ring as here no charge is

formed during the ring formation as the reaction happens through a dehydration reaction of the carbamates (Scheme 4-2). When water is present, the zwitterion can be destroyed by removing the H^+ from the amine. This amine can react with the carbamate forming the ring as the nucleophile is restored. The TGA shows the decreased release of CO_2 upon longer reaction times indicating that the formation of the cyclic urea is quite slow. The change in T_m shows that the original PEI has disappeared and more and more rings are formed, which lowers the melting temperature and eventually leads to an amorphous polymer with. These polymers also lost the softness and became brittle.

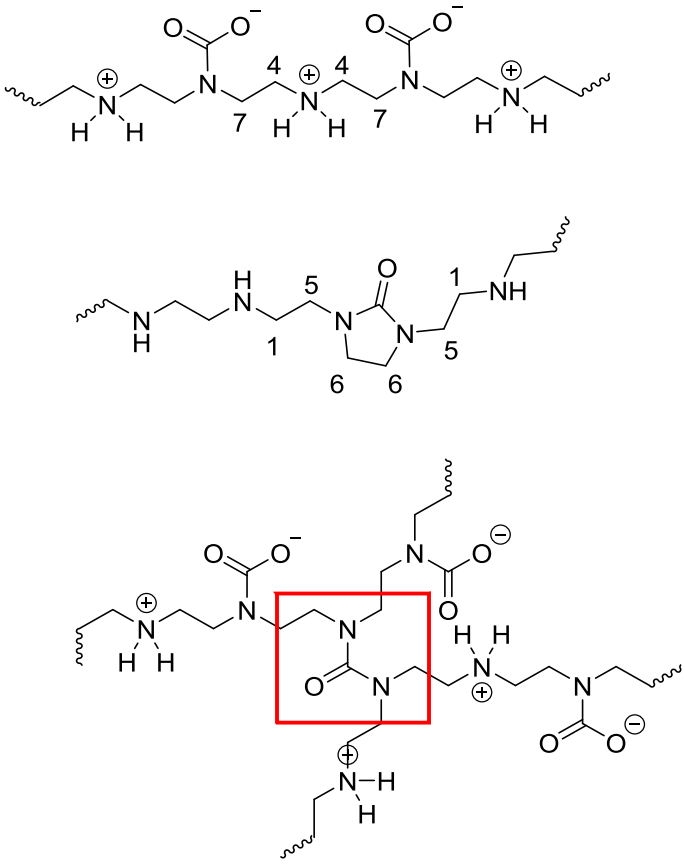

Figure 4-19 Overview of the different structures that are formed during $scCO_2$ treatment of L-PEI. Top: the zwitterionic carbamate is formed at the beginning in the reaction. Middle: formation of a cyclic urea, locking the carbamate on the backbone . Bottom: formation of a urea bond and as such cross linking between different polymer chains

In summary it can be concluded that the secondary amine on the L-PEI can react with the $scCO_2$ to form carbamates as indicated by the weight loss on the TGA. However after 2hr reaction time a decrease in weight loss on the TGA meaning that less CO_2 is released while the $scCO_2$ reaction time was longer. This decrease in weight loss is explained by the DSC, which shows that after longer reaction time the melting temperature of the L-PEI is lost indicating that the carbamate bonds are irreversible locked onto

the polymer backbone and the reversibility is lost by the formation of cyclic urea structures. The NMR studies confirms this hypothesis by showing that the present CH_2 groups can have different chemical environments. As shown in Figure 4-19 (top) at the beginning of the reaction the formation of a zwitterion occurs. Herewith only two CH_2 are recognized as either the PEI is converted into a carbamate(7) or protonated(4) (Figure 4-19 top). Already in the first moments of the reactions a second structure is formed that locks the carbamate by forming the cyclic urea bond. Here two CH_2 groups can be recognized, either (6) which is located in the ring or (5) which is located next to the ring, (Figure 4-19 middle). A last structure is proposed by the formation of a urea bond by cross linking two chains.(Figure 4-19, bottom).

The reaction mechanism to form the cyclic urea could also occur between multiple chains leading to chain coupling. The formed ring and the crosslinking bond have a similar chemical environment and therefore NMR cannot be used to see a distinction. Therefore SEC analysis was performed in HFIP, which is an excellent solvent for PEI like polymers. Caution still has to be taken, because the introduction of charges can induces more column interaction which may affect the measurement. This was indeed shown an the SEC traces are inconclusive

Due to the presence of the carbamate groups the formed polymers are fluorescent, which is induced by the close contact of the HOMO and the LUMO within one bond enabling delocalization of the excited electron. The fluorescence spectra of the polymers are shown Figure 4-20. Note that the polymers with the cyclic urea are still fluorescent and only a small shift towards lower wavelength is observed. In the case of the cyclic urea a different HOMO and LUMO is activated and thus different entities are exited. Figure 4-21 shows the difference between the absorption and the emission spectra of the 2h exposed polymer. The maximum of the absorbance spectrum can be found at 260 nm and for the fluorescence this is 470 nm, resulting in a Stoke shift of 210 nm. Which is of great importance as the larger the shift between both the better it is for fluorescence.

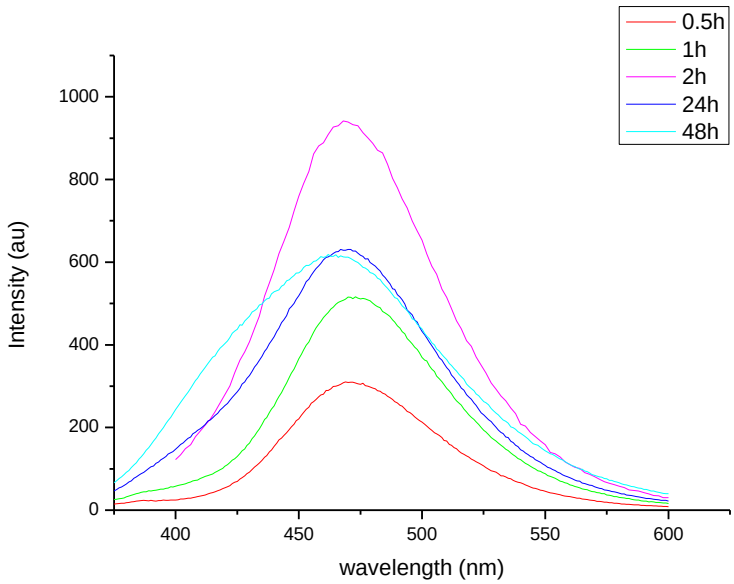

Figure 4-20 Fluorescence spectra of PEI-1(x) in water

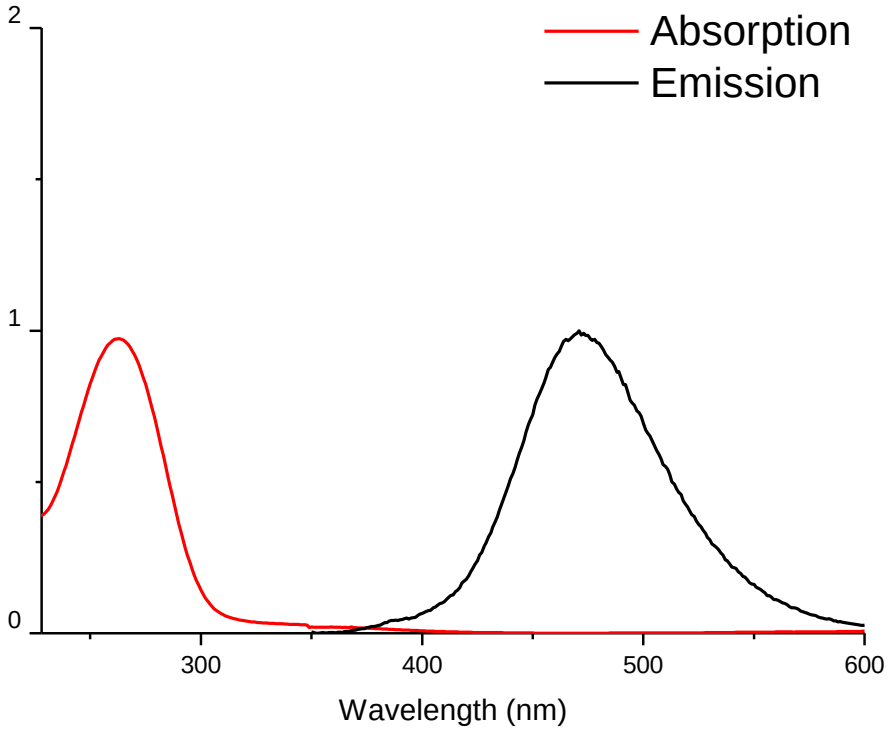

Figure 4-21. The comparison between the absorption and the emission of PEI-1(2large) in water.

The carbamate bond is a reversible bond and by heating the CO_2 is released. To confirm the formation of the cyclic urea the polymer was heated above 200°C to remove all carbamates. During this heat

treatment that was performed in a close reaction vessel, there was a clear pressure build-up by release of the CO_2, that ejected the septum of the microwave vial. The stacked plots of the ^1H NMR spectra (Figure 4-22)of the polymers before and after heat treatment clearly show the pure L-PEI is not regained, it was previously also shown by DSC. However, it is evident that peak H(6) is present confirming the earlier conclusion that this is the CH2 group of the cyclic urea. Similar conclusions can be drawn for peak (1) as this resembles the PEI-3(48). The broad peaks containing H(5) and H(6) probably have a lot of different small domains with different environments of L-PEI in between, which causes all kind of different chemical shifts and the corresponding peak broadening. Interestingly, the resulting polymer after heat treatment and removal of the carbamates still showed fluorescence indicating that the formed cyclic urea is also fluorescent, (Figure 4-23) for which the origin is unclear. The comparison to dendritic polyureas may give a hint, even though in literature no real consensus has been reached to explain such type of fluorescence. It was already shown that PAMAM urea dendrimers show intrinsic fluorescence, that is pH dependent[48] which is ascribed to the combination of the urea and the positive charged end groups.[74] In the case of the cyclic urea rings we have a similar system. First of all the polymer contains the needed urea ring and second of all the PEI units, that are still present can be protonated. An important observation is that the initial L-PEI is not water soluble and after $scCO_2$ treatment followed by heating *i.e.* by addition of the ring structure, a water soluble PEI is formed. This solubility most likely results from suppression of the crystallisation by the cyclic urea groups that also lead to intrinsic fluorescence of this L-PEI analogue.

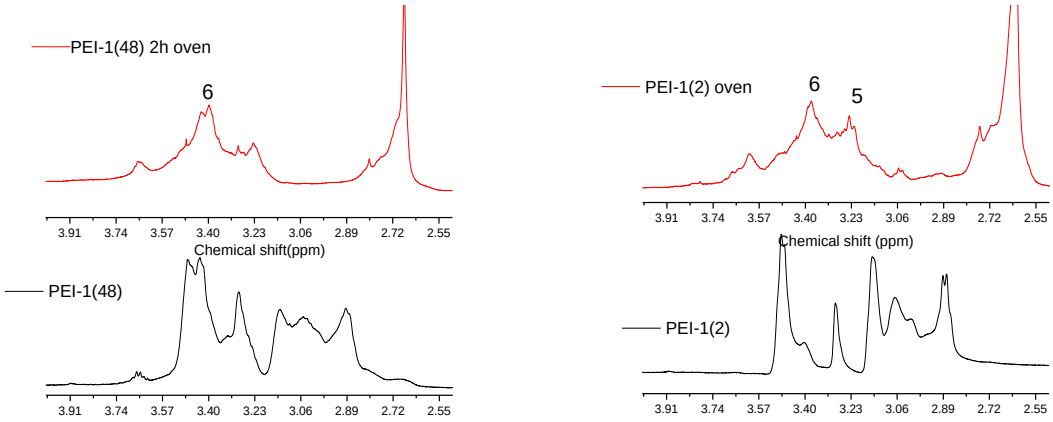

Figure 4-22 ^1H NMR spectra of PEI1-(2) (left) and (PEI-1(48) (right) before and after heat treatment at 200 ^oC (oven); all measured in D2O.

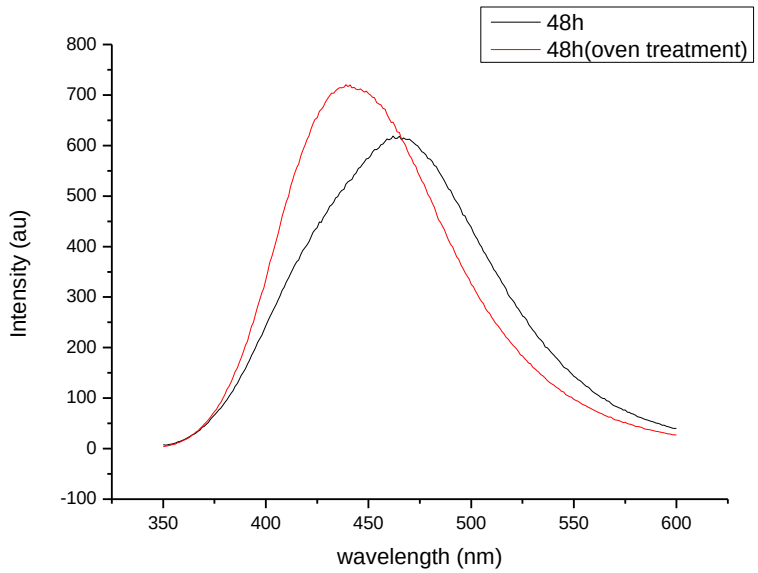

Figure 4-23 Fluorescence spectra of PEI-1(48) before and after heating in oven.

To see whether it was possible to do the modification of L-PEI with $scCO_2$ at lower temperatures, both PEI-1 and PEI-3 were also reacted with $scCO_2$ at 40°C for 24h and 27.58 MPa pressure. The difference between both PEI-1(24c) and PEI-3(24c) is shown Figure 4-24. The amount of CO_2 bound to the L-PEI is 34% and 24% respectively, calculated based on the ^{1}H-NMR spectra. TGA confirms this as it shows a higher weight loss for PEI-1(24c) compared to PEI-3(48) (Figure 4-24).

The DSC data of both polymers shows a distinct difference as the PEI-(24c) has a Tm of 86°C and the PEI-3(24c) has two melting points at 62.4 °C and 83.1°C in the second run. This can indicate that a part of the polymer sample still contains unmodified L-PEI units while another part is similar to the PEI-1(24). This reaction temperature of 40°C is well below the Tm of the starting polymers which means that the polymer is in a solid state. It may therefore be speculated that the high reaction temperature melts the polymer and all parts are easily accessible for reaction. For the low temperature modification, the porosity of the polymer sample influences the contact with $scCO_2$. The PEI-3 was indeed a more dense solid and had a more brittle appearance. The HFIP SEC shows that between the low and high temperature exposure to $scCO_2$ there is a clear difference as the low temperature treatment leads to much higher molar mass indicating significant interaction in coupling. The origin of this difference may lay in solubility, (Figure 4-25).

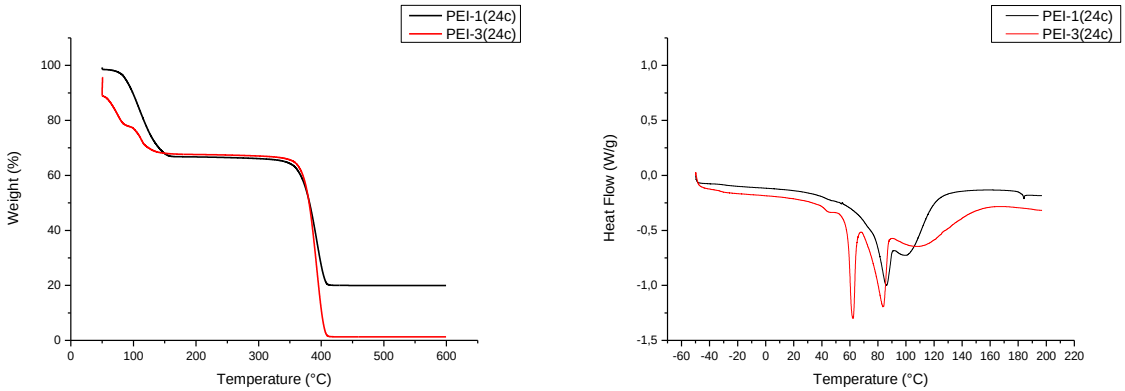

Figure 4-24 TGA of the PEI-1(24c) and PEI-3(24c) (left); DSC of the PEI-1(24c) and PEI-3(48c) (right)

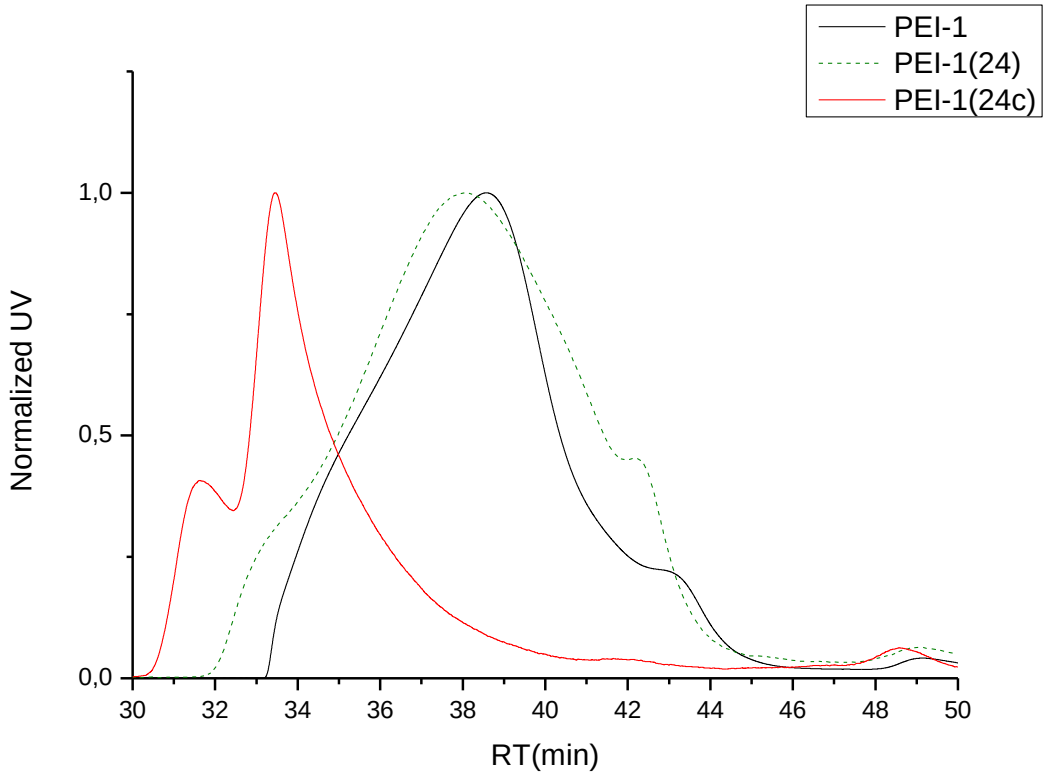

Figure 4-25 Normalized HFIP SEC-UV signal (375nm) PEI-1, PEI-1(24) and PEI-1(24c)

The ^{1}H NMR spectra overlay, Figure 4-26, indicates that the PEI-1(24C) reacted at 40°C shows similar peaks as the PEI-1(24). Indicating that this polymer has both the ring, the functionalized part and the PEI, hence the temperature does influence the ring formation. The PEI-3(24c) spectrum is similar to the PEI-

3(48) spectrum. This indicates that the formation of the ring happens at lower temperature and is merely influenced by the water content. This is opposite to literature reports that state that the presence of water blocks the formation of the rings as during the formation of the ring H_2O is released and the reaction is slowed down in presence of water.[75] However, in our case we have a catalytic amount of water present which can act as a charge carrier and promotes ring formation by the formation of H_3O^+.[56] This removes the charge from the protonated amine and enhances the nucleophilic attack of the lone pair of the amine onto the carbamate.

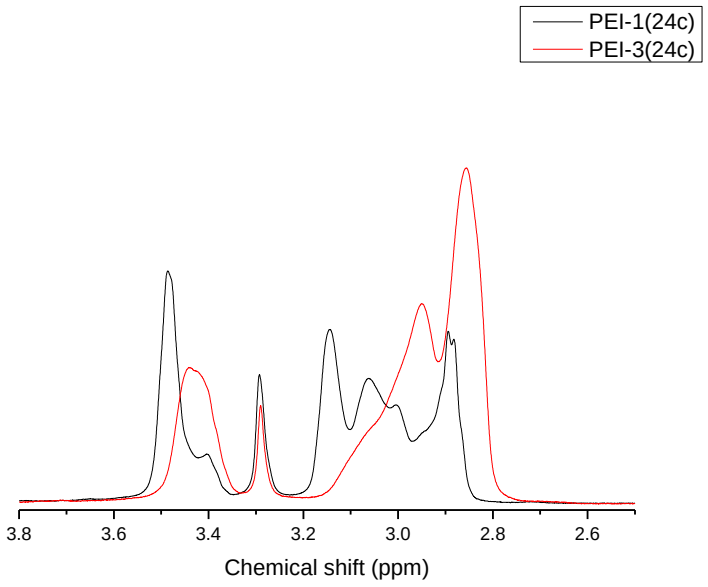

Figure 4-26 overlay of the ^{1}H-NMR spectra of PEI-1(24c) and PEI-3(48c)(D2O)

4.3.2 PEtOx-PEI functionalisation

In the second part of this work, we investigated whether it could be possible to make a fluorescent biocompatible polymer in $scCO_2$. Therefore, $PEtOx_{307}$-PEI_{93} was prepared by partial hydrolysis of $PEtOx_{400}$ and the resulting PEtOx-PEI copolymers was exposed to $scCO_2$ for different times at 135°C. It is important to state that the PEtOx-PEI has a block like distribution of PEI units along the chain as demonstrated in Chapter 2. The TGA degradation profile shows similarities with the PEI modified with $scCO_2$, because a weight loss is observed in between 100 and 150°C indicative of CO_2 loss due to formation of the carbamates. The polymers have a max weight loss after 2h and the max loading of 10% is much smaller compared to the L-PEI because less secondary amine groups are available. Also a 25% loading can never be achieved due to the formation of the zwitterion with a positive charge on the amine. After 48 h and 24h there is a decrease in weight loss indicating the locking of the carbamate in cyclic urea groups, which is facilitated due to the block-like distribution of the L-PEI units. The DSC is difficult to interpret as we have a polymer

with different domains. All of the polymers are however still amorphous after $scCO_2$ treatment although some shifts are observable.

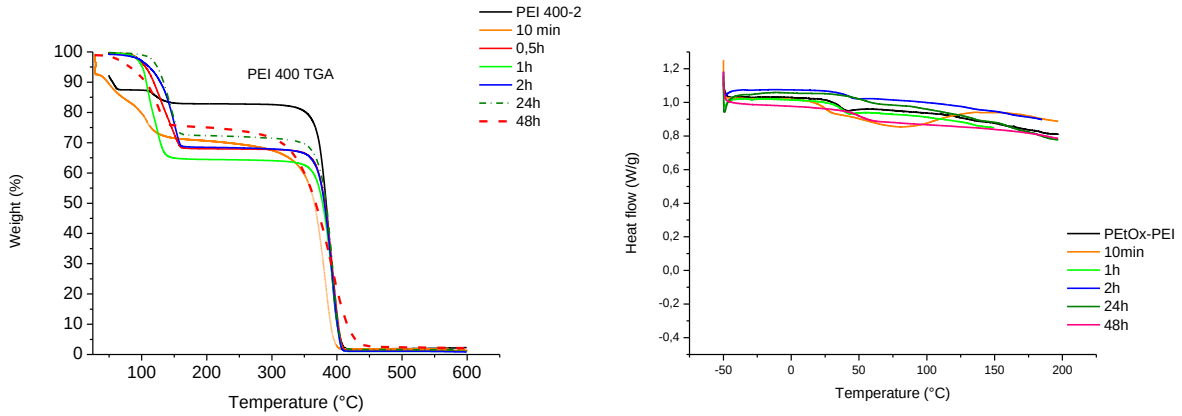

Figure 4-27 TGA of the PEtOx-PEI-2(x)(left) and DSC of the PEtOx-PEI-2(x)(right)

The ^{1}H-NMR spectra in Figure 4-28 shows that upon reaction the PEI peak at 2.8 ppm has vanished and that there is a shoulder in the backbone peak of 3.5 ppm. These results are similar to those previously discussed for the PEI indicating that there is formation of carbamates and possible rings upon exposure of PEtOx-PEI to $scCO_2$.

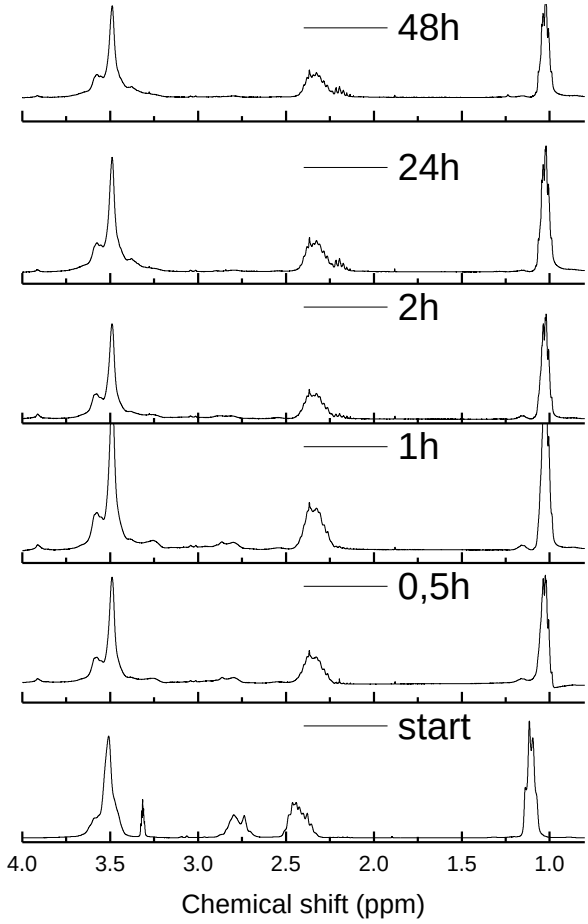

Figure 4-28 Stacked plot of the ^{1}H NMR spectra of PEtOx-PEI-(x) in D_2O

The ^{13}C-NMR had a very poor signal to noise ratio and it was difficult to interpret whether there was a formation of a carbamic acid due to the lack of carbonyl signal at 163 ppm. The HSQC also had too much noise and could not be interpret. Luckily the HMBC resolved the problem and an interesting conclusion could be drawn. In Figure 4-29 the HMBC spectrum is shown. As expected, there is a correlation between the CH_3 (C) signal at 1 ppm and the CH_2 (B) signal of the PEtOx at 2.4 ppm. There are extra cross peaks appearing in the region between 120-140 ppm, corresponding to dissolved CO_2. This is possible as the samples were not freshly prepared and there is a possible release of CO_2 due to the reversed reaction. The interesting part is seen in the CH_2 region of the backbone of PEtOx and the formed carbamates, both can be found around 3.6 ppm in the ^{1}H-spectrum. Different than the L-PEI carbamate the Cq signal of these polymers is located around 174 ppm. This indicates that the CH_2 groups next to the carbamate are in close contact with the PEtOx chain, hence the similar chemical shift. This indicates that the formed PEI blocks

as discussed earlier are rather small, as may be expected for this rather low degree of hydrolysis. A similar conclusion can be drawn from the PEtOx-PEI-2(48). The zoom of the HMBC spectrum is shown in Figure 4-30 and here it is clear that the shoulder also has a Cq contact. There is not enough data to draw conclusions as the ^{13}C-NMR is not well measured after multiple attempts.

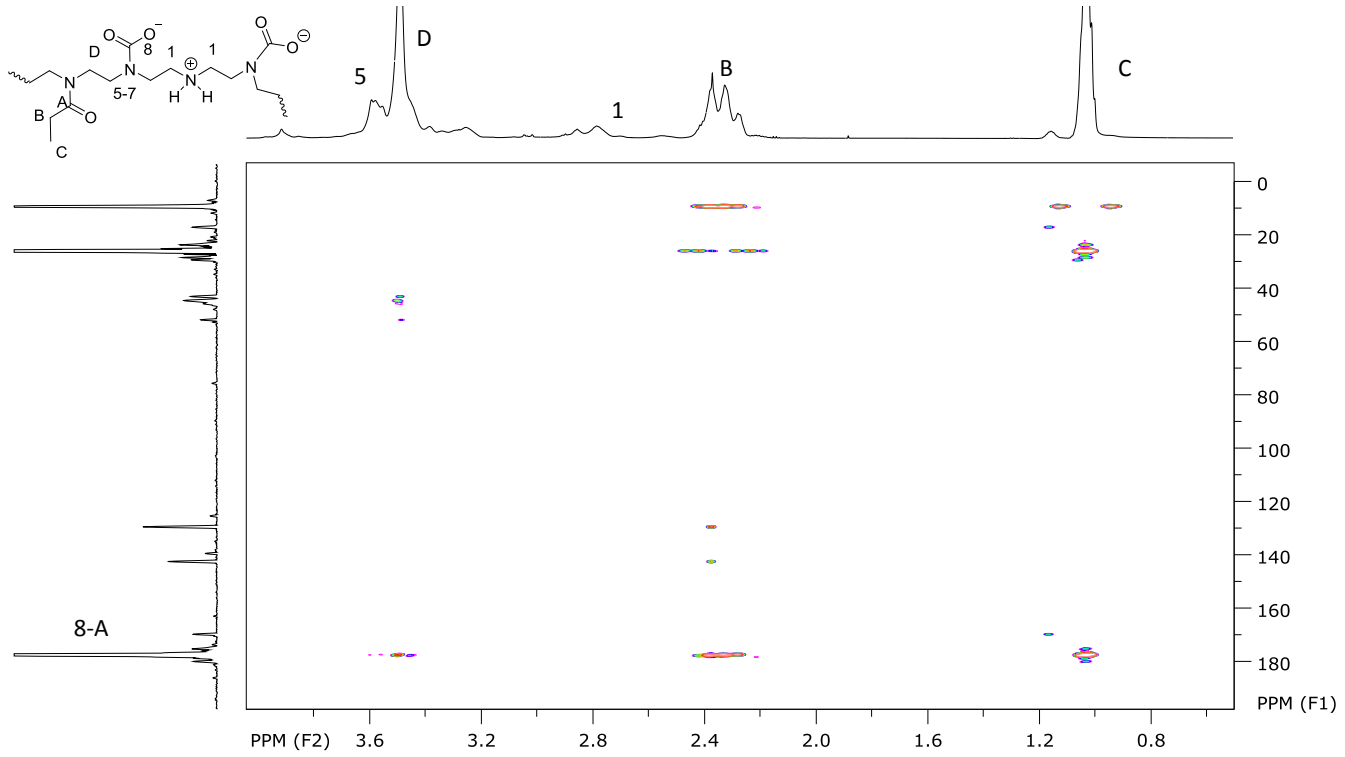

Figure 4-29 HMBC spectrum of the PEtOx-PEI-2(0.5) (D_2O).

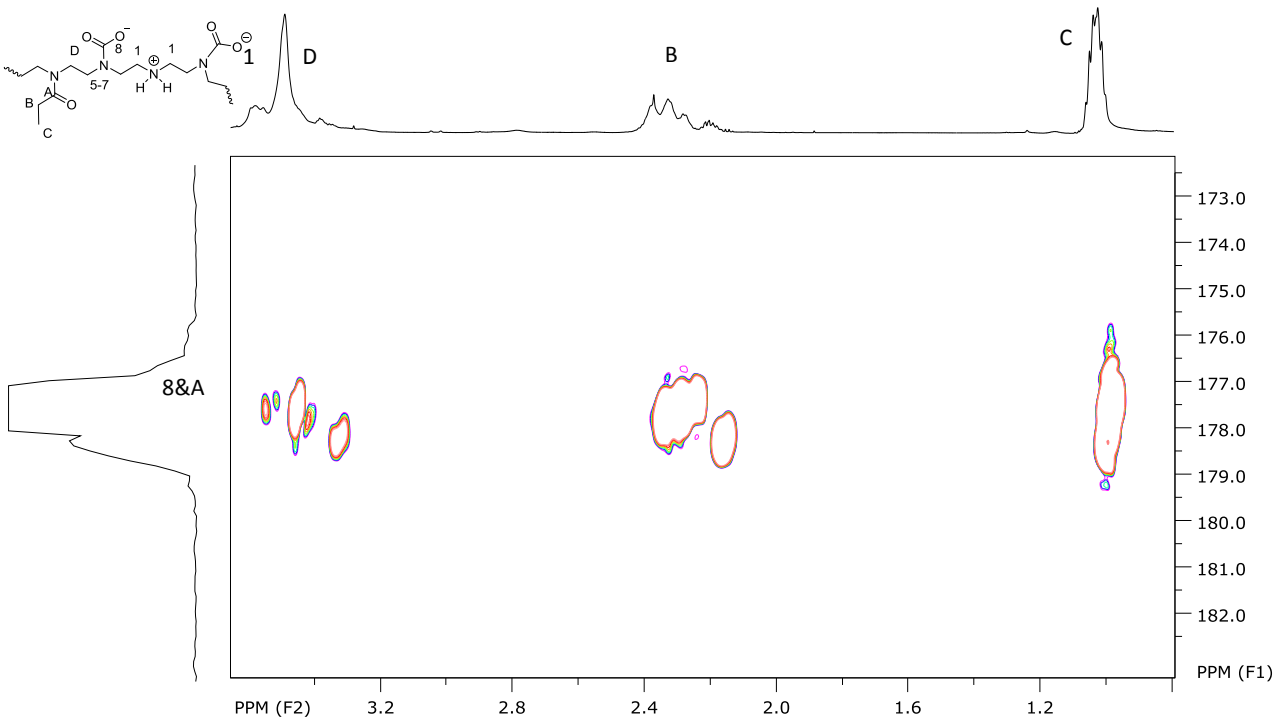

Figure 4-30 Zoom of the HMBC spectrum of PEtOx-PEI-2(48)(D_2O)

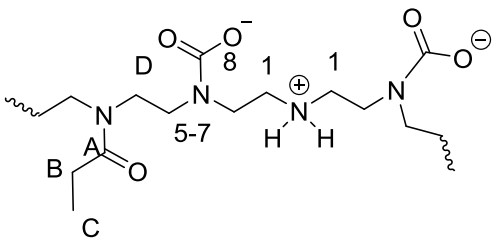

Figure 4-31 Polymer structure of modified PEtOx-PEI

The structure of the new polymers is shown in Figure 4-31. Different CH_2 groups can be found. The first type is the (D) which is the CH_2 group next to the original PEtOx unit. The (5-7) peaks are found next to the carbamate. The (1) signals is the same as in the L-PEI polymer and is located next to an protonated amine, as maybe assumed that all of the non-reacted amines are protonated. From the obtained data no conclusion can be drawn from possible ring formation.

The main goal was to make a fluorescent biomaterial on the PEtOx-PEI platform and the fluorescent spectrum (Figure 4-32) shows that the obtained materials are indeed fluorescent. The same shift as with the PEI-1 with longer reaction times towards a lower excitation value is observed, ascribed to the formation of urea groups.

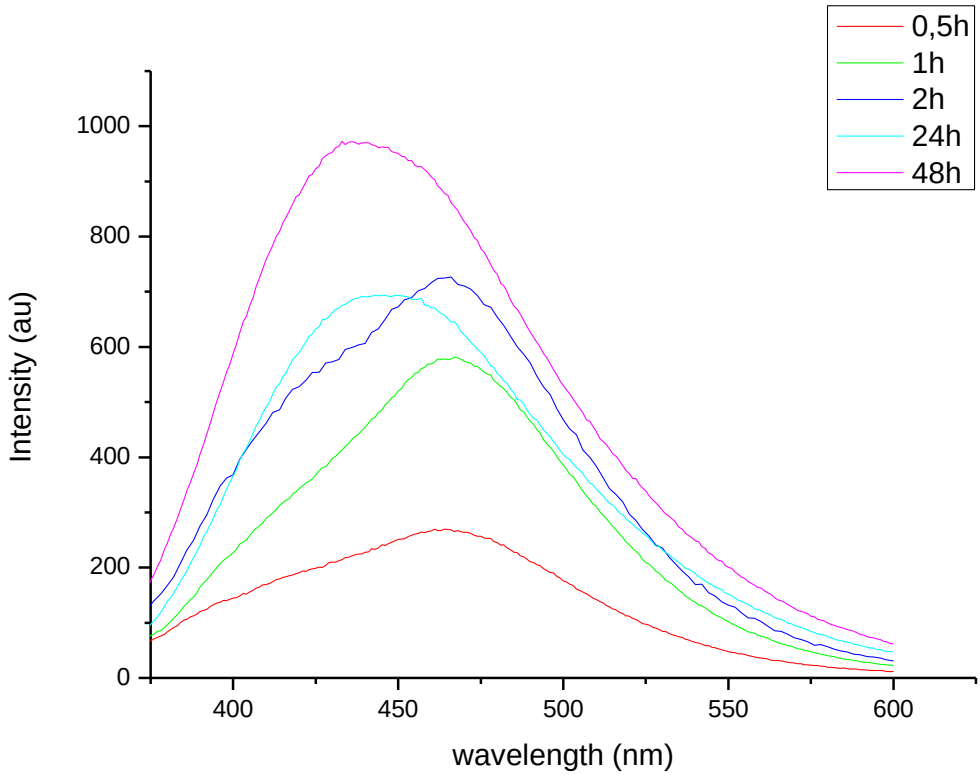

Figure 4-32 Fluorescence spectra of the PEtOx-PEI(x)

4.4 Conclusions

The goals of modifying the L-PEI with $scCO_2$ was successful leading to new fluorescent copolymers. Depending on the reaction time, two structures were formed. The first structure contained the deprotonated carbamate and a protonated amine. Due to a side reaction a second cyclic urea structure was formed. With longer reaction time this ring structure became more pronounced. There is also a possible cross linking reaction which may occur via the same mechanism. It was also shown that after removal of the carbamates the ring structure was preserved and this ring structure also showed intrinsic fluorescence. In the second part a PEtOx-PEI polymer was modified with sCO_2 resulting in fluorescent PEtOx. The formed carbamates do show a different value for the Cq as this was shifted towards a larger value. This is caused by the different chemical environment and the block like distribution of L-PEI units that makes it possible to have a PEtOx and the carbamate in close proximity. This interesting platform of course has to be further tested for further biomedical applications. First of all it has to be checked whether the amorphous functionalized PEI can be used in gene transfection yielding fluorescent polyplexes or even if the zwitterionic form is less toxic due to the neutralization of the positive charge. The PEtOx-PEI copolymer should be tested on toxicity and on the ability to be use the intrinsic fluorescence for microscopy visualization.

This chapter fits in the broader picture of post modification of L-PEI and PEtOx-PEI herewith expanding the chemical toolbox. It was indeed useful to see whether fluorescent materials could be made. This enables new types of polymers with a fluorescent tag. As the polymers are shown to be stable further examination is needed towards applications.

4.5 References

(1) Hoogenboom, R. *Angew. Chem. Int. Ed. Engl.* **2009**, *48* (43), 7978.
(2) Adams, N.; Schubert, U. S. *Adv. Drug Deliv. Rev.* **2007**, *59* (15), 1504.
(3) Luxenhofer, R.; Han, Y.; Schulz, A.; Tong, J.; He, Z.; Kabanov, A. V; Jordan, R. *Macromol. Rapid Commun.* **2012**, *33* (19), 1613.
(4) Qi, Y.; Chilkoti, A. *Curr. Opin. Chem. Biol.* **2015**, *28*, 181.
(5) Schöttler, S.; Becker, G.; Winzen, S.; Steinbach, T.; Mohr, K.; Landfester, K.; Mailänder, V.; Wurm, F. R. *Nat. Nanotechnol.* **2016**, *11* (February), 1.
(6) Guillerm, B.; Monge, S.; Lapinte, V.; Robin, J.-J. *Macromol. Rapid Commun.* **2012**, *33* (19), 1600.
(7) Sedlacek, O.; Monnery, B. D.; Filippov, S. K.; Hoogenboom, R.; Hruby, M. *Macromol. Rapid Commun.* **2012**, *33* (19), 1648.
(8) Verbraeken, B. K. H. R. In *Encyclopedia of Polymer Science and Technology*; 2014; pp 1–39.
(9) Lava, K.; Verbraeken, B.; Hoogenboom, R. *Eur. Polym. J.* **2015**, *65*, 98.
(10) Kem, K. M. *J. Polym. Sci. Polym. Chem. Ed.* **1979**, *17*, 1977.
(11) Ferrari, S.; Moro, E.; Pettenazzo, A.; Behr, J. P.; Zacchello, F.; Scarpa, M. *Gene Ther.* **1997**, *4* (10), 1100.
(12) Lungwitz, U.; Breunig, M.; Blunk, T.; Göpferich, A. *Eur. J. Pharm. Biopharm.* **2005**, *60*, 247.
(13) Jäger, M.; Schubert, S.; Ochrimenko, S.; Fischer, D.; Schubert, U. S. *Chem. Soc. Rev.* **2012**, *41* (13), 4755.
(14) Mees, M. A.; Effenberg, C.; Appelhans, D.; Hoogenboom, R. *Biomacromolecules* **2016**, *17* (12), 4027.
(15) Mees, M. A.; Hoogenboom, R. *Macromolecules* **2015**, *48* (11), 3531.
(16) Kanazaki, K.; Sano, K.; Makino, A.; Homma, T.; Ono, M.; Saji, H. *Nat. Sci. Reports* **2016**, *6* (August), 33798.
(17) Chujo, Y.; Sada, K.; Nomura, R.; Naka, A.; Saegusa, T. *Macromolecules* **1993**, *26* (21), 5611.
(18) Wyffels, L.; Verbrugghen, T.; Monnery, B. D.; Glassner, M.; Stroobants, S.; Hoogenboom, R.; Staelens, S. *J. Control. Release* **2016**, *235*, 63.
(19) de Macedo, C. V.; da Silva, M. S.; Casimiro, T.; Cabrita, E. J.; Aguiar-Ricardo, A. *Green Chem.* **2007**, *9*, 948.
(20) Bonifácio, V. D. B.; Correia, V. G.; Pinho, M. G.; Lima, J. C.; Aguiar-ricardo, A. *Mater. Lett.* **2012**, *81*, 205.
(21) Restani, R. B.; Conde, J.; Pires, R. F.; Martins, P.; Fernandes, A. R.; Baptista, P. V.; Bonifácio, V. D. B.; Aguiar-Ricardo, A. *Macromol. Biosci.* **2015**, *15* (8), 1045.
(22) Correia, V. G.; Bonifácio, V. D. B.; Raje, V. P.; Casimiro, T.; Moutinho, G.; da Silva, C. L.; Pinho, M. G.; Aguiar-Ricardo, A. *Macromol. Biosci.* **2011**, *11* (8), 1128.
(23) Belli Dell'Amico, D.; Calderazzo, F.; Labella, L.; Marchetti, F.; Pampaloni, G. *Biomacromolecules* **2012**, *12* (d), 3037.
(24) Vollrath, A.; Schubert, S.; Schubert, U. S. *J. Mater. Chem. B* **2013**, *1* (15), 1994.
(25) Hezinger, a F. E.; Tessmar, J.; Göpferich, a. *Eur. J. Pharm. Biopharm.* **2008**, *68* (1), 138.
(26) Carlos, L. D.; de Zea Bermudez, V.; Ferreira, R. a. S.; Marques, L.; Assunção, M. *Chem. Mater.* **1999**, *11* (9), 581.
(27) Shaner, N. C.; Steinbach, P. A.; Tsien, R. Y. *Nat. Methods* **2005**, *2* (12), 905.
(28) Chudakov, D.; Matz, M.; Lukyanov, S.; Lukyanov, K. *Physiol. Rev.* **2010**, *90* (3), 1103.
(29) Ruedas-Rama, M. J.; Walters, J. D.; Orte, A.; Hall, E. A. H. *Anal. Chim. Acta* **2012**, *751*, 1.
(30) Johnson, N.; Johnson, K. *ACS Chem. Biol.* **2007**, *2* (1), 31.
(31) Chalfie, M. Ghia Euskirchen, Y. Ward, W. Prasher, D. *Science* **1994**, *263* (5148), 802.
(32) Johnson, L. V; Walsh, M. L.; Chen, B.; Buchanan, J. M. *Proc. Natl. Acad. Sc. USA Cell Biol.* **1980**, *77* (2), 990.
(33) Dubertret, B.; Skourides, P.; Norris, D. J.; Noireaux, V.; Brivanlou, A. H.; Libchaber, A. *Science* **2002**, *298* (5599), 1759.

(34) Resch-Genger, U.; Grabolle, M.; Cavaliere-Jaricot, S.; Nitschke, R.; Nann, T. *Nat. Methods* **2008**, *5* (9), 763.
(35) Jaiswal, J. K.; Simon, S. M. *Trends Cell Biol.* **2004**, *14* (9), 497.
(36) Moghimi, S. M.; Szebeni, J. *Prog. Lipid Res.* **2003**, *42* (6), 463.
(37) Papadimitriou, S. A.; Salinas, Y.; Resmini, M. *Chem. A Eur. J.* **2016**, *22* (11), 3612.
(38) Fu, A.; Gu, W.; Larabell, C.; Alivisatos, a P. *Curr. Opin. Neurobiol.* **2005**, *15* (5), 568.
(39) Robin, M. P.; O'Reilly, R. K. *Polym. Int.* **2015**, *64* (2), 174.
(40) Zhu, M. Q.; Zhang, G. F.; Hu, Z.; Aldred, M. P.; Li, C.; Gong, W. L.; Chen, T.; Huang, Z. L.; Liu, S. *Macromolecules* **2014**, *47* (5), 1543.
(41) Mackiewicz, N.; Nicolas, J.; Handké, N.; Noiray, M.; Mougin, J.; Daveu, C.; Lakkireddy, H. R.; Bazile, D.; Couvreur, P. *Chem. Mater.* **2014**, *26* (5), 1834.
(42) Quadir, M. A.; Morton, S. W.; Deng, Z. J.; Shopsowitz, K. E.; Murphy, R. P.; Epps, T. H.; Hammond, P. T. *Mol. Pharm.* **2014**, *11* (7), 2420.
(43) Pu, H. L.; Chiang, W. L.; Maiti, B.; Liao, Z. X.; Ho, Y. C.; Shim, M. S.; Chuang, E. Y.; Xia, Y.; Sung, H. W. *ACS Nano* **2014**, *8* (2), 1213.
(44) Xu, J.; Wang, J.; Mitchell, M.; Mukherjee, P.; Jeffries-El, M.; Petrich, J. W.; Lin, Z. *J. Am. Chem. Soc.* **2007**, *129* (42), 12828.
(45) Van Mierloo, S.; Hadipour, A.; Spijkman, M.-J.; Van den Brande, N.; Ruttens, B.; Kesters, J.; D'Haen, J.; Van Assche, G.; de Leeuw, D. M.; Aernouts, T.; Manca, J.; Lutsen, L.; Vanderzande, D. J.; Maes, W. *Chem. Mater.* **2012**, *24* (3), 587.
(46) Wu, C.; Schneider, T.; Zeigler, M.; Yu, J.; Schiro, P. G.; Burnham, D. R.; Mcneill, J. D.; Chiu, D. T. .
(47) Levitus, M.; Schmieder, K.; Ricks, H.; Shimizu, K. D.; Bunz, U. H. F.; Garcia-Garibay, M. A. .
(48) Restani, R. B.; Morgado, P. I.; Ribeiro, M. P.; Correia, I. J.; Aguiar-Ricardo, A.; Bonifcio, V. D. B. *Angew. Chemie - Int. Ed.* **2012**, *51* (21), 5162.
(49) Wang, D.; Imae, T.; Miki, M. *J. Colloid Interface Sci.* **2007**, *306* (2), 222.
(50) Wu, D.; Liu, Y.; He, C.; Goh, S. H. *Macromolecules* **2005**, *38* (24), 9906.
(51) Wang, D.; Imae, T. *JACS Commun.* **2004**, *126*, 13204.
(52) Chu, C. C.; Imae, T. *Macromol. Rapid Commun.* **2009**, *30* (2), 89.
(53) Lee, W. I.; Bae, Y.; Bard, A. J. *J. Am. Chem. Soc.* **2004**, *126* (27), 8358.
(54) Pastor-Pérez, L.; Chen, Y.; Shen, Z.; Lahoz, A.; Stiriba, S. E. *Macromol. Rapid Commun.* **2007**, *28* (13), 1404.
(55) Hampe, E. M.; Rudkevich, D. M. *Tetrahedron* **2003**, *59* (48), 9619.
(56) Pan, X.; Wang, G.; Lay, C. L.; Tan, B. H.; He, C.; Liu, Y.; Tan, H.; He, C.; Liu, Y. *Sci. Rep.* **2013**, *3* (2763), 1.
(57) Murphy, L. J.; Robertson, K. N.; Kemp, R. A.; Tuononen, H. M.; Clyburne, J. A. C. *Chem. Commun.* **2014**, *51* (19), 3942.
(58) Ion, A.; Doorslaer, C. Van; Parvulescu, V.; Jacobs, P.; Vos, D. De. *Green Chem.* **2008**, *10* (1), 111.
(59) Belli Dell'Amico, D.; Calderazzo, F.; Labella, L.; Marchetti, F.; Pampaloni, G. *Chem. Rev.* **2003**, *103* (10), 3857.
(60) Aresta, M.; Ballivet-Tkatchenko, D.; Dell'Amico, D. B.; Boschi, D.; Calderazzo, F.; Labella, L.; Bonnet, M. C.; Faure, R.; Marchetti, F. *Chem. Commun.* **2000**, *8* (13), 1099.
(61) Sada, E.; Kumazawa, H.; Han, Z. Q. *Chem. Eng. J.* **1985**, *31* (2), 109.
(62) Crooks, J. E.; Donnellan, J. P. *J. Chem. Soc. Perkin Trans. 2* **1989**, *2* (4), 331.
(63) Wright, H. B.; Moore, M. B. *J. Am. Chem. Soc.* **1948**, *70* (11), 3865.
(64) Sayari, A.; Heydari-Gorji, A.; Yang, Y. *J. Am. Chem. Soc.* **2012**, *134* (33), 13834.
(65) Drage, T. C.; Arenillas, A.; Smith, K. M.; Snape, C. E. *Microporous Mesoporous Mater.* **2008**, *116* (1–3), 504.
(66) Hahn, M. W.; Jelic, J.; Berger, E.; Reuter, K.; Jentys, A.; Lercher, J. A. *J. Phys. Chem. B* **2016**, *120* (8), 1988.
(67) Bludau, H.; Czapar, A. E.; Pitek, A. S.; Shukla, S.; Jordan, R.; Steinmetz, N. F. *Eur. Polym. J.* **2016**, 1.
(68) Stubbe, B.; Li, Y.; Vergaelen, M.; Van Vlierberghe, S.; Dubruel, P.; De Clerck, K.; Hoogenboom, R. *Eur. Polym. J.* **2016**.
(69) Correia, V. G.; Ferraria, A. M.; Pinho, M. G.; Aguiar-Ricardo, A. *Biomacromolecules* **2015**, *16* (12),

3904.
(70) Ferreira, L. S.; Trierweiler, J. O. *IFAC Proc. Vol.* **2009**, *7* (PART 1), 405.
(71) Hartono, A.; Da Silva, E. F.; Grasdalen, H.; Svendsen, H. F. *Ind. Eng. Chem. Res.* **2007**, *46* (1), 249.
(72) Barzagli, F.; Mani, F.; Peruzzini, M. *Int. J. Greenh. Gas Control* **2011**, *5* (3), 448.
(73) Diefenbacher, J.; Piwowarczyk, J.; Marzke, R. F. *Rev. Sci. Instrum.* **2011**, *82* (7), 76107.
(74) Liang, H.; Jia, D.; Liu, H.; Gu, Y.; Liu, C.; Zhao, F.; Chen, P.; Wang, D. *Chem. Lett.* **2015**, *44* (4), 548.
(75) Sayari, A.; Belmabkhout, Y. *J. Am. Chem. Soc.* **2010**, *132* (18), 6312.

CHAPTER 5

Chapter 5 :
Functional poly(2-oxazoline)s by direct amidation of methyl ester side chains

Contributors to this chapter:

Joachim Van Guyse, Department of Organic and Macromolecular Chemistry ,Ghent University

Contributions of the candidate

Synthesis of the start polymers and all post modifications including all analysis

Part of this work was published as

Macromolecules, ***2015***, 48 *(11), pp 3531−3538*

CHAPTER 5

Prologue

PAOx polymers have excellent biocompatible properties and upon injection there is no immune response of the hosting organism. As discussed in the introduction these qualities are similar to PEG, the gold standard of biocompatible polymers. The advanced chemical versatility makes PAOx polymers superior to PEG. In this chapter different linkers are explored for the modification of PAOx, which can be used to couple bioactive molecules onto the polymer platform. To couple these linkers onto the polymer a post polymerisation approach was chosen where first the polymer was partially hydrolysed. It is known from chapter 2 that this proceeds in a block like fashion. The nucleophilic properties of the amine of the PEI units is used to couple a methyl ester group via four different linkers based on amide (oxazoline), tertiary amine, isocyanate and thioisocyanate. It is demonstrated that the methyl ester functionality can be converted into an amide via a direct amidation reaction with a wide range of (functional) amines. This model reaction can be used for future reactions with bioactive compounds containing amines.

5.1 Introduction

The story of poly(2-oxazoline)s started in 1966 when 4 independent research groups reported the cationic ring opening polymerisation (CROP) of 2-aryl-2-oxazolines and 2-alkyl-2-oxazolines, such as 2-phenyl-2-oxazoline and 2-methyl-2-oxazoline.[1–4] After this discovery, the CROP of 2-oxazolines has gained significant interest. Well-defined poly(2-alkyl/aryl-2-oxazoline)s (PAOx) can be obtained if the polymerisations are done under nucleophile free conditions to avoid side reactions such as chain transfer and termination.[5,6] After the flourishing of PAOx in the seventies and eighties, research interest was retracting in the nineties. Since the dawn of the new millennium, PAOx are quickly gaining interest again, as researchers have discovered their high potential for biomedical applications.[7–10] In addition, a microwave assisted polymerisation protocol was introduced about ten years ago to drastically reduce polymerisation times from days and hours to minutes.[11,12] The livingness of the CROP allows the preparation of defined PAOx with full control over polymer architectures including blocks,[13,14] gradients[15] and star-shaped structure[16]. Furthermore the properties of PAOx are highly tunable by variation of the side-chain R group as well as by copolymerisation of different monomers.[17–19]

The current interest in PAOx is more and more shifting towards biomedical applications stimulated by the high biocompatibility and stealth behaviour, which is especially documented for poly(2-methyl-2-oxazoline) (PMeOx) and poly(2-ethyl-2-oxazoline) (PEtOx).[7,20] In fact, they can arguably compete or even outperform the gold standards of the field, namely poly(ethylene glycol) and poly(*N*-hydroxypropylmethacrylamide).[21–24] For use of PAOx in biomedical applications, it is important to have easy and straightforward functionalization methodologies, either for conjugation of the polymers to

biological entities or substrates or to attach drug molecules, labels or targeting moieties. Up to three orthogonal functionalities can be (simultaneously) introduced in PAOx through initiation, termination and incorporation of functional monomers.[18,25] The choice of functional monomers is however limited to groups that are non-nucleophilic as any nucleophile will interfere with the polymerisation process.

A major advantage of PAOx over PEG is the possibility to introduce functionalities in the side chains by simple copolymerisation of a functional monomer with a non-functional monomer. However, many functional groups need to be protected during the CROP to avoid interference with the polymerisation conditions, as has been reported for monomers with acid,[12,19,26] alcohol,[19] amine,[12] thiol[19] and aldehyde[19,27,28] functionalities. An important exception are monomers containing double and triple bonds that are not affected by the living CROP. The direct introduction of internal and terminal double bonds as well as terminal triple bonds into PAOx has been demonstrated.[14,27,29,30] These polymers could further be utilized for efficient post-polymerisation modification by thiol-ene,[25,31,32] thiol-yne[32] and copper(I) catalysed azide-alkyne cycloaddion (CuAAC),[31,32] so called click reactions[33].

In this work, we report a novel straightforward post-polymerisation modification strategy for PAOx, which allows the incorporation of a wide range of side-chain functionalities by direct amidation of the side chain methyl ester groups with different amines as shown in Figure 5-1. The PAOx building blocks containing side-chain methyl ester groups can either be prepared by partial hydrolysis of PAOx followed by introduction of the methyl ester functionality by reaction with methyl succinyl chloride or other methyl ester containing electrophilic reagents or by copolymerisation of a non-functional 2-oxazoline monomer with 2-methoxycarbonylethyl-2-oxazoline.[4,34] Within this chapter we will demonstrate the versatility of this new synthetic methodology. The newly formed methyl ester containing groups can be modified into an amide via the direct amidation reaction.

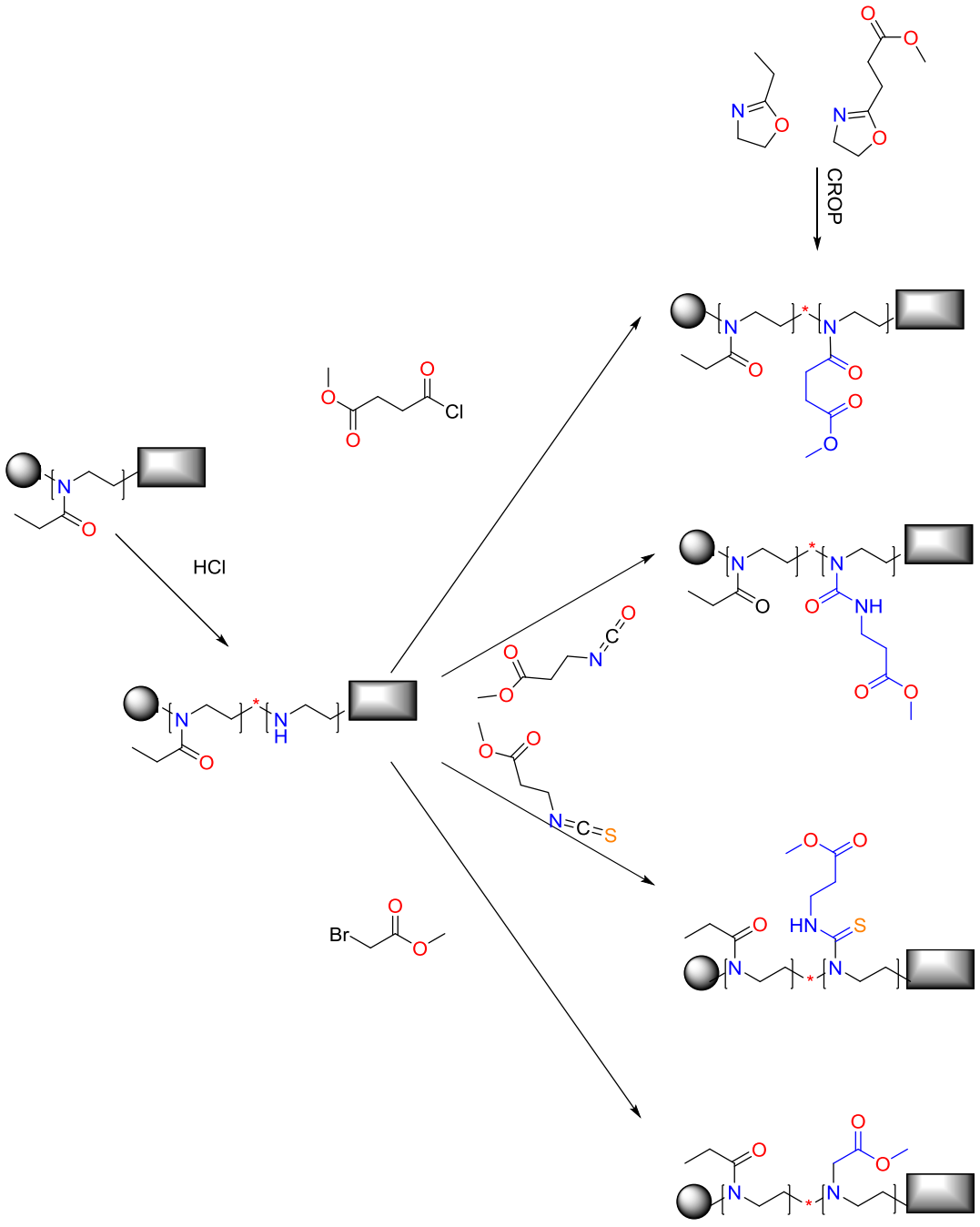

Scheme 5-1 Schematic representation of the partial hydrolysis of a poly(2-oxazoline) followed by modification with methyl succinyl chloride, methyl-isocyanopropanate, methyl-thiocyanopropanate, methyl bromoacetate . The direct synthesis of the methyl ester containing PAOx by copolymerisation is also included in the scheme as alternative route.[34] The grey sphere is the initiator part and the grey rectangle the termination agent part.

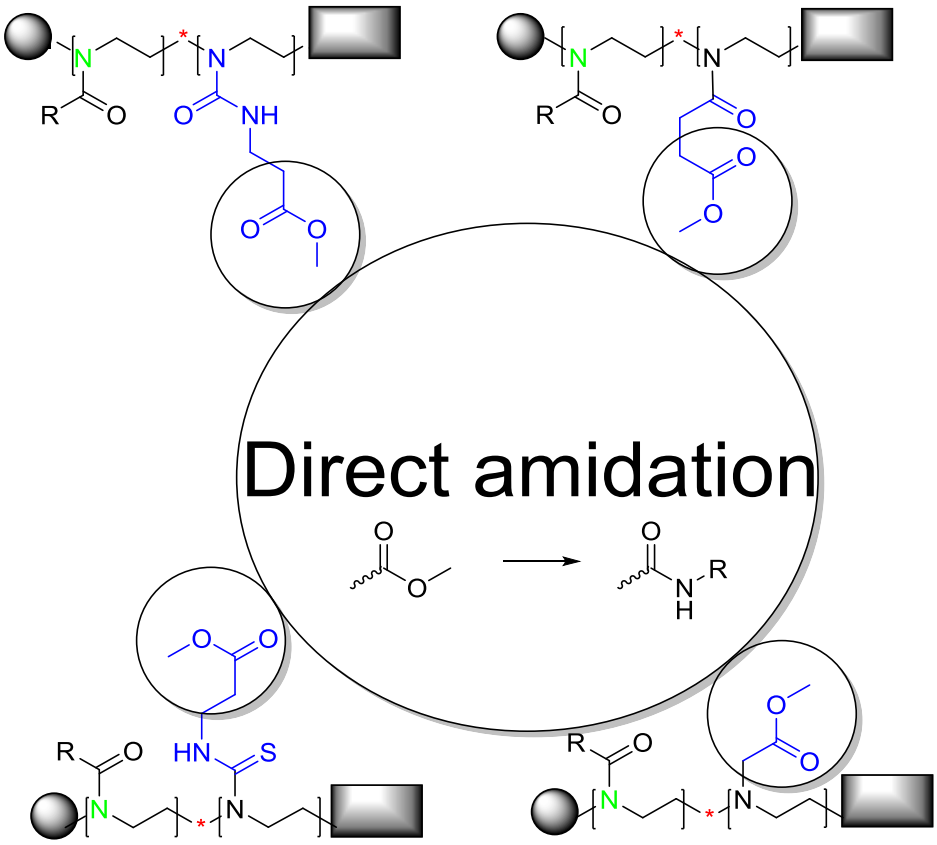

Figure 5-1 Direct amidation of the methylester containing groups

5.2 Materials and methods

5.2.1 Materials and Instrumentations

Poly(2-ethyl-2-oxazoline) (PEtOx; DP = 100, M_n 9700, PDI 1.13; measured on SEC with DMA as eluent) was synthesized following a literature protocol.[11] Hydrogen chloride, sodium hydroxide, dichloromethane, aminomethane, aminoethane, 1-aminopropane, dimethylamine, hydrazine, glycine, Leucine methyl ester, 1,3 aminopropanol, allylamine, 1-amino-3-butyn, allylamine, N,N'-dimethyl-1,2-ethylene diamine, 1,2 ethylene diamine, methyl succinyl chloride and amino ethanol were obtained from Sigma Aldrich and used as received. ^{1}H NMR and ^{13}C NMR spectra were recorded in $CDCl_3$ or in DMSO on a Bruker Avance 300 MHz or 500 MHz spectrometer. Size exclusion chromatography (SEC) was performed on a Agilent HPLC with a 1260 refractive index detector (RID) using dimethylacetamide containing 50 mM LiCl as eluent at a flow rate of 0.6 mL/min. Polymethylmethacrylate (PMMA) standards were used to calculate the molar mass values and the column set consisted of two PLgel 5 µm mixed D columns at 40°C and a similar guard column (Agilent) in series. Chromatograms were analyzed using Agilent Chemstation software with the GPC add on. The polymers obtained after amidation were analyzed by size exclusion chromatography (HFIP-SEC) using a Agilent HPLC with a 1260 refractive index detector (RID) with eluent of hexafluoro-2-isopropanol (HFIP) containing 20 mM Sodium trifluoroacetate at a flow rate of 0.3 mL/min. PMMA standards were used to calculate the molar mass values and the column set consisted of two PSS PFG 100Å gel 5 µm mixed D columns and a similar guard column (Agilent) at 35°C in series Chromatograms were analyzed using Agilent Chemstation software with the GPC add on. The FT-IR was performed on a Perkin Elmer 1000 FTIR spectrum meter with PIKE HATR module. All of the polymerisation were done in a Vigor glovebox. Matrix assisted laser desorption/ionization time of flight mass spectroscopy (MALDI-TOF MS) was performed on an Applied Biosystems Voyager De STR MALDI-TOF mass spectrometer equipped with 2 m linear and 3 m reflector flight tubes, and a 355 nm Blue Lion Biotech Marathon solid state laser (3.5 ns pulse). All mass spectra were obtained with an accelerating potential of 20 kV in positive ion mode and in reflector mode. 2-(4'-hydroxybenzeneazo)benzoic acid (HABA) (20 mg/mL in acetone) was used as matrix. Polymer samples were dissolved in acetone 2mg/mL analyte solutions were prepared by mixing 10 µl matrix and 5 µl polymer samples. Samples were applied using the dried droplet method.

5.2.2 Procedures

Partial hydrolysis of PEtOx.

The PEtOx (10 g) was dissolved in 50 mL of water with heating and stirring until everything was dissolved. Then 50 mL of 36% solution of HCl was added and the mixture was heated to 73°C (internal temperature) for 200 min. After the volatiles were removed on a rotary evaporator, the polymer was dissolved in water and the solution was basified to pH 10-11 using a NaOH solution. The solution was then lyophilized and the solid was dissolved in dichloromethane. The organic phase was washed with brine and then concentrated in vacuum to yield the PEtOx-PEI as a solid white product (7 g; 77% yield). *^{1}H-NMR (300 MHz, δ in ppm, $CDCl_3$): 1-1.2 (3 H,CH_2-C<u>H</u>3); 2.3-2.5 (4H,C<u>H</u>$_2$-CH_3); 2.6-2.8 (4 H,C<u>H</u>$_2$-NH); 3.2-3.5 (4 H,C<u>H</u>2NCH2).* The integral ratios between the peaks at 2.6-2.8 ppm and 3.2-3.5 ppm were utilized to calculate the degree of hydrolysis to be 18%.

Modification of PEtOx-PEI with methyl succinyl chloride.

7 g of the PEtOX-PEI (18%) was several times washed with toluene for the removal of any water. Subsequently, the polymer was dissolved in dry dichloromethane (6 mL/g of polymer) and the mixture was cooled to 0°C. Methyl succinyl chloride (4.5 mLmL, 3.65 mmol, 2eq.) was added to this solution of PEtOx-PEI followed by drop wise addition of triethylamine (2 eq, 0.3 mL). The mixture was stirred for 24 h after which the reaction mixture was directly precipitated in cold ether. The precipitated polymer was isolated by filtration and dried under vacuum to yield the PEtOx copolymer with methyl ester side chains (PEtOx-MestOx) in 84% yield (7.5 g). *^{1}H-NMR (300 MHz, δ in ppm, $CDCl_3$): 1-1.2 (3 H,CH_2-C<u>H</u>$_3$); 2.3-2.5 (4H,C<u>H</u>$_2$-CH_3); 2.6-2.8 (4 H,C<u>H</u>$_2$-NH); 3.2-3.5 (4 H,C<u>H</u>2N-CH2); 3.7 (3 H,O-C<u>H</u>$_3$).* SEC-data M_w 1.76 10^4; M_n 1.67 10^4 g/mol and Đ 1.1. The IR spectrum showed following peaks (cm^{-1}): 1731 (CH_3-O, ester) 1630 (all amides).

Modification of PEtOx-PEI with methyl thio(isocyanate).

Methyl-isocyanatopropanoate (3 eq, 290 mg, 2.25 mmol) or methyl-(thio) isocyanatopropanoate (3eq., 33 mg, 2.25 mmol) was added toghether with the polymer (0.5 g) in a microwave vial. The reaction was carried out in the microwave for 5 min. at 150°C. Purification was done by preparative SEC (PD10).

^{1}H-NMR(300 MHz, δ in ppm, $CDCl_3$): 1-1.2 (3 H,CH_2C<u>H</u>$_3$); 2.3-2.5 (4H,C<u>H</u>$_2$-CH_3); 2.6-2.8 (4 H,C<u>H</u>$_2$-CH_2); 3.2-3.5 (4 H,C<u>H</u>2NCH2); 3.7 (3 H,O-C<u>H</u>$_3$). 4.7 ppm (1 H, CH_2N<u>H</u>-CO-NH); 3.9 (1 H, CH_2N<u>H</u>-CS-NH)

Modification of PEtOx-PEI with methyl bromoacetate.

3 g of the PEtOX-PEI (15%) was dissolved in 30 mLmL if acetonitrile. Subsequently, 0.3 g K_2CO_3 and methyl bromoacetate (200µl, .0.0018 mol,10eq) were added to this solution. The mixture was refluxed for 12 h. After evaporation of the solvent DCM was added and the solution was filtered. A cold precipitation in ether was done to remove all residual reactants. After precipitation the samples was lyophilised. *^{1}H-NMR(300 MHz, δ in ppm, CD_3OD): 1-1.2 (3 H,$CH_2C\underline{H_3}$); 2.3-2.5 (2H,$C\underline{H_2}$-CH_3); 2.6-2.8 (4 H,$C\underline{H_2}$-CH_2); 3.2-3.5 (4 H,$C\underline{H_2}NCH_2$); 3.7 (3 H,O-$C\underline{H_3}$).*

Amine coupling method 1: (aminomethane, aminoethane, 1-aminopropane, hydrazine).

The PEtOx-PMestOx copolymer/PEtOx-Poly((thio)ureum)methylester/PEtOx-Poly(amine acetate) (300 mg) was directly dissolved in an excess of amine (~6 mL). The reaction was stirred for 2 days at 70°C after which the solution was evaporated to dryness. Purification was done using preparative SEC, PD 10 column with water ass eluent, to yield the modified polymers in near-quantitative yields.

Amine coupling method 2: (amino ethanol, amino propanol, allylamine, amino-3-butyne, N, N dimethylethylene diamine).

The PEtOx-PMestOx (300 mg, 4.6 * 10^{-4} mol) copolymer was dissolved in 6 mL of acetonitrile; for amines that are not soluble in acetonitrile the solvent was changed to DMF. In the case where the amines where part of on an amino acid, such as glycine or Leucine, water with a pH of 9 was used to ensure that all amines where deprotonated. A concentrated solution of amine (3 equivalents to the methyl ester) was then added and the reaction mixture was stirred for 1 day at 40 °C. After evaporation of the solution under reduced pressure, the remaining polymer was purified by preparative SEC, PD 10 column with water as eluent yielding the modified polymers in near-quantitative yields.

Polymerisation of the methyl ester functionalized monomer (MestOx) DP 20.

The MestOx monomer was synthesised as described earlier.[34] The polymerisation was carried out in a 20 mL microwave vial. The methyl tosylate (0.34 mL; 0.002 mol) was dissolved in a solution containing MestOx monomer (7 g; 0.04 mol) and 8 mL of acetonitrile obtaining a 3 M polymer solution. The reaction mixture was prepared in the glovebox ensuring an oxygen and water free environment. The polymerisation was performed by heating the mixture for 2.35 minutes to 140 °C in the microwave. After polymerisation the reaction was terminated by addition of 1 mL of a 1 M solution KOH in methanol. The acetonitrile was then removed *via* reduced pressure and the polymer was dissolved in dichloromethane

and precipitated in cold diethyl ether (10-fold excess). The polymer was then dissolved in water and freeze dried to obtain a white powder (3.311 g; yield 65%). *^{1}H-NMR (500 MHz, δ in ppm, D_2O): ;2.5-2.7(4H , CO-CH_2-CH_2-CO-OCH); 3.2-3.5 (4 H,CH_2N-CH_2); 3.7 (3 H,O-CH_3)*. SEC-data M_w 6600; M_n 5800 g/mol and Đ 1.12.

5.3 Results and discussion

5.3.1 Synthesis of PEtOx-MestOx via hydrolysis and modification of PEtOx

To evaluate the newly proposed post-polymerisation modification platform of PAOx copolymers with methyl ester side chains with amines (Figure 5-1), a well-defined PEtOx was first prepared as starting material, whereby the narrow dispersity (Đ) will facilitate the evaluation of the products after each reaction step by SEC. Therefore, a large batch (10 g) of PEtOx with a DP of 100 was prepared using the previously optimized microwave assisted polymerisation protocol yielding well-defined PEtOx with a Đ of 1.1 determined by SEC with DMA as eluent.[11]

Next, the well-defined PEtOx was hydrolysed in controlled acidic conditions and based on the previously established hydrolysis kinetics, a good control can be achieved over the hydrolysis rate.[35] As shown in chapter 2 there is a block like distribution of the PEI units along the backbone. This hydrolysis reaction allows for an easy control over the amount of secondary amines in PEtOx-PEI and, thus, provides control over the amount of methyl ester functional groups that can be attached to the main chain. To aim for a hydrolysis degree around 20% the hydrolysis was performed in ~6.8 N hydrochloric acid at 73°C for 200 min. The degree of hydrolysis was determined by ^{1}H-NMR spectroscopy. The integral ratio of signals corresponding to the backbone of PEtOx at δ 3.5 ppm and the backbone of PEI at δ 2.8 ppm was used to calculate the degree of hydrolysis, as shown in Figure 5-2. It is shown that 18% of the PEtOx units were hydrolysed yielding a $PEtOx_{82}$-PEI_{18} copolymer. Purification of this PEtOx-PEI was done by first drying the reaction mixture on a rotary evaporator to remove the water, propionic acid and excess of hydrochloric acid. Subsequently the polymer is dissolved in a small amount of water and the pH is adjusted to pH 10-11 with NaOH, to deprotonate the PEI units, followed by lyophilization. The resulting white powder is subsequently dissolved in dichloromethane and extracted with brine and water to remove the traces of propionate as well as the NaOH. The final purified polymer is collected by evaporation of the dichloromethane. This partially hydrolysed copolymer can no longer be analysed by SEC in DMA due to too strong interactions between the amine groups and the column material leading to tailing of the signal and with higher hydrolysis degrees even to complete sticking of the polymer to the column. Therefore, SEC of PEtOx-PEI was measured with hexafluoroisopropanol (HFIP) as eluent,[36] revealing a M_n of 1.5 x 10^4 Da and Đ of 1.3. The broadening of size distribution can be ascribed to the SEC system and column set as

the PEtOx starting polymer revealed a M_n of 7.6 x 10^3 Da and a Đ of 1.4 on this SEC system with HFIP. The counterintuitive increase in M_n upon removal of 18% of the side chains is in line with previous observations and can be ascribed to the larger hydrodynamic volume of the partially hydrolysed copolymer in HFIP, presumably due to better hydrogen bonding of the HFIP to the polymer chains.

The prepared PEtOx-PEI represents a well-defined reaction platform containing the biocompatible PEtOx as main structure together with the nucleophilic secondary amine units from the PEI. A wide variety of modification reactions of such partially hydrolysed polymers have already been reported in literature.[37] In this work, the PEtOx-PEI copolymer was first reacted with methyl succinylchloride to reintroduce a side chain amide group similar to the native PAOx structure containing a latent methyl ester functionality yielding $PEtOx_{82}MestOx_{18}$. The ^{1}H-NMR spectrum of PEtOx-MestOx revealed the disappearance of the PEI backbone resonances at 2.6 ppm as well as the appearance of the methyl ester peak at 3.7 ppm demonstrating the success of the modification reaction. Furthermore, the IR spectrum also revealed the representative methyl ester carbonyl vibration at 1730 cm^{-1}. The SEC trace of PEtOx-PMestOx in HFIP also revealed a decrease in M_n caused by the change in hydrodynamic volume while the Đ remained the same (Đ = 1.3). Overlays of the SEC traces and ^{1}H NMR spectra of PEtOx, PEtOx-PEI and PEtOx-MestOx are shown in Figure 5-2 to illustrate the successful modifications.

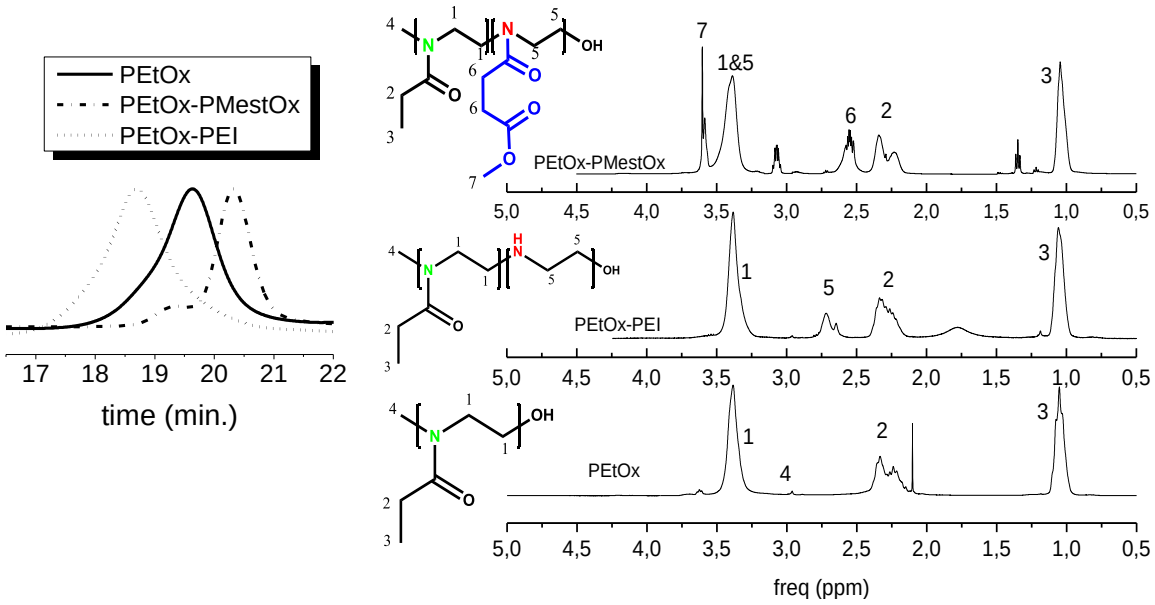

Figure 5-2. Overlay of the SEC traces in HFIP (Left) and ^{1}H NMR spectra of PEtOx, PEtOx-PEI and PEtOx-MestOx in $CDCl_3$.

As mentioned in the introduction PEtOx-MestOx can also be obtained by direct copolymerisation of 2-ethyl-2-oxazoline (EtOx) and 2-methoxycarboxyethyl-2-oxazoline (MestOx). Although the direct polymerisation seems to be a more straightforward method compared to the here presented two-step hydrolysis-modification method, it should be noted that EtOx is available in bulk quantities while MestOx has to be custom synthesized in a two-step synthetic protocol when starting from methyl succinyl chloride with 57% overall yield, including double purification by distillation.[34] In this perspective, the demonstrated hydrolysis-modification method may actually be more cost-effective and time-efficient than the direct polymerisation method. Moreover, the hydrolysis-modification route is also more versatile as different reactive linkers, such as methyl bromopropionate, methyl acrylate or methyl iso(thio)cyanatopropionate may be used to install similar methyl ester side chains as will be discussed in the following section.[38]

5.3.2 Synthesis of methyl ester functional PEtOx via reaction of PEtOx-PEI with (thio)urea or methyl bromo acetate

A similar synthesis as above is proposed for the synthesis of a PAOx polymer containing either a urea or thio urea bond in the side chain. The reaction between isocyanates and partially hydrolysed PAOx was already explored for the synthesis of hydrogels with a PMeOx-PEI polymer.[39] Here a reaction between methyl-3-isocyanatopropanoate or methyl-3-thioisocyanatopropanoate with PEtOx-PEI is performed by heating in the microwave at 150°C with no catalyst.[40] The ^{1}H-NMR spectra before and after the reaction are shown in Figure 5-3 revealing that the PEI peak at 2.8 ppm has disappeared showing the coupling of the iso(thio)cyanate onto the backbone of the polymer. A pronounced new peak is seen at 3.7 ppm which indicates the formation of a methyl ester side chain. As we know from the previous part this shows a successful coupling to the backbone. By this method two types of polymer are coupled, urea and thio urea both bearing the methyl ester that can be used for further modification.

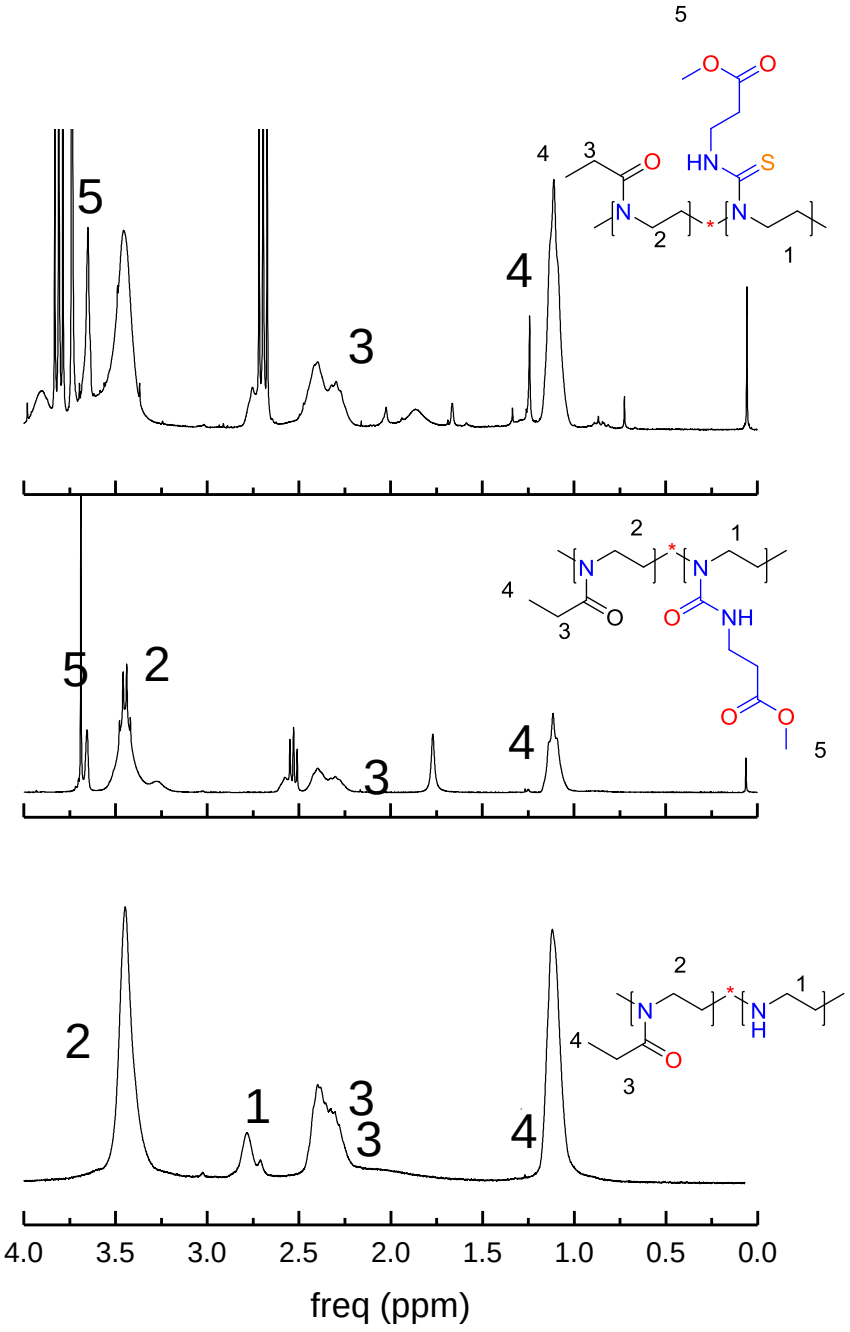

Figure 5-3 NMR overlay of the (thio)urea modified copolymers. Bottom (PEtOx-PEI(15%)), middle PEtOx-Poly(urea methyl ester), top PEtOx-Poly(thiourea methyl ester).

A final modification strategy to introduce the methyl ester side chains in PEtOx-PEI that was explored is by reaction with methyl bromoacetate. Hereby, the amine of PEI attacks methyl bromo acetate and forms a tertiary amine with the methyl ester on the side chain. The reaction is performed under reflux

conditions and is pushed by the formation of KBr, which precipitates in the acetonitrile. The ^{1}H-NMR spectrum shows that the reaction was successful, although the reaction was not complete as there are still PEI units left as the signal left at 2.8 ppm has not disappeared from the ^{1}H-spectrum, (Figure 5-4).

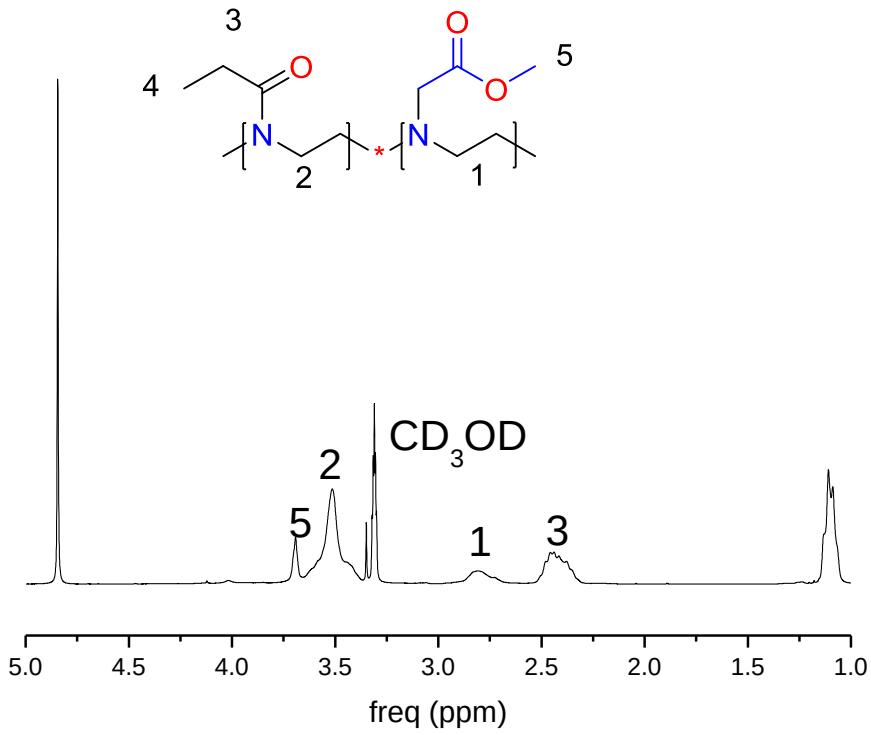

Figure 5-4 ^{1}HNMR spectrum (CD_3OD) of the PEtOx-Poly(amino methyl acetate)

5.3.3 Post-polymerisation modification of PEtOx-MestOx by direct amidation

After establishing a robust procedure for the preparation of PEtOx-MestOx, we focused our attention to the amidation of the methyl ester side chains. Even though it is commonly accepted that a direct amidation is not feasible under mild conditions, we did try this out by stirring the PEtOx-MestOx copolymer for two days in neat *n*-propylamine at 70 °C. ^{1}H NMR spectroscopic analysis of the resulting polymer after precipitation revealed that the methyl ester resonance at 3.7 ppm disappeared and a new amide signal appeared at 7.9 ppm indicating successful amidation. The disappearance of the methylester peaks proves that there is a full conversion from an ester to an amide. In addition, FT-IR also confirmed the successful amidation by disappearance of the methyl ester band at 1730 cm^{-1} and appearance of a new band at 1531 cm^{-1} representative for the NH bending in a secondary amide group. Furthermore, SEC

analysis in DMA revealed an increase in M_n from 9.7 x 10^3 Da for PEtOx to 11 x 10^3 for PEtOx-MestOx to 17.8 x 10^3 Da for the *n*-propyl modified polymer. Importantly, the Đ remained constant at 1.1 indicating that no side reactions take place. Even though it is not fully clear why the direct mild amidation of PEtOx-MestOx is possible, it may be speculated that this is due to the very high concentration and large excess of amine groups, possibly in combination with a neighbouring group effect in which the amide groups attached to the PAOx backbone participate in the reaction mechanism by stabilization of the transition state *via* the formation of H-bonds.

Inspired by the success of this first direct amidation reaction, we continued to explore the scope of this post-polymerisation modification reaction for PEtOx-MestOx. Several other readily available and cheap amines, namely aminomethane, aminoethane and hydrazine-hydrate, were utilized using the same Method 1, whereby the reaction is performed in a solution of the amine. ^{1}H NMR spectroscopy, FT-IR and SEC again revealed the success of these direct amidation reactions (Table 1). The hydrazine modified polymer is especially interesting as it contains hydrazide side-chains that may be further utilized for conjugation of ketone containing molecules *via* a pH-degradable hydrazone linker.[41] In a next step, a series of more complex functional amines was explored for direct amidation of PEtOx-MestOx. As these amines are more expensive and often occur as viscous liquids, the reaction conditions were modified resulting in Method 2. In this second method, the polymer is dissolved in acetonitrile and three equivalents of the amine are added. The resulting solution is stirred at 40 °C overnight. Only if the amine is not soluble in acetonitrile, the reaction was performed in a similar manner in DMF, which was the case for allylamine and 1-amino-3-butyne. In the case of amino acids such as leucine ester and glycine a deprotonation was needed. Therefore basic water was used as a reaction medium. The different tested amines are listed in Table 1 and successful direct amidation was found based on ^{1}H NMR and FT-IR spectroscopy as well as SEC for dimethylamine, leucine methyl ester, glycine, 1,2-aminoethanol and 1,3-aminopropanol, allylamine, 1-amino-3-butyne, *N*,*N*-dimethyl-1,2-ethylenediamine and 1,2-ethylenediamine. As such, we could include a wide variety of functional groups in the side chains of PAOx based on the same PEtOx-MestOx reactive platform. It is important to note, that the reaction with 1,2-ethylenediamine led to a minor increase of Đ and a decrease in M_n. This observation can be ascribed to tailing of the SEC trace due to interaction of the free amine group with the column materials. There is no evidence of double molar mass shoulders indicating that no cross-linking took place. A series of representative ^{1}H NMR spectra, FT-IR spectra and SEC traces of the PEtOx-MestOx and some products after amidation are shown in Figure 5-5, 5-6 and 5-7, respectively. The ^{1}H-NMR spectra clearly show that the peak at 3.7 ppm of the methyl ester group in PEtOx-PMestOx disappears upon amidation. There is also a notable change of signal 6, which after reaction with the amine moves closer to, and partially overlap with the peak around 2.2 ppm. These peaks merge together because of the similarity between the side chain of the PEtOx and the side chain of the succinyl. FT-IR clearly shows the disappearance of the band at 1730 cm^{-1} of the methyl ester

carbonyl and reveals the appearance of a new band in the region between 1530-1560 cm $^{-1}$a finger print of the NH bending. Finally, SEC analysis clearly shows that the polymer molar mass distributions have very similar shape before and after amidation demonstrating that no polymer coupling occurred.

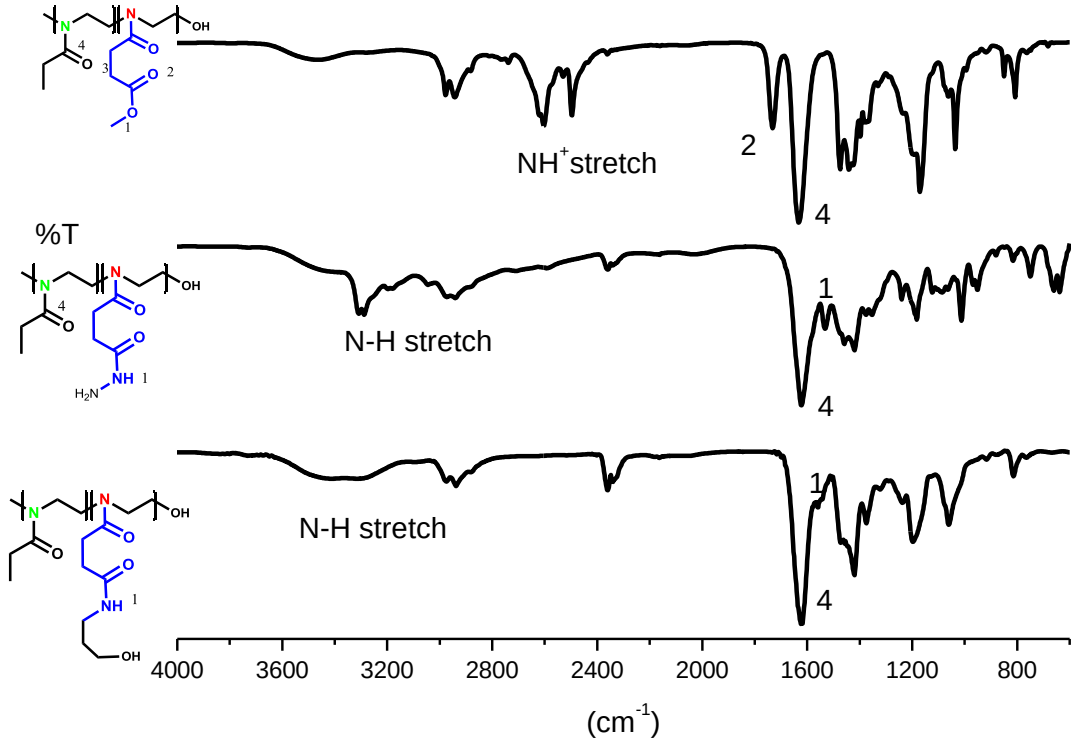

Figure 5-5: FT-IR data starting from the top with the PEtOx-MestOx and below two examples of polymers after the direct amidation

Table 1: Overview of the direct amidation of PEtOx-MestOx with various amines.

	R_1-group	Chemical shift amide proton(ppm)[1]	Mn (kDa)[2]	Đ[2]	Method[3]
aminomethane		6.4	17.7	1.1	1
aminoethane	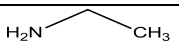	6.5	17.7	1.1	1
1-amino propane	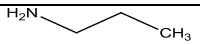	7.9	17.8	1.1	1
N-metylmethaanamine	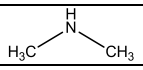	6.3	17.8	1.1	2(water)
hydrazine monohydrate		9	17.7	1.1	1
leucine methylester	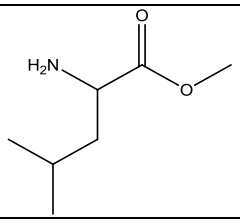	nd[4]	18	1.1	2(basic water)
glycine	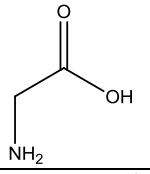	nd[4]	18	1.1	2(basic water)
2-aminoethanol	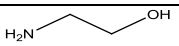	nd[4]	22	1.1	2(acetonitrile)
3-amino-1-propeen	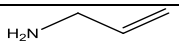	nd[4]	16.5	1.1	2(DMF)
1-amino-3-butyne	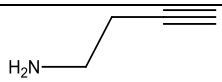	7.8	16.7	1.1	2(DMF)
N,N'-dimethyl-1,2-ethyleen diamine	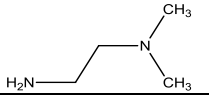	8.2	16.6	1.1	2(DMF)
1,2 ethylene diamine	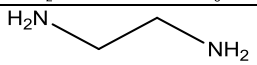	nd[4]	14	1.3	1

1 Chemical shift in 1H-NMR spectra recorded in $CDCl_3$.

2 Calculated from SEC analysis with DMA as eluent and PMMA as calibration.

3 Method 1: amine is used as reaction solution; method 2: The amidation reaction is done in another solvent specified between brackets.

4 Not distinguishable as the 1H-NMR-spectra were recorded in DMSO and the NH peak could not be seen.

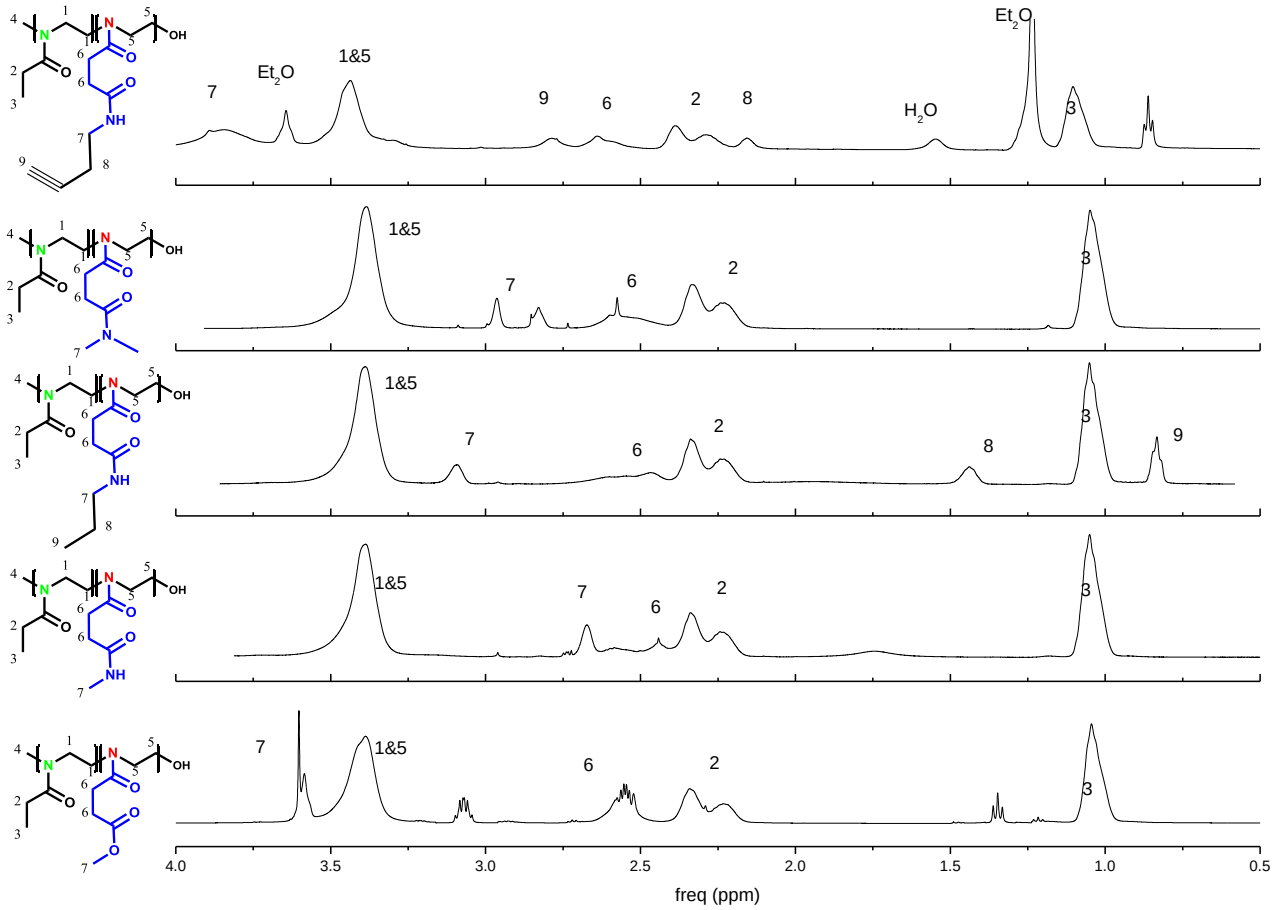

Figure 5-6: Overlay of the ^{1}H-NMR spectra of PEtOx-MestOx and four products after direct amidation with different amines.

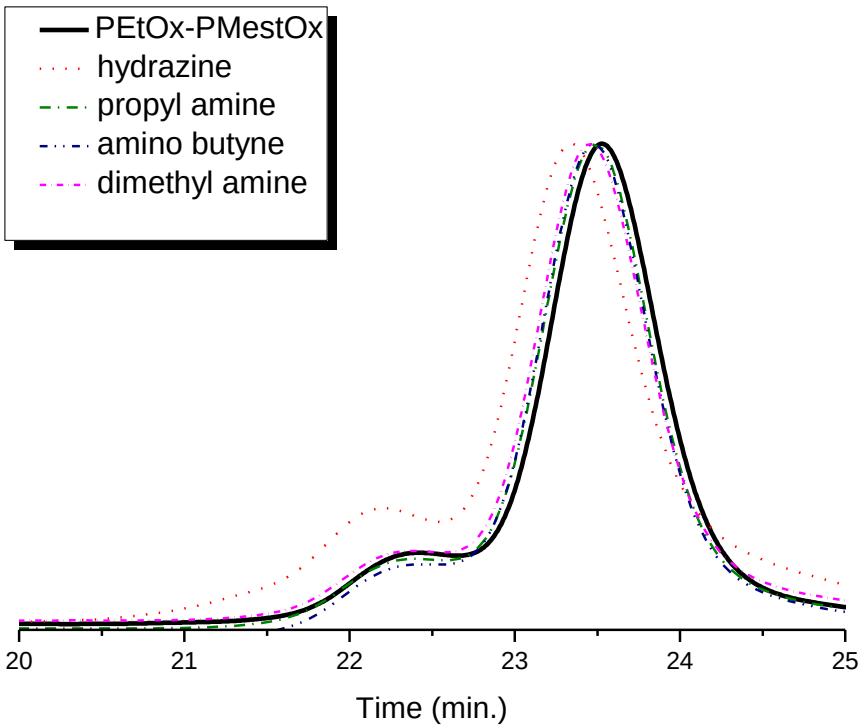

Figure 5-7: Overlay of normalized SEC (HFIP) traces of PEtOx-PMestOx and four examples of amidated polymers functionalized with hydrazine, allyl amine, 1-amino-3-butyne, cystamine

To show that the direct amidation is also possible on homopolymers, PMestOx with DP 20 was synthesized by CROP of MestOx using methyl tosylate as initiator. This resulting polymer was analyzed by 1H-NMR spectroscopy, MALDI-TOF MS and SEC revealing the formation of a defined polymer with a low polydispersity (Đ=1.13; Figure 5-6). This polymer was subsequently modified with 1-aminopropane *via* method 1 (bulk method) by dissolving the polymer in 1-aminopropane and stirring overnight at 37°C. The MALDI-TOF mass spectrum of the resulting polymer clearly shows that there is a shift in mass in comparison to the begin product (Figure 5-6). MALDI-TOF MS of the PMestOx revealed the expected spacing of 157 m/z corresponding to the MestOx monomer while after reaction the spacing increased to 184.24 m/z corresponding to the amidopropane side chain. Furthermore, the exact mass of 3197 m/z for PMestOx corresponds to a polymer with 20 repeat units and methyl and OH end-groups charged with a sodium cation. After the amidation reaction, the exact mass of 3738 is found corresponding to the amido-propane functionalized polymer with methyl and OH end-groups and charged with a sodium cation. These results confirm a clean amidation of all methyl ester side chains. The 1H-NMR spectra also demonstrate that the methyl ester groups disappeared after amidation while 3 new peaks appeared

corresponding to the propyl side chains (signals 4-6 in Figure 5-7). Finally, SEC confirmed an increase in hydrodynamic volume after the amidation reaction while the Đ mildly increased from 1.13 to 1.17, albeit no clear shoulders are observable (Figure 5-8).

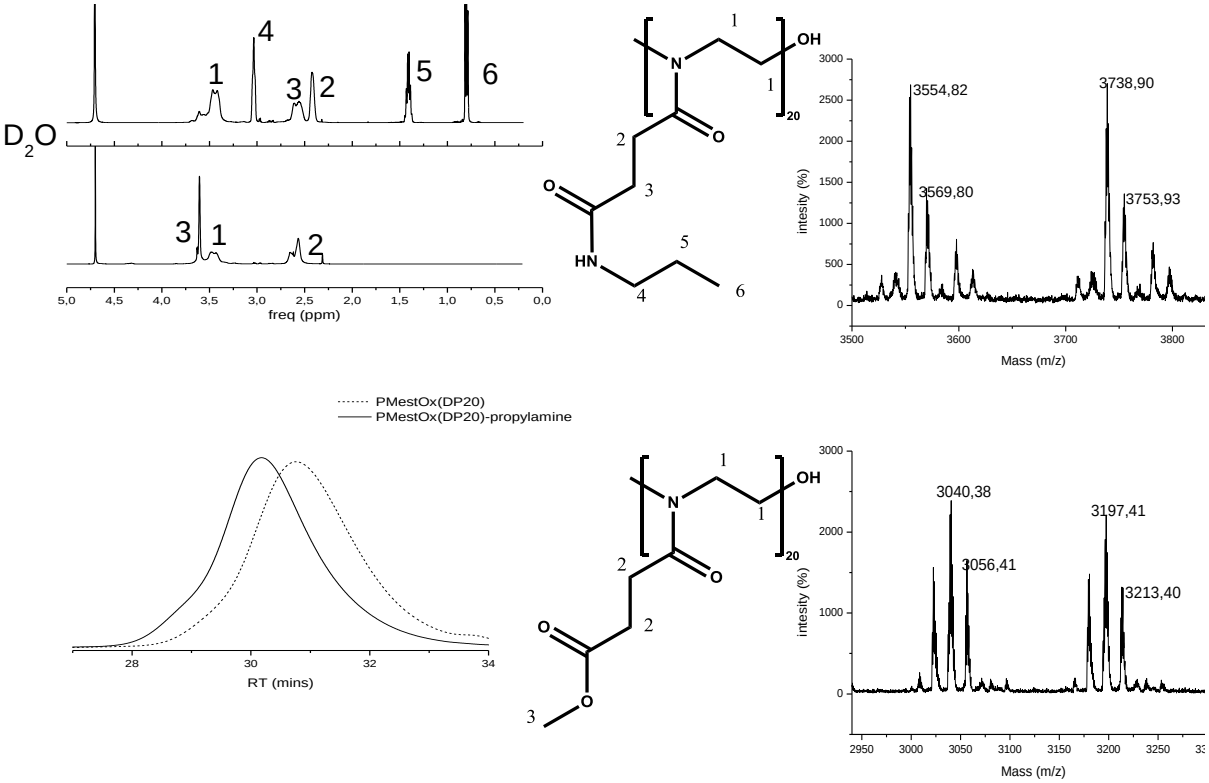

Figure 5-8 Overview of the ^{1}H-NMR data in D_2O (top left), MALDI-TOF MS (right) and SEC (DMA as eluent; bottom left) analysis of the pure PMestOx with 20 repeating units before and after amidation with 1-aminopropane. The bottom ^{1}H NMR and MALDI TOF mass spectra show PMestOx and the top spectra show the polymer after amidation with propylamine.

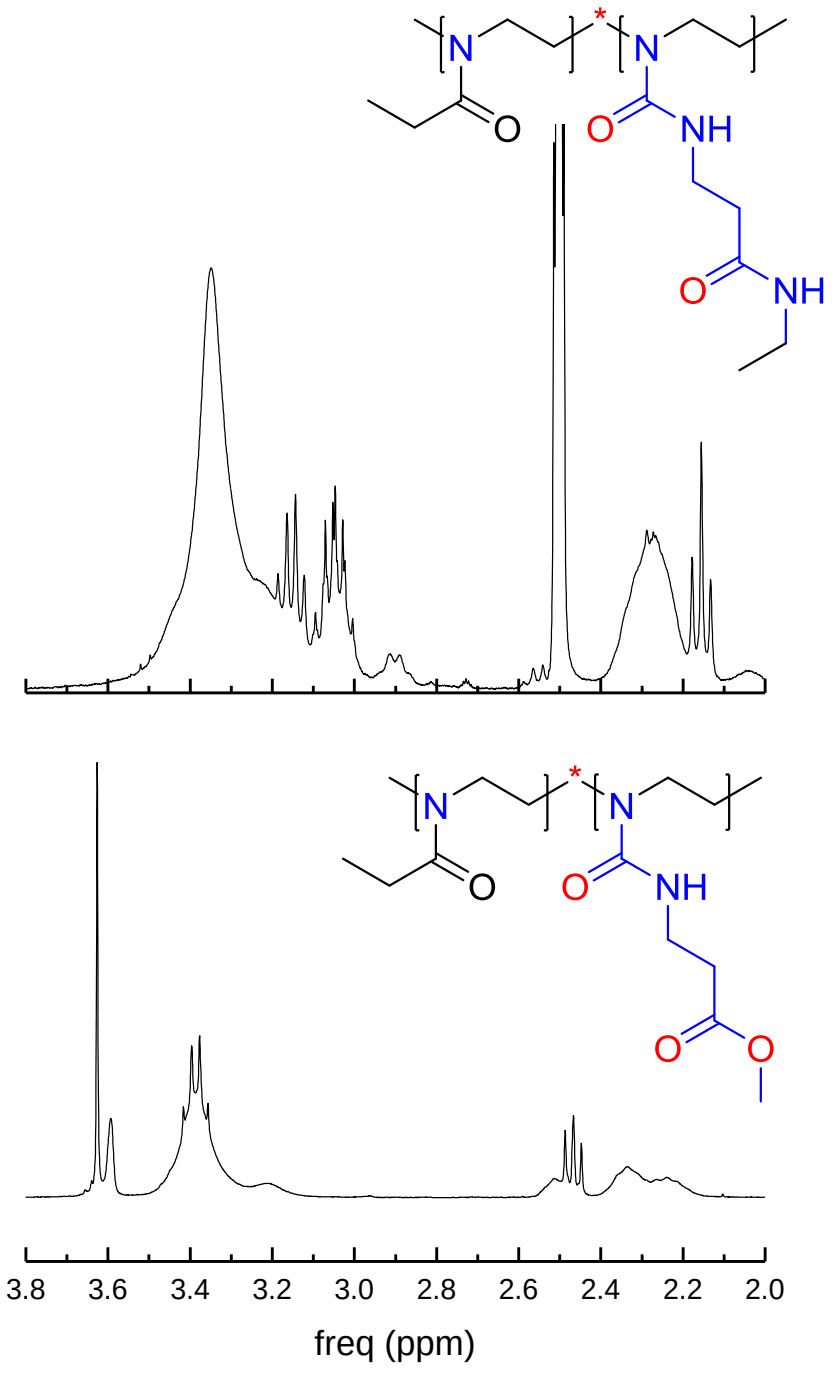

Figure 5-9 Conversion of the PEtOx-poly(urea) methyl ester with ethylamine

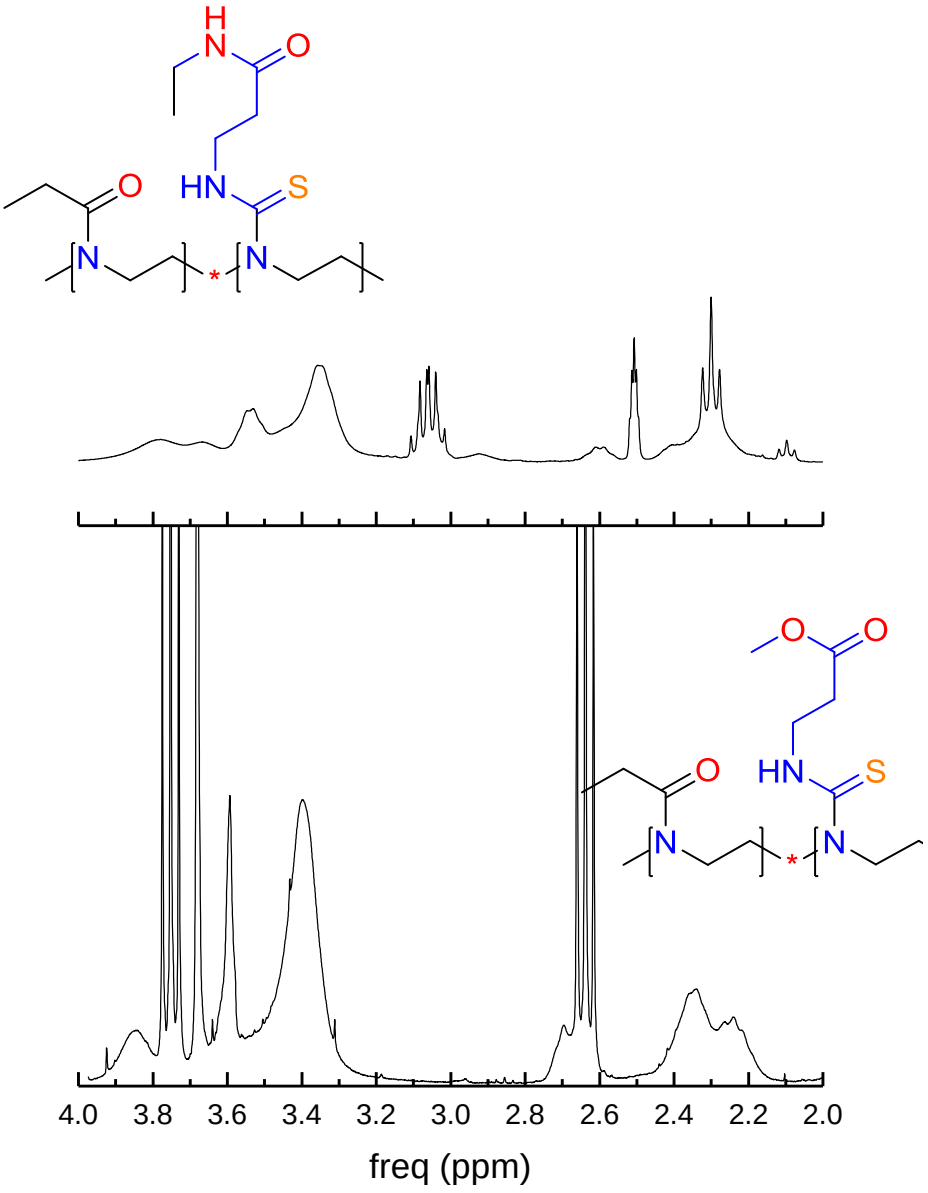

Figure 5-10 Conversion of the PEtOx-poly(thiourea) methyl ester with ethylamine

The versatility of the methyl ester conversion was introduced by combining the amines with the methyl esters formed out the (thio)urea reaction. This enlarges the system versatility. It also shows that the methyl ester located on the side chain is a potent reactive group and the reactivity is independent of the linker.

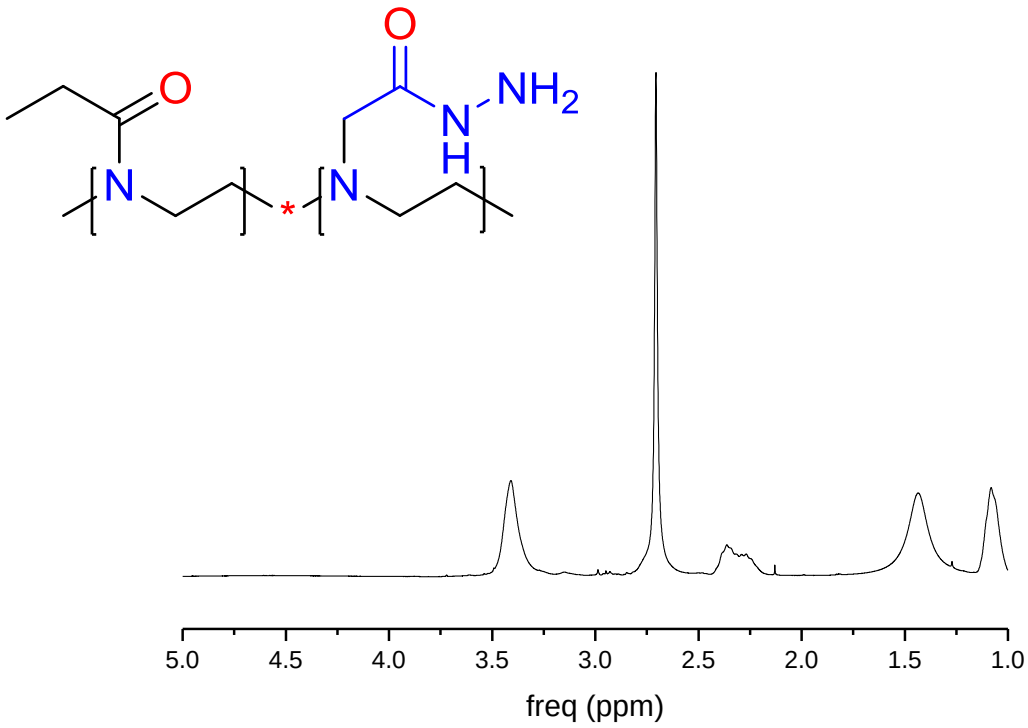

Figure 5-11 Converted quaternary amine changed with hydrazine.

5.4 Conclusion

We successfully showed a novel modification procedure to expand the chemical toolbox for poly(2-oxazoline)s PEtOx. Starting from the controlled hydrolysis of well-defined PEtOx a copolymer is obtained with a specific amount of amine units to control the number of functional groups that can be incorporated. These amine units are subsequently reacted with methyl succinyl chloride restoring the poly(2-oxazoline) side chain structure while installing a methyl ester functionality. Even though such methyl ester functionalized copolymers can also be obtained *via* a direct polymerisation method, the post polymerisation modification route is, arguably, more cost effective and less time consuming. The synthesis of three different methyl ester containing linkers was also demonstrated, based on urea, thiourea and a tertiaire amine, showing the further versatility of the PEtOx-PEI platform.

The copoly(2-oxazoline)s containing methyl ester side chains methyl ester group is demonstrated to undergo a direct amidation reaction, enabling the installation of a wide-range of side chain amide groups and functionalities. An important feature is that these reactions efficiently proceed without a catalyst, proposedly due to activation by neighbouring amide groups. Furthermore, we also demonstrated the synthesis of a PMestOx homopolymer with 20 repeat units by direct CROP of MestOx. The direct amidation of this model polymer with 1-aminopropane clearly revealed that all methyl ester side-chains can be modified.

We are confident that this direct amidation side-chain modification approach will be an important extension of the PAOx toolbox that will lead to the development of novel applications of these polymers. By using the PAOx-PEI platform in these post-polymerisation modification reactions we have accessed four new types of polymers with reactive and functional side chains. These four different structures can be further developed to couple drug or bioactive molecules in future work. This novel methodology shows that the chemical versatility of the PAOx polymer family is large.

5.5 References

(1) Tomalia, D. a; Sheetz, D. P. *J. Polym. Sci. Part A-1 Polym. Chem.* **1966**, *4* (9), 2253.
(2) Seeliger, W.; Aufderhaar, E.; Diepers, W.; Feinauer, R.; Nehring, R.; Thier, W.; Hellmann, H. *Angew. Chem. Int. Ed. Engl.* **1966**, *5* (10), 875.
(3) T, K.; Narisaw, S.; Maeda, T.; Kenichi, F. *Polym. Lett.* **1966**, *4*, 441.
(4) Levy A,Bassiri, L.; Bassiri, L.; Levy, A.; Litt, M. *J.Polym.Sci.PartB:Polym.Lett* **1968**, *5* (1), 2253.
(5) Aoi, K.; Okada, M. *Prog. Polym. Sci.* **1996**, *21* (95), 151.
(6) Kobayashi, S. *Prog. Polym. Sci.* **1990**, *15* (5), 751.
(7) Hoogenboom, R. *Angew. Chem. Int. Ed. Engl.* **2009**, *48* (43), 7978.
(8) Adams, N.; Schubert, U. S. *Adv. Drug Deliv. Rev.* **2007**, *59* (15), 1504.
(9) Schlaad, H.; Hoogenboom, R. *Macromol. Rapid Commun.* **2012**, *33* (19), 1599.
(10) Luxenhofer, R.; Han, Y.; Schulz, A.; Tong, J.; He, Z.; Kabanov, A. V; Jordan, R. *Macromol. Rapid Commun.* **2012**, *33* (19), 1613.
(11) Hoogenboom, R.; Paulus, R. M.; Pilotti, Å.; Schubert, U. S. *Macromol. Rapid Commun.* **2006**, *27* (18), 1556.
(12) Kempe, K.; Lobert, M.; Hoogenboom, R.; Schubert, U. S. *J. Comb. Chem.* **2009**, *11* (2), 274.
(13) Kjøniksen, Anna-lena, H. R. *Macromolecules* **2012**, *45*, 4337.
(14) Persigehl, P.; Jordan, R.; Nuyken, O. *Macromolecules* **2000**, *33* (cmc), 6977.
(15) Milonaki, Y.; Kaditi, E.; Pispas, S.; Demetzos, C. *J. Polym. Sci. Part A Polym. Chem.* **2012**, *50* (6), 1226.
(16) Fetsch, C.; Luxenhofer, R. *Macromol. Rapid Commun.* **2012**, *33* (19), 1708.
(17) Guillerm, B.; Monge, S.; Lapinte, V.; Robin, J.-J. *Macromol. Rapid Commun.* **2012**, *33* (19), 1600.
(18) Verbraeken, B. K. H. R. In *Encyclopedia of Polymer Science and Technology*; 2014; pp 1–39.
(19) Rossegger, E.; Schenk, V.; Wiesbrock, F. *Polymers (Basel).* **2013**, *5* (3), 956.
(20) Huntsville, J. M.; Huntsville, M. D.; Madison, K.; Madison, Z.; Maria, F. Activated polyoxazolines and compositions comprising the same, 2011.
(21) Knop, K.; Hoogenboom, R.; Fischer, D.; Schubert, U. S. *Angew. Chem. Int. Ed. Engl.* **2010**, *49* (36), 6288.
(22) Barz, M.; Luxenhofer, R.; Zentel, R.; Vicent, M. J. *Polym. Chem.* **2011**, *2* (9), 1900.
(23) de la Rosa, V. R.; Bauwens, E.; Monnery, B. D.; De Geest, B. G.; Hoogenboom, R. *Polym. Chem.* **2014**, *5*, 4957.
(24) Sedlacek, O.; Monnery, B. D.; Filippov, S. K.; Hoogenboom, R.; Hruby, M. *Macromol. Rapid Commun.* **2012**, *33* (19), 1648.
(25) Kempe, K.; Hoogenboom, R.; Jaeger, M.; Schubert, U. S. *Macromolecules* **2011**, *44* (16), 6424.
(26) Mais, U.; Binder, W. H.; Knaus, S.; Gruber, H. **2000**, 2115.
(27) Taubmann, C.; Luxenhofer, R.; Cesana, S.; Jordan, R. *Macromol. Biosci.* **2005**, *5* (7), 603.
(28) Legros, C.; De Pauw-Gillet, M.-C.; Tam, K. C.; Lecommandoux, S.; Taton, D. *Eur. Polym. J.* **2015**, *62*, 322.
(29) Diehl, C.; Schlaad, H. *Macromol. Biosci.* **2009**, *9* (2), 157.
(30) Englert, C.; Tauhardt, L.; Hartlieb, M.; Kempe, K.; Gottschaldt, M.; Schubert, U. S. *Biomacromolecules* **2014**, *15* (4), 1124.
(31) Kempe, K.; Weber, C.; Babiuch, K.; Gottschaldt, M.; Hoogenboom, R.; Schubert, U. S. *Biomacromolecules* **2011**, *12* (7), 2591.
(32) Luxenhofer, R.; Jordan, R. *Macromolecules* **2006**, *39* (10), 3509.
(33) Lava, K.; Verbraeken, B.; Hoogenboom, R. *Eur. Polym. J.* **2015**, *In press*, 1.
(34) Bouten, P. J. M.; Hertsen, D.; Vergaelen, M.; Monnery, B. D.; Boerman, M. a.; Goossens, H.; Catak, S.; van Hest, J. C. M.; Van Speybroeck, V.; Hoogenboom, R. *Polym. Chem.* **2014**, *6* (4), 514.
(35) Van Kuringen, H. P. C.; Lenoir, J.; Adriaens, E.; Bender, J.; De Geest, B. G.; Hoogenboom, R. *Macromol. Biosci.* **2012**, *12* (8), 1114.

(36) Lambermont-Thijs, H. M. L.; van der Woerdt, F. S.; Baumgaertel, A.; Bonami, L.; Du Prez, F. E.; Schubert, U. S.; Hoogenboom, R. *Macromolecules* **2010**, *43* (2), 927.
(37) Jäger, M.; Schubert, S.; Ochrimenko, S.; Fischer, D.; Schubert, U. S. *Chem. Soc. Rev.* **2012**, *41* (13), 4755.
(38) Hoogenboom, R. Polyoxazoline polymers and methods for their preparation, conjugates of these polymers and medical uses thereof, 2013.
(39) Chujo, Y.; Yutaka, Y.; Sada, K.; Saegusa, T. *Macromolecules* **1989**, *22* (3), 1074.
(40) Lee, M.-J.; Sun, C.-M. *Tetrahedron Lett.* **2004**, *45* (2), 437.
(41) Bildstein, L.; Dubernet, C.; Couvreur, P. *Adv. Drug Deliv. Rev.* **2011**, *63* (1–2), 3.

Chapter 6 :
Sweet polymers: poly(2-ethyl-2-oxazoline) glycopolymers by reductive amination

Contributors to this chapter:

Christiane Effenberg, Leibniz institute of Polymer Research Dresden

Dietmar Appelhans Leibniz institute of Polymer Research Dresden

Contributions of the candidate

Synthesis of the start polymers and DLS characterization

Is integrally published as

Biomacromolecules, **2016**, *17* (12), pp 4027–4036

Prologue

This chapter is an example of the post-polymerisation modification on the PAOx-PEI platform. By using this platform we can couple carbohydrates on to this platform. These carbohydrates can act as a model in the further development of more complicated carbohydrates. As carbohydrates play an important role in all kinds of biological processes this coupling could introduce a useful functionality. It gives the opportunity to introduce new and more complex structures.

6.1 Introduction

Carbohydrates are a crucial part of living organisms and function as structural components, energy sources, and in cellular communication and recognition.[1,2] As glycoconjugates, carbohydrates can be integrated with proteins (glycoproteins) or with lipids (glycolipids). Galactin is an example of a carbohydrate binding protein, which interacts with polylactosamines on the cell surface and is crucial in cellular activation, differentiation and survival. An example of a glycoconjugate is hyaluronan, a polysaccharide that is highly abundant in the extracellular compartment of cartilage and synovial fluid and which induces cell adhesion by binding to various proteins.[3] The carbohydrates interact through weak forces with low selectivity, such as hydrogen bonds, chelation, electrostatic and hydrophobic interactions.[4,5] In nature, these low-affinity interactions occur between multiple, oligomeric binding site/pockets for monomeric/oligomeric sugar units. The binding becomes stronger due to multivalency,[5] which also generates reversible interactions that differentiate multivalency from covalent interactions[6] and generally results in stronger binding, as observed in lectin[7]. A great way to mimic these glycoconjugates is fabricating carbohydrate-containing polymers or glycopolymers; unlike glycoproteins, glycopolymers can be easily produced on a large scale.[8–13] This process of biomimicry uses a simplified system, which facilitates the understanding of biological systems without the burden of difficult syntheses.

To obtain these polymers, two strategies can be followed: the first consists a polymerisation of a carbohydrate-containing monomer, whereas the second consists of a post-polymerisation-modification in which the carbohydrate is coupled to a preformed polymer. In the case of the carbohydrate-containing monomer, the combination of a hydrophilic sugar component and a hydrophobic backbone often gives solubility problems due to the large differences in polarity. Therefore, living radical polymerisation and free radical polymerisation are often applied in solvent mixtures such as methanol:water or water:DMF.[14] Some examples of the direct polymerisation of unprotected sugar-containing monomers include the reversible addition-fragmentation chain transfer (RAFT) polymerisation of methacrylates,[15–17] atom-transfer radical polymerisation (ATRP) of poly(oligoethylene glycol) methacrylate[18] and single electron

transfer living radical polymerisation (SET-LRP).[19,20] The ring opening polymerisation of substituted N-carboxyanhydride yields a large range of polypeptides depending on the (protected) carbohydrate.[13] Nonetheless, protecting groups must be introduced to the carbohydrate, which requires the use of a deprotection step.

The second approach for the preparation of glycopolymers is the post-polymerisation modification of a reactive polymer with a sugar. In this approach, the sugar units do not intervene in the polymerisation, which provides more control and requires no subsequent deprotection step. An azide group is often used to click the sugar onto the polymer.[16,21–23] The use of thiol-ene and NHS-esters to couple sugar units onto a polymer chain have also been described.[13,14] Moreover, reductive amination has been used to couple sugars to amine-containing polymers.[13,24–27]

For further biomedical applications, the choice of polymer is crucial because this determines, to a large extent, the properties and biocompatibility of the material. Ideal candidates have high water solubility, do not interact with the immune system, show no toxic effects, and are well defined and easily accessible. Therefore, poly(2-oxazoline)s (PAOx) were chosen in this work not only for their biocompatibility[28–30] but also for the easy introduction of functionalities.[29,31–33] These polymers are readily accessible by cationic ring opening polymerisations (CROP), which enables different architectures and functionalities. Earlier publications have already shown the preparation of glyco-PAOx using carbohydrate initiators, which resulted in chain-end functionalized PAOx.[34,35] Furthermore, poly(2-methyl-2-oxazoline) and other PAOx have been grafted onto the polysaccharide chitin yielding graft copolymers.[36,37] The first report on the CROP of a protected sugar-functionalized 2-oxazoline monomer was by Takasu,[38] who copolymerised a sulfur-modified galactosyl containing a 2-oxazoline monomer with 2-methyl-2-oxazoline and with 2-benzyl-2-oxazoline. The second publication by Schubert reported the copolymerisation of a 2-oxazoline monomer with a protected sugar with 2-ethyl-2-oxazoline or 2-decenyl-2-oxazoline.[39] The main disadvantage of this copolymerisation route, however, is that the carbohydrates interfere with the CROP, necessitating protection of the hydroxyl groups of the sugar and deprotection after the polymerisation. Therefore, the post-polymerisation modification route is preferred for the preparation of these types of glyco-PAOx polymers. For example, Diehl et al[40] reported the glycosylation of PAOx *via* thiol-ene chemistry in which the double bond was located on the side chain of the polymer; related polymers have been reported by the same and other research groups.[41–45] This route enables the synthesis of well-defined polymers with a variety of functionalities, although the synthesis of a functional 2-oxazoline monomer is required for the thiol-ene mediated introduction of the carbohydrates.

Therefore, in this work, an alternative post-polymerisation modification route starting from a well-defined poly(2-ethyl-2-oxazoline) (PEtOx) homopolymer is proposed. The PEtOx was easily converted into a copolymer of PEtOx-PEI with a controllable percentage of PEI *via* acidic hydrolysis.[46–48] The resulting copolymer contained the biocompatible PEtOx and a secondary reactive amine that was

subsequently used to couple the carbohydrate. In this step the amount of PEI in the partially hydrolysed PEtOx controlled the number of carbohydrates that could be incorporated. A major advantage of this modification of the PEtOx-PEI copolymer is that a biocompatible polymer was obtained. During the polymerisation of PEtOx, there is the possibility of further tailoring the end groups with functional terminators/initiators[31] to enable the introduction of specific targeting groups or labels. The targeting groups could deliver polymers in specific tissue or organs. Also labels or traces can be coupled so the polymers can be used as tracking devices. As shown in earlier reports, sugar moieties can be coupled to primary amines through reductive amination; this approach has been used to introduce sugar moieties into hyperbranched PEI.[24–26] However, such direct modification of the linear PEI (co)polymer has not been reported to date, and it is not directly clear whether the efficient modification *via* reductive amination is possible on the more sterically hindered secondary amine groups.

Here, we report the preparation of defined PEtOx-PEI copolymers and the subsequent coupling of carbohydrates *via* the aldehyde of the linear form to yield an imine linkage, which was then reduced to a tertiary amine group in situ, so-called reductive amination (Scheme 1). The carbohydrates may increase bioavailability or even render a higher rate of accumulation in, for example, tumors due to the higher nutrient intake of cancer cells. This also could be the start of a new field of polymers where PEtOx and specific oligosaccharides are combined. The success of coupling the sugar onto copolymers with different amounts of PEI was investigated *via* size exclusion chromatography (SEC) and ^{1}H and ^{13}C NMR spectroscopy. The temperature-dependent solution behavior of the resulting glyco-PAOx was also investigated using dynamic light scattering (DLS). Finally, we demonstrated the biological affinity of the obtained glycopolymers by studying their interaction with Concanavalin A *via* DLS.[39]

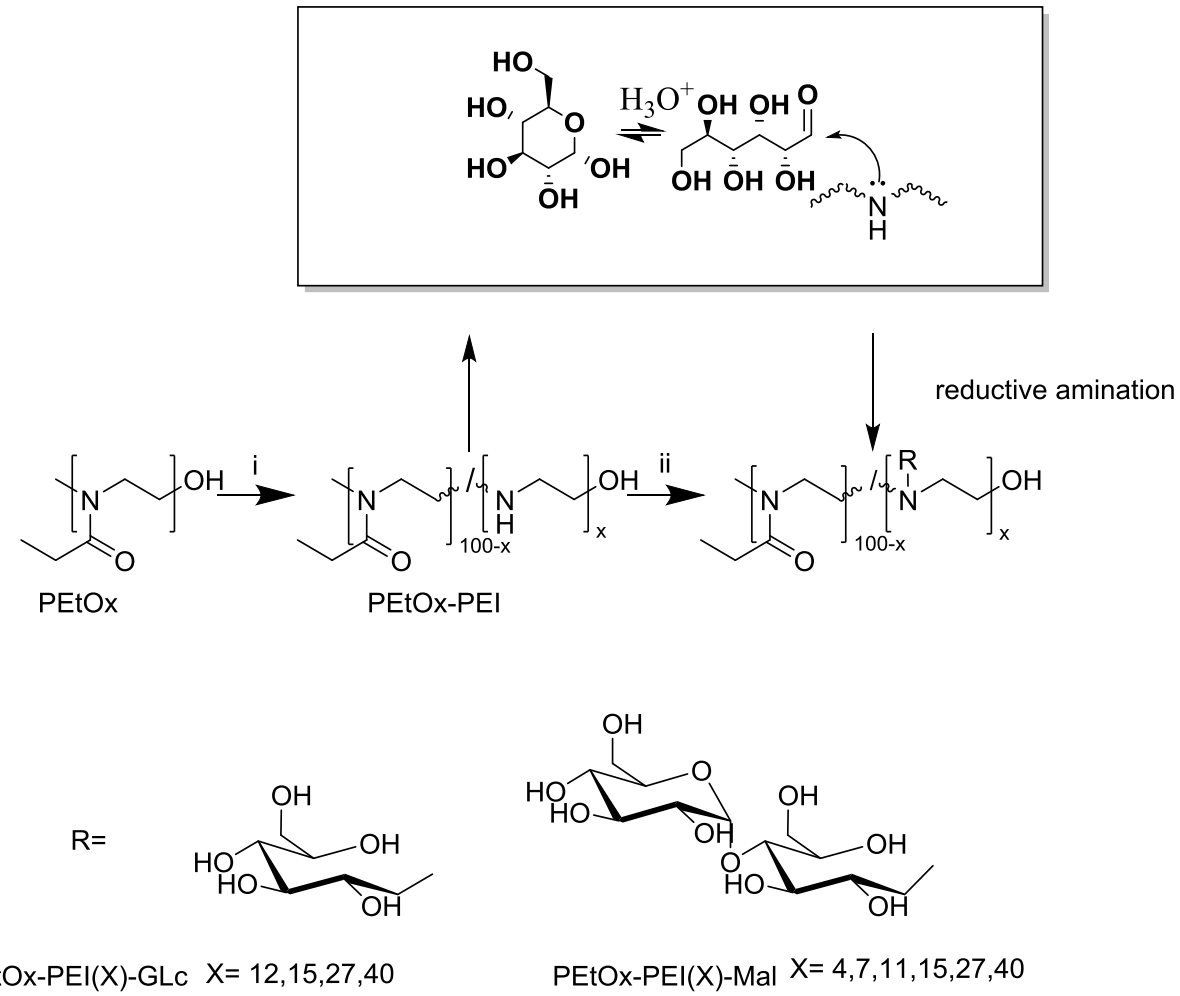

Scheme 1 Synthetic approach for synthesizing PEtOx$_{(100-x)}$-PEI$_x$-Glc and PEtOx$_{(100-x)}$-PEI$_x$-Mal. Reaction conditions: i) acid hydrolysis (6 M HCl) at 73°C; ii) excess Glc (10eq) or Mal (20 eq) and excess BH_3*Py (8 M) in sodium borate buffer (0.1 M) at 50°C for 7 days. The amount of x can be found in Table 1 of the SI. The upper box shows the formation of an imine *via* nucleophilic attack; the imine is subsequently reduced to an amine

6.2 Materials and methods

PEtOx with a degree of polymerisation (DP) of 100 was synthesized as reported earlier (M_n = 9700 kg/mol; Đ = 1.13).[49,50] Hydrogen chloride, sodium hydroxide, dichloromethane, Concanavalin A (ConA) (Canavalia ensiformis, 25.5 kDa per monomer), maltose monohydrate, anhydrous glucose and borane-pyridine complex (BH_3*Py) were purchased from Sigma-Aldrich and were used without further purification. Dialysis membranes with a molecular weight cut-off of 1000 g/mol were purchased from Roth (Germany).

Dynamic light scattering (DLS) was recorded on a Zeta Sizer Nano device (Malvern) using disposable polystyrene latex cuvettes. The concentration of the polymers was 5 mg/mL in MilliQ water. Unless otherwise mentioned, all samples were filtrated and sonicated before measurements were taken. Size exclusion chromatography (SEC) was performed using an Agilent HPLC equipped with a 1260 refractive index detector (RID) with 1,1,1,3,3,3-hexafluoro-2-isopropanol (HFIP) containing 20 mM sodium trifluoroacetate as the eluent at a flow rate of 0.3 mL/min (HFIP-SEC). Polymethylmethacrylate (PMMA) standards were used to calculate the molar mass values. The column set consisted of two PSS PFG 100Å gel 5 µm MIXED-D columns and a similar guard column (Agilent) in series at 35°C. Chromatograms were analyzed in Agilent Chemstation software using the GPC add-on.

The *NMR measurements* were carried out on a Bruker DRX 500 NMR spectrometer operating at 500.13 MHz for ^{1}H and at 125.75 MHz for ^{13}C. All samples were measured in D_2O. Sodium 3-(trimethylsilyl)-3,3,2,2-tetradeuteropropionate was added for internal calibration (δ (^{13}C) = 0 ppm; δ (^{1}H) = 0 ppm). The signal assignments were done by combination of 1D and 2D NMR experiments using the standard pulse sequences provided by Bruker. All chemical shifts are given in ppm.

Partial hydrolysis of PEtOx for the synthesis of PEtOx$_{(100-x)}$-PEI$_x$

PEtOx was fully dissolved in 50 mL of water with heating and stirring. Then, 50 mL of a 36 wt% solution of HCl (concentrated HCl) was added and the mixture was heated to 73°C or 100°C for a defined period of time, which was adjusted to obtain the desired amount of partial hydrolysis of PEtOx to PEtOx-PEI based on the hydrolysis kinetics described in an earlier work by our group[46]: PEtOx$_{96}$-PEI$_4$ (25 min, 73 °C); PEtOx$_{93}$-PEI$_7$ (35 min, 73 °C); PEtOx$_{89}$-PEI$_{11}$ (50 min, 73 °C); PEtOx$_{85}$-PEI$_{15}$ (180 min, 73 °C); PEtOx$_{73}$-PEI$_{27}$ (50 min, 100 °C); and PEtOx$_{60}$-PEI$_{40}$ (120 min, 100 °C).[46,47] After the hydrolysis, the volatiles were removed on a rotary evaporator. The polymer was basified to pH 10-11 by the addition of a NaOH solution. The solution was then lyophilized, and the solid was dissolved in dichloromethane. The organic phase was washed with brine and then concentrated under reduced pressure to yield a solid, white product. The

integral ratio between the peaks at 2.6-2.8 ppm (PEI backbone) and 3.2-3.5 ppm (PEtOx backbone) in the ^{1}H-NMR spectra were used to calculate the degree of hydrolysis.

PEtOx$_{96}$-PEI$_4$: ^{1}H NMR (D_2O): δ (ppm) = 0.9 – 1.25 (m, 3H, d); 2.1 – 2.55 (m, 2H, c), 2.6 – 3.0 (m, 4H, b); 3.15 – 3.95 (m, 4H, a). ^{13}C NMR (D_2O): δ(ppm) = (D_2O): δ (ppm) = 11.98 (CH_3, d); 28.6 and 28.9 (CH_2, c); 50.0 – 52.0 (CH_2, a and b); 180.2 (C=O, e). M_n = 10000 kg/mol; Đ = 1.13).

PEtOx$_{93}$-PEI$_7$: ^{1}H NMR (D_2O): δ (ppm) = 0.9 – 1.25 (m, 3H, d); 2.1 – 2.55 (m, 2H, c), 2.6 – 3.0 (m, 4H, b); 3.15 – 3.95 (m, 4H, a). ^{13}C NMR (D_2O): δ = (D_2O): δ (ppm) = 11.98 (CH_3, d); 28.6 and 28.9 (CH_2, c); 50.0 – 52.0 (CH_2, a and b); 180.2 (C=O, e). M_n = 11000 kg/mol; Đ = 1.11).

PEtOx$_{89}$-PEI$_{11}$: ^{1}H NMR (D_2O): δ (ppm) = 0.9 – 1.25 (m, 3H, d); 2.1 – 2.55 (m, 2H, c), 2.6 – 3.0 (m, 4H, b); 3.15 – 3.95 (m, 4H, a). ^{13}C NMR (D2O): δ = (D2O): δ (ppm) = 11.98 (CH_3, d); 28.6 and 28.9 (CH_2, c); 50.0 – 52.0 (CH_2, a and b); 180.2 (C=O, e). M_n = 12000 kg/mol; Đ = 1.11).

PEtOx$_{88}$-PEI$_{12}$: ^{1}H NMR (D_2O): δ (ppm) = 0.9 – 1.25 (m, 3H, d); 2.1 – 2.55 (m, 2H, c), 2.6 – 3.0 (m, 4H, b); 3.15 – 3.95 (m, 4H, a). ^{13}C NMR (D_2O): δ = (D_2O): δ (ppm) = 11.98 (CH_3, d); 28.6 and 28.9 (CH_2, c); 50.0 – 52.0 (CH_2, a and b); 180.2 (C=O, e). M_n = 12500 kg/mol; Đ = 1.15).

PEtOx$_{85}$-PEI$_{15}$: ^{1}H NMR (D_2O): δ (ppm) = 0.9 – 1.25 (m, 3H, d); 2.1 – 2.55 (m, 2H, c), 2.6 – 3.0 (m, 4H, b); 3.15 – 3.95 (m, 4H, a). ^{13}C NMR (D_2O): δ = (D_2O): δ (ppm) = 11.98 (CH_3, d); 28.6 and 28.9 (CH_2, c); 50.0 – 52.0 (CH_2, a and b); 180.2 (C=O, e). M_n =12000 kg/mol; Đ = 1.13).

PEtOx$_{73}$-PEI$_{27}$: ^{1}H NMR (D_2O): δ (ppm) =1.07 (s, 3H, d); 2.15 – 2.55 (m, 2H, c); 2.55 – 2.95 (m, 4H, b); 2.95 – 4.0 (m, 4H, a). ^{13}C NMR (D_2O): δ = (D_2O): δ (ppm) = 11.98 (CH_3, d); 28.6 and 28.9 (CH_2, c); 50.0 – 52.0 (CH_2, a and b); 180.2 (C=O, e). M_n = 15000 kg/mol; Đ = 1.10).

PEtOx$_{60}$-PEI$_{40}$: ^{1}H NMR (D_2O): δ (ppm) = 0.85 – 1.15 (m, 3H, d and A); 2.1 – 2.25 (q, 2H, A); 2.25 – 2.5 (m, 2H, c); 2.5 – 3.0 (4H, b); 3.0 – 4.0 (m, 4H, a). ^{13}C NMR (D_2O): δ (ppm) = 11.98 (CH_3, d); 13.1 (CH_3, A); 28.6 and 28.9 (CH_2, c); 33.5 (CH_2, A); 45.0 – 52.0 (CH_2, a and b); 180.2 (C=O, e); 187.6 (C=O, A). M_n = 25000 kg/mol; Đ = 1.2). Signals assigned with A belong to the residual propionic acid formed during the partial hydrolysis of PEtOx.

General procedure for the synthesis of maltose- or glucose-modified PEtOx$_{(100-x)}$-PEI$_x$

The precursor PEtOx$_{(100-x)}$-PEI$_x$ (x = mol percent of hydrolysed EtOx unit in PEtOx into the PEI unit), maltose monohydrate (360.31 g/mol) or anhydrous glucose (180.16 g/mol) and borane-pyridine complex (BH_3*Py, 8 M) was dissolved in a sodium borate buffer (0.1 M). The solution was stirred at 50 °C for 7 days. The crude product was purified by dialysis (1000 MWCO) against deionized water for 2 days. A solid product was obtained by freeze drying. Further information about the molar ratios used between the

precursor and other chemicals are presented in Table 1. The yields of these materials were between 40 and 80%.

Table 1. Molar ratio of components for the synthesis of PEtOx-PEI(x)-Carbohydrate (x = 4, 7, 11, 15, 27, 40).

	Precursor eq. [PEI: x mol] [mg]		Carbohydrate eq. [mol] [g]	BH_3*Py [8 M] eq. [mol] [ml]	borate buffer [ml]	Mn	Đ
PEtOx-PEI4-Mal	PEtOx-PEI4	1 1.9 x 10-4 200	20 3.8 x 10-3 1.37	20 3.8 x 10-3 0.48	10	14400	1.4
PEtOx-PEI7-Mal	PEtOx-PEI7	1 3.3 x 10-4 200	20 6.7 x 10-3 2.41	20 6.7 x 10-3 0.84	10	14000	1.3
PEtOx-PEI11-Mal	PEtOx-PEI11	1 5.3 x 10-4 200	20 10.7 x 10-3 3.85	20 10.7 x 10-3 1.34	10	15600	1.2
PEtOx-PEI15-Mal	PEtOx-PEI15	1 5.8 x 10-4 200	20 11.6 x 10-3 4.176	20 11.6 x 10-3 1.45	15	14000	1.4
PEtOx-PEI27-Mal	PEtOx-PEI27	1 12.5 x 10-4 200	20 25.1 x 10-3 9.044	20 25.1 x 10-3 3.14	10	17900	1.2
PEtOx-PEI40-Mal	PEtOx-PEI40	1 18.6 x 10-4 200	20 37.2 x 10-3 13.4	20 37.2 x 10-3 4.7	15	15000	1.4
PEtOx-PEI12-Glc	PEtOx-PEI12	1 4.3 x 10-4 150	10 4.3 x 10-3 0.782	10 4.3 x 10-3 0.54	10	17000	1.4
PEtOx-PEI27-Glc	PEtOx-PEI27	1 9.4 x 10-4 150	10 9.4.1 x 10-3 1.695	10 9.4.1 x 10-3 1.18	10	21600	1.4
PEtOx-PEI40-Glc	PEtOx-PEI40	1 18.6 x 10-4 150	10 18.6 x 10-3 3.35	10 18.6 x 10-3 2.40	15	18700	1.3

PEtOx$_{88}$-PEI$_{12}$ -Glc: ^{1}H NMR (D_2O): δ (ppm) = 0.8 – 1.3 (m, 3H, d); 2.0 – 2.55 (m, 2H, c); 2.55 – 3.2 (m, 4H, 1′ + b); 3.2 – 4.45 (m, a + 2′-6′). ^{13}C NMR (D_2O): δ (ppm) = 11.9 (CH_3, d); 28.6 and 28.9 (CH_2, c); 45.0 – 50.0 (CH_2, a); 52.0 – 57.0 (CH_2, b); 59.3 (CH_2, 1′); 65.7 (CH_2, 6′); 73.0 – 81.0 (CH, 2′-5′); 180.2 (C=O, e). SEC data: M_n = 17000 kg/mol; Đ = 1.4.

PEtOx$_{85}$-PEI$_{15}$ -Glc: ^{1}H NMR (D_2O): δ (ppm) = 0.8 – 1.3 (m, 3H, d); 2.0 – 2.55 (m, 2H, c); 2.55 – 3.2 (m, 4H, 1′ + b); 3.2 – 4.45 (m, a + 2′-6′). ^{13}C NMR (D_2O): δ (ppm) = 11.9 (*C*H_3, d); 28.6 and 28.9 (*C*H_2, c); 45.0 – 50.0 (*C*H_2, a); 52.0 – 57.0 (*C*H_2, b); 59.3 (*C*H_2, 1′); 65.7 (*C*H_2, 6′); 73.0 – 81.0 (*C*H, 2′-5′); 180.2 (C=O, e). SEC data: M_n = 19500 kg/mol; Đ = 1.2.

PEtOx$_{73}$-PEI$_{27}$-Glc: ^{1}H NMR (D_2O): δ (ppm) = 0.8 – 1.3 (m, 3H, d); 2.0 – 2.55 (m, 2H, c); 2.55 – 3.2 (m, 4H, 1′ + b); 3.2 – 4.45 (m, a + 2′-6′). ^{13}C NMR (D_2O): δ (ppm) = 11.9 (*C*H_3, d); 28.6 and 28.9 (*C*H_2, c); 45.0 – 50.0 (*C*H_2, a); 52.0 – 57.0 (*C*H_2, b); 59.3 (*C*H_2, 1′); 65.7 (*C*H_2, 6′); 73.0 – 81.0 (*C*H, 2′-5′); 180.2 (C=O, e). SEC data M_n = 21600 kg/mol; Đ = 1.4.

PEtOx$_{60}$-PEI$_{40}$-Glc: ^{1}H NMR (D_2O): δ (ppm) = 0.8 – 1.3 (m, 3H, d); 2.05 – 2.52 (m, 2H, c); 2.55 – 3.2 (m, 4H, 1′ + b); 3.2 – 4.45 (m, a + 2′-6′). ^{13}C NMR (D_2O): δ (ppm) = 11.9 (*C*H_3, d); 28.6 and 28.8 (*C*H_2, c); 45.0 – 50.0 (*C*H_2, a); 52.0 – 56.0 (*C*H_2, b); 59.2 (*C*H_2, 1′); 65.6 (*C*H_2, 6′); 73.0 – 81.0 (*C*H, 2′-5′); 180.2 (C=O, e). SEC data: M_n = 18700 kg/mol; Đ = 1.3.

PEtOx$_{96}$-PEI$_{4}$-Mal: ^{1}H NMR (D_2O): δ (ppm) = 0.8 – 1.3 (m, 3H, d); 2.0 – 2.55 (m, 2H, c); 2.55 – 3.2 (m, 4H, 1′ + b); 3.2 – 4.45 (m, a + 2′-6′). ^{13}C NMR (D_2O): δ (ppm) = 11.9 (*C*H_3, d); 28.6 and 28.9 (*C*H_2, c); 45.0 – 50.0 (*C*H_2, a); 52.0 – 57.0 (*C*H_2, b); 59.3 (*C*H_2, 1′); 65.7 (*C*H_2, 6′); 73.0 – 81.0 (*C*H, 2′-5′); 180.2 (C=O, e). SEC data: M_n = 14400; Đ = 1.4.

PEtOx$_{93}$-PEI$_{7}$-Mal:^{1}H NMR (D_2O): δ (ppm) = 0.8 – 1.3 (m, 3H, d); 2.0 – 2.55 (m, 2H, c); 2.55 – 3.2 (m, 4H, 1′ + b); 3.2 – 4.45 (m, a + 2′-6′). ^{13}C NMR (D_2O): δ (ppm) = 11.9 (*C*H_3, d); 28.6 and 28.9 (*C*H_2, c); 45.0 – 50.0 (*C*H_2, a); 52.0 – 57.0 (*C*H_2, b); 59.3 (*C*H_2, 1′); 65.7 (*C*H_2, 6′); 73.0 – 81.0 (*C*H, 2′-5′); 180.2 (C=O, e). SEC data: M_n = 14000 kg/mol; Đ = 1.3.

PEtOx$_{89}$-PEI$_{11}$-Mal: ^{1}H NMR (D_2O): δ (ppm) = 0.8 – 1.3 (m, 3H, d); 2.0 – 2.55 (m, 2H, c); 2.55 – 3.2 (m, 4H, 1′ + b); 3.2 – 4.45 (m, a + 2′-6′). ^{13}C NMR (D_2O): δ (ppm) = 11.9 (*C*H_3, d); 28.6 and 28.9 (*C*H_2, c); 45.0 – 50.0 (*C*H_2, a); 52.0 – 57.0 (*C*H_2, b); 59.3 (*C*H_2, 1′); 65.7 (*C*H_2, 6′); 73.0 – 81.0 (*C*H, 2′-5′); 180.2 (C=O, e). SEC data: M_n = 15600 kg/mol; Đ = 1.2.

PEtOx$_{88}$-PEI$_{12}$-Mal: ^{1}H NMR (D_2O): δ (ppm) = 0.8 – 1.3 (m, 3H, d); 2.0 – 2.55 (m, 2H, c); 2.55 – 3.2 (m, 4H, 1′ + b); 3.2 – 4.45 (m, a + 2′-6′). ^{13}C NMR (D_2O): δ (ppm) = 11.9 (*C*H_3, d); 28.6 and 28.9 (*C*H_2, c); 45.0 – 50.0 (*C*H_2, a); 52.0 – 57.0 (*C*H_2, b); 59.3 (*C*H_2, 1′); 65.7 (*C*H_2, 6′); 73.0 – 81.0 (*C*H, 2′-5′); 180.2 (C=O, e). SEC data: M_n = 14000 kg/mol; Đ = 1.4.

PEtOx$_{85}$-PEI$_{15}$-Mal: ^{1}H NMR (D_2O): δ (ppm) = 0.8 – 1.3 (m, 3H, d); 2.0 – 2.55 (m, 2H, c); 2.55 – 3.2 (m, 4H, 1′ + b); 3.2 – 4.45 (m, a + 2′-6′). ^{13}C NMR (D_2O): δ (ppm) = 11.9 (*C*H_3, d); 28.6 and 28.9 (*C*H_2, c); 45.0 – 50.0 (*C*H_2, a); 52.0 – 57.0 (*C*H_2, b); 59.3 (*C*H_2, 1′); 65.7 (*C*H_2, 6′); 73.0 – 81.0 (*C*H, 2′-5′); 180.2 (C=O, e). SEC data: M_n = 17900 kg/mol; Đ = 1.2.

PEtOx$_{73}$-PEI$_{27}$-Mal: ^{1}H NMR (D_2O): δ (ppm) = 0.8 – 1.3 (m, 3H, d); 2.25 – 2.55 (m, 2H, c); 2.55 – 3.0 (m, 4H, 1′ + b); 3.3 – 4.1 (m, 2-6 + 2′-6′); 4.9 – 5.45 (s, 1H, 1). ^{13}C NMR (D_2O): δ (ppm) = 11.98 (*C*H_3, d); 28.6

and 28.9 (*C*H_2, c); 45.0 – 50.0 (*C*H_2, a); 53.0 – 56.5 (*C*H_2, b); 59.8 (*C*H_2, 1′); 63.3 (*C*H_2, 6); 65.1 and 65.6 (*C*H_2, 6′); 71.8 (*C*H, 2′); 72.2 (*C*H, 4); 74.5 (*C*H, 2, 3′); 75.3 (*C*H, 5); 75.5 (*C*H, 5′); 75.8 (*C*H, 3); 83.3 (*C*H, 4′); 103.5 (*C*H, 1); 180.2 (C=O, e). SEC data: M_n = 15000 kg/mol; Đ = 1.4.

PEtOx$_{60}$-PEI$_{40}$-Mal: ^{1}H NMR (D_2O): δ (ppm) = 0.8 – 1.3 (m, 3H, d); 2.25 – 2.55 (m, 2H, c); 2.55 – 3.3 (m, 4H, 1′ + b); 3.3 – 4.5 (m, 2-6 + 2′-6′); 4.8 – 5.45 (s, 1H, 1). ^{13}C NMR (D_2O): δ (ppm) = 11.9 (*C*H_3, d); 28.6 and 28.9 (*C*H_2, c); 45.0 – 50.0 (*C*H_2, a); 51.0 – 56.0 (*C*H_2, b); 59.8 (*C*H_2, 1′); 63.2 (*C*H_2, 6); 65.1 and 65.6 (*C*H_2, 6′); 71.6 (*C*H, 2′); 72.2 (*C*H, 4); 74.4 (*C*H, 2, 3′); 75.3 and 75.8 (*C*H, 3, 5, 5′); 84.6 and 85.2 (*C*H, 4′); 103.4 (*C*H, 1); 180.2 (C=O, e). SEC data: M_n = 18700 kg/mol; Đ = 1.3.

General procedure for the DLS measurements with ConA

The concentration of the sugar-grafted PEtOx$_{(100-x)}$PEI$_x$ copolymers was kept constant at 0.4 mmol/L in phosphate buffered saline (PBS). The polymer was weighed (PEtOx$_{85}$-PEI$_{15}$-Mal 2.5 mg/mL; PEtOx$_{88}$-PEI$_{12}$-Mal 3.5 mg/mL; PEtOx$_{73}$-PEI$_{27}$ -Mal 2.9 mg/mLPEtOx$_{60}$-PEI$_{40}$ -Mal 2.5/mL mgPEtOx$_{60}$-PEI$_{40}$-Glc 2.5 mg/mL) and dissolved in PBS buffer solution. The concentration of the ConA solution was 5 mg/mL (0.4 mM) in PBS buffer. The ConA was added drop-wise to the polymer solution, and the resulting mixture was immediately measured in the DLS at 37°C.

6.3 Results and discussion

6.3.1 Synthesis of polymers

Previously, carbohydrates have been attached to hyperbranched PEI and aminopropyl methacrylamide by reductive amination.[24,26,27,51,52] In this work, we evaluated whether carbohydrates can be coupled to the secondary amines of linear PEI units contained with defined statistical PEtOx-PEI copolymers with varying amounts of PEI. The starting PEtOx can be readily prepared *via* microwave-assisted CROP with narrow Đ values and high purity. This seems a good starting product for further applications because the PEtOx polymer is easily obtained in high purity based on the readily available EtOx monomer, making it significantly cheaper than other functional PAOx that have been used to prepare glyco-PAOx while avoiding the sometimes difficult process of monomer synthesis. Several publications show that PEtOx has an excellent biocompatibility, and PEtOx is claimed to be a good alternative for PEG, the gold standard in this field.[19,21,46,47,53] The partial acidic hydrolysis of PEtOx is straightforward, and the degree of hydrolysis can be kinetically controlled by adjusting the temperature and time or by stoichiometric control over the variation of the amount of acid.[46–48] Scheme 1 shows that there is a statistical distribution of PEI along the backbone, whereby it should be noted that the exact monomer distribution for such partially hydrolysed polymers is more block-like as shown in chapter 2. In this work, the hydrolysis was performed at 73°C or 100°C, which were selected based on a previous work and depending on the amount of PEI required. When a higher percentage of PEI was required, the reactions were performed at a higher temperature to increase the reaction speed, whereas a lower degree of hydrolysis was performed at a lower temperature to have more accurate control over the final degree of hydrolysis. The $PEtOx_{(100-x)}$-PEI_x copolymers (Table 1) were prepared with 4 mol% until 40 mol% of PEI units. The resulting copolymers were analyzed by ^1H and ^{13}C NMR spectroscopy in D_2O. Figures 6-1, 6-2 and 6-3 show the respective ^1H-NMR spectra of $PEtOx_{60}$-PEI_{40}, $PEtOx_{60}$-PEI_{40} modified with glucose and modified with maltose. The ^{13}C NMR spectra of all $PEtOx_{60}$-PEI_{40}, are presented in the Figures 6-5,6-6 and 6-7. The ^1H and ^{13}C NMR spectra of $PEtOx_{73}$-PEI_{27} are shown in Figures 6-4 and 6-5. The PEI units appear at 2.5-3 ppm in the ^1H-NMR spectrum (CH_2-groups assigned as b) and at 45 and 52 ppm in the ^{13}C-NMR spectrum (CH_2-groups assigned as b), whereas the residual CH_2-

groups of PEtOx appear at 3.2-3.7 ppm in the ^{1}H-NMR spectrum and at 45 and 52 ppm in the ^{13}C-NMR spectrum (assigned with "a" in Figure 6-4). The degree of hydrolysis in the PEtOx-PEI copolymers was calculated based on the integrals of the CH_2 groups of (a) PEtOx and the CH_2-groups of (b) PEI units.[46]

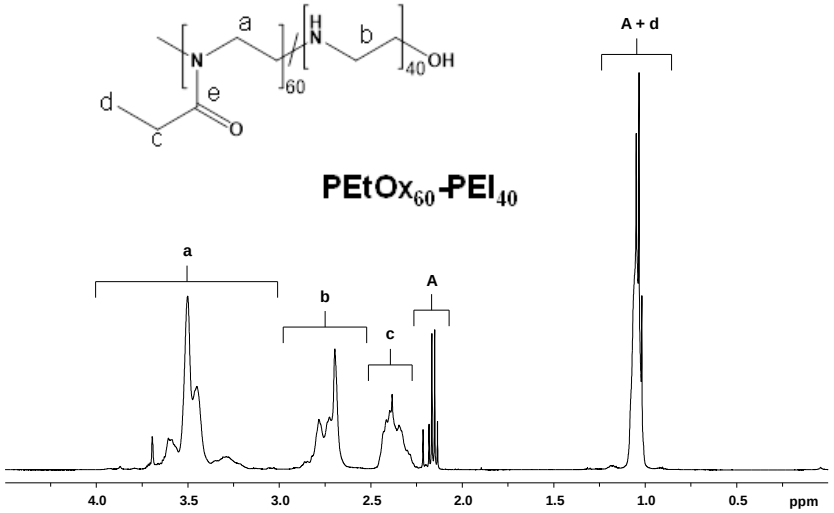

Figure 6-1: ^{1}H-NMR spectrum of the $PEtOx_{60}$-PEI_{40} copolymer (D_2O). The signal (A) corresponds to propionic acid.

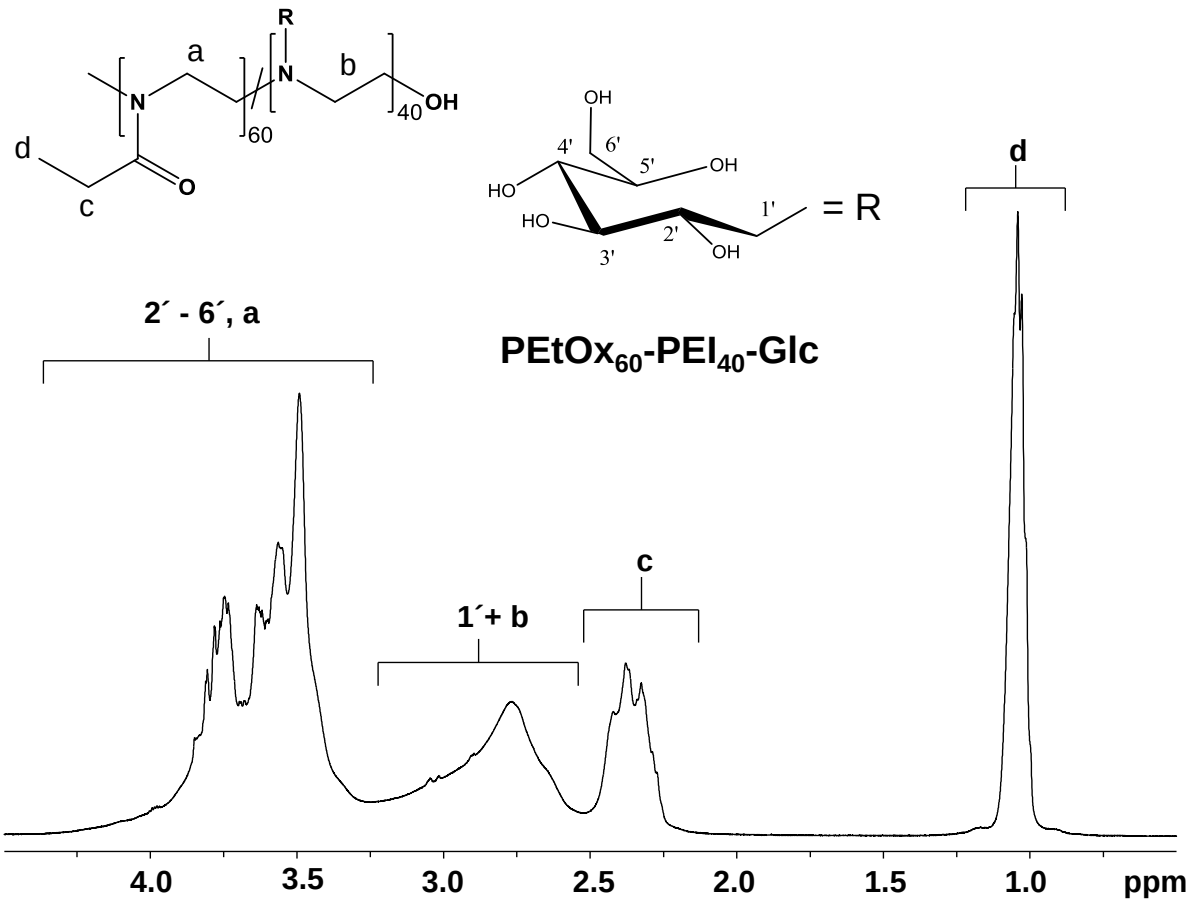

Figure 6-2: ^{1}H NMR spectrum of $PEtOx_{60}$-PEI_{40}-Glc (x = 40) obtained from reductive amination of $PEtOx_{60}$-PEI_{40} in the presence of excess glucose (Glc). (D_2O)

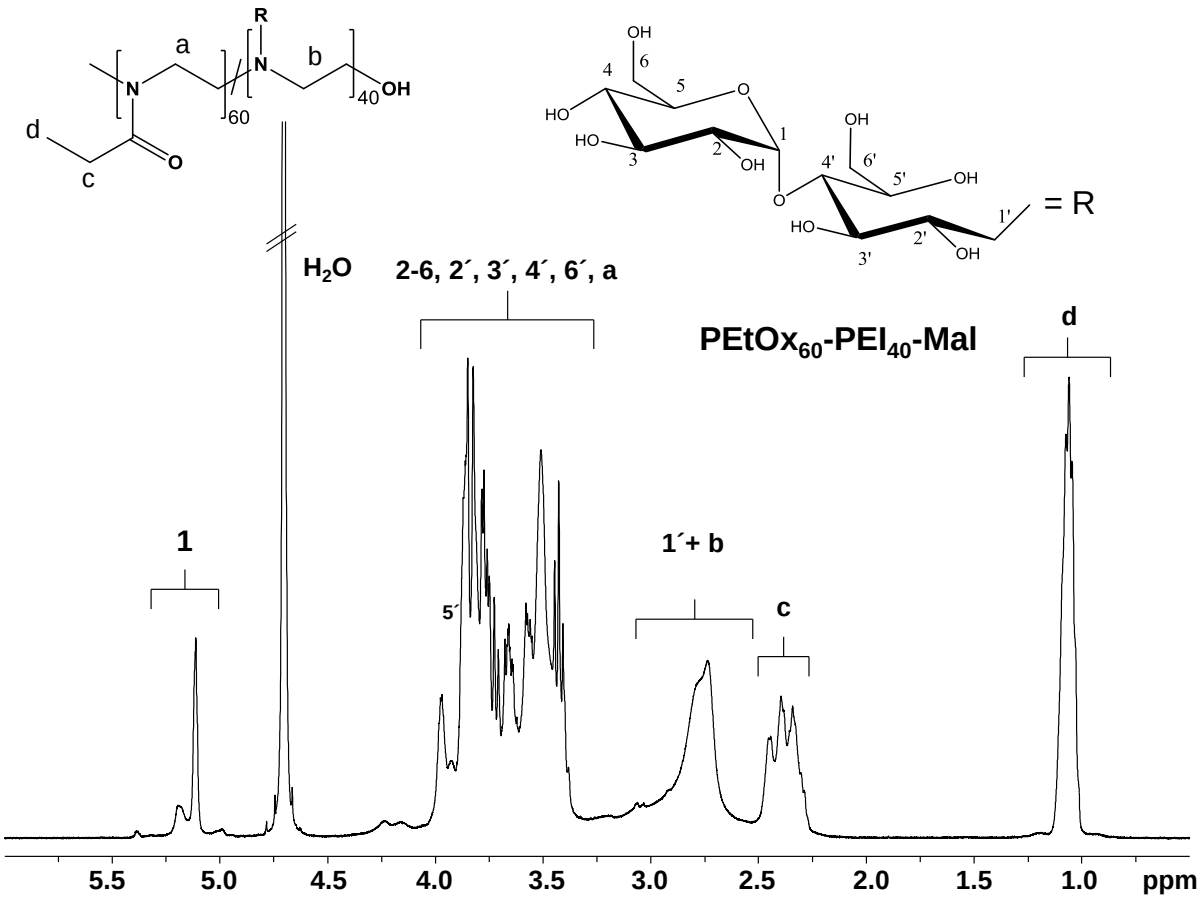

Figure 6-3: ^{1}H NMR spectrum of $PEtOx_{60}$-PEI_{40}-Mal (x = 40) obtained from reductive amination of $PEtOx_{60}$-PEI_{40} in the presence of excess maltose (Mal). (D_2O).

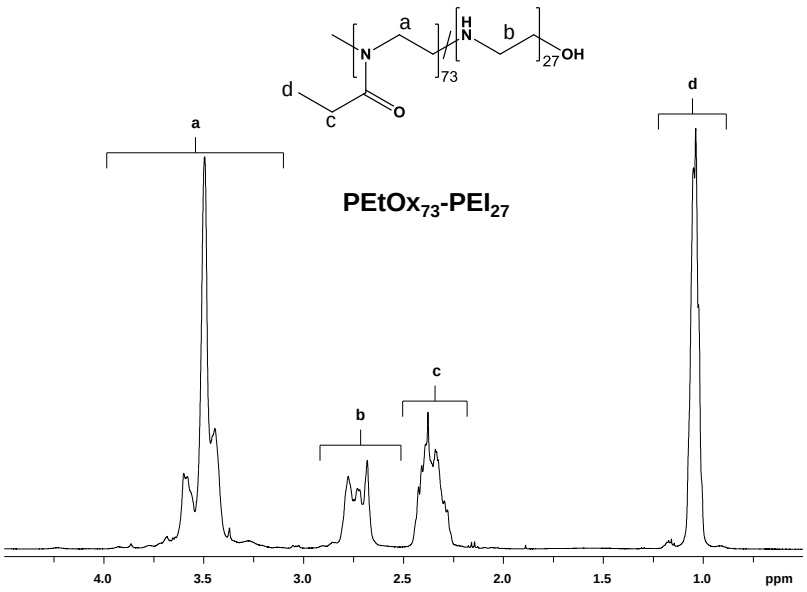

Figure 6-4: ^{1}H NMR spectrum of PEtOx-PEI27 (x = 27) obtained from 27% hydrolysis of PEtOx with 100 repeating units. (D_2O)

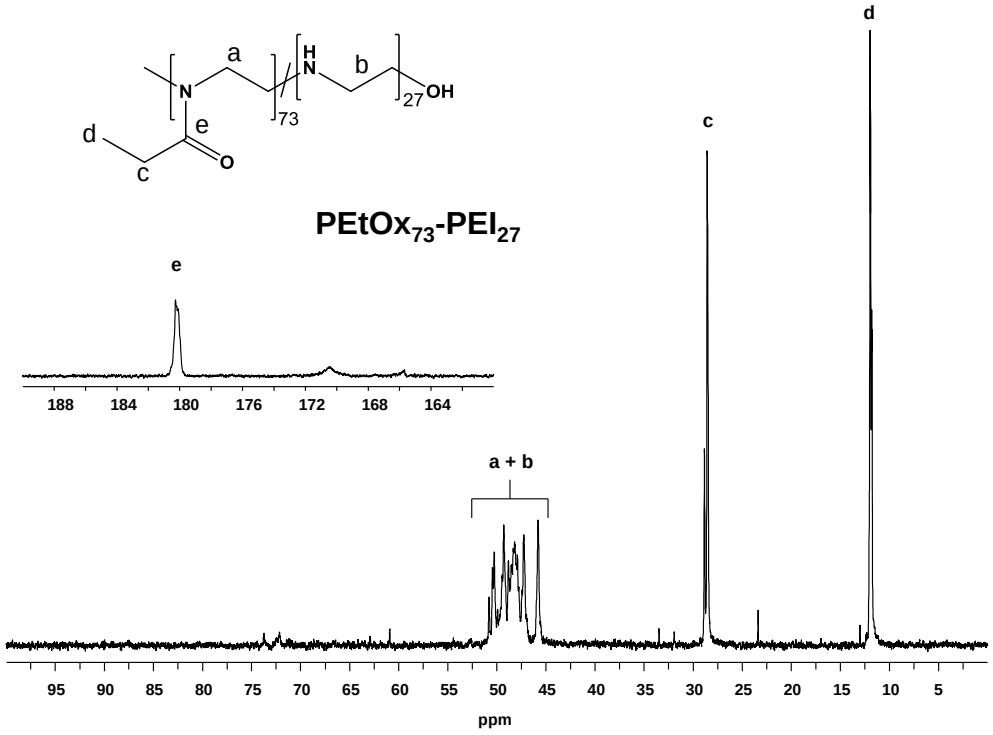

Figure 6-5: ^{13}C NMR spectrum of PEtOx-PEI27 (x = 27) obtained from 27% hydrolysis of PEtOx with 100 repeating units. (D_2O)

After purification, the formed propionic acid could be removed by evaporation and precipitation from all hydrolysed $PEtOx_{(100-x)}$-PEI_x copolymers, except $PEtOx_{60}$-PEI_{40}, which still contained some propionic acid (shown as signal assignment "A" in the NMR spectra of $PEtOx_{60}$-PEI_{40} in Figure 6-1), and $PEtOx_{73}$-PEI_{27} (Figure 6-4) which still contained a very small amount of propionic acid after purification. The larger

retention of propionic acid in the $PEtOx_{(100-x)}$-PEI_x, which contained a larger PEI content, can be ascribed to stronger hydrogen bonding interactions that increased the difficulty of evaporating the propionic acid. Although the remaining propionic acid could be removed by dialysis, using a higher vacuum for evaporation, or preparative SEC, the obtained copolymers were directly used for the reductive aminations because the presence of the propionic acid was not expected to interfere with the reductive amination process.

The reductive amination of PEtOx-PEI was first investigated with the monosaccharide glucose (Table 1: $PEtOx_{88}$-PEI_{12}, $PEtOx_{73}$-PEI_{27} and $PEtOx_{60}$-PEI_{40}, SI) to evaluate whether all of the secondary amine units in the PEtOx-PEI derivatives could be modified. The PEtOx-PEI derivatives were reacted with a large excess of glucose in the presence of a borane-pyridine complex to reduce the formed imine linkage to a stable tertiary amine *in situ* (Scheme 1). The most abundant structure of glucose in aqueous solution is the cyclic hemiacetal form; only a minor portion of aqueous glucose is present as the linear aldehyde structure, which is required for the reductive amination. Due to this equilibrium or the low accessibility of the secondary amine, a large excess of carbohydrate was used and longer reaction times were needed. The secondary amine functionality of the PEI attacked the aldehyde of the ring-opened glucose, which yielded the desired glucose-containing PEtOx-PEI derivatives after reduction (Scheme 1).[26] The glucose-containing copolymers were analyzed by NMR spectroscopy (Figure 6-2 and Figures 6-6 and 6-7) and HFIP-SEC (Figure 6-8 and 6-18). The ^{1}H NMR spectrum of $PEtOx_{60}$-PEI_{40}-Glc revealed broadening of the linear EI units (CH_2-groups assigned as "b" in Figure 6-2), indicating the successful coupling of glucose units to the secondary amine units of $PEtOx_{60}$-PEI_{40} leading to tertiary amine groups. Successful coupling was further supported by the analysis of the ^{13}C NMR spectrum of $PEtOx_{60}$-PEI_{40}-Glc (Figure 6-6), in which the presence of the CH_2 next to the tertiary amine units was found at 52-56 ppm showing the conversion of the imine group. Moreover, the successful coupling of Glc units to PEI units in $PEtOx_{60}$-PEI_{40} was supported by the conversion of the quaternary carbon of the aldehyde group in Glc into a CH_2-group at 59.2 ppm in the ^{13}C-NMR spectrum (assigned as 1′). These new CH2-groups (1′) demonstrate the presence of the tertiary amino groups by addition of the saccharide unit to the secondary amine group. These structural patterns are in agreement with those reported for other PEI glycoarchitectures.[26] Moreover, $PEtOx_{60}$-PEI_{40}-Glc did not contain any low molar mass impurities, including propionic acid, which was still present in $PEtOx_{60}$-PEI_{40} after purification by dialysis.

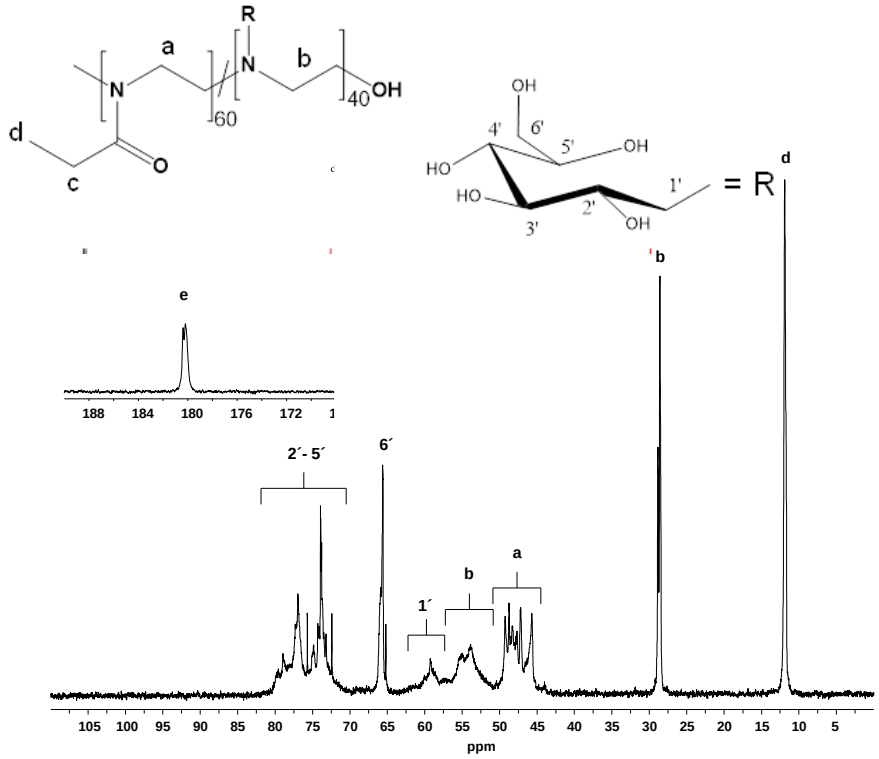

Figure 6-2: ^{13}C NMR spectrum of PEtOx-PEI40-Glc (x = 40) obtained from reductive amination of PEtOx-PEI40 in the presence of excess glucose (Glc). (D_2O)

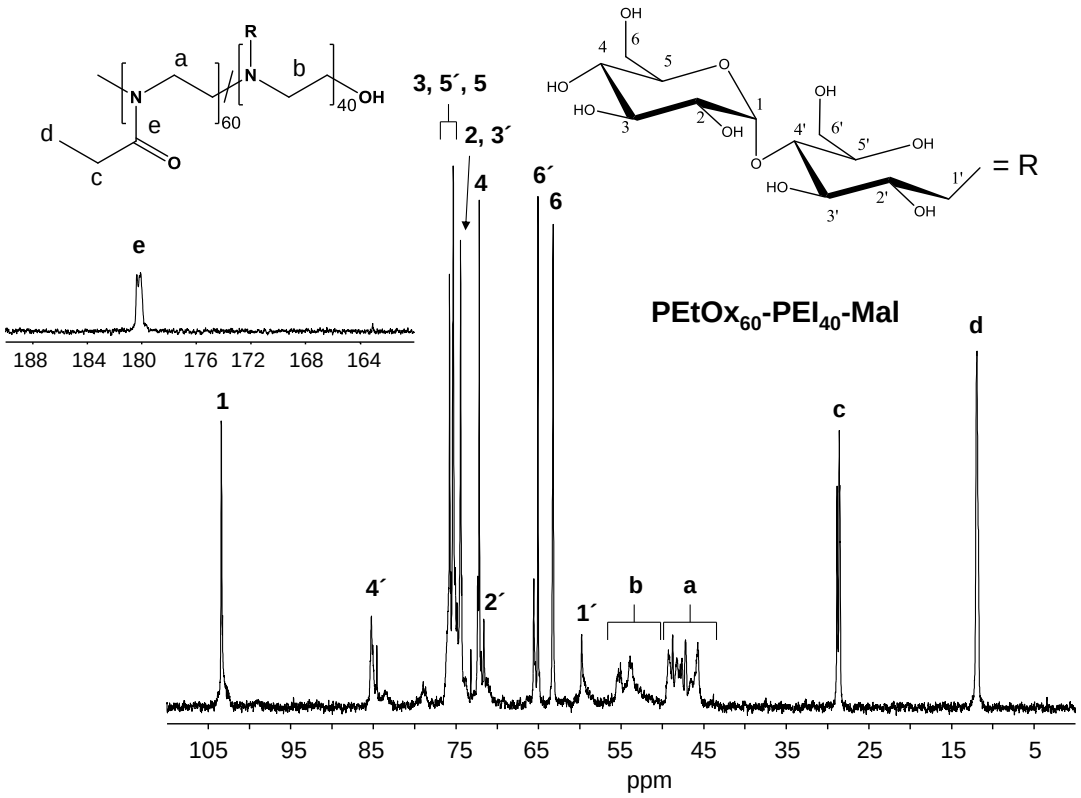

Figure 6-7: ^{13}C NMR spectrum of PEtOx-PEI40-Mal (x = 40) obtained from reductive amination of PEtOx-PEI40 in the presence of excess maltose (Mal). (D_2O)

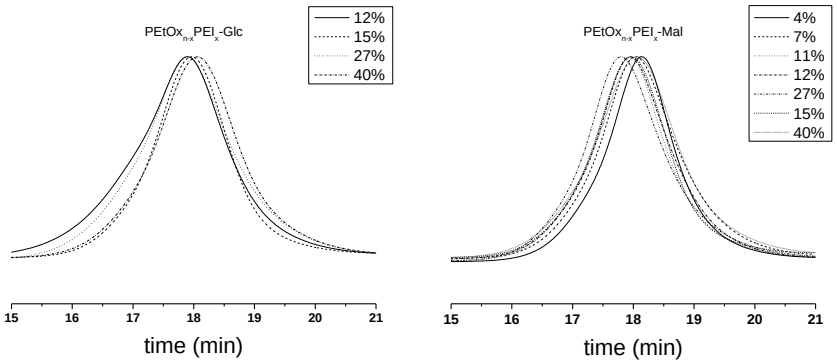

Figure 6-8: SEC traces of $PEtOx_{(100-x)}$-PEI_x-Glc (left) and $PEtOx_{(100-x)}$-PEI_x-Mal (right) measured using HFIP as the eluent.

The degree of functionalization accompanied by the conversion of secondary into tertiary amines was calculated *via* quantitative ^{13}C NMR spectroscopy as shown in Figure 6-9. This was done for both $PEtOx_{60}$-PEI_{40}-Glc and $PEtOx_{73}$-PEI_{27}-Glc. The integrals of the C atom C6′ of glucose and the methyl group of residual EtOx units were used. The signal of the methyl PEtOx was calibrated to 60 and the value of 6' was 34 giving the exact amount of coupled sugars. The degree of glucose functionality was: 34 EI units (85%) with glucose for $PEtOx_{60}$-PEI_{40}-Glc, and 23 EI units (85%) for $PEtOx_{73}$-PEI_{27}-Glc. Size exclusion chromatograms of glycosylated PEtOx-PEI derivatives were obtained using HFIP as the eluent (Figure 6-8 and 6-17) and showed that the desired glycopolymers had a narrow molar mass distribution with $Đ \leq 1.4$. The increase in Đ may be caused by column interactions resulting from the addition of the highly polar carbohydrates as seen with other PEtOx copolymers before.[47] This value indicated that neither chain coupling nor degradation occurred. Moreover, the low dispersity of the obtained glycopolymers may be beneficial for further biomedical applications.

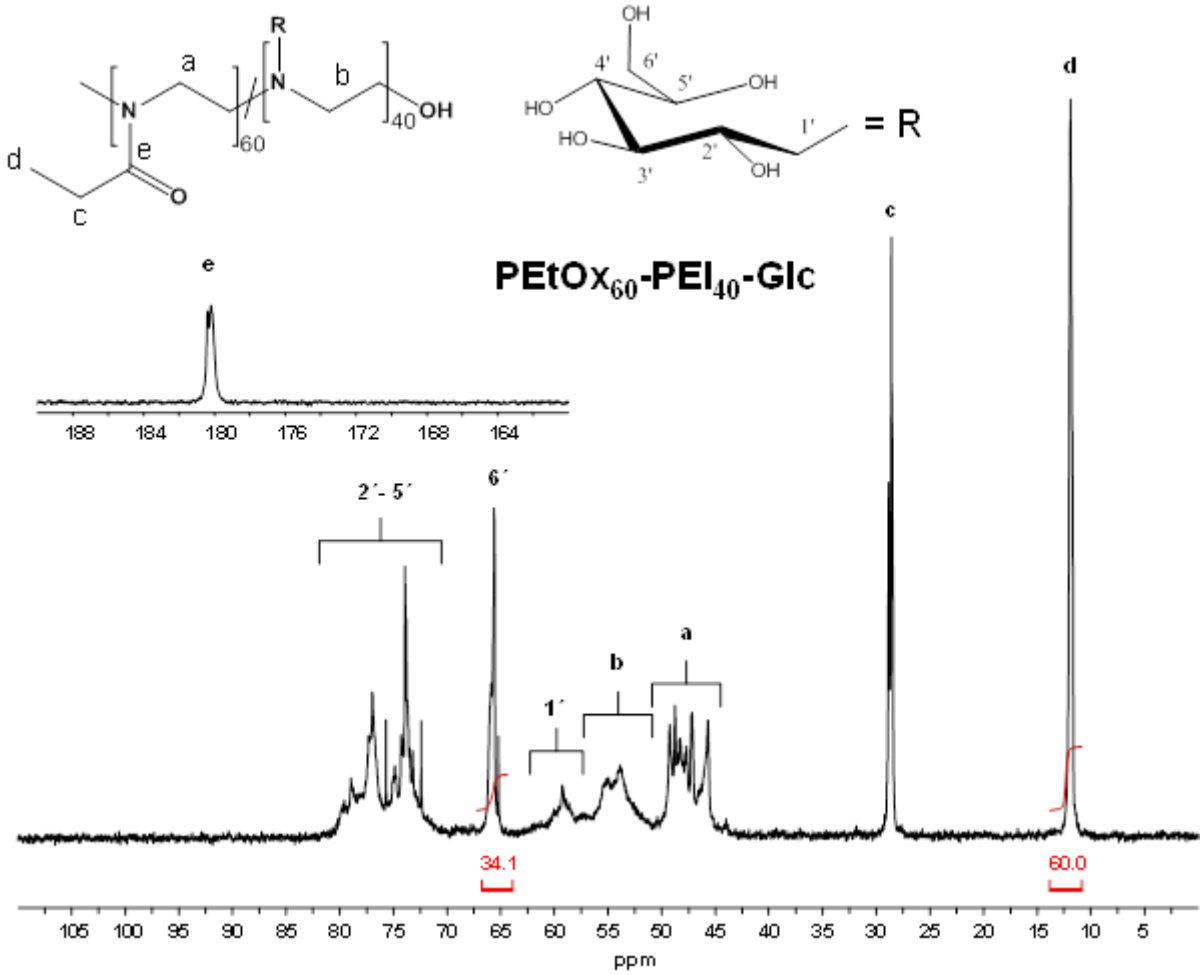

Figure 6-9: Determination of attached glucose in PEtOx60-PEI40-Glc is given by the direct read out of the integral number of 13C signal C6′, when 13C signal of d is calibrated with 60 (1C of EtOx x 60 repeating units in PEtOx60-PEI40-Glc).

Even though glucose grafted glycopolymers were successfully obtained, they contained the ring-opened glucose in the side chain, which is not efficiently recognized by carbohydrate binding proteins such as lectins. This implies that this sugar modification strategy will not have further useful applications in a biological context except to enhance the biocompatibility of those polymers. In preparing biologically active glycopolymers based on the reductive amination of $PEtOx_{(100-x)}$-PEI_x,(Scheme 1) we, therefore, focused our attention on the introduction of a disaccharide, namely maltose. The first saccharide unit of maltose was used in its linear aldehyde form as a linker in the coupling *via* the reductive amination reaction. The second saccharide unit, however, remained intact as a cyclic structure, enabling the biological recognition of the obtained glycopolymers. For this purpose, maltose was coupled to various $PEtOx_{(100-x)}$-PEI_x derivatives (Table 1) under reductive amination conditions in the presence of excess maltose (Scheme 6-1). The resulting maltose-containing copolymers $PEtOx_{96}$-PEI_4-Mal, $PEtOx_{93}$-PEI_7-Mal, $PEtOx_{89}$-PEI_{11}-Mal, $PEtOx_{88}$-PEI_{12}-Mal, $PEtOx_{85}$-PEI_{15}-Mal, $PEtOx_{73}$-PEI_{27}-Mal and $PEtOx_{60}$-PEI_{40}-Mal were analyzed by NMR spectroscopy and SEC. Figure 6-10 depicts the ^{1}H NMR and Figure 6-7 the ^{13}C NMR spectra of $PEtOx_{60}$-PEI_{40}-Mal as representative examples. Similar structural characteristics (e.g., the appearance of the PEI unit and the conversion of the aldehyde group into a CH_2-group) were identified in $PEtOx_{60}$-PEI_{40}-Mal and $PEtOx_{60}$-PEI_{40}-Glc. A comparison with a previously reported maltosylated hyperbranched PEI obtained by reductive amination[54] further confirmed the successful quantitative coupling of maltose to the PEtOx-PEI derivatives. Moreover, the chemical structure of PEtOx in $PEtOx_{60}$-PEI_{40}-Mal remained intact after the successful integration of maltose into the PEtOx-PEI derivatives (Figure 6-3). SEC traces of the polymers showed narrow dispersity, which proved that the coupling but no degradation of the polymer chains occurred (Figure 6-8). However, the higher Đ is probably caused by the column interaction.

Additionally, the functionalization was calculated *via* 1H NMR spectroscopy using the integrals for PEtOx60-PEI40-Mal as shown in Figure 6-10. The integrals of the signal of the anomeric proton of the residual glucose ring in maltose, (1), was used as well as the integrals of the signal of the methyl group of residual PEtOx (d). The latter was calibrated and, thus, allows calculation of the converted EI units to be 37.5 (94%) for PEtOx60-PEI40-Mal, and 24 EI units (88%) PEtOx73-PEI27-Mal. When using the quantitative 13C NMR spectra to calculate the conversion, the signal of the C atom of the C6´and the C6 of maltose in the corresponding PEtOx60-PEI40-Mal and PEtOx73-PEI27-Mal were used as well as the signal of the methyl group of residual EtOx units. The degree of functionalization using this method is determined to be 99% for PEtOx60-PEI40-Mal and of 96% for EI for PEtOx73-PEI27-Mal.

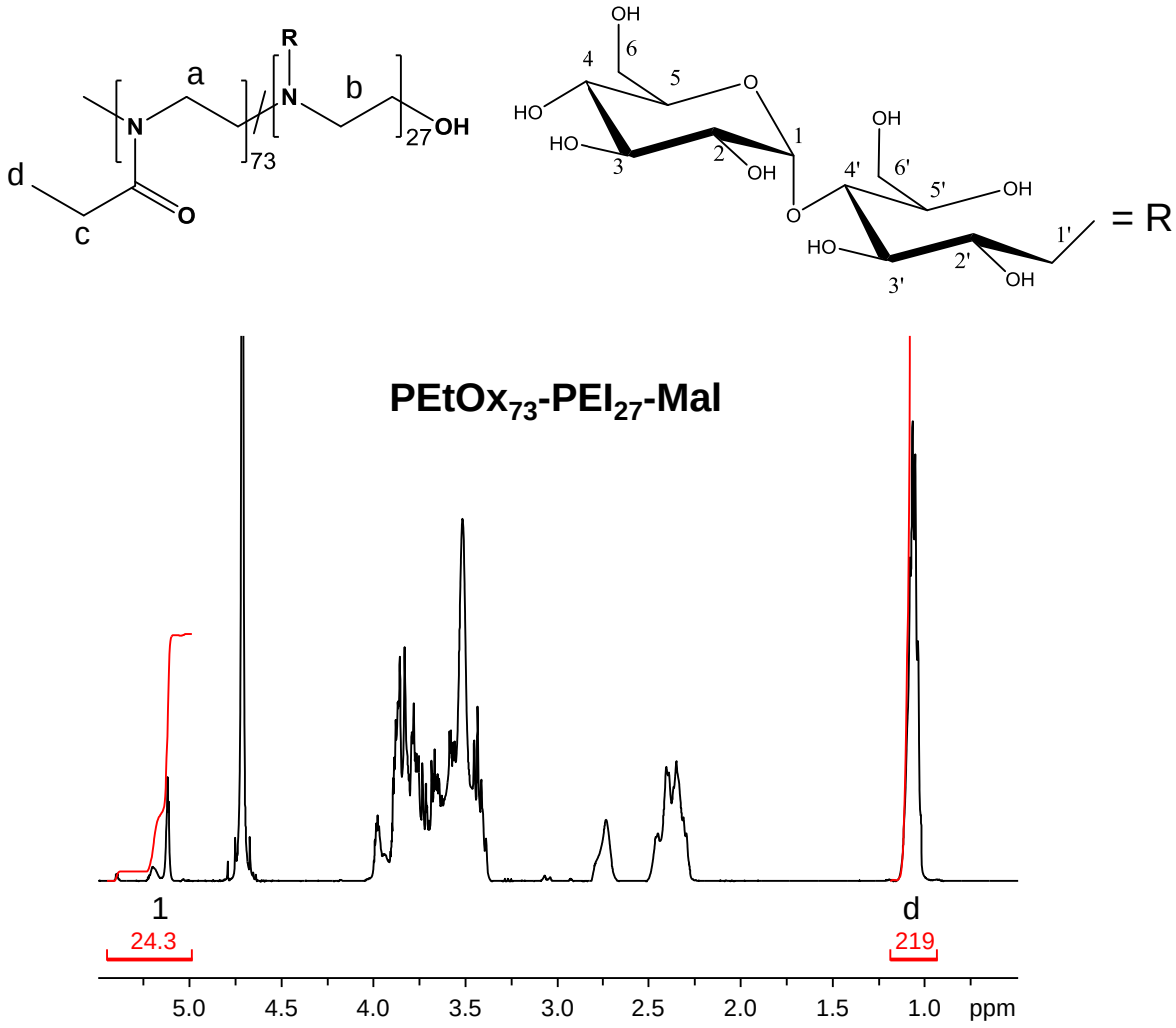

Figure 6-10: Determination of attached maltose in $PEtOx_{73}$-PEI_{27}-Mal is given by the direct read out of integral number for ^1H signal 1, when ^1H signal d is calibrated with 219 (3H x 73 repeating units in $PEtOx_{73}$-PEI_{27}-Mal).

6.3.2 Solution behavior

The solution behavior of the synthesized glycopolymers was thoroughly investigated by DLS to investigate whether the polymers were soluble as unimers, were thermo-responsive, or whether they formed aggregates. This is of great importance in a biomedical context, in which macroscopic aggregation must be avoided. Before the temperature-dependent DLS was measured, the stability of the glycopolymers in solution was assessed by measuring a sample that was equilibrated for a few hours before and after filtration. As shown in Figure 6-5 the equilibrated $PEtOx_{60}$-PEI_{40}-Glc revealed the presence of large aggregates; these aggregates were no longer observed after filtration. The syringes have a 0.22 µm threshold, so either the aggregates remained on the filter, or they were destroyed by shear forces when the sample was pushed over the filter due to their loosely bound state and, thus, their ease of dissociation.

Therefore, the derived count rate before and after filtration was compared, which revealed a minor decrease from 127.33 kcps before filtration to 94.66 kcps after filtration. Although some polymer appears to remain on the filter, the major fraction of aggregates was transformed back into unimers, indicating that mostly loose aggregates were formed, which could be easily disaggregated by filtration.

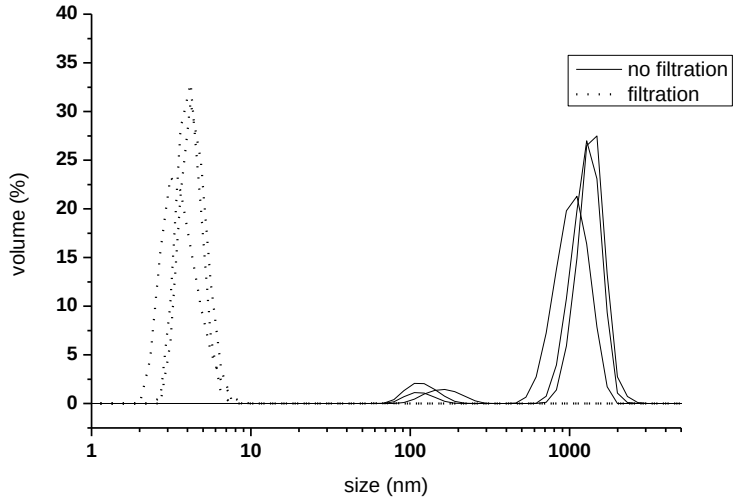

Figure 6-11: Effect of the filtration on DLS measurements of $PEtOx_{60}$-PEI_{40}-Glc. The dotted lines indicate the filtered polymer solution; the solid line indicates the unfiltered solution.

Because the parent PEtOx showed a lower critical solution temperature (LCST) occurring approximately 60 °C,[55,56] the temperature-dependent solubility behaviors of the glycopolymers were subsequently investigated. The temperature-dependent DLS was measured in water between 10 °C and 70 °C (Figure 6-12) and clearly indicated the difference between the glucose and maltose grafted glycopolymers. All of the PEtOx-PEI-Glc polymers (Figure 6-12, left) show macroscopic aggregation at all temperatures; though the DLS of PEtOx73-PEI27-Glc did not show large aggregates, a macroscopic precipitate was formed on the bottom of the cuvette. The strong agglomeration of these glucose modified polymers was ascribed to the strong intermolecular hydrogen bonding between the PEtOx amide groups and the hydroxyl groups of the linear grafted glucose units, as well as between the glucose units.

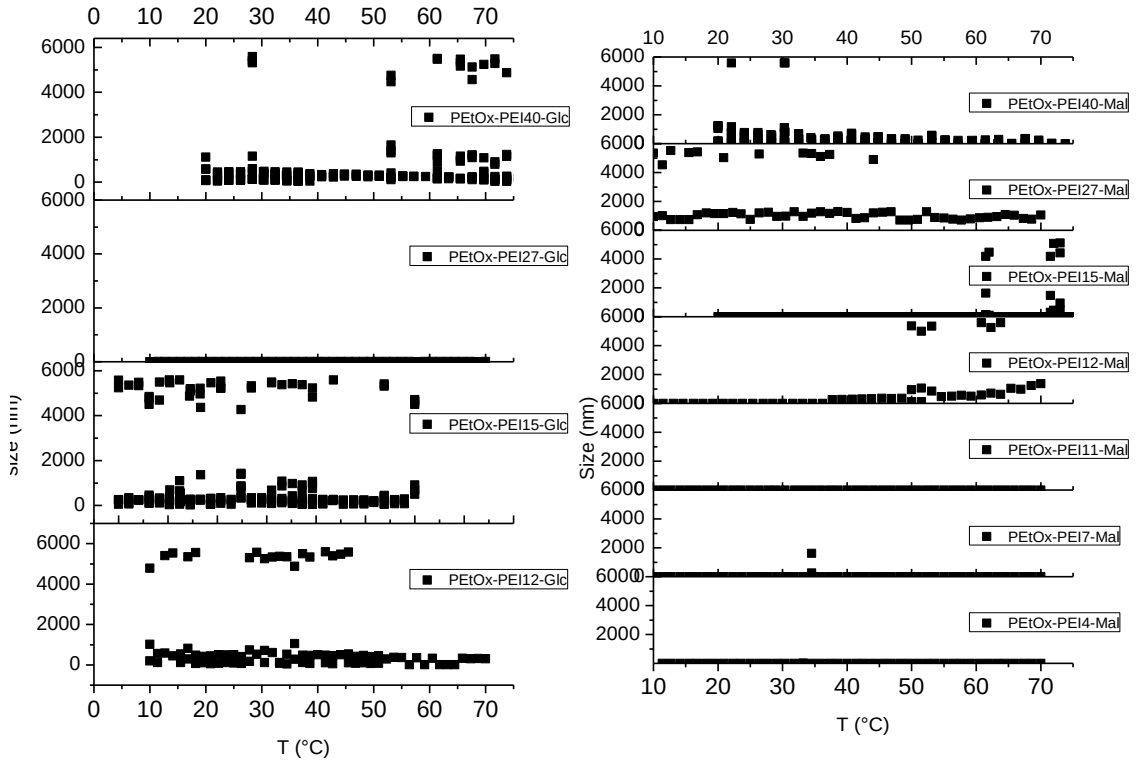

Figure 6-12: Temperature-dependent hydrodynamic diameter of $PEtOx_{(100-x)}$-PEI_x-Glc (left) and $PEtOx_{(100-x)}$-PEI_x-Mal (right) as obtained by DLS (z-average size from cumulant analysis). (pH ~8)

In contrast, the PEtOx-PEI-Mal glycopolymers (left Figure 6-12) containing low amounts of maltose (less than 12%) did not show aggregation, and only unimers were detected by DLS at all temperatures. It may be speculated that the larger size of the saccharide side chain, in combination with the cyclic saccharide unit, suppresses the hydrogen bonding interactions with the amide groups in the polymer backbone. The maltose glycopolymers with 12 and 15% showed LCST behaviors with cloud point temperatures of 37 °C and 60 °C, respectively. These behaviors were probably caused by an increase in the hydrogen bonding interactions between the sugar units and the polymer backbone, which competes for hydration and lowers the solubility of the polymers. Even higher percentages of maltose induced macroscopic aggregation and thus behaved similarly to the glucose-functionalized glycopolymers, supporting the proposed decrease in polymer solubility resulting from enhanced competition for efficient hydration by interpolymer hydrogen bonding.

In addition to temperature dependence, the pH-responsive solution behavior of the glycopolymers was also investigated based on the (de)protonation of the tertiary amine groups of the glyco-PAOx prepared by reductive amination.

13 shows the DLS measurements for the 40% grafted copolymers containing either glucose or maltose. These polymers were expected to reveal the largest pH-responsiveness, as they contained the largest amount of tertiary amine groups. The initial polymer solutions had a pH of ~8 in PBS buffer. The pH was raised to 12 by the addition of NaOH and lowered to pH 2 by the addition of HCl to ensure full deprotonation and protonation of the tertiary amine groups, respectively. Also the pH was lowered to pH 6.22 to see the solubility effect. Unexpectedly, neither glycopolymer showed a large change in solution behavior as a function of pH despite the (de)protonation state of the tertiary amine groups indicating that the amine groups are shielded by the sugar side chains and have little influence on the polymer solubility as was also found for the partially hydrolysed poly(22-n-propyl-2-oxazoline)s in chapter 3.

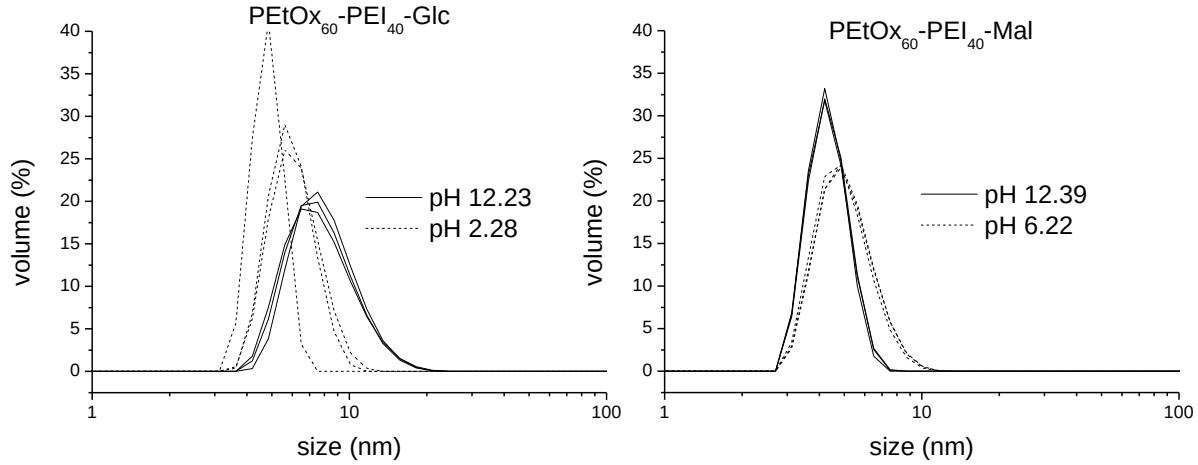

Figure 6-13: pH dependence of $PEtOx_{60}$-PEI_{40}-Mal (left) and $PEtOx_{60}$-PEI_{40}-Glc (right) measured by DLS at 25°C (solutions in PBS).

The biomedical relevance of the synthesized glycopolymers was investigated by studying their interaction with the glucose binding protein Concanavalin A (ConA). This lectin specifically binds to glucose or maltose[12]. First, the binding of $PEtOx_{60}$-PEI_{40}-Glc to ConA was investigated at 37°C; no aggregation was observed upon the addition of ConA to the glycopolymer (Figure 6-14 and 6-15). The absence of interactions between this polymer and ConA was anticipated because the polymer was functionalized with the linear form of glucose, which is not recognized by this lectin. Subsequently, the interaction between $PEtOx_{60}$-PEI_{40}–Mal and ConA was studied, as this glycopolymer was functionalized with maltose; in this glycopolymer, the first glucose unit (in the linear form) was used for conjugation and the second glucose unit, which remained intact in its cyclic form, was predicted to be able to bind ConA.

Figure 6-11 shows the DLS volume plots of the $PEtOx_{60}$-PEI_{40}–Mal unimers after filtration (bottom). Upon the addition of ConA, the solution immediately became turbid, and the DLS measurements shows in Figure 6-16 middle and Figure 6-19) revealed the presence of large aggregates of approximately 1000 nm as well as some smaller aggregates with a hydrodynamic size of 200 nm. This clear agglutination of ConA with $PEtOx_{60}$-PEI_{40}-Mal confirmed that the second glucose unit after the conjugation of maltose to $PEtOx_{60}$-PEI_{40} was still biologically active and was thus prone to interact with ConA. To further prove that the interaction between the glycopolymer and ConA was based on specific saccharide binding, an excess of glucose was added to the agglutinated solution, resulting in the destruction of the aggregates due to the interactions between the large excess of soluble glucose with ConA, which freed the polymer as unimers (Figure 6-16, top). The 15 % grafted maltose showed that this contained not enough glucose units to interact with the Con A (Figure 6-20).

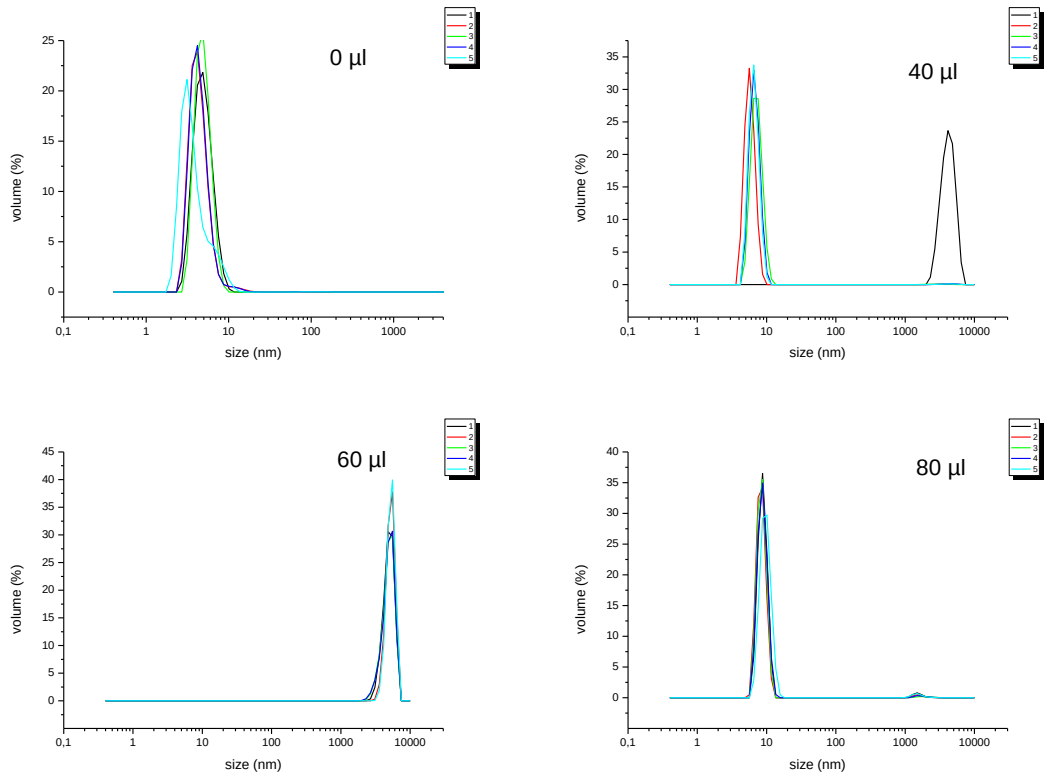

Figure 6-14: DLS volume plot of the 27% glucose grafted polymer with different amounts of the Concavalin A.

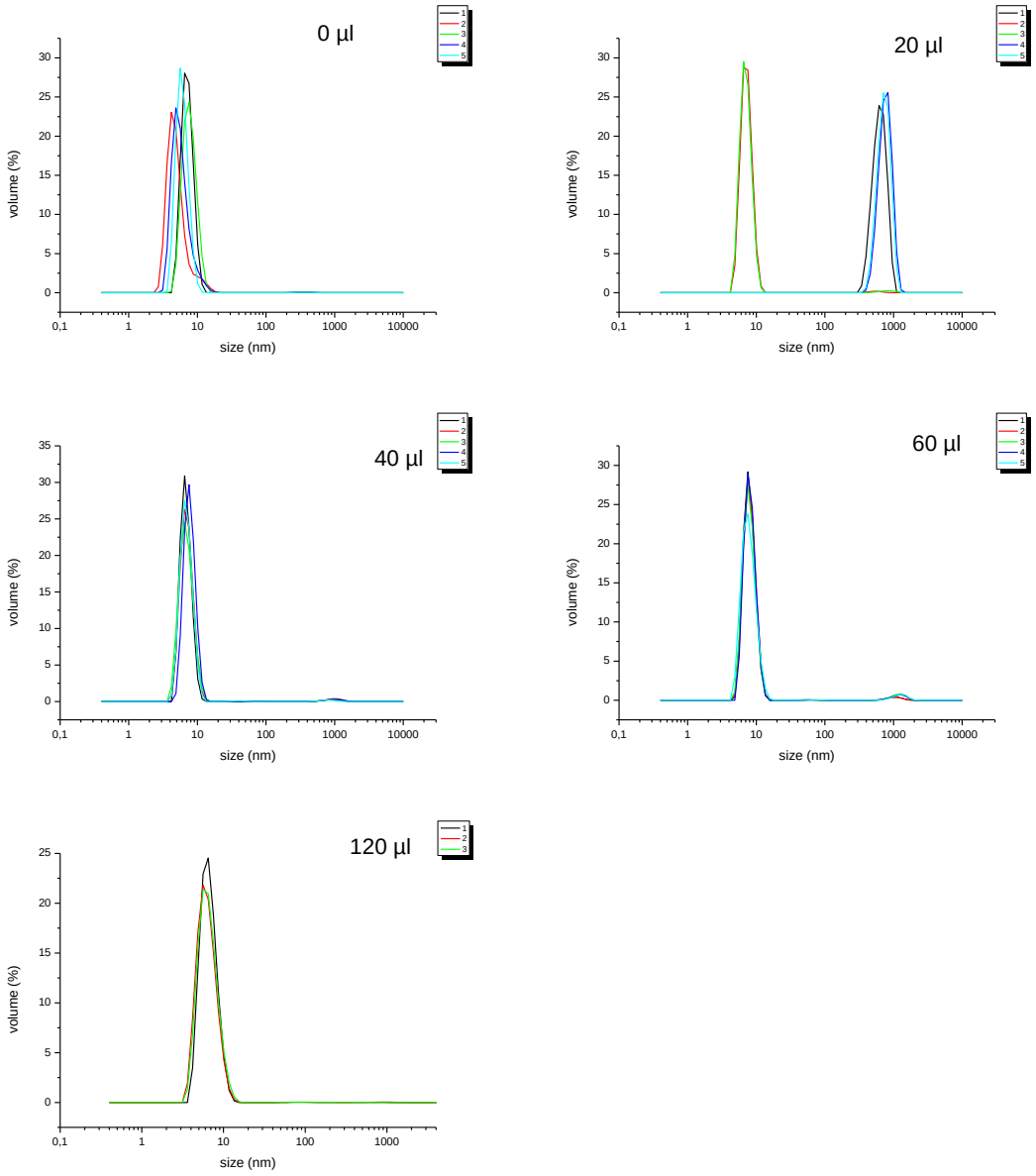

Figure 6-15: DLS volume plot of the 12% glucose grafted polymer with different amounts of the Concavalin A.

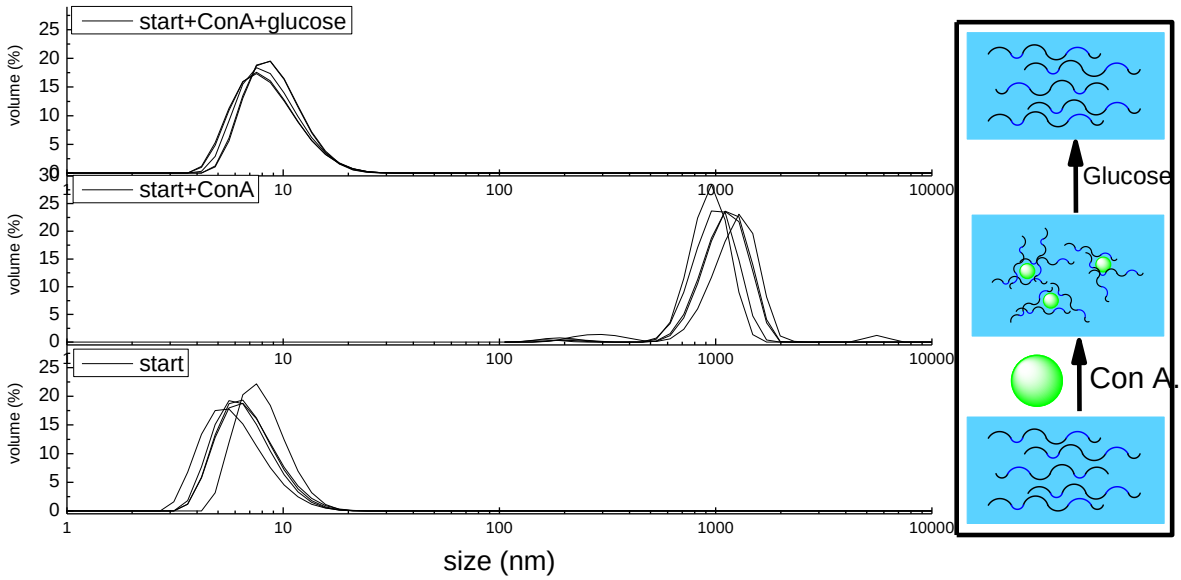

Figure 6-16: DLS volume plots of $PEtOx_{60}$-PEI_{40}–Mal (10 mg/mL in PBS buffer at 37 °C) measured after filtration (bottom), after the addition of 40 µL of Concanavalin A solution (middle), and after the further addition of an excess of glucose (top).

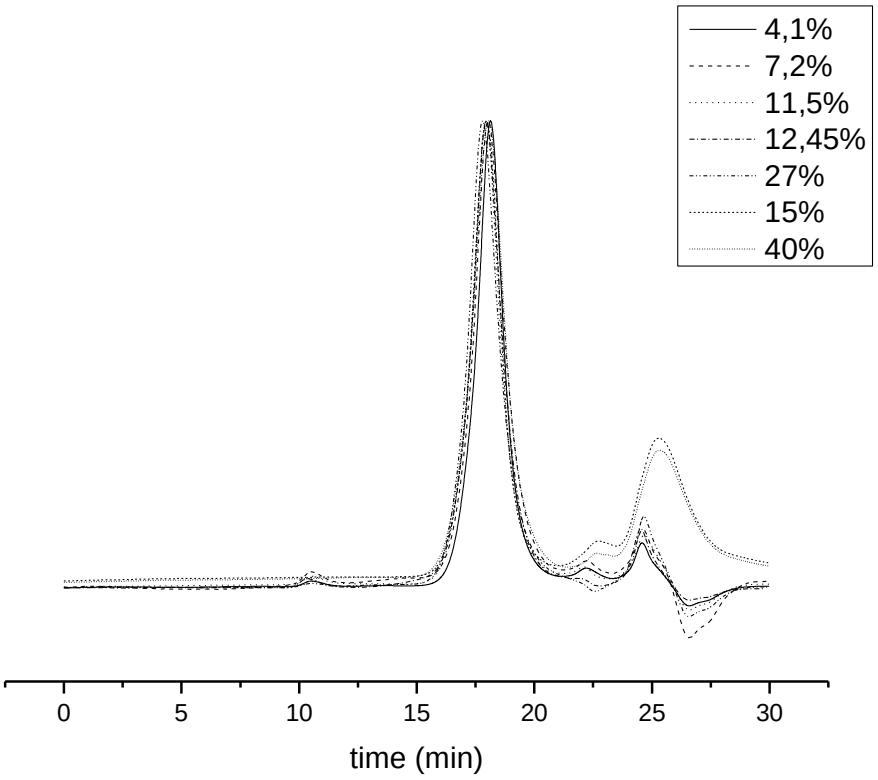

Figure 6-17: HFIP-SEC of PEtOx-PEI-Mal (x) obtained from reductive amination of PEtOx-PEI in the presence of excess maltose (Mal).

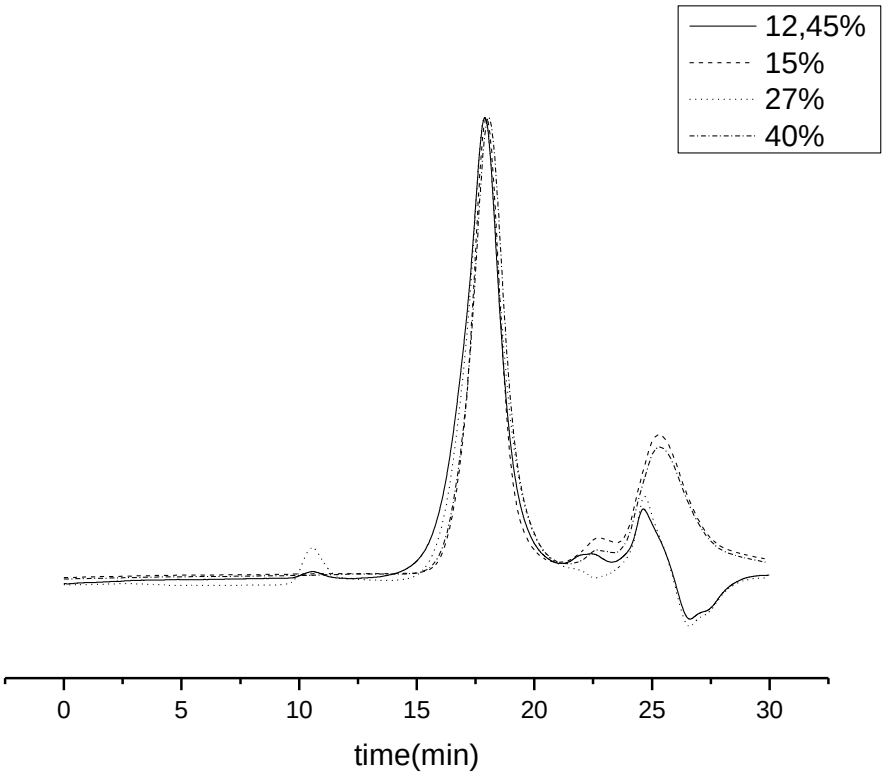

Figure 6-18: HFIP-SEC of PEtOx-PEI-GlC (x) obtained from reductive amination of PEtOx-PEI in the presence of excess maltose (Glc)

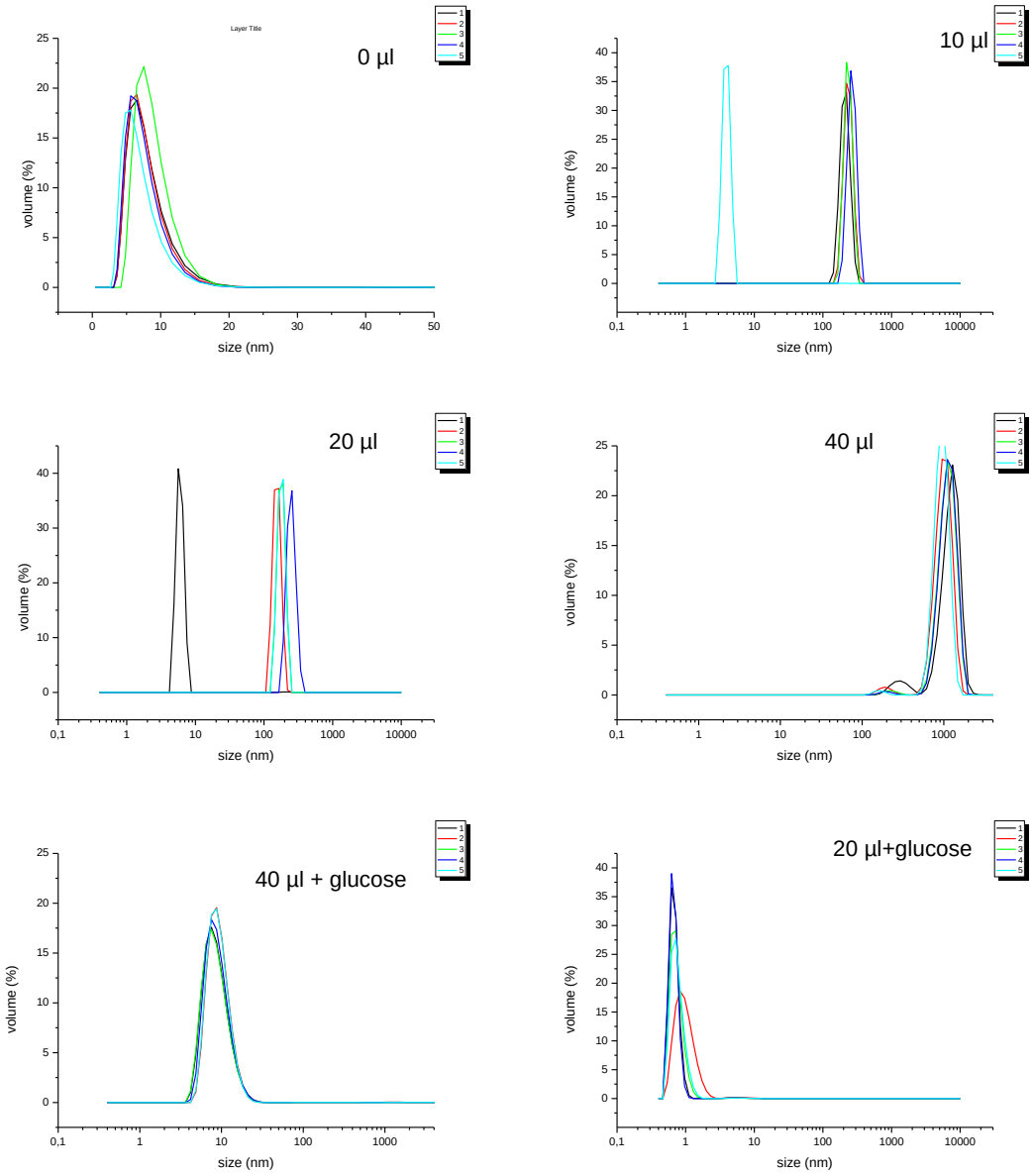

Figure 6-19: DLS volume plot of the 40% maltose grafted polymer with different amounts of Concavalin A in µl.

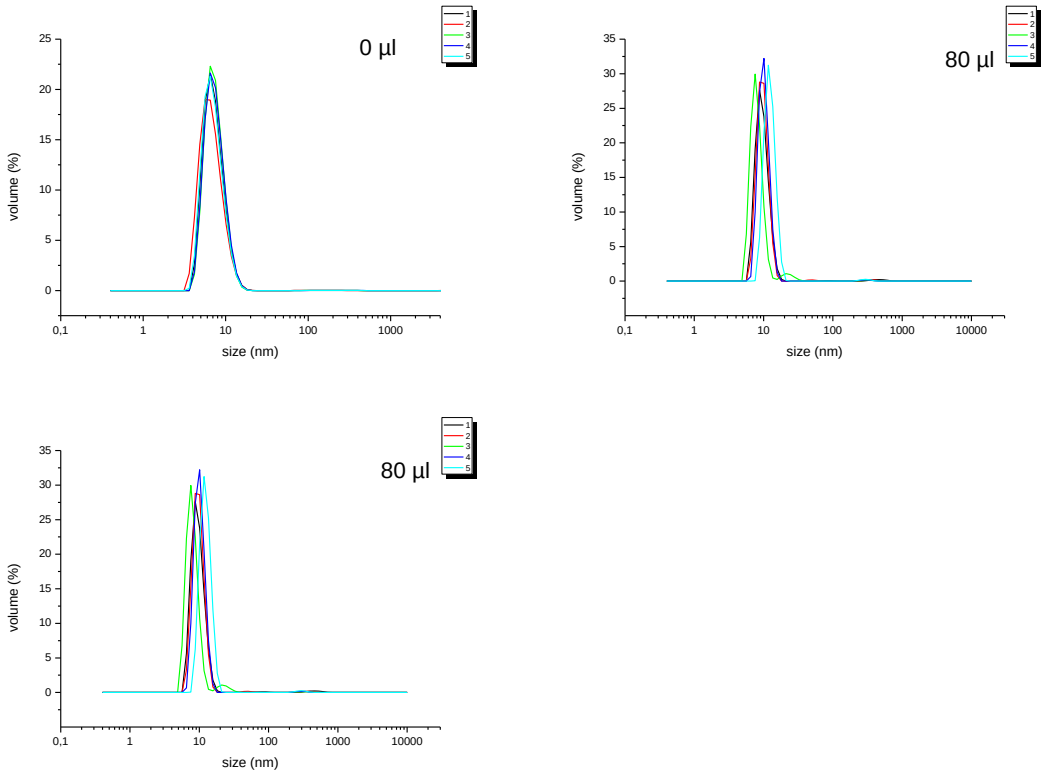

Figure 6-20: DLS volume plot of the 15% maltose grafted polymer with different amounts of the Concavalin A

6.4 Conclusion

The successful exploration of PEtOx-PEI as a reactive platform for post-polymerisation modification was shown by the coupling of two sugars, glucose and maltose, *via* reductive amination to yield glyco-PAOx. The linear aldehyde form of glucose efficiently forms imine linkages with the secondary amine units of PEI followed by the in situ reduction to the stable tertiary amines. The solution behavior of the resulting glycopolymers shows that there are strong interactions *via* hydrogen bonding between the backbone and the side chains, leading to the formation of the loose aggregates of all glucose-modified copolymers. The maltose functionalized copolymers containing less than 12% maltose are stable as unimers, whereas polymers with 12% to 15% maltose show LCST behavior. Higher maltose contents resulted in aggregation. Because our aim is the development of glycopolymers for biomedical applications, the interaction of the obtained glyco-PAOx with ConA, a sugar binding lectin, was investigated. As expected, the glucose modified copolymers do not interact with ConA, as they contain linear glucose units. The polymer grafted with maltose does, however, still contain a ring closed glucose unit that is available for binding and leads to the efficient and specific agglutination with ConA. Future works will focus on using the developed synthetic strategy for the preparation of glyco-PAOx containing more biologically relevant sugars that show specific interactions with certain tissues or proteins associated with certain diseases, such as influenza or HIV. The carbohydrate will then be used as a targeting agent or as an inhibitor. We also hope that this work inspires the use of the PEtOx-PEI platform for coupling of other biologically relevant carbohydrates.

This coupling of carbohydrate is of vast importance for the PAOx field as the carbohydrates are important in all kind of biological processes. It may open up a new field of post polymerisation added carbohydrates making polymers which may be used in cell trafficking or other biological processes.

6.5 References

(1) Vollrath, A.; Schubert, S.; Schubert, U. S. *J. Mater. Chem. B* **2013**, *1* (15), 1994.
(2) Hezinger, a F. E.; Tessmar, J.; Göpferich, a. *Eur. J. Pharm. Biopharm.* **2008**, *68* (1), 138.
(3) Carlos, L. D.; de Zea Bermudez, V.; Ferreira, R. a. S.; Marques, L.; Assunção, M. *Chem. Mater.* **1999**, *11* (9), 581.
(4) Shaner, N. C.; Steinbach, P. A.; Tsien, R. Y. *Nat. Methods* **2005**, *2* (12), 905.
(5) Chudakov, D.; Matz, M.; Lukyanov, S.; Lukyanov, K. *Physiol. Rev.* **2010**, *90* (3), 1103.
(6) Ruedas-Rama, M. J.; Walters, J. D.; Orte, A.; Hall, E. A. H. *Anal. Chim. Acta* **2012**, *751*, 1.
(7) Johnson, N.; Johnson, K. *ACS Chem. Biol.* **2007**, *2* (1), 31.
(8) Chalfie, M. Ghia Euskirchen, Y. Ward, W. Prasher, D. *Science* **1994**, *263* (5148), 802.
(9) Johnson, L. V; Walsh, M. L.; Chen, B.; Buchanan, J. M. *Proc. Natl. Acad. Sc. USA Cell Biol.* **1980**, *77* (2), 990.
(10) Dubertret, B.; Skourides, P.; Norris, D. J.; Noireaux, V.; Brivanlou, A. H.; Libchaber, A. *Science* **2002**, *298* (5599), 1759.
(11) Resch-Genger, U.; Grabolle, M.; Cavaliere-Jaricot, S.; Nitschke, R.; Nann, T. *Nat. Methods* **2008**, *5* (9), 763.
(12) Jaiswal, J. K.; Simon, S. M. *Trends Cell Biol.* **2004**, *14* (9), 497.
(13) Moghimi, S. M.; Szebeni, J. *Prog. Lipid Res.* **2003**, *42* (6), 463.
(14) Papadimitriou, S. A.; Salinas, Y.; Resmini, M. *Chem. A Eur. J.* **2016**, *22* (11), 3612.
(15) Fu, A.; Gu, W.; Larabell, C.; Alivisatos, a P. *Curr. Opin. Neurobiol.* **2005**, *15* (5), 568.
(16) Robin, M. P.; O'Reilly, R. K. *Polym. Int.* **2015**, *64* (2), 174.
(17) Zhu, M. Q.; Zhang, G. F.; Hu, Z.; Aldred, M. P.; Li, C.; Gong, W. L.; Chen, T.; Huang, Z. L.; Liu, S. *Macromolecules* **2014**, *47* (5), 1543.
(18) Mackiewicz, N.; Nicolas, J.; Handké, N.; Noiray, M.; Mougin, J.; Daveu, C.; Lakkireddy, H. R.; Bazile, D.; Couvreur, P. *Chem. Mater.* **2014**, *26* (5), 1834.
(19) Quadir, M. A.; Morton, S. W.; Deng, Z. J.; Shopsowitz, K. E.; Murphy, R. P.; Epps, T. H.; Hammond, P. T. *Mol. Pharm.* **2014**, *11* (7), 2420.
(20) Pu, H. L.; Chiang, W. L.; Maiti, B.; Liao, Z. X.; Ho, Y. C.; Shim, M. S.; Chuang, E. Y.; Xia, Y.; Sung, H. W. *ACS Nano* **2014**, *8* (2), 1213.
(21) Wu, D.; Liu, Y.; He, C.; Goh, S. H. *Macromolecules* **2005**, *38* (24), 9906.
(22) Wang, D.; Imae, T. *JACS Commun.* **2004**, *126*, 13204.
(23) Wang, D.; Imae, T.; Miki, M. *J. Colloid Interface Sci.* **2007**, *306* (2), 222.
(24) Chu, C. C.; Imae, T. *Macromol. Rapid Commun.* **2009**, *30* (2), 89.
(25) Lee, W. I.; Bae, Y.; Bard, A. J. *J. Am. Chem. Soc.* **2004**, *126* (27), 8358.
(26) Restani, R. B.; Morgado, P. I.; Ribeiro, M. P.; Correia, I. J.; Aguiar-Ricardo, A.; Bonifcio, V. D. B. *Angew. Chemie - Int. Ed.* **2012**, *51* (21), 5162.
(27) Pastor-Pérez, L.; Chen, Y.; Shen, Z.; Lahoz, A.; Stiriba, S. E. *Macromol. Rapid Commun.* **2007**, *28* (13), 1404.
(28) Pan, X.; Wang, G.; Lay, C. L.; Tan, B. H.; He, C.; Liu, Y.; Tan, H.; He, C.; Liu, Y. *Sci. Rep.* **2013**, *3* (2763), 1.
(29) Murphy, L. J.; Robertson, K. N.; Kemp, R. A.; Tuononen, H. M.; Clyburne, J. A. C. *Chem. Commun.* **2014**, *51* (19), 3942.
(30) Ion, A.; Doorslaer, C. Van; Parvulescu, V.; Jacobs, P.; Vos, D. De. *Green Chem.* **2008**, *10* (1), 111.
(31) Hampe, E. M.; Rudkevich, D. M. *Tetrahedron* **2003**, *59* (48), 9619.
(32) Belli Dell'Amico, D.; Calderazzo, F.; Labella, L.; Marchetti, F.; Pampaloni, G. *Chem. Rev.* **2003**, *103* (10), 3857.
(33) Wright, H. B.; Moore, M. B. *J. Am. Chem. Soc.* **1948**, *70* (11), 3865.
(34) Crooks, J. E.; Donnellan, J. P. *J. Chem. Soc. Perkin Trans. 2* **1989**, *2* (4), 331.
(35) Aresta, M.; Ballivet-Tkatchenko, D.; Dell'Amico, D. B.; Boschi, D.; Calderazzo, F.; Labella, L.;

Bonnet, M. C.; Faure, R.; Marchetti, F. *Chem. Commun.* **2000**, *8* (13), 1099.
(36) Sada, E.; Kumazawa, H.; Han, Z. Q. *Chem. Eng. J.* **1985**, *31* (2), 109.
(37) Belli Dell'Amico, D.; Calderazzo, F.; Labella, L.; Marchetti, F.; Pam. *Biomacromolecules* **2012**, *12* (d), 3037.
(38) Drage, T. C.; Arenillas, A.; Smith, K. M.; Snape, C. E. *Microporous Mesoporous Mater.* **2008**, *116* (1–3), 504.
(39) Sayari, A.; Heydari-Gorji, A.; Yang, Y. *J. Am. Chem. Soc.* **2012**, *134* (33), 13834.
(40) Hahn, M. W.; Jelic, J.; Berger, E.; Reuter, K.; Jentys, A.; Lercher, J. A. *J. Phys. Chem. B* **2016**, *120* (8), 1988.
(41) de la Rosa, V. R.; Bauwens, E.; Monnery, B. D.; De Geest, B. G.; Hoogenboom, R. *Polym. Chem.* **2014**, 5, 4957.
(42) Ferrari, S.; Moro, E.; Pettenazzo, A.; Behr, J. P.; Zacchello, F.; Scarpa, M. *Gene Ther.* **1997**, *4* (10), 1100.
(43) Hoogenboom, R. *Angew. Chem. Int. Ed. Engl.* **2009**, *48* (43), 7978.
(44) Sedlacek, O.; Monnery, B. D.; Filippov, S. K.; Hoogenboom, R.; Hruby, M. *Macromol. Rapid Commun.* **2012**, *33* (19), 1648.
(45) Guillerm, B.; Monge, S.; Lapinte, V.; Robin, J.-J. *Macromol. Rapid Commun.* **2012**, *33* (19), 1600.
(46) Verbraeken, B. K. H. R. In *Encyclopedia of Polymer Science and Technology*; 2014; pp 1–39.
(47) Kanazaki, K.; Sano, K.; Makino, A.; Homma, T.; Ono, M.; Saji, H. *Sci. Rep.* **2016**, *6* (August), 33798.
(48) de Macedo, C. V.; da Silva, M. S.; Casimiro, T.; Cabrita, E. J.; Aguiar-Ricardo, A. *Green Chem.* **2007**, *9*, 948.
(49) Bonifácio, V. D. B.; Correia, V. G.; Pinho, M. G.; Lima, J. C.; Aguiar-ricardo, A. *Mater. Lett.* **2012**, *81*, 205.
(50) Restani, R. B.; Conde, J.; Pires, R. F.; Martins, P.; Fernandes, A. R.; Baptista, P. V.; Bonifácio, V. D. B.; Aguiar-Ricardo, A. *Macromol. Biosci.* **2015**, *15* (8), 1045.
(51) Correia, V. G.; Bonifácio, V. D. B.; Raje, V. P.; Casimiro, T.; Moutinho, G.; da Silva, C. L.; Pinho, M. G.; Aguiar-Ricardo, A. *Macromol. Biosci.* **2011**, *11* (8), 1128.
(52) Stubbe, B.; Li, Y.; Vergaelen, M.; Van Vlierberghe, S.; Dubruel, P.; De Clerck, K.; Hoogenboom, R. *Eur. Polym. J.* **2016**.
(53) Correia, V. G.; Ferraria, A. M.; Pinho, M. G.; Aguiar-Ricardo, A. *Biomacromolecules* **2015**, *16* (12), 3904.
(54) Ferreira, L. S.; Trierweiler, J. O. *IFAC Proc. Vol.* **2009**, *7* (PART 1), 405.
(55) Hartono, A.; Da Silva, E. F.; Grasdalen, H.; Svendsen, H. F. *Ind. Eng. Chem. Res.* **2007**, *46* (1), 249.
(56) Barzagli, F.; Mani, F.; Peruzzini, M. *Int. J. Greenh. Gas Control* **2011**, *5* (3), 448.
(57) Diefenbacher, J.; Piwowarczyk, J.; Marzke, R. F. *Rev. Sci. Instrum.* **2011**, *82* (7), 76107.
(58) Liang, H.; Jia, D.; Liu, H.; Gu, Y.; Liu, C.; Zhao, F.; Chen, P.; Wang, D. *Chem. Lett.* **2015**, *44* (4), 548.
(59) Sayari, A.; Belmabkhout, Y. *J. Am. Chem. Soc.* **2010**, *132* (18), 6312.

Chapter 7 :
Summary and outlook

CHAPTER 7

7.1 English Summary and outlook

During this PhD research the world of poly(2-alkyl-2-oxazoline)s (PAOx) was explored. This class of polymers was discovered in 1966 by four independent research groups.[1–4] Nowadays, these polymers find their applications mostly in the biomedical field as the polymers show excellent behavior in a biomedical context.[5] When PAOx is brought in contact with a living organism no adverse reactions are observed.[6] Although specific protein adsorption is observed, these proteins actually ensure that macrophages do remove the polymer.[7] These beneficial biological properties in combination with the large chemical versatility could potentially make PAOx *"the new kid on the block"* in the field of polymer therapeutics. The future is prosper as the first PAOx drug conjugate, SER 214, has entered phase I of the clinical trials. SER 214 is a PAOx-Parkinson drug developed by Serina Therapeutics and many more are expected to follow.

Next to its excellent biomedical behavior PAOx is known as the precursor of L-PEI.[8] L-PEI is obtained either via an acidic or basic hydrolysis of PAOx, to remove all the amide side chains of the PAOx.[9] If only a part of the side chains is removed we obtain PAOx-PEI copolymers, that contain the original polymer and newly formed L-PEI units.[10–12] These copolymers are used in gene transfection and in post-polymerisation modification procedures.[13,14] In this thesis we focused on the post-polymerisation modification of PEI-units along the backbone. For the development of new polymer therapeutics a polyvalent polymer platform is needed with a broad range of chemical versatility. For PAOx this includes the functionalisation of the side chains and/or the end groups either *via* termination agents and/or initiators. The third option for functionalisation is the post polymerisation modification route. This route uses well-defined homopolymers such as PEtOx or PMeOx as a starting point. The polymerisation of these polymers can happen in a defined way, in large scale and the polymers are commercially available in different grades. The latter is important for labs which have no specific installation for the synthesis of PAOx and cannot synthesise special polymers. The amines of the PEI units can be used in post polymerisation modification steps as it is a good nucleophile. However the distribution of PEI units along the backbone is not known. Knowing this distribution is of great importance as it will influence the behavior and reactivity in further steps.

In chapter 2 the acidic hydrolysis was investigated via different 1D NMR techniques, namely ^{1}H-NMR, ^{13}C-NMR spectroscopy and 2D NMR techniques namely HSQC, HMBC and COSY spectroscopy. These techniques were used to gain insight in the distribution of L-PEI units along the PAOx chain after partial hydrolysis. (Figure 7-1, center) Three types of CH_2 in the PEI units were revealed. All three CH_2 groups have different chemical environment and, therefore, could be identified in the ^{13}C-NMR spectrum with the help of various 2D NMR techniques. The first CH_2 type is surrounded by other CH_2 groups originating from PEI and was identified as the middle of a block of PEI units, an all PEI triad. The second type of CH_2

is the frontier of the block as it showed interactions with CH_2 groups of both PEI and PEtOx. The third type of CH_2 only showed interactions with CH_2 originating from PEtOx. The three types of CH_2 reflect three types of PEI-units, indicating that the hydrolysis proceeds in a block like fashion as already at lower hydrolysis degree all PEI triads were present. This means that starting from one PEI-unit the neighbouring groups are more likely to be hydrolysed into PEI. We stipulate that the block formation is caused by the presence of the neighbouring protonated amine. This facilitates the reaction by the formation of a seven-membered intramolecular ring thereby overcoming the repulsion effect which is induced by the protonation of the amines. The seven ring induces an acceleration during the beginning of the hydrolysis reaction which was already observed in the kinetics, while at higher hydrolysis degree the effect of the protonation becomes significant and decreases the hydrolysis speed.[9,11] With increasing hydrolysis degrees a higher percentage of block-like PEI structures were found as expected. The second proof for the block like PEI distribution was given by straightforward statistics. The random hydrolysis can be compared with Bernoulli statistics, meaning that the effect of the neighbouring group is nonexistent. The experimental data showed that the experimental hydrolysis does not agree with the Bernoulli statistics and that there is an effect of neighbouring groups on the hydrolysis. After 50 years the question of the PEI units distribution resulting from partial hydrolysis is finally answered, as it yields block-like PAOx-PEI copolymers. The investigated hydrolysis reactions were performed in HCl. The effect of adding different kinds of salt could potentially influence the protonation and related seven ring formation. Different effects on the protonation, like addition of salts, could provide some mechanistic insights and probably could make it possible to prepare statistical copolymers. The option of different solvents could also be interesting as this influences the protonation and the solubility of the resulting PEI units. With this chapter the copolymer distribution is unraveled and this knowledge can be used to understand the polymer behavior in the following chapters and maybe useful for functionalisation.

The hydrolysis of PPrOx was investigated in the third chapter (Figure 7-1, left top corner). For the hydrolysis of PAOx into L-PEI mostly PMeOx and PEtOx are used due to their good water solubility. The PPrOx is water soluble at room temperature, but the polymer has a temperature dependent solubility and crashes out of solution at elevated temperatures as used during the hydrolysis reactions. Therefore the hydrolysis of PPrOx was investigated and the kinetics were determined, showing a slower hydrolysis for PPrOx compared to PEtOx and PMeOx.[8,15] This result was anticipated as the extra carbon present in the side chain obstruct the access to the amide. The Tcp of PPrOx of 25°C makes that the polymer is insoluble at the reaction temperature thereby decreasing the reaction speed. Due to the presence of the PEI units along the backbone an increase in T_{cp} was observed for the PPrOx-PEI copolymers. A higher percentage of PEI induced a higher T_{cp} as expected as the hydrophobic propyl side chains were removed. The solubility behavior of the PPrOx-PEI copolymers was examined in different salts and this showed that the hydration layers are influenced by the salt addition, when there was an addition of a “salting in” salt there

was an even higher increase for the T_{CP}. There was no pH influence on the $T_{cp.}$ After the thorough examination of the hydrolysis reaction of PPrOx, polymers with different lengths were partially hydrolysed and used to prepare polyplexes with DNA for transfection experiments. These polymers formed well-defined particles, which could subsequently act as a scaffold when heated beyond the T_{CP}. When forming the particles the positive charges were found on the outside, enabling a strong interaction with the DNA. This chapter showed that together with PEtOx and PMeOx, PPrOx could have potential as non-viral gene vector for gene transfection. For further work the polymer could be modified or partially cross-linked to form hydrogels in situ.

In the fourth chapter both PEI and PEtOx-PEI were used to develop a post-polymerisation modification procedure (Figure 7-1, right top corner). By using the well-known reaction between an amine and CO_2, a carbamate containing polymer could be obtained. However the reaction between a secondary amine and CO_2 is slow and therefore the modification reactions were done in $scCO_2$ yielding partially carbamate functionalized PEI and PEtOx. It was however impossible to convert all of the PEI units into carbamates with $scCO_2$ due to the formation of a zwitterion. The zwitterionic carbamate was formed when remaining amines of L-PEI were protonated and the carbamate was deprotonated. The deprotonation by the amines is important as this stabilizes the carbamate. A detailed NMR study on the formed polymer structure revealed the occurrence of a side reaction at longer exposure times leading to the formation of a cyclic urea that was irreversibly formed by locking the CO_2 on the backbone. The introduction of this cyclic urea had a huge influence on the properties of the final polymers. The polymers with the cyclic urea showed fluorescence similar to the carbamate polymer. After removal of the carbamate units by using heat, a linear PEI analogue was obtained having some cyclic urea groups, which suppresses the crystallization making it better water-soluble while simultaneously providing intrinsic fluorescence. Such amorphous fluorescent PEI analogues have huge prospect for gene delivery and cell trafficking. Also zwitterionic polymers are getting more attention in biomedical context as they show non-fouling behaviour. The carbamate functionalized PEtOx also have intrinsic fluorescence making them interesting for biomedical applications and for theranostic.

In the fifth chapter, the PEtOx-PEI reaction platform was further explored (Figure 7-1, left bottom corner). Expanding the chemical toolbox is important as this could help the development of new polymer therapeutics. Four different copolymers bearing methyl ester side chains were synthesised. Al linkers were coupled by using a reaction between the amine of the PEI unit and a reactive group. The first modification reaction with an acid chloride yielded a copolymer with the original PEtOx and the newly formed PMestOx. The second and the third copolymers used a thiourea and urea group to couple the linker. The last linker formed a tertiary amine and was developed by the reaction of L-PEI with bromo-acetate. All of the polymers have a latent methyl ester functionality, which could be transformed in an amide via a direct

amidation reaction with an excess of amine. Different kind of amines were used to transform the methyl ester group into an amide to introduce a wide range of (functional) side chains. This chapter not only showed the versatility of PEtOx-PEI platform, it also introduced new linkers. The linkers could be used to couple drugs, peptides or any other active molecule in future works.

In the sixth chapter the PEtOx-PEI platform was examined as basis for carbohydrate containing polymers (Figure 7-1, right bottom corner) This is important as there is a need for biocompatible polymers with potential targeting groups. This was done by the synthesis of PEtOx-PEI copolymers containing different hydrolysis degrees. The PEI units were subsequently reacted with a carbohydrate via a reductive amination. This reductive amination of the linear form of carbohydrates was already shown on the primary amino groups of branched PEI, however not on copolymers with L-PEI that only contain secondary amino groups. The successful synthesis of these polymers showed that PEtOx-carbohydrate copolymers were accessible, whereby the first part of the carbohydrate is ring opened. In our case two carbohydrates were used, glucose and maltose. The solution behaviour of the resulting polymers was examined and the possibility for binding with ConA was evaluated. This showed that the second carbohydrate unit was still available for binding with the enzyme when a disaccharide was used, whereby one ring is opened for coupling to the PEtOx-PEI but the second ring remains intact. The reductive amination is however not a straightforward process, so it could be suggested that carbohydrates should be coupled via different methods as carbohydrates with all kind of functionalities are being developed.

This work provides some insights in the world of post polymerisation modification of PAOx-PEI. It could potentially help to ensure a better access to the PAOx class. The polymer class is pushing its way to the top of the polymer therapeutic field. However if there will be no FDA approval, polymer therapeutics based on PAOx are just a dream. Luckily a firm such as Serina Therapeutics is focused on developing and exploring the PAOx platform. The PAOx field could learn a lot from Serina as they used different molecules than those often found in polymer papers. The main factor to convince the pharmaceutical and biomedical community is by producting biological relevant data.

If PAOx cannot play a role in polymer therapeutics it will play a role in the field of macroscopic polymers. Here the FDA approval is not crucial and the Dutch company GATT is brining PAOx polymer to the patient and the medical world. This is of vast importance for the PAOx field showing that innovation and new products can push the gates open to new markets.

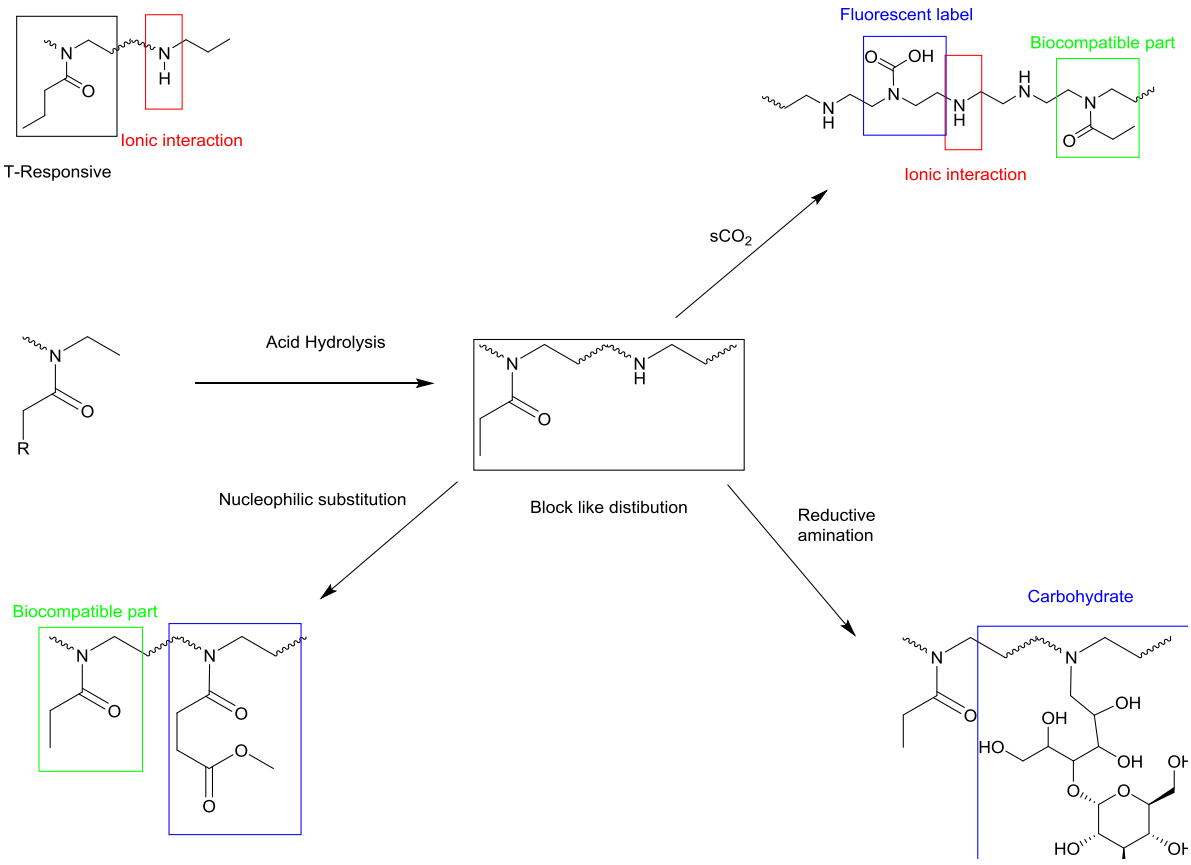

Figure 7-1: Overview figure

References

(1) Tomalia, D. a; Sheetz, D. P. *J. Polym. Sci. Part A-1 Polym. Chem.* **1966**, *4* (9), 2253.

(2) Seeliger, W. H. H.; Aufderhaar, E.; Diepers, W.; Feinauer, R.; Nehring, R.; Their, W.; Hellmann, H. *Polym. Lett.* **1966**, *5* (1), 871.

(3) Kagiya, T.; Maeda, T.; Fukui, K.; Narisawa, S. *Polym. Lett.* **1966**, *4*, 441.

(4) Levy, A.; Litt, M. *Polym. Lett.* **1967**, *5*, 881.

(5) Bauer, M.; Lautenschlaeger, C.; Kempe, K.; Tauhardt, L.; Schubert, U. S.; Fischer, D. *Macromol. Biosci.* **2012**, *12* (7), 986.

(6) Bauer, M.; Schroeder, S.; Tauhardt, L.; Kempe, K.; Schubert, U. S.; Fischer, D. *J. Polym. Sci. Part A Polym. Chem.* **2013**, *51* (8), 1816.

(7) Koshkina, O.; Westmeier, D.; Lang, T.; Bantz, C.; Hahlbrock, A.; Würth, C.; Resch-Genger, U.; Braun, U.; Thiermann, R.; Weise, C.; Eravci, M.; Mohr, B.; Schlaad, H.; Stauber, R. H.; Docter, D.; Bertin, A.; Maskos, M. *Macromol. Biosci.* **2016**, No. 16, 1287.

(8) Kem, K. M. J. Polym. Sci. Polym. Chem. Ed. **1979**, 17, 1977.

(9) Van Kuringen, H. P. C.; De La Rosa, V. R.; Fijten, M. W. M.; Heuts, J. P. A.; Hoogenboom, R. *Macromol. Rapid Commun.* **2012**, *33* (9), 827.

(10) Fernandes, J. C.; Qiu, X.; Winnik, F. M.; Benderdour, M.; Zhang, X.; Dai, K.; Shi, Q. *Int. J. Nanomedicine* **2013**, *8*, 4091.

(11) Mees, M.; Haladjova, E.; Momekova, D.; Momekov, G.; Shestakova, P. S.; Tsvetanov, C. B.; Hoogenboom, R.; Rangelov, S. *Biomacromolecules* **2016**, *17* (11), 3580.

(12) Shah, R.; Kronekova, Z.; Zahoranová, A.; Roller, L.; Saha, N.; Saha, P.; Kronek, J. *J. Mater. Sci. Mater. Med.* **2015**, *26* (4), 157.

(13) Englert, C.; Trützschler, A.-K.; Raasch, M.; Bus, T.; Borchers, P.; Mosig, A. S.; Traeger, A.; Schubert, U. S. *J. Control. Release* **2016**, *241*, 1.

(14) Mees, M. A.; Effenberg, C.; Appelhans, D.; Hoogenboom, R. *Biomacromolecules* **2016**, *17* (12), 4027.

(15) Van Kuringen, H. P. C.; Lenoir, J.; Adriaens, E.; Bender, J.; De Geest, B. G.; Hoogenboom, R. *Macromol. Biosci.* **2012**, *12* (8), 1114.

7.2 Nederlandstalige samenvatting

In dit doctoraat werd de wondere wereld van poly(2-alkyl-2-oxazoline)s (PAOx) verder onderzocht. Deze polymeren behoren tot de klasse van de biomedische polymeren en werden gelijktijdig door 4 onderzoeksgroepen ontdekt in 1966. PAOx zijn enorm geschikt voor toepassingen in het medische veld door excellente farmaceutische kwaliteiten. Wanneer deze polymeren in contact komen met een organisme, bijvoorbeeld in de bloedbaan, wordt geen afstotingsgedrag opgemerkt. Ze zijn als het ware onherkenbaar voor het immuunsysteem waardoor ze ideale kandidaten zijn voor toepassingen in de farmaceutische wereld. Daarnaast biedt dit polymeer ook een enorme chemische diversiteit omdat de polymeren op verschillende niveaus chemisch gemodificeerd kunnen worden, dit via de eindgroepen en de zijketens. Daarom is het ook fantastisch nieuws dat voor het eerst een PAOx gebaseerd medicijn naar fase I van de klinische trials wordt getest door de farmaceutische firma Serina Therapeutics.

Naast hun kwaliteiten op biologisch vlak zijn deze PAOx polymeren ook gekend als precursors van lineair poly(ethylene imine) (L-PEI). Dit polymeer is een van de belangrijkste referenties op het vlak van gen transcriptie. Via een zure of basische hydrolyse van PAOx wordt het L-PEI verkregen. Niet alleen het volledig gehydrolyseerd polymeer kan worden verkregen maar ook copolymeren, die bestaan gedeeltelijk uit het PAOx en PEI. De PAOx-PEI polymeren hebben hun toepassingen op het vlak van gen therapie maar kunnen daarnaast ook dienen als startpolymeer voor het maken van nieuwe copolymeren. Door de vele ontwikkelingen in het veld op het vlak van goed gedefinieerde polymeren kunnen startpolymeren worden verkregen met een $Đ < 1.1$. Hiermee kunnen zeer goed gedefinieerde polymeren op maat van de toepassing gemaakt worden met als groot voordeel dat er geen moeilijke monomeersynthese moeten worden gedaan. Daarnaast zijn deze startpolymeren commercieel beschikbaar en is de hydrolyse een proces waarbij geen gespecialiseerde apparatuur voor nodig is.

Omdat de gedeeltelijke hydrolyse van PAOx een zo belangrijke rol kan spelen moet deze eerst tot in het detail gekend zijn. In het eerste deel van dit doctoraat werd daarom nagegaan hoe de zure hydrolyse in zijn werk gaat. Via nucleaire magnetische resonantie technieken werd de monomeer distributie langs de keten onderzocht. Hierbij kwamen we tot de conclusie dat er drie types L-PEI methyleen populaties aanwezig zijn in het copolymeer. Het eerste type is de methyleen populatie waarbij deze enkel en alleen is omringd door andere methyleen molecule van PEI. Dit wil zeggen dat deze methyleen groep zich in het midden van een PEI block bevindt. De tweede populatie wordt omringd door enerzijds PEI methyleen en anderzijds een PEtOx methyleen. Deze vormt de grens van een PEI gebied en een PEtOx gebied. De laatste methyleen populatie bevindt zich in een PEtOx rijke omgeving. Tijdens de hydrolyse wordt blokvorming verkregen die niet overeenkomt met een willekeurige hydrolyse. Dit werd aangetoond via de Bernoulli statistiek, waarbij de kans zeer klein is dat willekeurig drie methyleen PEI units naast elkaar komen te

staan by lage hydrolyse graad. De blokvorming wordt verkregen doordat de NH geprotoneerd is en zo een zeven ring kan vormen met de carbonyl van het amide op de zijketen. Hierdoor is dit amide veel gevoeliger voor een nucleofiele aanval. Het zou het zeker interessant zijn om te kijken wat de invloed is van het zuur en de eventuele toevoeging van zouten op deze zure hydrolyse. Indien er enige optimalisatie gebeurt zou het mogelijk moeten zijn om de hydrolyse uit te voeren waarbij statistische polymeren worden verkregen.

Vervolgend op het verhaal van de hydrolyse van PEtOx werd ook de hydrolyse van poly(n-propyloxazoline) (PPrOx) bestudeerd. Dit polymeer vertoont temperatuurafhankelijk oplossingsgedrag wat wil zeggen dat het PPrOx boven de 25°C onoplosbaar wordt en dat de oplossing melkachtig wordt. De hydrolyse werd onderzocht en gedeeltelijk gehydrolyseerde polymeren werden bekomen. Door de additie van hydrofiele PEI blokken langs de keten werd de Tcp hoger dan deze van het startpolymeer. Hoe hoger de PEI fractie hoe hoger de Tcp. Daarnaast werden ook polymeren gemaakt met verschillende ketenlengten en verschillende PEI hoeveelheden voor de complexatie met DNA. Bij het vormen van de complexen werd opgemerkt dat het temperatuurgedrag van de polymeren terug was gewijzigd en dat er nanogelen werden gevormd. De lading van de polymeren in oplossing, zeta potentiaal, waren boven de LCST gegroepeerd aan de buitenzijde. Deze werden dan verder onderzocht in het kader van gen transfer.

In het vierde hoofdstuk werd een andere post modificatie reactie geïntroduceerd waarbij zowel L-PEI als PEI-PEtOx in super kritisch CO_2 werden gebracht. Door deze modificatie vertoonde deze polymeren fluorescent gedrag door de gevormde carbamaat binding. Opmerkelijk was wel dat er ook een zijreactie optrad waardoor de carbamaat verder reageerde naar het cyclisch ureum. Deze was opmerkelijk genoeg ook nog steeds fluorescent. Het mooie aan deze polymeren is dat ze zwitterionisch zijn maar toch nog steeds positieve ladingen dragen op de keten waardoor interactie mogelijk is met DNA.

In het vijfde hoofdstuk werd de verscheidenheid aangetoond van het polymeer platform door de synthese van 4 verschillende copolymeren van PEtOx. Vier verschillende linkers werden gekoppeld aan het PEtOx-PEI platform. De eerste linker werd gekoppeld met een zuurchloride waarbij het amide werd gevormd. Bij de twee volgende linkers werden respectievelijk een ureum en een thio-ureum gevormd door het koppelen van een isocyanaat en een thio-isocyanaat. De koppeling vormde een tertiair amine door de reactie van het amine met bromo-methylacetaat. Elk van de vier linkers hebben een methyl ester die kan reageren met een amine en zo een amide vormt. Verschillende types amines werden dan ook onderzocht voor de reacti met het methylester via directe amidatie. De gevormde polymeren kunnen als basis dienen in verschillende toepassingen en zeker op het vlak van polymeer drug conjugaten. De linker methode is simpel en verscheidene, zelfs degradeerbare, linkers kunnen worden ingebouwd.

In het laatste hoofdstuk van dit doctoraat werd het PEtOx-PEI platform verder uitgebreid naar het koppelen van carbohydraten. Deze koppeling verliep via een reductieve aminatie waarbij de aldehyde van de ring geopende versie van het suiker werd verbonden via een imine linker op de backbone. Deze trage reactie was succesvol en toonde aan dat carbohydraten bevattende polymeren ook een optie zijn voor het

PEtOx platform en uitgevoerd kan worden op de secundaire amine van de L-PEI groepen in gedeeltelijk gehydrolyseerde polymeren. De karakterisatie van het gedrag in oplossing toonde aan dat naargelang het koppelen van verschillende suikers diverse gedraging optraden. Het gekoppelde maltose toonde aan dat het glucose die aanwezig was in de zijketen kon gebruikt worden voor bio recognitie met ConA. De reductieve aminatie is niet het gemakkelijks en meest zuinig proces dus in de toekomst zou het zeker mogelijk moeten zijn om via gefunctionaliseerde carbohydraten PEtOx-PEI te modificeren.

7.3 Publication list of the candidate

1. **Thermoresponsive polymeric temperature sensors with broad sensing regimes.** *Qilu Zhang, Gertjan Vancoillie, Maarten A. Mees, Richard Hoogenboom. Polym. Chem., 2015,6, 2396-2400 DOI: 10.1039/C4PY01747A*
2. **Functional Poly(2-oxazoline)s by Direct Amidation of Methyl Ester Side Chains** *Maarten A. Mees and Richard Hoogenboom, Macromolecules, 2015, 48 (11), pp 3531–3538 DOI: 10.1021/acs.macromol.5b00290*
3. **Partially Hydrolyzed Poly(n-propyl-2-oxazoline): Synthesis, Aqueous Solution Properties, and Preparation of Gene Delivery Systems** *Maarten Mees, Emi Haladjova, Denitsa Momekova, Georgi Momekov, Pavletta S. Shestakova, Christo B. Tsvetanov, Richard Hoogenboom, and Stanislav Rangelov Biomacromolecules, 2016, 17 (11), pp 3580–3590 DOI: 10.1021/acs.biomac.6b01088*
4. **Sweet Polymers: Poly(2-ethyl-2-oxazoline) Glycopolymers by Reductive Amination**, *Maarten A. Mees, Christiane Effenberg, Dietmar Appelhans, and Richard Hoogenboom Biomacromolecules, 2016, 17 (12), pp 4027–4036 DOI: 10.1021/acs.biomac.6b01451*
5. **Synthesis of novel boronic acid-decorated poly(2-oxazoline)s showing triple-stimuli responsive behavior** *Gertjan Vancoillie, William L. A. Brooks, Maarten A. Mees, Brent S. Sumerlin and Richard Hoogenboom Polym. Chem., 2016,7, 6725-6734 DOI: 10.1039/C6PY01437B*
6. **Understanding the partial hydrolysis of poly(2-alkyl-2-oxazolines: Is it random or is it block like** *Maarten A. Mees, Dieter Buyst, Timothee Courtin, José C.Martins, Richard Hoogenboom. Submitted*
7. **Controlled Synthesis of Novel Fluorinated Copolymers via Cobalt-Mediated Radical Copolymerization of Perfluorohexylethylene and Vinyl Acetate** *Jérémy Demarteau, Bruno Améduri, Maarten A. Mees, Vincent Ladmiral, Richard Hoogenboom, Antoine Debuigne, Christophe Detrembleur. Submitted to Macromolecules*
8. **The plunge of PEI into CO_2.***Maarten A. Mees, Prof. Steve Howdle, Thomas McAllister, Silvio Curia. Manuscript in preparation(2017)*
9. **Rose Bengal Poly(2-alkyl-2-oxazolines) for cancer treatment.** *Maarten A. Mees, Nathalie De Laet, Niels Vandamme, Geert Berx, Annemieke Madder, Richard Hoogenboom. Manuscript in preparation(2017)*
10. **Unraveling the tacicity of poly(2-alkyl-2-oxazoline)s via oligomers.** *Maarten. A. Mees, Guillia Morgese, Edmundo Benetti, Richard Hoogenboom Manuscript in preparation*

Acknowledgment

Ge zyt miskien geen lichtend voorbeeld maar ge èt tenminste gebrand

De Feesters

Waarschijnlijk de enige pagina die door iedereen met zoveel aandacht gelezen wordt. Ik kan het bijna niet geloven maar toch. De laatste pagina's van mijn doctoraat…

Toen ik een kleine 5 jaar geleden het idee had om mijn master thesis te doen bij Richard Hoogenboom had ik geen idee waar ik aan begon, ik kwam terecht in een startende groep waar vele dingen nog niet echt geregeld was maar toch had ik het gevoel dat ik thuis kwam (cliché maar zo waar). Het moment dat Richard me vroeg om te doctoreren had ik niet onmiddellijk ja gezegd (playing hard to get, but he already had me at hello) natuurlijk heb ik ja gezegd. Ik moet toegeven dat Richard waarschijnlijk de enigste persoon was die het lef had (of naïef genoeg was) om mij in zijn onderzoeksgroep op te nemen. Ik was geen top student en toonde zeker geen ambitie om een top onderzoeker te worden. Toch is hij er in geslaagd om me, ik geef het niet graag toe, te veranderen. Ik leerde van hem onderzoek doen, kritisch denken en vooral creatief omgaan met chemie. Ik had het gevoel dat we in onze onderzoeksgroep meespeelden op internationaal vlak en zoals vaak leer je van de groten het meest. Ik hoop dan ook dat de Ugent niet te klein wordt voor je, maar ik vrees ervoor. Bedankt.

Daarnaast wil ik zeker Gertje (Héhéhé) bedanken. Hij was voor mij de eerste reden om naar de groep te komen en wat ben ik blij dat ik zijn madness (die voorhoofd ader) van vlakbij heb mee gemaakt. De volgende quote "*Wie zet er nu een lezing om half 9 achter een feestje*" met een Bary White stem zullen mij altijd bijblijven. Ook onze diepe gesprekken samen met ons Patricia vergeet ik niet. Over onze muzikale smaak valt er weinig te twijfelen, de cantina band en o zo veel meer. *You're insecure don't know what for.*

De persoon waarmee ik de laatste 4 jaar het meest mee heb opgetrokken en samen heb gezeten zonder me een moment te vervelen, dat is Jim. Moest een van ons twee een vrouw zijn hadden we nu al kindjes en hadden we een huisje gekocht, iedereen zijn unanieme mening. Ik zal zeker onze honeymoon suite niet vergeten in Riva en daarbij horend koffie meisje (chiao Bella), ons Brooks en de Riva bar is dan ook weer eentje om in te kaderen. Die keer dat er een Chinees in ons toilet zat is ook eentje om te onthouden, zeker nadat ik je had gered omdat je verdwaalt was. Ons kindje "Jimmy" is niet wat het moest worden maar we hebben ons best gedaan, sommige zaken zijn dan ook niet recht te trekken. En ik hoop dat je in de toekomst toch toegeeft dat ik veel gelijk heb :p

Daarnaast wil ik ook twee mensen bedanken die toch vrienden zijn geworden (als ze dat al niet waren), Joa en Bart. Joa, ik versta nog steeds niet hoe en waar je opmerkingen haalt maar toch slaag je erin om elk

gesprek dood te laten lopen. Ik vergeet niet vlug hoe je altijd en overal in slaap kan vallen maar ik ben blij dat we de remedie hebben gevonden(Praagse boobies). En die frietjes gaan we nog eens gaan stekken met een halve liter. Tuub merci om elke dag onze lieve buurman te kloten en termen als *"ik ben pegel*" en "*ik moet plassen als een pony*" zullen me altijd bijblijven. Er zijn toch veel gelijkenissen tussen jij en Tyrion Lannister(You drink en you know things) Hierbij wil ik ook ons "mama" Kathleen bedanken. We hebben al veel mensen moeten dag zeggen in onze groep maar jij mis ik toch het meest.

The Supra group. I would like to thank you guys and girls. I might say that this was the best group to work with, how cool is it when you can work with friends. Sometimes we had our issues but still I hope you enjoyed as much as I enjoyed working in our group. I will probably not have a working place like in the Supra group (if my future colleagues read this, it is a high bar to reach). I will not sum up all the people who joined and left our group, I would like to thank all of you. We had special moments on the group trips and many other occasions (washing machines and octopussies, losing thesis students and post docs). I would like to thank some of the post docs as you guys showed me how not to act as a post doc.

Er zijn ook enkele mensen buiten onze eilandje in de S4 dat ik wil bedanken. Jos wil ik ten zeerste bedanken omdat hij altijd klaar stond om ons uit de nood te helpen. Bedankt om ons (niet verplicht) verder te helpen. Natuurlijk stond Jos klaar om de laatste roddels te aanhoren en te vertellen. Idem dito voor Tim van den NMR, bedankt dat ik nooit echt moeten wachten heb om stalen te meten. En om al die tijd die we hebben verdaan met onze diepe gesprekken over de diepere filosofie van de menselijkheid.

Van de "Madder" groep wil ik ook zeker Nathalie bedanken voor de vele leuke roze gesprekken. Ik voel het er kan nog steeds een Nature paper uitkomen. Mien, Bram, Jantje (zag eens pruimen hangen), Johan, Ellen, Duchan (speedy Gonzalez), Vincent, Jimmy, Kurt, Lieselot(the crazy one). Hen wil ik bedanken voor al die keer dat ik jullie in het lab ben komen" inspecteren" en jullie zich waarschijnlijk af vroegen maar wat doe die toch allemaal.

Ook wil ik de mensen bedanken van de werkplaats Marc, Mario, Tim, Theo en Joris. Jullie hebben mij veel uit de nood geholpen en het deed altijd eens deugd om eens bij jullie binnen te springen. De mensen van de administratie, Paul en Veerle hebben mij ook vaak geholpen en ik moet jullie hiervoor bedanken. Ik wil me ook verontschuldigen voor al die keer dat ik jullie snoep heb opgegeten.

During my visit in Sofia I got the honor to work together with some fun and remarkable people at the Bulgarian academia of Science, I would like to thank all the people there. Emi, special thanks for you, you gave me a warm welcome in the beautiful Sofia and I really enjoyed the time we spent together.

In England/Notingham I was glad to work two weeks in the lab of Steve Howdle (aka He-Man), one of the few chemistry professors with songs on Youtube. Probably the only professor I impressed by finding

the best pub in town after half a day. I especially want to thanks Thomas for taking care of me and wondering what the Belgian was mumbling. May the force be with you… Carbamates synthesise we will.

Er zijn ook nog veel vrienden en vriendinnen die ik wil bedanken. Zeker Michael wil ik niet vergeten. We hebben samen vijf jaar "gestudeerd" en we zien elkaar veel te weinig maar ik geniet ervan om elke keer samen te zijn. Jelle "de maestro" De Vos, ik heb de bijl al en jij kijkt voor het boerenpaard en de rest zien we wel ☺. Andere mensen zoals Olivier, Debbie, Boris, Laura, Heidi, Lieselot (the small one), Laure-Anne, Jonas, JOACHIM, Justine, Els, Mieke, Sam, Charlotte, Jasper, Lana, Nathalie, Karolina, Esther, sexy ass, Giel, Sylvie, Niels, Kristof, Patrick en nog zo veel meer. Bedankt om samen zo veel leuke/minder leuke momenten samen te beleven. Ook wil ik zeker al onze buren bedanken voor de vele warme momenten samen, betere een goede buur dan een verre vriend, laat die buren maar goede vrienden zijn…

Ik wil zeker ook al mijn broers en schoonzussen bedanken, ten eerste omdat jullie zo jullie best hebben gedaan om een nest schone en leuke kindjes te maken. Ten tweede het is altijd leuk om samen te komen met de hele mezen bende. Hierbij wil ik mijn ouders ook bedanken voor de vele hulp, het af en toe(ja Wouter af en toe) eens strijken en klussen. Ik zeg het misschien niet genoeg maar bedankt voor de vele liefde en ik hoop dat jullie hier ook van kunnen genieten. Want ik vermoed dat jullie meer stress hebben gehad dan mezelf.

En last but no least. De persoon die in feite verantwoordelijk is dat dit doctoraat is wat het is. Mijn Babiettje. Niet alleen hebben we samen ons doctoraat geschreven maar hebben we ook samen alle dieptes en hoogtes meegemaakt van het onderzoek. Blijkbaar is samen het doctoraat schrijven een relatie test maar dat hebben we zelf niet gemerkt. Kapotte auto's dat is pas een test : Jij hebt me ook elke keer weer geambeteerd waarom dit of dat nuttig zou zijn en gepusht. Maar het belangrijkste is dat jij een o zo lief slim meisje bent die mijn hart heeft gestolen (en nog zo veel meer). Ik vond het soms ambetant om te wachten op je maar ik wacht liever op de liefde van mijn leven dan op de trein. Ik moet je dan ook bedanken dat we nu al zo lang samen zijn en dat we vanaf nu Dr Catrysse en Dr Mees zijn(en dat we eindelijk doktertje kunnen spelen).

And though where the road then takes me,
I cannot tell
We came all this way
But now comes the day
To bid you farewell

I bid you all a very fond farewell

CHAPTER 7